DEVELOPMENT OF AN ULTRASONIC NEEDLE GUIDE AS AN AID TO PERCUTANEOUS PUNCTURE OF BLOOD VESSELS

by

PETER JOSEPH KOLB

Submitted to the University of Cape Town in partial fulfilment of the requirements for the degree of Master of Science in Medicine in the field of Biomedical Engineering

September 1982

ABSTRACT

The puncturing of blood vessels is often a "hit and miss" procedure which may take even a skilled physician considerable time to perform. Perhaps even more important than the time taken by medical personnel is the trauma inflicted on patients when the procedure is unnecessarily prolonged.

A needle guide was developed, based on the well-known Doppler ultrasound principle. Two transducers,on sliding bars,are used to locate the vessel. A unique mechanical arrangement was devised for aiming the needle at the intersection point of the two ultrasonic beams.

An account is given of the theory, engineering philosophy, design parameters and step-by-step development of the guide. Full mechanical and electronic drawings and photographs of the prototype also appear in this work.

Mike Price

Peter Kolk

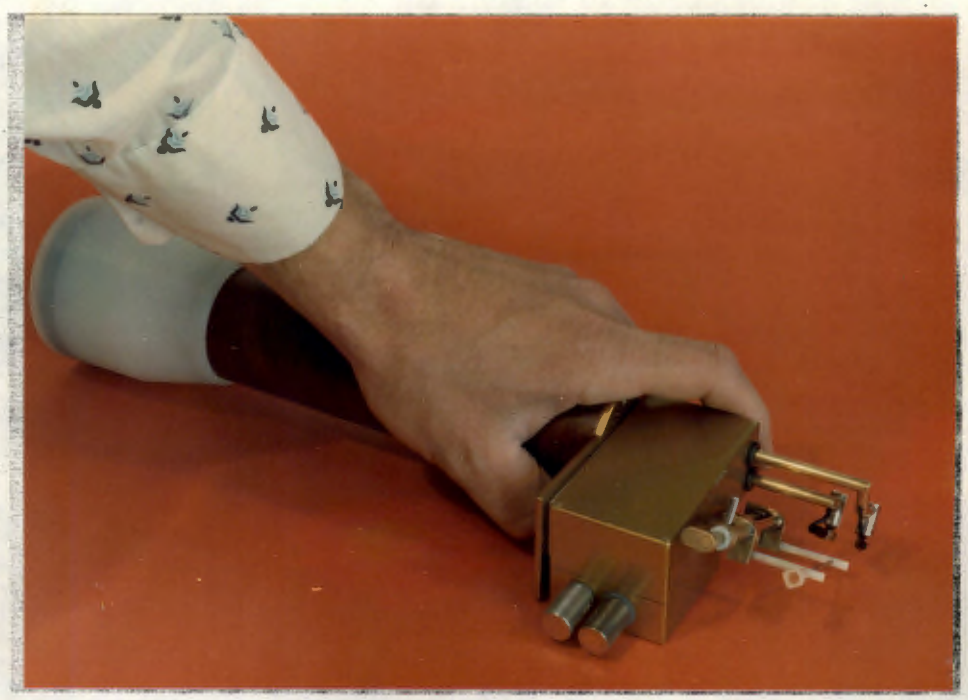

ULTRAGUIDE

CONTENTS

INTRODUCTION

There is at present no general purpose instrument available to medical personnel to help them insert needles into blood vessels. When one reflects on the amount of costly time wasted and the dangers to the patients of prolonging the puncture procedure, one wonders why this problem has earned so little attention.

There have been some attempts at using ultrasound to guide needles into blood vessels. These have involved very simple adaptations to existing ultrasound equipment. Perhaps this simple approach has not been adequate in addressing the problem. For this reason a very different approach was used in developing the *Ultraguide*. No effort was spared at making the instrument as clinically acceptable as possible.

Development of this instrument involved multidisciplinary integration, including:

- *Ergonomics
- *Clinical considerations
- *Electrical engineering
- *Mechanical engineering

The major part of this work deals with the development of the guidance mechanism. Design of the transducers and associated driving circuitry is given less emphasis, since commercial blood flow detectors are already well established.

Since this was a Biomedical Engineering project, it was not considered sufficient to simply demonstrate the feasibility of such a system, but rather to design, construct and test an instrument which would be clinically useful and which was likely to be used. This has necessitated limiting the discussion of certain aspects, such as acoustics. Some of these aspects, such as the design of a suitable transducer system, lend themselves to thesis topics in their own right.[1]

---

[1] *See reference list on page 193*

CHAPTER ONE

ULTRAGUIDE — THE CONCEPT

§1.1 NEED FOR THE GUIDE

During my visits to various hospital departments at the beginning of 1981, I came across several blood vessel puncture procedures, most of which appeared to be inordinately lengthy. One such procedure which made a lasting impression on me was a Swan Ganz catheterization performed on a seriously ill patient in the respiratory intensive care unit. The young doctor was clearly inexperienced and nervous. He fought bravely for about an hour and a half before the consultant arrived and with his skill managed to insert a fresh catheter within a few minutes. The patient was visibly distressed by the whole procedure and the doctor seemed very relieved when it was all over. A catheter costing R100 was discarded.

Subsequent investigations revealed that this was not an isolated case. Discussions with an experienced consultant in Angiography brought up some interesting information. For example, while an expert can puncture an Internal Jugular Vein in the first 'stab' on average, an inexperienced intern takes more than ½hour (Appendix 1-1). While he had done over 150 Jugular Veins himself, about 3% still gave him trouble, and that means they take more than ½hour. A Subclavian Vein can take over two hours, while a Femoral Vein takes a novice between 20 minutes and an hour. An anaesthetist I spoke to was of the opinion that it can take between five minutes and ½hour to find a single artery.

Although time taken for these procedures has been emphasized, it is perhaps not so much the time wasted that is important, as the danger to the patient in unnecessarily prolonging such invasions.

The risks involved in invading the body are well known.[2] Catheterization of the Subclavian Vein, for example, is fraught with dangers. Pneumothorax is a typical complication that can result and was reported in one study[2] to be as high as 6%.

The accidental placement of catheters in the mediastinal or pleural spaces has also been known to occur, sometimes followed by the infusion of large volumes of fluid into these spaces.[2] A study has shown that out of over eleven hundred attempts at cannulating the Internal Jugular Vein, 4.2% ended with a cannula in the carotid artery. While this in itself is not that serious, subsequent heparinization of the patient can lead to haematomas forming in the neck and this could lead to compromised airways.[2]

Damage to blood vessels is a problem commonly encountered in puncture procedures. This is particularly serious in the case of the Subclavian where haemothorax can occur. Other results of vessel damage include exsanguination from the puncture site and one attempt on the subclavian was reported to have resulted in an arteriovenous fistula.[2]

Frequency of vessel puncture

A survey was carried out to determine the frequency with which vessel punctures are performed at Groote Schuur hospital. In order to get some idea of the total number of vessel punctures performed at the hospital the surgical stores were approached for information on the issue of needles that are known to be used exclusively for puncturing blood vessels. These include small vein sets, cannulae needles, butterfly infusion sets and butterfly intermittent sets. Not included are short and long bevelled hypodermic needles, since there is no way of knowing what proportion is used for simple subcutaneous puncture. Catheters are also not included since some are used for urinary puncture. The number of needles in all four classes issued annually is 17 200 000. If we consider that there are 600 doctors working at the hospital, it turns out that on average 78 needles are used per doctor every day. Although quite obviously not all the needles can be inserted by the doctors, this figure does give some indication of the importance of blood vessel puncture.

A second estimate on the number of punctures performed at the hospital was obtained from the chemical pathology laboratory. One of the doctors there revealed that the laboratory receives

more than 234 000 blood samples annually; each sample requires a fresh vascular puncture. There are a number of other laboratories in the hospital, of which Haematology was likely to get a similar number of samples.

The point here is that even if a small percentage of the needle punctures performed give trouble, the numbers are still enormous and any attempt at helping the situation must surely be worthwhile.

§1.2 THE STARTING CONCEPT

The next question to be asked was: "What do the medical doctors think about the idea of using a needle guide for percutaneous puncture of vessels?" So discussions were held with some of the people who would ultimately use the instrument.

First a model was built, based on an idea that evolved as a result of some work I had previously done on a commercial Doppler ultrasonic velocimeter. The guide was initially conceived as a black box containing the electronic circuitry necessary for

Fig.1-1

driving two ultrasonic transducers. The transducers were to be mounted on one end of a pole protruding from the box.

One of the transducers would transmit ultrasound in the form of a pencil beam into the tissue, while the other would receive the reflected signal. By processing the two signals electronically, the sound of blood flow could be heard from the speaker mounted in the other end of the box, when the transducers point directly at flowing blood. A special guiding mechanism could then be used to steer the needle down the length of the two beams towards the vessel. This model was intended to serve as a basis for discussing the concept with medical practitioners.

18 Medical doctors were approached for their views on the proposed instrument. Their comments are summarized in appendix 1-1. Of the 18 questioned, three did not consider the device to be a potentially useful instrument. It is interesting to note that these three were the only ones no longer routinely practicing blood vessel puncture. The other 15 ranged from being pleased with the idea to being very enthusiastic. Enthusiasm was particularly marked among the anaesthetists.

One point that came up several times during earlier discussions with various medical doctors was the problem that young doctors might have in developing skills associated with vessel puncture if they were to rely on a 'gadget.' There are two important observations to be made here. Firstly, it takes a good few months of practice before a doctor is reasonably competent with a needle. Since practicing percutaneous puncture on dummies is not a feature of medical training, one supposes that human beings at various stages of illness are being used for practice. This is no fault of the medical profession since they have no alternative. However, to reject the concept of an assist device which could prevent iatrogenic complications on the grounds that doctors would be deprived of medical experience, is patently immoral.

The second point that should be made is that the instrument could, in fact, assist the doctor in getting experience in percutaneous puncture much more rapidly than he might without it. One could argue that if he had an assist device he would soon learn how and where to position the needle to optimize his success rate. He would then learn to handle the needle in much the same way without the device.

§1.3 CONCLUSION

The large number of vessel punctures performed, the difficulty in certain cases of performing the procedure, the danger to patients, the waste of costly time, the potential aid to teaching and the strong support particularly from the anaesthetists all go to indicate a strong need for a needle guide.

CHAPTER TWO

LITERATURE SURVEY

The research work was started with a search for literature on instrumentation for transcutaneous blood flow measurement. Such instruments are widely used and the principle of determining the location of the blood vessel by detecting the blood flow in it forms the basis of the needle guide. The next step is to decide on a physical principle to use for blood flow detection. The principle should be well established and understood. The object of this work is not to re-invent or improve a particular detection technique, but rather to exploit it for use in the needle guide. Of the various techniques that were considered (§2.1), the doppler ultrasound method suggested itself as the most suitable.

Over the last ten years ultrasound systems appear to have dominated the field of blood flow measurement. Many of the papers written on this subject discuss ways of improving the dependability of velocimeters. However, since we are concerned with blood flow detection and not velocimetry, most of these works are of little value to us.

The search for literature uncovered about fifty papers that were at first thought to contain potentially useful material, but few of which were to prove relevant to the project. In an attempt to get some order into this survey, the papers were classified under the following headings:

1. Non-invasive blood flow measurement other than ultrasound.
2. Ultrasonically guided percutaneous puncture.
3. Relevant signal processing.
4. Modulated Doppler techniques.
5. Ultrasonic transducers and fields.
6. Ultrasonic catheter probes.
7. Clinical aspects of cannulation.
8. General.

Only papers that were to prove useful to this project are discussed here. Thus only topics *1* and *2* will be covered. Pertinent aspects of clinical cannulation have already been discussed.

§2.1 NON-INVASIVE BLOOD FLOW MEASUREMENT OTHER THAN ULTRASOUND

Roberts[3] wrote a review article on non-invasive blood flow measurement techniques most of which, while not lending themselves to the localization of blood vessels, should nevertheless be mentioned for the sake of completeness.

Plethysmography for example, is the most reliable and simplest technique for the quantitative determination of net volume flow rate to a limb.[4] Since it does not relate to any particular blood vessel but rather to blood flow to the extremity as a whole, it cannot be used to detect vessels.

Impedance plethysmography is a technique in which the change in electrical impedance across a limb or body section is used as an indicator of change of blood volume in that section. It also does not lend itself to vessel detection.

The nuclei of various atoms, such as those of hydrogen, can be considered as extremely small magnets which line up in the presence of an external magnetic field.[3] Both the alignment and disalignment processes are functions of time. By measuring the extent of alignment or residual magnetism downstream from an applied magnetic field, one can calculate the rate of blood flow. This technique is know as "nuclear magnetic resonance." It is unlikely that this technique could be adapted for detecting blood vessels.

Lee[5] described a method whereby skin electrodes pick up voltages generated by blood flowing through powerful magnetic fields. Since blood can be considered as a moving conductor, this is just an application of the Hall effect. What makes this technique particularly unsuitable for blood flow detection is that a computerized data processor is required to distinguish blood flow signals from background noise.

Powers[6], Phung Le Cong[7], and Phillips[8] discuss the application of LASERS to blood flow velocimetry. These instruments are extremely bulky and very complex. They are used, for example, for tracking individual erythrocytes as in microcirculation studies before grafting. They frequently require surgical procedures to gain access to the proximity of the study region. One would only resort to these instruments when the work is too delicate to be handled by ultrasonic equipment. While laser doppler anemometers may not be useful for general blood vessel location, there may well be potential for this technique in paediatrics as in scalp vein puncture.

Finally, a technique that should be investigated further is the thermal blood flow detector. No literature was found on this instrument, but it is thought that it depends on the elevated temperature of arteries for detection. Obscurity alone was deemed sufficient grounds for rejecting this technique.

§2-2 ULTRASONICALLY GUIDED PERCUTANEOUS PUNCTURE

Ultrasonically guided puncture has become indispensible as a clinical procedure in aspiration biopsy, nephrostomy, liver biopsy,intra-abdominal fluid collection and amniocentesis amongst others. These applications of transcutaneous puncture have been comprehensively discussed in a recently published text book[9].

The basic technique is a logical extension to ultrasonic diagnostic imaging and can be considered analogous to missile guidance by radar. Short pulses of ultrasound are transmitted through the tissue. Reflections are either presented on A-scan where the amplitude of the returned signal is plotted as a function of time from the pulse transmission, or on B-scan where the amplitude is used to modulate the brightness of a spot along the line. In the B-mode a full map of the area scanned can be drawn on the screen. In order to achieve this the transducer has to be attached to articulated arms that are ground referenced by means of position sensors. The problem of ground referencing has been overcome in some instruments by the development of multi-element transducer arrays.

The earliest reference to ultrasonically guided puncture suggests that it was first tried before 1969 by Kratochwill[10], who discussed it at the first world congress on ultrasonic diagnostics in medicine in Vienna in June 1969. Subsequently Holm and Kristensen appear to have dominated the pioneering work done in this field.

In 1972 Holm[11] described a method whereby a biopsy needle was passed through a canal made in a transducer of a standard ultrasonic scanner. Firstly the target is mapped on B-scan. Then the range of the target is measured from the A-scan presentation and marked off on the needle. The needle is then guided through the canal in the transducer to the depth marked off. One of the difficulties with this system is that the progress of the needle cannot be monitored since it passes down the centre of the ultrasonic beam. So in 1975 Holm[12] designed an attachment to guide the needle across the axes of a multi-element array made up of many small transducers lying next to each other and fired sequentially to produce a real time B-scan map of the area under examination. Since the needle crossed the ultrasonic beam at an angle, its progress could readily be monitored on the screen. A number of other researchers applied Holm's ideas directly or in modified form.

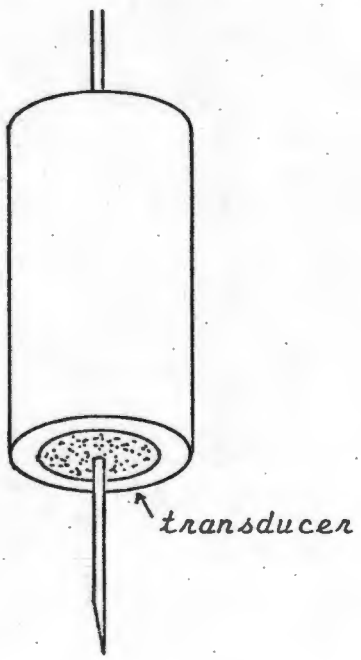

Fig.2-1

Pulsed echo ultrasonic imaging could unquestionably be used for localization of blood vessels. It does, however, have certain disadvantages. The equipment is relatively bulky and expensive and the output is visual, which is not thought ideal for vessel puncture. One could also conceivably mistake blood vessels for other structures.

This latter problem was very cleverly solved in 1972 by Mozersky[13] when he used a pulsed ultrasonic velocity detector in which only the Doppler shifted return signals were used to brightness modulate

the beam of a CRT. In this way a plot was obtained of intensity as a function of time after pulse transmission. This then was a typical B-presentation map, but only targets having a finite velocity showed up. This principle is ideal for angiography. But far more interesting from the point of view of this project, was a Doppler controlled needle director he described in 1973[14]. It was developed as an aid in angiography to puncture arteries in paediatric patients and in those patients with proximal occlusive vascular diseases.

The guide was very similar in design to that of Holm. It consisted of a 35mm cylinder axially pierced by a canal. Two 4mm^2, 8MHz piezoelectric crystals were mounted at one end on either side of the canal and at 75^o to it. These were connected to a standard PARKS Doppler flow detector. Once a blood vessel has been detected and the position of the dowel optimized for maximum doppler intensity, the needle could be passed down the central canal and out between the two transducers into the target area. The two ultrasonic beams from the two crystals were focused at a distance of 10mm. They converged for 5mm on either side of this point. The diameter of the converged ultrasonic beam was said to be about 20mm, but optimal signals were obtained in a much narrower range. In the laboratory, dog vessels as small as two millimeters in diameter were successfully impaled with the device. However, Mozersky's discussion is very concise and comments on the success of the instrument are sparse.

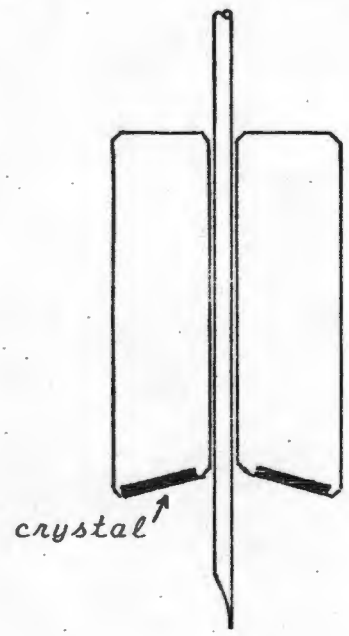

Fig.2-2

In 1976 Petzoldt[15] developed a similar device, primarily for puncturing the subclavian vein. A detachable clip mounted over a transducer pair was designed to accommodate the needle. A feature of this clip was that it could be opened for

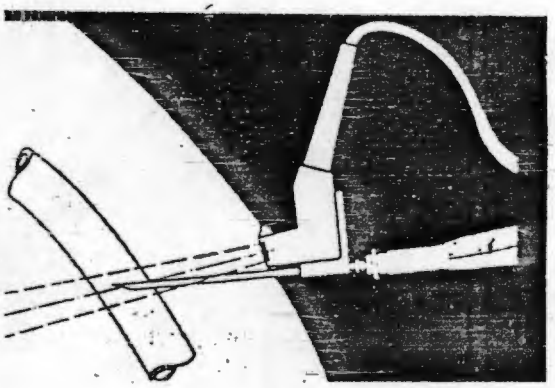

Fig.2-3[15]

convenient separation of the needle following successful puncture.

The criterion for successful vessel location was considered to be maximum intensity of the returned signal, since this occurs when there are a maximum number of scatterers in the beam intersection volume. (One could argue that if the velocity profile in the vessel is parabolic, then the optimum position occurs when the frequency or pitch is at a maximum.)

Of 50 punctures, 48 were successful and entirely without complications. In two cases puncture was contra-indicated for various reasons, although the vessels had been successfully located. Petzold suggested that the system could be used for other vessels but failed to mention why he did not try this himself.

While both Mozersky and Petzoldt developed very interesting instruments, there are a number of objections to their schemes. These include: the problems of puncturing vessels at shallow angles to the skin; the accommodation of standard needles such as short butterfly infusion needles and the location of vessels beyond the focal point of the beams.

Of great interest is also why the instruments are not commonly seen in hospitals. This alone has led me to conclude that there may be faults associated with their concepts, and that some new ideas are required. While this may not necessarily be true, this line has been adopted and some new ideas will be discussed in chapter 6.

CHAPTER THREE

BIOMEDICAL REQUIREMENTS

§3.1 BIOMEDICAL ENGINEERING

A crucial and perhaps most controversial task is that of marrying an engineering solution to a clinical problem.

The first step is to clearly identify the problem. It is quite possible for an engineer in a field such as medicine to miss something while trying to read a problem. This may not become evident until the equipment has been designed and built.

The second step is to clearly identify the important parameters and constraints within which the engineering solution is to be found. Since these parameters are open to subjective interpretation, there is yet another weak link in the design chain.

Thirdly, an engineering solution must be conceptualized and created on paper before it can finally be constructed. Now, assuming that the instrument has been constructed correctly and works according to the drawing, it may still fail as a result of something having gone wrong in one of the two steps discussed above.

The problem was approached with these three pitfalls very much in mind. The idea was to build a prototype from a design based on a personal assessment of the problem, a subjective evaluation of the design parameters and an engineering solution which appeared appropriate at the time. (Since two engineers examining the same problem are likely to come up with entirely different solutions, there must be a very significant role played by subjectivity, foreign though this is to scientific thinking.)

The prototype was to be an instrument that could be used by medical personnel in the clinical environment, in order to generate more objective design parameters for a final model. While the prototype is not expected to be the final answer, it was hoped that by careful planning it might be possible to get very close to it.

This necessitated a considerable amount of attention to detail, while ironically, the major concepts could still be considered under debate.

Perhaps a more controversial issue is that of deciding to what extent the end user should have a say in the design of the system. It is my opinion that the Engineer alone should decide what sort of information he requires from the physician and what sort of parameters are important. He alone should also decide on what sort of instrument is appropriate for the task. The following factors influenced the formation of this opinion:

* Doctors often do not know what they want.
* Doctors often do not know what sort of solution is practically feasible.
* Various potential end users frequently have contradictory requirements.
* Medical personnel are often so well established in some or other technique that they cannot see past the methods they are used to. This closes the doors to potentially very useful engineering ideas.
* Experience has taught senior Engineers that one can frequently not trust the "experts." [16]
* Good ideas can be destroyed by exessive interference from those who have different ideas. This can seriously demoralize the designer.

This does not imply that one should not consult the end user. What it does mean is that the Engineer should in the final analysis trust his own judgement more than that of others.

§3.2 CLINICAL ASPECTS

In order to start the project and to get a feel for the problem, several percutaneous puncture procedures were attended, and some discussions with physicians took place. It soon became clear that there were five identifiable difficulties associated with vessel puncture:

1. Locating the vessel in the first instance may not be that difficult in superficial vessels of normal, healthy people. However, obese patients tend to have their vessels obscured by fat rendering arteries impalpable and veins not visible. (Veins cannot be palpated since they do not pulsate sufficiently.)

2. Once a vessel has been successfully palpated, it may still be difficult to aim a needle at it, particularly in the case of children, where these structures are small.

3. A major problem in puncturing vessels is that of "furrowing". This happens when a first attempt is unsuccessful. A furrow or groove is formed in the tissue and it is often impossible to get the needle out of this groove. Often fresh puncture sites have to be chosen, but these will get progressively more difficult to deal with since the easiest ones are tried first.

4. Another major problem is that of wall compression, particularly in veins. When the tip of the needle presses on a vessel, the vessel gets compressed and the needle shoots through both walls. The situation can usually be saved by withdrawing the needle slowly until blood issues out through the lumen of the needle. In veins, however, the pressure is often so low that blood does not issue from the needle even if the tip of the needle is inside the vessel.

5. The vessel frequently "jumps out of the way" when a needle is pressed on it. This is more a problem with the tough skinned arteries.

It was initially the purpose of this work to examine all aspects of the difficulties associated with vessel puncture, but it soon became clear that the last two issues were separate problems and could not be covered in this work. However, at this stage it might be sensible to make some suggestions on avenues that could be explored in solving these two difficulties.

Firstly, wall compression can be minimized by increasing the pressure inside the vessel relative to the outside at the site of

the needle's tip. This could be achieved by proximal occlusion of the veins draining, for example the limb, with a suitable cuff. One can also increase the hydrostatic pressure inside the veins by simply lowering the puncture site as far as possible below the phlebostatic plane. It was rather surprizing to find that this technique is not employed more frequently.

Instead of increasing the pressure inside the vein one might also be able to decrease the pressure immediately outside the vessel by applying a negative pressure to the lumen of the needle just before it enters the vessel wall. In this way it might be able to "suck" its way through the wall.

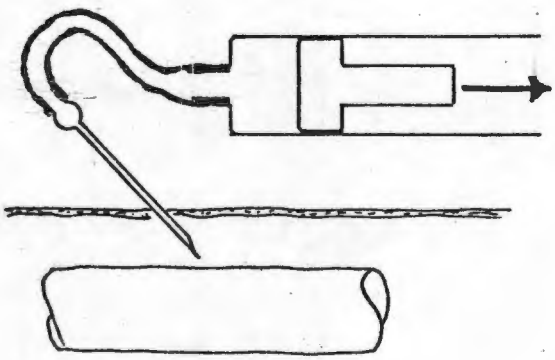

Fig.3-1

Another alternative might be to apply a negative pressure to the area around the puncture site by means of some sort of suction cup. The negative pressure under the suction cup would temporarily be transmitted through the skin and into the tissue until the extracellular fluid floods the area.

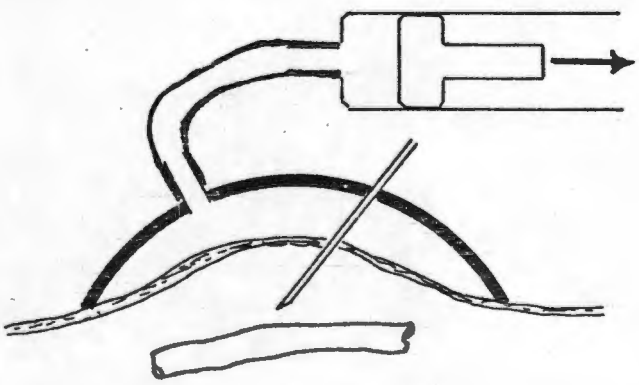

Fig.3-2

These last two suggestions might also minimise the effect of vessels jumping out of the way when stabbed with a needle.

§3.3 PROBLEM DEFINITION

The basic problem that will be of concern in this work is that of locating blood vessels prior to invasion and ensuring that the needle hits its target, assuming that the vessel does not jump around when speared. Given that a solution can be found, the problem of furrowing will no longer be relevant.

As was discussed in chapter 2, ultrasonic blood flow detectors are commercially available. The best known of these is probably the range of blood flow velocimeters manufactured by PARKS. As was discussed earlier, there have also been attempts at guiding needles using ultrasound, particularly for puncturing really difficult vessels such as the Subclavian. However, there are no general purpose instruments to be found in the hospital to aid in vessel puncture.

Commercial detectors lack the needle guidance facility. They also cannot distinguish between overlying vessels. While they can indicate an axis along which a needle has to be driven in order to find its target, they cannot indicate the depth of the vessel and can therefore not be used, in general, during the puncture process. One would first have to locate the axis, or direction in which the vessel is lying, memorize it and then try to place the needle accordingly. This can be done if the vessel is reasonably superficial and large. These points will become clearer in Chapter 6.

It is worth repeating that although ultrasound has been around for many decades and ultrasonically guided percutaneous puncture was first attempted over 10 years ago, commercial guides are either not available or just not popular. Problems associated with guiding a needle between a transmitted and reflected beam will be discussed in chapter 6.

Blood flow detection is already a commercial reality. *The purpose of this project is therefore to use this technology and develope a clinically acceptable guidance mechanism that will aim a needle at any blood vessel normally punctured by trial and error.* It is recognized that the prototype will in all probability not be sufficiently sensitive to deal with very small vessels such as paediatric scalp veins.

§3.4 DESIGN CRITERIA

Having defined the problem, the next stage is to list the constraints within which the system has been designed in order to make it as potentially successful as possible. The design criteria have been rather subjectively selected. Each parameter has been star rated to indicate its relative importance. Setting a value to these parameters is essential, since frequently one of two mutually contradictory parameters has to be compromised.

***** The instrument should be a portable device, suitable for general use in all wards, theatres and ICU's.
***** It should be able to deal with most vessels which are normally punctured by trial and error.
**** It should be a single unit not requiring coupling to other equipment. It should be possible to take the instrument off the shelf with one hand without having bits hanging from it.
* It should be a low cost device which can easily be constructed.
**** It should be completely washable.
***** The relevant parts must be sterilizable or disposable.
***** It should be reliable.
** It should be durable.
**** It should be very easy to operate.
**** It should accommodate most standard size needles.
***** It should be possible to remove the instrument from the needle without having to withdraw the needle from the patient.

These were the general constraints within which it was hoped to find a suitable engineering solution.

§3.5 SPECIFICATIONS - Needle Entry

Before commencing with the design, some more clinical information was needed. Although I personally attended several procedures to get a "feel" for what was going on, it was nevertheless essential to get some specific information from the doctors. Essentially this was a process of translating the clinical art of vessel puncture into engineering terms. Specifically what was

needed known was the depth of these vessels, their size and at what angle they were attacked. It was also important to know the relative frequency of each procedure in the event that a compromise solution had to be found. To this end a questionnaire was drawn up and with the help of an aneasthetist, copies were distributed to 16 medical doctors, together with covering letters.

Four replies were received. Not altogether unexpectedly the results were not really amenable to exact scientific evaluation. For example, different individuals commented on different procedures so that there was little or no overlap in some cases. Nevertheless, the results were averaged as well as possible and summarized diagrammatically in appendix 3-2. A copy of the questionnaire appears in appendix 3-1.

Perhaps the procedure most difficult to describe is cannulation of the Subclavian, and it was not possible to represent this on a simple diagram. It is, however, a very important procedure and one for which the guide should be of use.

The Subclavian vein is a continuation of the Axillary which drains blood from the upper limb. It has a tributary, the External Jugular from the head. The Subclavian is a short but wide vessel joining the Internal Jugular to form the Brachio-Cephalic which continues into the Superior Vena Cava. It begins at the outer border of the first rib and ends behind the clavicle (hence Subclavian) about 25mm from the sterno-clavicular joint. In order to puncture it a needle is lined up at the point where the sterno-cleido- mastoid muscle joins the clavicle. The needle is driven to a depth of 40 to 60 mm under the clavicle (posterior to it) at about 45° to the horizontal and in the direction of the opposite nipple. Access is extremely difficult for neophytes and poses special problems to ultrasonic guidance because of the bony covering, limited access window and considerable depth of the vessel. This discussion is important when the mechanical arrangement for the guide is considered in chapter 6.

While there were far too few replies to make the results really meaningful, they did form a basis for developing the prototype. The most important result is that the *angle of entry of the needle in nearly all cases varies from* 5° *to* 30° *relative to the*

skin. The Femoral Artery is punctured only rarely and when it is it is punctured at 90° when arterial blood samples are required, but this was not reflected in the replies.

Small vessels that are punctured are relatively superficial, while the deeper ones are larger. This stands to reason, since it would be unreasonable to attempt piercing a small vessel deep down in the tissue. The smallest vessel encountered is in the order of 1,5mm in diameter on average.

The results obtained were for adults although they were marginally influenced by a single return from paediatrics. While there is no question that the guide would be most useful for puncturing infants, it was thought that the instrument should first be made applicable to adults. Once this has been achieved a paediatric model, or better still a more universal model can be considered. Paediatrics is a very specialized field where techniques and dimensions and even illnesses are very differnet from those in the adult world.

§3.6 THE ENGINEERING SOLUTION

There is no doubt that with present technology the answer to detection lies in Doppler ultrasound. But before discussing the reasons for this choice, it is necessary to outline the principles involved here. The continuous wave Doppler ultrasound system works as follows:

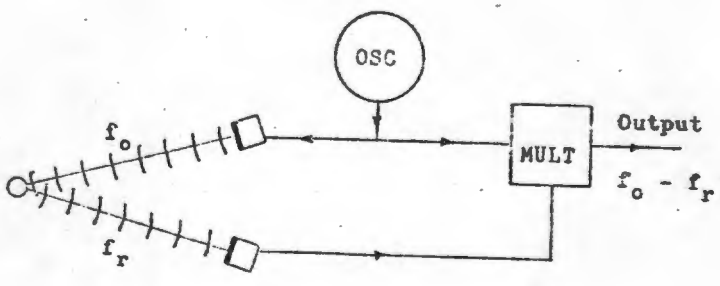

Continuous Wave Doppler Ultrasound System

Fig.3-3

The transmitting crystal is excited by a fixed frequency oscillator and transmits a continuous signal. Part of the oscillator output is fed to a mixer, where it is multiplied by a signal coming from

the receiving crystal. The two crystals are piezoelectric transducers which simply change electrical energy into mechanical vibration and vice versa. The output from the mixer contains a signal with a frequency equal to the difference between the frequencies of the two incoming signals. All signals returned from stationary objects will yield zero output, because the difference frequency is zero. Moving targets, however, cause the returned signal to be doppler shifted. That means that they are at a higher or lower frequency, depending on which way the target is moving. Moving targets will therefore cause the mixer to have a signal at its output. Output from the mixer is amplified and used to drive a loudspeaker, which presents the signal to the operator as the sound of flowing fluid.

Continuous wave doppler ultrasound was chosen for the following reasons:

1. Apart from some variations on the ultrasound principle, there appears at this stage to be no practical alternative.
2. Doppler ultrasound is well established as a transcutaneous blood flow detection technique. It is well known amongst hospital personnel.
3. Only moving targets have an output.
4. The output is in the form of sound in the audio spectrum which in itself has certain advantages:
   (a) Input is provided to a sense which is not being used for anything else during the puncture procedure. (A video display, for example, would be unacceptable.
   (b) The ear is particularly sensitive to sound colour. There is a wealth of information available from the mixer which is very useful without any further processing. For this reason one can readily detect the difference between an artery and a vein, since the blood flow pattern differs markedly between the two.
5. The output is readily interpreted as the flowing of fluid.
6. The system is electronically simple and can readily be made portable.
7. Ultrasound is very directional. In fact one can obtain quite a sharp pencil beam from the transducer.

8. At the power levels we deal with it is very safe.
9. It is completely non-invasive.
10. It is cheap, reliable and rugged.
11. Although some of the stages have to be tuned, these stages can be made stable without fear of drift.

As far as the mechanical guidance system is concerned, it was found that the simple principle of guiding a needle down the ultrasound beam had certain drawbacks and a more complex but flexible system was developed. The development of the mechanical arrangement is fully covered in chapter 6.

§3.7 SAFETY CONSIDERATIONS

After the Thalidomide catastrophe of the early 1960's, the safety of diagnostic ultrasound has come under heavy scrutiny. Innumerable investigations have been made into possible side effects associated with ultrasound. There has so far been no evidence to suggest that at the power levels presently used, any damage is caused to *in vivo* tissue. In fact, Sikov and Hildebrand suggest that current clinical procedures with doppler techniques have a factor of safety of at least 1650 ranging to a possible maximum of 7500[63].

Ultrasound is known to be destructive to tissue at high intensities. Interaction between ultrasound and tissue can be classified into two broad categories. Firstly, there are the effects related to the mechanics of wave propagation, such as cavitation. The second category includes those effects which lead to heat generation by absorption of ultrasonic energy.

In experimental situations where tissue suspensions are used, cellular damage usually results from cavitation. In stable cavitation, microbubbles of gas contract and expand, resonating at the frequency of the sound applied. Together with microstreaming, stable cavitation can lead to damage to subcellular structures in the liquid. At 1-4 MHz this can take place at intensities as low as $0,2W/cm^2$.[64]

In transient cavitation there is a more violent reaction in which

microbubbles collapse completely. This takes place in suspensions at intensities higher than 300W/cm^2.

There is sufficient and conclusive evidence that with c.w. or pulsed ultrasound there is no damage to organized mammalian tissues, from wave mechanics phenomena and cavitation up to peak intensity levels of approximately 1500W/cm^2 at frequencies of 2-3MHz.[63,64] Below these intensity levels the potential for damage lies in the temperature rise due to absorption of the acoustical energy. There is evidence that no significant bioeffect of ultrasound occurs in mammalian tissues without concomitant elevation of temperature.[64] (It is known that organogenesis in fetuses is extremely sensitive to temperature. It is for this reason that ultrasonic power levels in obstetrics are kept especially low.)

After a study of the biological effects reported with the use of ultrasound, the American Institute of Ultrasound in Medicine (AIUM) issued a statement on mammalian *in vivo* ultrasonic biological effects (AIUM Committee Report 1977/78). This in part states: *In the low megahertz frequency range there have been (as of this date) no independently confirmed significant biological effects in mammalian tissues exposed to intensities below 100mW/cm^2. Furthermore, for ultrasonic exposure times less than 500 seconds and greater than 1 second, such effects have not been demonstrated even at higher intensities, when the product of intensity and exposure time is less than 50 joules/cm^2.* [63,64]

For peripheral work as in blood flow detection, high frequencies (8-10MHz) are used. These are less penetrating and because of the smaller signals associated with blood flow detection, higher intensities are applied. Baker[58] indicates that some commercial machines have intensities as high as 600mW/cm^2.

In view of the fact that this instrument is to be used for peripheral blood flow detection in the high Megahertz region where penetration is low, and since the on-time is likely to be short, intensities of a few hundred mW/cm^2 can be tolerated.

CHAPTER FOUR

ACOUSTICS

§4.1 DOPPLER PRINCIPLE

Up till now not much has been said about the Doppler principle or how it is applied to the detection of blood flow. The Doppler effect is the change in pitch that is observed when a source of sound changes its velocity relative to the observer.

Consider a source of ultrasound and a receiver focussed at a small tube carrying blood at velocity u as illustrated.

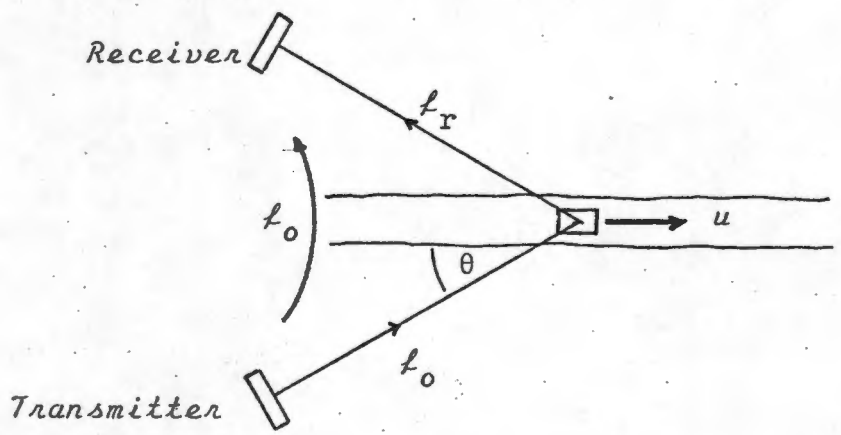

Fig.4-1

If the transmitter transmits ultrasound at velocity c and frequency f_0 then the frequency of the reflected signal f_r is obtained as follows:

$$\Delta f = f_o - f_r$$

and from appendix 4-1 we have that

$$\Delta f = f_o\left[\frac{2u}{c}\cos\theta\right] \qquad (4\text{-}1)$$

hence

$$f_r = f_o\left[1 - \frac{2u}{c}\cos\theta\right] \qquad (4\text{-}2)$$

The receiver does not hear only this doppler shifted signal. There is also leakage flux from the transmitter which is added to it.

If the transmitted signal is given by $A\cos(\omega_0 t)$ and the doppler shifted signal is given by $B\cos\{(\omega_0 + \Delta\omega)t + \phi\}$ where ϕ represents the phase difference between the two signals, then the signal picked up at the receiver is given by

$$C = A\cos\omega_0 t + B\cos\{(\omega_0 + \Delta\omega)t + \phi\} \qquad (4\text{-}3)$$

Physically these signals can be represented by two vectors.[17] The transmitted or leakage flux A is added to the doppler shifted one B to yield resultant C. C can therefore be considered to result from the modulation of carrier A in phase and amplitude by the doppler shifted reflected signal B.

Fig.4-2 shows the importance of keeping the leakage flux as small as possible. The smaller the signal to leakage ratio, the greater has to be the sensitivity of the multiplier.

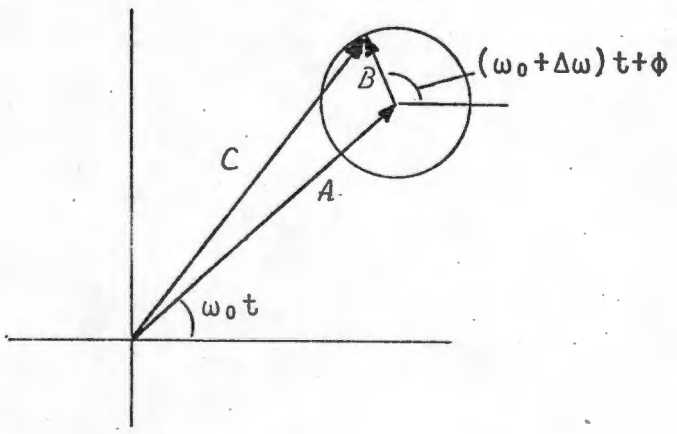

Fig.4-2

If the returned signal is electronically amplified and multiplied by the transmitted signal, then the output from the multiplier would be:

$$E = (A\cos\omega t + B\cos\{(\omega+\Delta\omega)t + \phi\})D\cos\omega t$$

$$= AD\cos^2\omega t + BD\cos\omega t\cos\{(\omega+\Delta\omega)t+\phi\} \qquad (4\text{-}4)$$

In general we have

$$\cos\theta_1\cos\theta_2 = \tfrac{1}{2}(\cos(\theta_1+\theta_2) + \cos(\theta_1-\theta_2))$$

and substituting for θ_1 and θ_2 we get

$$E = \tfrac{1}{2}AD(\cos(2\omega t)+1) + \tfrac{1}{2}BD(\cos\{(\omega+\Delta\omega)t+\phi+\omega t\} +$$

$$+ \cos\{(\omega+\Delta\omega)t+\phi-\omega t\})$$

Hence

$$E = \tfrac{1}{2}AD(\cos 2\omega t+1) + \tfrac{1}{2}BD(\cos(2\omega t+\Delta\omega t+\phi) + \cos(\Delta\omega t+\phi)) \quad (4\text{-}5)$$

Equation 4-5 shows us that the output contains frequency components at 2ω, $2\omega+\Delta\omega$, $\Delta\omega$ and 0. Both the very high frequency components and the DC value can be filtered off, leaving just the $\Delta\omega$ term. This is done in practice and its full implementation will be considered in chapter 5.

§4.2 BANDWIDTH OF OUTPUT

Numerous texts were consulted for information on blood flow velocities in the type of vessels to be puncture. This was found to be difficult to extract, because the available information for man does not lend itself to such an assessment. There are, however, tables available for blood flow in the vessels of dogs [18,19,20]. Since 1888 the vascular bed of dogs has been carefully analysed and extensive tables of blood vessels have been drawn up giving the total area of all the vessels of a given size in the vascular tree. From this information the blood flow rate can be estimated by dividing the cardiac output by the total area of vessels of a particular diameter. In principle one could therefore make a reasonable estimate at least for a dog. Sadly, neither the type of dog used, nor the animal's mass, nor its cardiac output appear on these tables, making extrapolation or interpolation to the physiology of man impossible.

A concise table of blood flow rates through some selected vessels in man was found, however, and is reproduced here[21].

Vessel	Radius cm	Mean flow vel. cm/s
Asc. Aorta	1,25	25
Inf.Vena Cava	1,75	12
Arteriole	0,01	1

While the Aorta, Vena Cava and arterioles do not fall into the categories of vessels to be punctured by means of the guide, figures for these vessels provide absolute upper and lower limits

of blood flow velocities likely to be encountered. It should be mentioned that systolic blood flow in the Aorta has been estimated at roughly three times the average flow rate[22]. It should also be remembered that the flow profile is such that higher velocities are obtained in the centre of the vessel than at the walls.

Typical ultrasound frequencies used for blood flow velocimetry are between 5 and 10 MHz. The frequency to be used in the prototype is 9,1MHz. In order to determine the bandwidth of the doppler spectrum, we have to estimate the peak arterial flow. Estimates of peak flow are usually given at around 3 times average flow, which from the table on p25 gives us a peak flow rate of 0,75 m/s in the Aorta. The minimum flow rate would be the average found in the smallest vein to be punctured, or half that in an arteriole (say 5mm/s). If we assume that the beams will impinge on the vessels at around 45°, and using a value for c of 1500m/s (Wells[23]), the Doppler equation (4-1) tells us that the maximum shift in frequency we can expect is

$$\Delta f_{max} = \frac{2u}{c} f \cos\theta$$

$$= \frac{2 \cdot 0,75}{1\ 500} \cdot 9,1 \cdot 10^{6} \cos 45^{\circ}$$

$$= 6\ 400 \text{ Hz}$$

and the minimum

$$\Delta f_{min} = \frac{2 \cdot 0,005}{1\ 500} \cdot 9,1 \cdot 10^{6} \cos 45^{\circ}$$

$$= 43 \text{ Hz}$$

Apart from the very low end of the spectrum, these maximum and minimum values are covered neatly by the audio range. While one can accept that this estimate of the lowest frequency encountered could be considerably lower than we might expect for reasons already discussed, then from the point of view of ensuring inclusion of the smaller veins in the range of vessels to be successfully located, one would hesitate to use carrier frequencies much below 9MHz. In fact it might be desirable to shift the whole spectrum a little higher. However, there are other consideration that have to be taken into account in determining this frequency.

§4.3 RADIATION FROM A TRANSDUCER

Fundamental to the principle on which the needle guide is based, is the ability of ultrasound to be contained in a narrow beam, so that the position of the blood vessel can be determined by the relative positions of the transducers when doppler returns are received. It is therefore important that we have some idea of the shape of the ultrasonic beam produced by the transducer.

The intensity distribution of the ultrasonic beam follows Huygen's principle in that it can be considered to be established by the summation of all the little wavelets arriving at a particular point. Wavelets that are in phase interfere with one another to form intensity peaks, while out of phase wavelets cancel each other.

The intensity distribution along the axis of a circular transducer is given by:[24]

$$I_{\theta_0} = 2\rho_0 c U_0^2 \sin^2(\tfrac{1}{2}k\{\sqrt{r^2+a^2}-r\}) \qquad (4\text{-}6)$$

where $$k = \frac{2\pi}{\lambda} = \frac{\omega}{c} \qquad (4\text{-}7)$$

and is known as the wavelength constant

and
ρ_0 = density of the acoustic medium
c = velocity of sound in the acoustic medium
U_0 = peak velocity at the surface of the transducer
r = distance from the transducer
a = radius of the transducer

Along the axis we therefore get intensity peaks and troughs whenever

$$\tfrac{1}{2}k(\sqrt{r^2+a^2}-r) = \tfrac{1}{2}n\pi \qquad (4\text{-}8)$$

when $n = 1,3,5.....$ we get maxima and
when $n = 2,4,6.....$ we get minima

Substituting for k (eq.4-7) and rearranging we get:

$$\frac{2\pi}{2\lambda}(\sqrt{r^2+a^2}-r) = \tfrac{1}{2}n\pi$$

$$\sqrt{r^2+a^2} = \tfrac{1}{2}n\lambda + r$$

$$r^2+a^2 = (\tfrac{1}{2}n\lambda)^2+r^2+2(\tfrac{1}{2}nr\lambda)$$

$$r(n\lambda) = a^2-(\tfrac{1}{2}n\lambda)^2$$

Hence
$$r = \frac{a^2}{n\lambda} - \frac{n\lambda}{4} \qquad (4\text{-}9)$$

The last trough occurs at $r \simeq \frac{a^2}{2\lambda}$ and the last peak when $r \simeq \frac{a^2}{\lambda}$

This holds for $a>>\lambda$ as is usually the case. The axial intensity can be plotted as follows:[25]

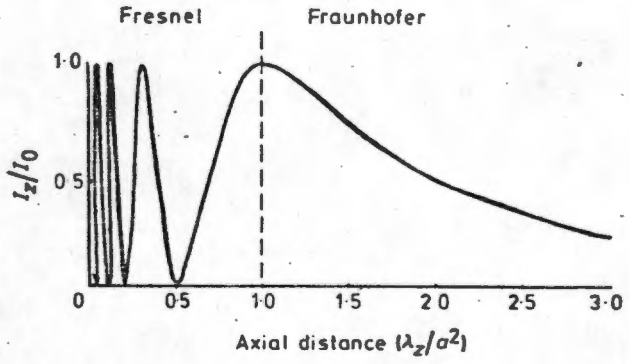

Fig.4-3

Before the last peak in the *near field* region we get Fresnel type diffraction, while in the *far field* region Fraunhofer diffraction takes place.

Off Axis Intensity

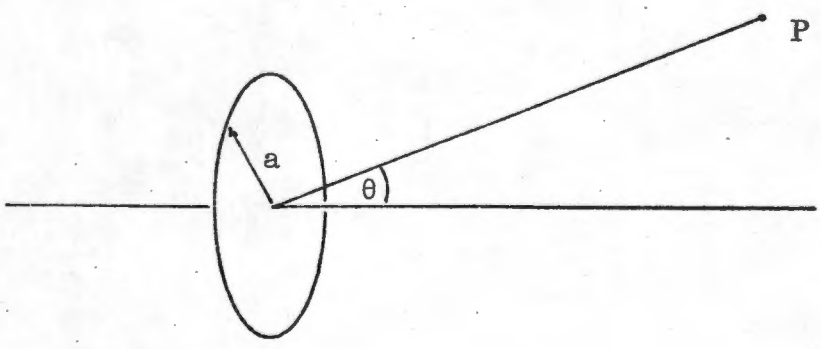

Fig.4-4

In the far field region the intensity distribution is given by:[26]

$$I = \frac{\rho c k^2 U_0^2 \pi^2 a^4}{8\pi^2 r^2} (D^2) \qquad (4\text{-}10)$$

where $$D = \frac{2J_1(ka\ \sin\theta)}{ka\ \sin\theta} \qquad (4\text{-}11)$$

and is called the *Directivity Function.*
J_1 is a first order Bessel function of the first kind and θ is the off axis angle as shown in Fig.4-4.

Apart from the directivity function the expression is the same as the intensity for a simple source in an infinite baffle. The directivity function for a circular piston appears conveniently tabulated in appendix 4-2. Plotting $\frac{2J_1(x)}{x}$ from this table we get:[27]

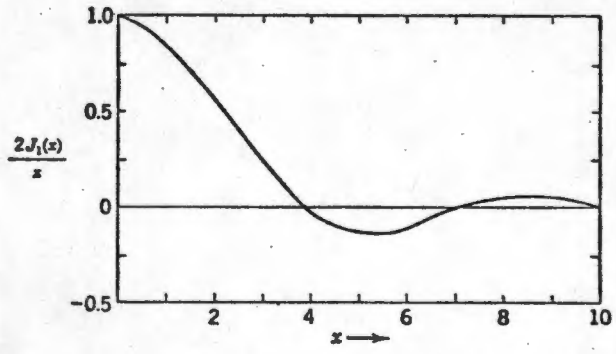

Directivity function for a circular piston.

Fig.4-5

Now, along the axis $\theta = 0$

Therefore $x = ka\ \sin\theta$

$\theta = 0$

and $D = 1$

So intensity $$I_{\theta_0} = \frac{\rho_0 c k^2 a^2 U_0^2}{8r^2} \qquad (4\text{-}12)$$

This shows us that the intensity along the axis in the far field region falls off with the square of the distance from the source.

The intensity at a point on a spherical surface of radius 'r' decreases with increasing θ and becomes zero whenever

$$ka\ \sin\theta = 3{,}83;\ 7{,}02;\ 10{,}15 \text{ etc} \qquad (4\text{-}13)$$

the values being derived from Fig.4-5 or appendix 4-2.

The intensity distribution therefore consists of a central lobe of beam width 2 arc sin(3,83/ka), surrounded by many smaller lobes. If *ka* is larger than 3,83, then there is one major lobe surrounded by minor lobes. The larger *ka* is the more lobes we get and the smaller is the angular width of the major lobe. If *ka* is less than 3,83, then there is no angle that satisfies arc sin(3,83/ka) and only the major lobe exists. It will be remembered that *k* is the wavelength constant and is proportional to frequency.

$$ka = \frac{2\pi}{\lambda} \cdot a$$

The polar radiation patterns of a flat piston are plotted in Fig.4-6 for 3 different frequencies.[27] Log *I* is plotted against θ for:

(a)	$\lambda = 8a$	$(ka = \pi/4)$
(b)	$\lambda = 2a$	$(ka = \pi)$
(c)	$\lambda = a/2$	$(ka = 4\pi)$

Radial distances in this graph are proportional to log *I*.

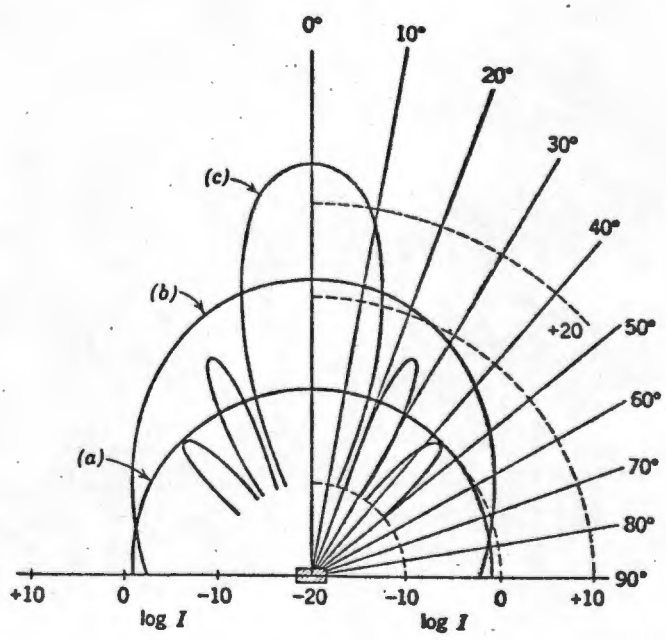

Fig.4-6

Since the first side lobe has a maximum intensity at the first turning point of the directivity function (Fig.4-5; or appendix 4-2) one can readily calculate the intensity of this side lobe relative to that of the major lobe. From the tables, the maximum

was found where: $x = ka \sin\theta_1$

$= 5,0$

i.e.: $\theta_1 = \text{arc sin}(5,0 / ka)$

Also since $|D| = 0,131$ at $x = 5,0$ and since

$$I_{\theta_1} = I_{\theta_0} D^2$$

we have that $I_{\theta_1} = I_{\theta_0} (0,131)^2$

$= 0,0172\ I_{\theta_0}$

Since the side lobes have relatively little power, we need to look at a system with as narrow a major lobe as possible, while the proliferating minor lobes can be ignored. To this end we have to ensure that the wavelength λ is very much smaller than a as was shown above.

Sound Intensity in the Near Field

In the near field the sound intensity pattern is so complex that it is not generally discussed in elementary texts. The field consists of a number of complex rings about the central axis as illustrated in the following diagram:[28]

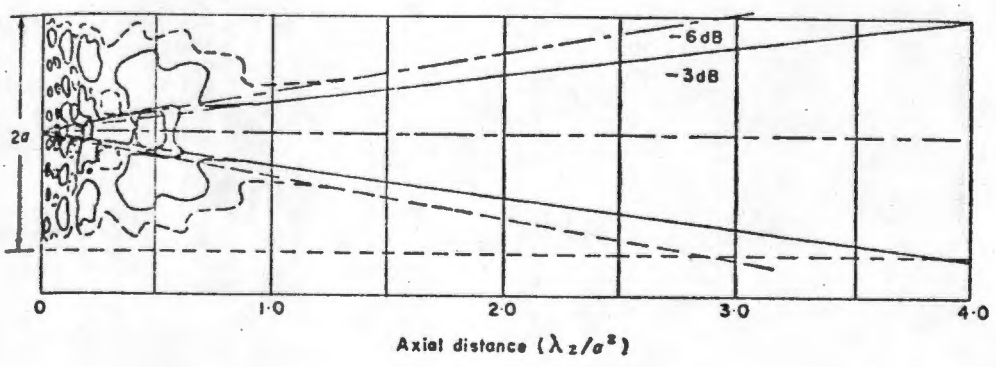

Fig. 4-7

Along the axis the intensity in the near field region is given by equation 4-6. For the sake of completeness we should demonstrate that this reduces to equation 4-12 in the far field region.

$$(r^2+a^2)^{\frac{1}{2}} = r\left[1+\left(\frac{a}{r}\right)^2\right]^{\frac{1}{2}}$$

$$= r\left[1+\tfrac{1}{2}\left(\frac{a}{r}\right)^2 - \frac{1}{2\cdot 4}\left(\frac{a}{r}\right)^4 \ldots\ldots\right]$$

which is simply the Taylor series expansion. For $a<<r$ we can truncate this after the second term. Therefore from eq.6

$$I_{\theta_0} = 2\rho_0 c U_0^2 \sin^2 \tfrac{1}{2}k\left(r+\tfrac{1}{2}\frac{a^2}{r}-r\right)$$

and since in general we have that for small θ, $\sin\theta = \theta$

$$I_{\theta_0} = 2\rho_0 c U_0^2 \left[\tfrac{1}{2}k\cdot\tfrac{1}{2}\frac{a^2}{r}\right]^2$$

$$= \frac{\rho_0 c U_0^2 k^2 a^4}{8r^2} \qquad \text{Q.E.D.}$$

In the near field region, the radiated sound may be thought of as being confined within a cylinder of radius a.[29]

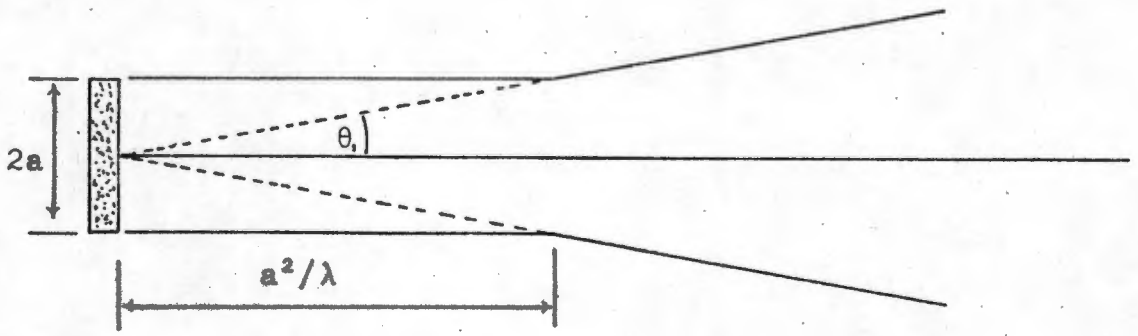

Fig. 4-8

Divergence beyond this depends on the directivity function. Beamwidth could be defined as the angle containing the major lobe and therefore twice the angle at which the intensity first is zero. From eq. 4-13 we have that:

$$\theta_1 = \text{arc sin}(3{,}83/ka)$$

therefore *beam width* $= 2\theta_1$

$$= 2\,\text{arc sin}(0{,}61\lambda/a)$$

Since, however, the intensity is never in practice measured to be zero, definition of the angular beam width is somewhat arbitrary and has not been standardized.

It should also be pointed out here that the equations derived above are based on a piston radiating from a point on an infinite baffle, which is never the case in practice. The discussion is therefore somewhat idealized.

A great deal of importance is attached to the radiation pattern of the transducer which is to be used. The polar radiation pattern could give some insight into the directivity of the instrument, which is of fundamental importance in the needle guide. It has been plotted as follows:

The average intensity transmitted by the crystal into the medium is given by:

$$I' = \frac{\text{Power}}{\text{Area}}$$

$$= \frac{\text{Mean square vel. of face} \times \text{Acoust. impedance}}{\text{Area of Transducer}}$$

by analogy with electric circuit theory.

$$I' = \tfrac{1}{2}U_0^2(\rho cA) \times \frac{1}{A} \qquad (4\text{-}14)$$

where ρc is the *specific* acoustic impedance and must be multiplied by the area of the transducer to give the *acoustic impedance*. Hence, from equation 4-10 we have:

$$\frac{I}{I'} = \left(\frac{2\pi}{\lambda}\right)^2 \frac{a^4}{4r^2} \times D^2 \qquad (4\text{-}15)$$

where D is again the directivity factor.
The iso-intensity lines where $I/I' = \alpha$ are given by

$$r = \frac{2\pi}{\lambda} \times \frac{a^2}{2} \times \frac{D}{\sqrt{\alpha}} \qquad (4\text{-}16)$$

In the table of appendix 4-2, $D = \frac{2J_1(x)}{x}$ is given for various x. Since

$$x = ka \sin\theta$$

$$\theta = \text{arc sin}(x/ka)$$

Thus we can plot $r(\theta)$ from equation 4-16. This was done using

a computer program shown in appendix 4-3.

Values of a and λ for the transducers used in the prototype were chosen as follows:

a Was made as small as possible, but not that small that it became unmanageable to handle. It was felt that a transducer with a 1mm radius was about as small as could comfortably be handled in a prototype. A factor that still had to be considered was that the crystal had to have wires soldered onto its faces. The amount of space these take up has to be small relative to the area of the transducer so that the sound field pattern and resonance of the transducer are not disturbed too much. The crystal had to be small since the smaller the cross sectional area of the beam becomes, the more likely it is that small diameter blood vessels can be isolated. Although the sound field was to have a diameter in the order of 2mm, it was still thought possible that 1mm vessels could be located, since the peak intensity of the beam was to be found along the central axis (as is indeed well illustrated in the field plots (Fig.4-9).

A frequency of 9,1MHz was chosen (to be discussed later). The average speed of propagation of ultrasound in tissue is around 1500m/s [30] and thus the wavelength is

$$\lambda = c/f$$

$$= \frac{1500}{9,1\times10^{6}}$$

$$= 0,165\text{mm} \qquad (\text{i.e.: } a > \lambda)$$

What is very interesting about the plots in Fig.4-9, is the insignificance of the side lobes and the excellent directivity one should be able to obtain because of the high axial intensity. The picture indicates very clearly that any misalignment of the beam relative to even a minute target, should be readily detectable as a drop in intensity. In principle one should therefore be able to locate blood vessels much smaller than the diameter of the transducer, especially in the far field.

What we have not taken into account, however, is the scattering of ultrasound by the tissue which is likely to smudge these curves.

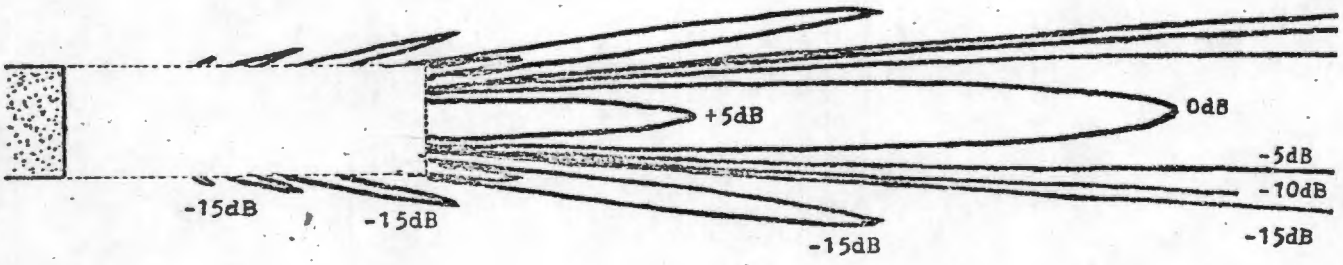

f = 9,1 MHz
a = 1 mm
a^2/λ = 6 mm
ak = 38

Fig.4-9a

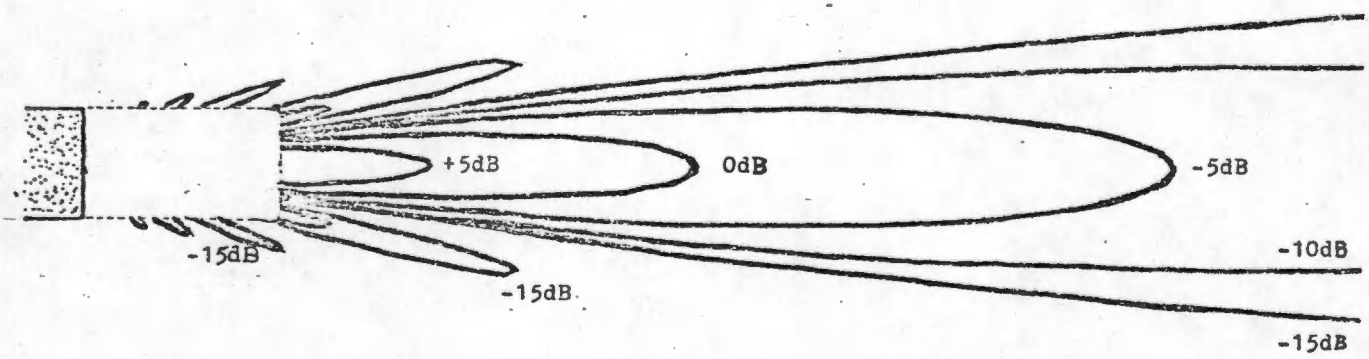

f = 5 MHz
a = 1 mm
a^2/λ = 3,3 mm
ak = 21

Fig.4-9b

A 5MHz field is plotted in Fig.4-9b. to illustrate the effect of frequency. The high frequency field has a longer near field region and improved directivity with which we associate higher concentrations of energy along the axis.

While these results hold for a circular transducer, the transducers that were eventually used were 2 × 2,5mm rectangular ones, since this is easier to cut. It should also be said that the circular transducers are generally used in pulse-echo systems, while those in CWDU systems are rectangular [31]. The rectangular transducer is more difficult to analyse, but the results correspond closely. The near field region of a rectangular transducer is mathematically even more complex than that of a circular one, although the inhomogeneities are less marked. The near field also extends slightly further [32].

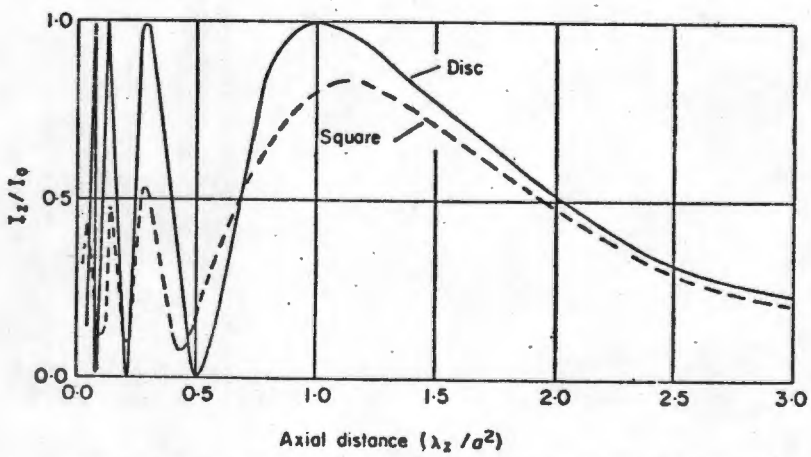

Computed amplitude contours in the plane of the central axis of a plane disc transducer ($a/\lambda = 5{\cdot}0$) and a plane square transducer $1/2\lambda = 5{\cdot}0$). (Data of Stenzel, 1952.)

Fig. 4-10

§4.4 RECIPROCITY

Assuming that the transmitting crystal transmits a beam as discussed above, how does the receiving crystal respond to signals arriving from different regions in the acoustic medium? Is there a directivity function associated with the receiving crystal? These questions are answered by the general acoustic reciprocity theorem first stated by Rayleigh. The mathematical statement of the theorem is not important to us, but its application is. Using the theorem it can be shown [33] "*that the directivity pattern of a rigid plane piston acting as a radiator of sound, is identical with its receiving pattern when it is acting as the diaphragm of a microphone.*" This very important result verifies our initial assumption that vessel identification could be effected by two directional beams, i.e.: a transmitted ultrasound beam and a received "beam".

§4.5 ATTENUATION AND BACKSCATTER

To establish rigorous design parameters of a doppler ultrasound system, one needs to know what fraction of the transmitted signal can be expected to be returned to the receiving crystal. Both attenuation and backscatter are very complex subjects and are not fully understood. In fact Shung[34] commented in 1976: "The properties of scattering in biological tissues, unfortunately, are virtually unknown. This is true even in the case of blood, despite the fact that the operation of Ultrasonic flowmeters in cardiology and blood flow studies depends directly on the scattering properties of red blood cells."

In the final analysis it is debatable whether it is entirely necessary in a project such as this to discuss these details. It is not the purpose of this project to re-invent doppler ultrasound velocimetry,nor indeed to improve on it. Having established the all-important properties of the ultrasonic beam, it now remains to harness this technology. Because of all the variables, it was decided to develop the electronic circuit in such a way that the gain could be set experimentally at the various stages. Discussion on attenuation and backscatter will therefore be very limited.

Attenuation of ultrasound in a medium is due to absorption (with corresponding conversion into heat) and scatter. Figures for attenuation in ultrasound in biological materials are not well established[35] but the following graph[36] summarizes information that has been gathered from a large number of sources. The coefficient

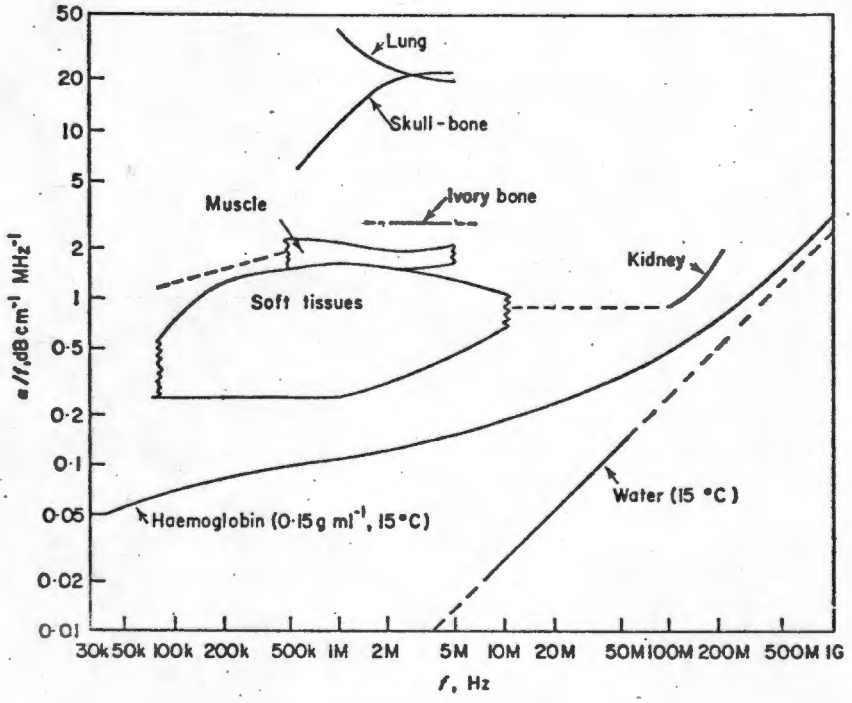

Fig.4-11

of attenuation α has been plotted as α/f vs. f. Attenuation is approximately proportional to frequency.

Tissue to be punctured could fall into the general category of "soft", although in practice it is not uniformly so. From Fig.4-11 α/f for soft tissue is in the order of 1dB/cm/MHz, but this can be expected to vary considerably from one puncture site to another. This figure may also be a little low for muscle.

Scatter by blood, while forming one component of attenuation, is also fundamental to the whole concept of ultrasonic blood flow velocimetry and detection. It has been verified that only the erythrocytes in the blood contribute to scattering[37]. Investigations into scattering by blood are not common, largely because of difficulties in measuring the very weak returned signals which in the case of whole blood are at least 70 dB below those reflected

from a stainless steel plane surface[37].

Some interesting work on this subject was done by Shung[34]. He showed that the scattering coefficient of blood was a parabolic function of Haematocrit (Fig. 4-12.) He also measured the backscatter as a function of frequency and verified that it was proportional to the fourth power of frequency (Fig.4-13). This confirmed the theory of Lord Rayleigh on scattering from particles whose diameter is very much smaller than the wavelength.

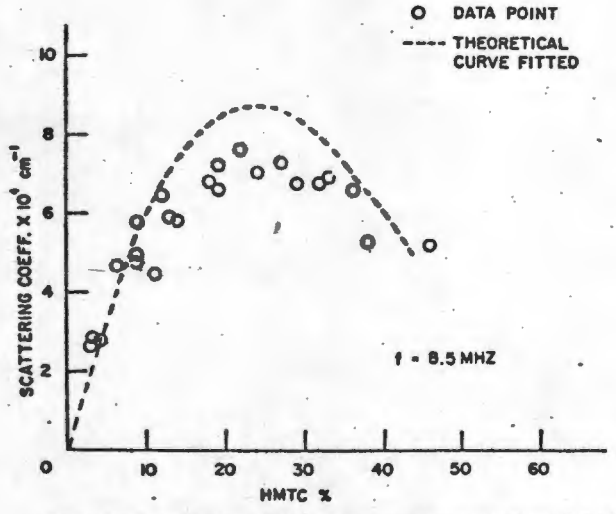

Scattering coefficient is plotted versus hematocrit at 8.5 MHz.

Fig.4-12 [34]

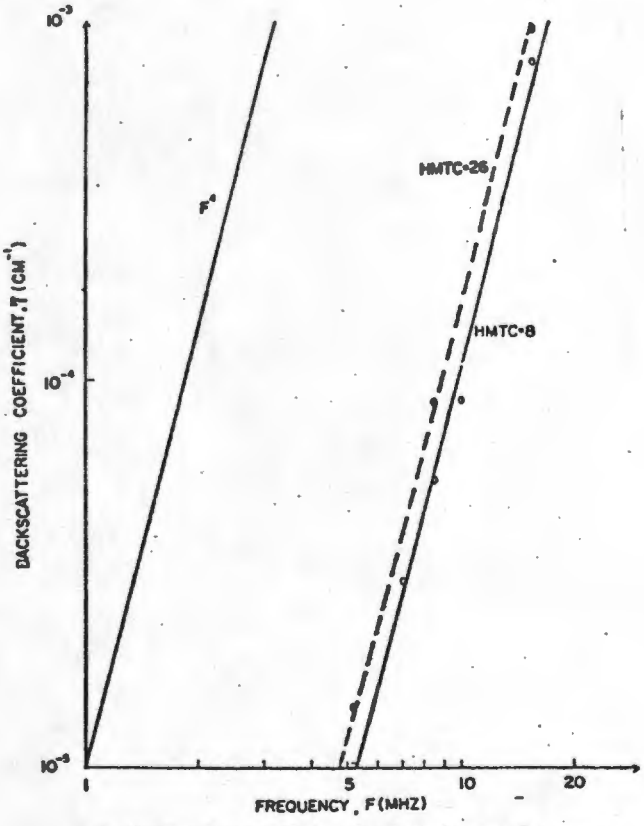

Backscattering coefficient is plotted versus frequency.

Fig.4-13 [34]

Morse and Ingard[37] derived a sound scattering formula which showed that for these small particles the scattering depends on the adiabatic compressibility and density of the particles relative to that of the imbedded medium. There is, in fact, a difference of 7% in density and 17% in compressibility between plasma and erythrocytes. Ahuja elaborated on this formula by including a term which took into account the viscous nature of the particle in a frictional medium. Both theories were tested by Shung experimentally. The results are plotted in Fig.4-14.

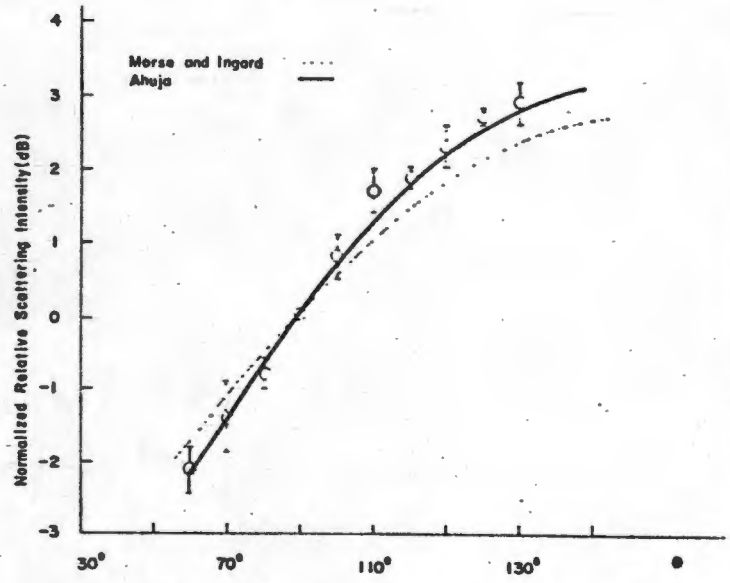

Measured angular scattering intensity normalized with respect to I (90°) was plotted along with theoretical predictions. Dashed line shows the theoretical curve based on the formula of Morse and Ingard. Solid line is the theoretical curve based on the formula of Ahuja.

Fig.4-14 [37]

This curve is relevant to us in as much as it gives some indication of the directionality of the back-scattered signal. Since the relevant formulae describe the situation of blood flowing in a cylinder immersed in a tank of water, and since this situation is very different from that of blood vessels buried in animal tissue, these formulae are of little real value to us. They do provide insight into the mechanism of scattering, but because of their complexity they do not warrant treatment here.

§4.6 SIGNAL TO NOISE OPTIMIZATION

Since absorption is a linear function of frequency, and backscatter varies according to the fourth power of frequency, there is presumably some point at which a system will operate under optimal signal to noise conditions. McLeod[38] formulated such a relationship. He determined that:

$$\frac{S}{N} \propto \frac{V_v}{V_B} \frac{\sigma\, e^{-2\alpha R}}{R^2 \eta (BW)} P_a \qquad (4\text{-}17)$$

where $\sigma = \sigma(f^4)$ is the scattering cross section of blood.

$\alpha = \alpha(f)$ is the tissue absorption coefficient.

R is the depth of the scatterer.

P_a is the average emission power.

V_v is the volume of vessel lumen falling within sound beam.

V_B is volume of sound beam within boundary set by system noise threshold.

BW = BW(f) is the system bandwidth dictated by maximum doppler shift.

η is the electronic noise component.

f is the operating frequency

If only the frequency terms are included, we can rewrite this equation as:

$$\frac{S}{N} \propto \frac{f^4}{fR^2} e^{-2\alpha fR} \qquad (4\text{-}18)$$

In order to optimise the signal to noise ratio, we differentiate eq.4-18 and set the result equal to zero.

$$\frac{d}{df}\left(\frac{f^3}{R^2} e^{-2\alpha fR}\right) = \frac{3f^2}{R^2} e^{-2\alpha fR} + \frac{f^3}{R^2}(-2\alpha R)e^{-2\alpha fR}$$

$$= 0$$

$$\text{hence} \qquad f = \frac{3}{2\alpha R} \qquad (4\text{-}19)$$

Now the attenuation, γ, is customarily given in dB/cm/MHz, while α defines the power ratio[39]

$$\frac{A_R}{A_o} = e^{-\alpha R}$$

$$\text{When R= 1} \qquad \gamma = -10\log \frac{A_1}{A_0}$$

$$= -10\log e^{-\alpha}$$

$$= 10\alpha \log e$$

$$\alpha = \frac{\gamma}{10\log e} \qquad (4\text{-}20)$$

Substituting eq.4-20 into eq 4-19 we get

$$f = \frac{15 \log e}{R\gamma}$$

$$= \frac{41}{R\gamma} \qquad (4\text{-}21)$$

Fig.4-15 shows the range of frequencies considered optimal by McLeod, Reid and Gill[40]. Equation 4-21 is plotted for muscle

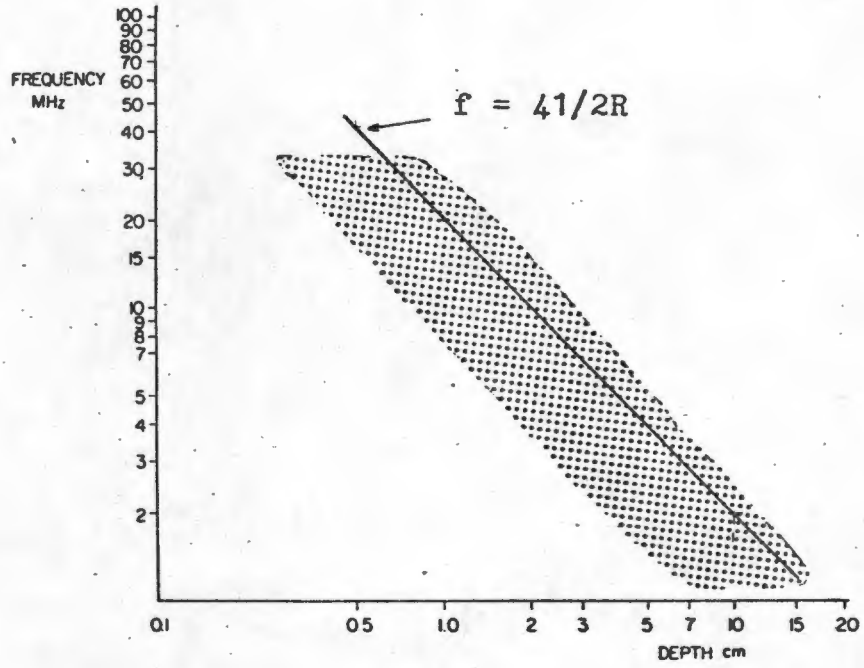

Calculations from several laboratories to determine the optimal frequency for maximum signal-to-noise ratio versus depth all fall within the dotted area. The precise value is influenced by a number of complex trade-offs concerning the design of specific instruments. New instrument developments will probably lead to improved signal-to-noise ratios at greater depths..

Fig.4-15

(γ = 2dB/cm/MHz) on the same axes in Fig.4-15.

There are factors other than signal to noise ratio which play a role in deciding on a particular frequency. For example, in our case a narrow pencil beam is required, which in turn necessitates a small transducer. In order to ensure that the beam does not diverge, one needs to keep ak large, i.e.: the frequency high. Then there are practical considerations in prototyping such as difficulties in working with high frequencies and the availability of transducers.

Transducer material is virtually impossible to obtain in South Africa, but two crystals were found in our stores, one with a 9,1MHz series resonance frequency and the other resonating at 5MHz. Since most of the work was expected to be done at short ranges from 5 to 10 mm, with only occasional Subclavian punctures at 40mm, the 9,1 MHz crystals were chosen. This turns out to be a good compromise frequency. It was also interesting to learn that doctors at the Vascular Laboratory (Deep Vein Thrombosis Clinic),

who routinely use doppler ultrasound in assessing vascular disfunctioning, prefer working with the 9MHz probes. All subsequent design work was therefore confined to 9,1 MHz operation.

While some investigation was done into the theory surrounding reflected waves, it soon became clear that a more heuristic approach was necessary. Rigorous design formulae have not been developed, and the theory is insufficiently known to allow for a formal design procedure. Since this project is primarily concerned with the *application* of ultrasound technology, and since resources are limited, this approach is felt to be justified.

The characteristics of a typical CWDU device will be examined in chapter 5, and the design of the electronic system will be based on that.

§4.7 PIEZOELECTRIC TRANSDUCERS

The piezoelectric (PE) effect is exhibited by materials that undergo a change in their physical dimensions when an electric field is applied across them. Conversely, these materials generate an electric field of their own when subjected to mechanical stress.

PE materials are anisotropic, i.e.: their crystal structures have no centres of symmetry. There are several naturally occuring PE materials, but the most popular ones at the moment are the synthetic ferroelectrics of which the ceramics form an important group. They are made in much the same way as insulating ceramics. They can be grown to any size and shape, and they are chemically inert, immune to humidity and mechanically hard. During manufacture various chemicals can be added to enhance one or more of the properties depending on the application.

The ceramics are only anisotropic below the Curie temperature. They are cooled through the Curie temperature in the presence of a strong electric field which lines up all the small electric dipoles. They are called ferroelectric by analogy with the manufacturing process of ferromagnetic materials.

When the material is stressed below the Curie temperature, the net dipole moment of the crystal is changed. This is a linear and

reversible process. Similarly if an electric field is applied across the crystal it either elongates and narrows or shortens and widens depending on the direction of the field w.r.t. the poling axis.

As has already been discussed, two transducers are to be used in the instrument, one being a transmitter and the other a receiver of ultrasound. Both must be connected to electronic circuits, and therefore their electrical characteristics must be known. It turns out that their electrical properties are largely dictated by their mechanical behaviour, which in turn is a function of the transducer material, dimensions of the crystals, method of mounting and acoustic impedance of the material into which they transmit energy.

The following section deals with the electromechanical relationships of the transducers so that their electrical characteristics can be determined. It will be demonstrated that the crystals can be represented by equivalent electrical circuits and that values of the various components can be determined. In this way, for example, a relationship between driving voltage and output power can be obtained.

Piezoelectric Relations

There are two electrical and two mechanical variables associated with PE materials. These are related to one another by a number of interdependent PE constants. These variables are as follows:

E = Electric Field (volts/length)
D = Dielectric Displacement (charge/area)
S = Strain $(\Delta \ell / \ell_0)$
T = Stress (force/area)

Consider a crystal subjected to a compressive stress T. The open circuit voltage and hence field strength E is proportional to this stress and is related to it by the PE voltage constant g:

$$E = -gT \qquad (4\text{-}22)$$

We also know that for an unstressed dielectric material placed in an electric field E, the field strength and dielectric displacement D are related by the permittivity ε of the material. Thus:

$$D = \varepsilon E \tag{4-23}$$

or

$$E = D/\varepsilon \tag{4-24}$$

Piezoelectricity involves the interaction between the electrical and mechanical variables. Thus from equations 4-22 and 4-24 we have the total electric field E given by:

$$E = -gT + \frac{1}{\varepsilon}D$$

Similarly for electro-mechanical conversion, the strain of an unstressed material resulting from the application of an electric field E is given by:

$$S = dE \tag{4-25}$$

where d is the piezoelectric charge constant. Again, in the absence of an electric field the strain resulting from applied stress T is given by

$$S = sT$$

where s is the compliance of the material. Thus the total strain in a piezoelectric element is given by the sum of these two components:

$$S = sT + dE$$

The choice of independent variables is arbitrary, provided one is mechanical and one is electrical. The following list is a summary of all these relations: [41]

$$S = s^{E}T + dE \tag{4-26}$$

$$D = dT + E\varepsilon^{T} \tag{4-27}$$

$$E = -gT + D/\varepsilon^{T} \tag{4-28}$$

$$S = s^{D}T + gD \tag{4-29}$$

$$E = -hS + D/\varepsilon^{S} \tag{4-30}$$

$$T = c^{D}S - hD \tag{4-31}$$

$$D = eS + \varepsilon^{S}E \tag{4-32}$$

$$T = c^{E}S - eE \tag{4-33}$$

In each case the superscript refers to the variable being held constant when the particular PE constant is defined. The piezoelectric constants are summarized in the following list:

s = specific elastic compliance (strain to stress ratio)
ε = permittivity of the material
d = PE charge constant
g = PE voltage constant
c = elastic stiffness
h,e = piezoelectric stress constants

Piezoelectric transducers are operated in one of two classes, either resonant or non-resonant. Non-resonant applications of PE materials include phonograph pickups, microphones and loudspeaker elements.[42] But the most important category covers the PE resonators.

Another constant which should be mentioned because of its importance is the coupling coefficient k, which may be considered to be the square root of the ratio of electrical (mechanical) work which can be done under ideal conditions to the total energy stored from a mechanical (electrical) source below resonance.[43] It is not an efficiency, since dissipative mechanisms are not taken into account, and unconverted energy can be recovered.[44] Efficiency is defined as the usefully converted power to the input power. Properly tuned & matched PE transducers operating at resonance can achieve efficiencies of over 90%. If they are unmatched or operate at low frequencies, the efficiency is very low.[45]

The PE constants depend on the directions of the applied electric field, dielectric displacement, stress and strain. For piezoelectric ceramics the poling axis is taken to be in the z-direction. Since the materials have symmetry about the poling axis, the sense of x and y is not important. Directions x, y and z are represented respectively by 1, 2 and 3, while shear about these axes is represented by 4, 5 and 6 respectively.

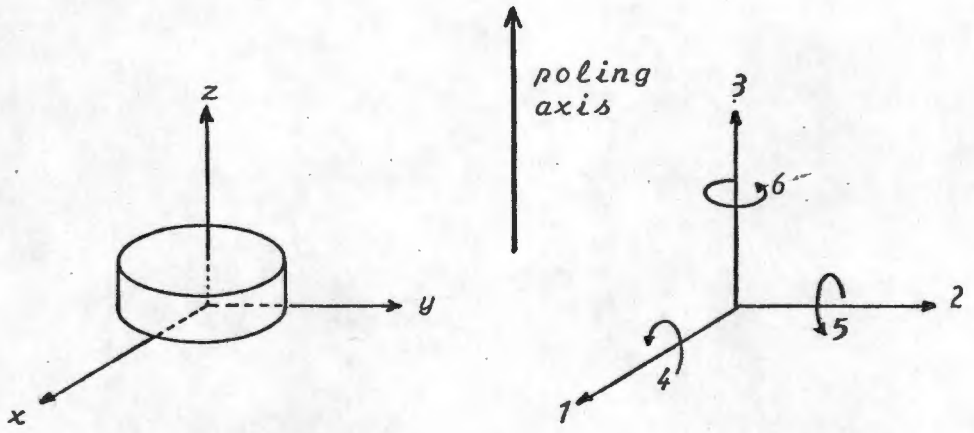

Fig.4-16

Piezoelectric constants are associated with two subscripts relating to their direction dependence. For example, s_{13} is the compliance of a crystal when the strain is measured in the 1 or x direction and the stress is applied in the 3 or z direction. The following table lists the direction dependence of these constants.[46]

	Direction of:			
	E	D	T	S
ε_{ij}	j	i		
s_{ij}			j	i
d_{ij}	i	i	j	j
g_{ij}	i	i	j	j
h_{ij}	i	i	j	j

From this table and from equations 4-26 to 4-33 it is clear that d,g and h can be defined in two different ways.

Equivalent Electric Circuit [47]

Since the transducer has to be coupled to an electronic circuit, it is useful to transform the mechanical behaviour of the transducer into an equivalent electrical circuit. This can be done using the principles of wave mechanics, electric circuit theory and the piezoelectric relations.

Consider the following mass-spring representation of the PE transducer.

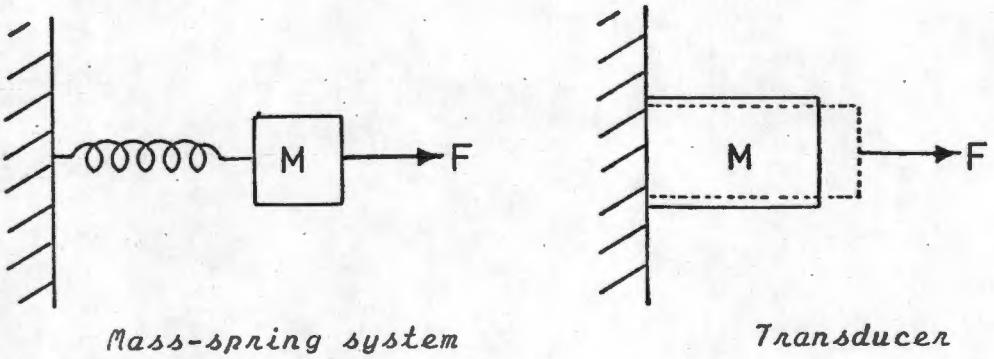

Mass-spring system *Transducer*

Fig.4-17

From Hooke's and Newton's laws it can be shown that the equation of motion of the system is:

$$F = M \frac{d^2x}{dt^2} + R_m \frac{dx}{dt} + \frac{1}{C_m} x \qquad (4\text{-}34)$$

where the R_m term has been included to account for damping due to friction and:

M = mass of the system

C_m = compliance of the spring

x = displacement

F = force applied to the system

This equation has the same form as that describing the charge flowing through an RLC circuit, with which we are perhaps more familiar.

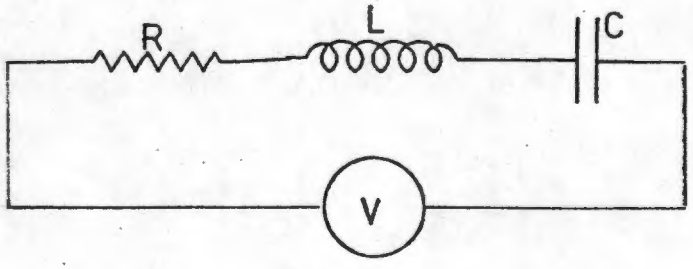

Fig.4-18

$$V = L \frac{d^2q}{dt^2} + R \frac{dq}{dt} + \frac{1}{C} q \qquad (4\text{-}35)$$

By analogy with the well-known solution to the electrical circuit equation, the solution to the equation describing the mass-spring

system is:

$$u = \frac{dx}{dt} = \frac{F}{z_m} \tag{4-36}$$

where $$z_m = R_m + j\left(\omega M - \frac{1}{\omega C_m}\right) \tag{4-37}$$

z_m Is the mechanical impedance and u the velocity of the mass. At resonance the two reactive components cancel and

$$\omega_r = \frac{1}{\sqrt{MC_m}} \tag{4-38}$$

These results will be used a little later.

Now, if the two electrodes on the transducer are short-circuited, then the applied electric field is zero and equations 4-26 and 4-27 reduce to:

$$S = s^E T \tag{4-39}$$

and $$D = dT \tag{4-40}$$

From equation 4-32 we have:

$$D = eS \tag{4-41}$$

If we substitute for S from equation 4-26 we get

$$D = e(s^E T)$$

hence $$\frac{D}{T} = es^E$$

From equation 4-27 we have

$$d = \frac{D}{T}$$

hence $$e = \frac{d}{s^E} \tag{4-42}$$

This result will also be used later.

Consider once again a transducer undergoing a strain S:

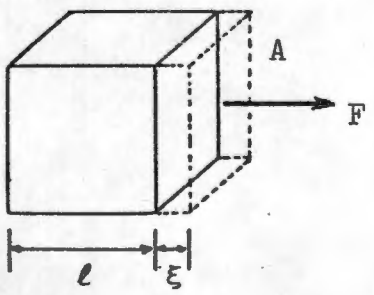

$$S = \frac{\xi}{\ell}$$

The velocity of the face is

$$u = \frac{d\xi}{dt} = \ell\frac{dS}{dt}$$

The current flowing through the device on short circuit is:

$$i = \frac{dQ}{dt}$$

$$= A \frac{dD}{dt}$$

and from equation 4-41

$$\frac{dD}{dt} = e\frac{dS}{dt}$$

hence $$i = \frac{Ae}{\ell} u$$

$$i = \alpha_T u \qquad (4\text{-}43)$$

where $$\boxed{\alpha_T = \frac{Ae}{\ell}} \qquad (4\text{-}44)$$

and is known as the transformation ratio.

When the crystal is clamped the strain S = 0 and the stress is compressive, i.e.: negative. Hence equation 4-26 becomes:

$$S = -Ts^E + dE = 0$$

$$T = \frac{d}{s^E} E$$

and from equation 4-42 we have

$$T = eE$$

i.e.: $$\frac{F}{A} = e\frac{V}{\ell}$$

hence $$F = \frac{Ae}{\ell} V$$

$$= \alpha_T V \qquad (4\text{-}45)$$

From equation 4-36 we had

$$u = \frac{F}{z_m}$$

$$= \frac{\alpha_T V}{z_m}$$

so $$z_m = \frac{\alpha_T V}{u} \qquad (4\text{-}46)$$

The equivalent electrical impedance looking into the crystal is

$$z = V/i = \frac{V}{\alpha_T u}$$

Hence $$z = \frac{z_m}{\alpha_T^2} \tag{4-47}$$

Hence the equivalent electric circuit elements are:

$$\boxed{1/C = 1/C_m\alpha_T^2} \tag{4-48}$$

$$\boxed{R = R_m/\alpha_T^2} \tag{4-49}$$

$$\boxed{L = M/\alpha_T^2} \tag{4-50}$$

The next step is to determine R_m, C_m and M in terms of known quantities.

The boundary conditions for the solution of differential equation 4-34 were set with one face of the transducer fixed. Under these conditions we can show from wave mechanics that at resonance the thickness ℓ of the crystal is equal to $\lambda/4$ where λ is the wavelength of sound in the crystal.[48]

From wave mechanics it can be shown that[49]

$$c^2 = \frac{1}{s\,\rho} \tag{4-51}$$

where c = wave velocity in the transducer material
ρ = density of the transducer material
s = specific elastic compliance (1/mod.of elast.)

The resonant frequency is

$$f_r = c/\lambda_r = \frac{1}{4\ell\sqrt{s\rho}} \tag{4-52}$$

and equating this to equation 4-38 we have

$$\frac{1}{2\pi\sqrt{MC_m}} = \frac{1}{4\ell\sqrt{s\rho}} \tag{4-53}$$

Now $$M = \rho A \ell \tag{4-54}$$

Hence $$C_m = \frac{4s\ell}{\pi^2 A} \tag{4-55}$$

To achieve this in practice the transducer has to be backed by an identical transducer whose free surface radiates into an identical acoustic load or into a load whose characteristic impedance is

negligible, such as air. This is thus effectively an air backed half wavelength transducer. Since the effective thickness t, i.e.: the thickness for which these equations hold is half the actual thickness of the transducer we have that:

$$\boxed{M = \tfrac{1}{2}\rho A t} \qquad (4\text{-}56)$$

$$\boxed{C_m = \frac{2st}{\pi^2 A}} \qquad (4\text{-}57)$$

The *specific* acoustic impedance is also derived from wave mechanics and is given by:[50]

$$Z_m = \rho' c' \qquad (4\text{-}58)$$

where ρ' = density of the acoustic medium

c' = velocity of sound in the acoustic medium

The acoustic resistance is given by

$$R_m = Z_m A$$

$$\boxed{R_m = \rho' c' A} \qquad (4\text{-}59)$$

At resonance the impedance of the medium to the transducer is given by

$$z_m = R_m$$

i.e.: z_m is entirely real. Hence the power delivered to the load is given by:

$$W = V^2/R$$

$$= \frac{\alpha_T^2}{R_m} V^2$$

Hence $$\boxed{W = \frac{\alpha_T^2 V^2}{\rho' c' A}} \qquad (4\text{-}60)$$

and intensity $$\boxed{I = \frac{\alpha_T^2 V^2}{\rho' c' A^2}} \qquad (4\text{-}61)$$

Apart from the mechanical components that have been transformed into electrical terms through the transformation factor α_T, the transducer also has two electrical components. These are the very important capacitance between the plates of the electrodes C_o and

the parallel resistance R_o representing the dielectric losses. This quantity is usually omitted since R_o is relatively large and therefore plays an insignificant role. The capaciatance on the other hand, plays a very major role in the behaviour of the transducer and usually turns out to be very much larger than the equivalent capacitance transformed from the compliance. The value of C_o as for any parallel plate capacitor is simply

$$C_o = \frac{\varepsilon A}{t} \qquad (4\text{-}62)$$

The full equivalent electric circuit for the transducer is given in Fig. 4-19.

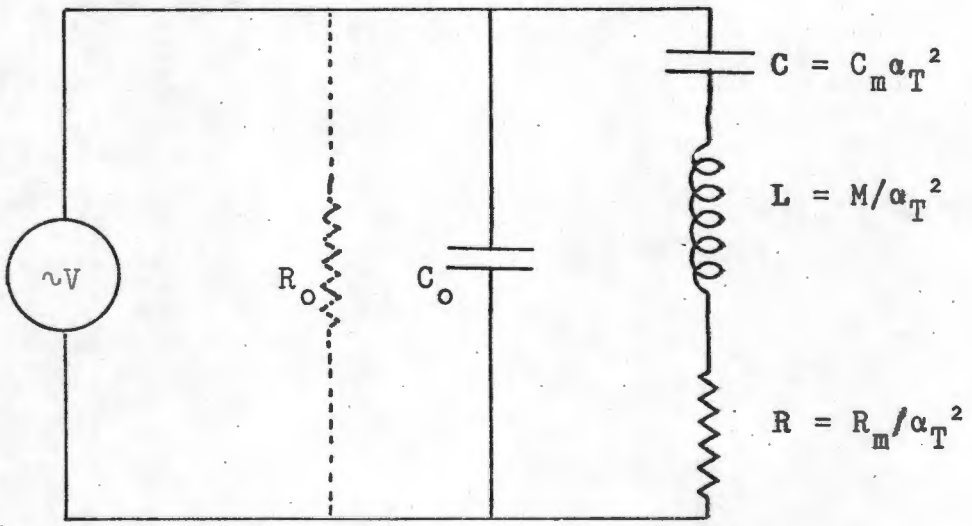

Fig. 4-19

From this circuit it can be seen that two resonant circuits exist. Mechanical resonance is determined by C_m, M and R_m and is responsible for a minimum impedance at the series resonance frequency, while the parallel resonance of C_o with the mechanical impedance produces an impedance maximum. For our application the transducer is operated at the half-wavelength series resonance frequency so that the driving circuit sees a pure resistance in parallel with C_o. An inductance can then be added in parallel or in series with the crystal to tune out C_o.

Selection of a transducer material

Perhaps the most popular modern transducer material is Lead Zirconate Titanate which is marketed under different codes by several manufacturers. PZT is the trade mark of a British manufacturer, LTZ is that of an American company while Philips produces the PXE range. Producers seem to specify those PE constants they consider important. Comprehensive tables are given by Don Belincourt[51] for the PZT materials. They do not correspond exactly with those of the PXE range, although there is some general correlation. The electrical capacitance C_o, for example, was found to be four times higher for a 2×2,5mm PXE5 crystal resonating at 9 MHz than for a similar crystal made of LTZ material.

Initial tests were carried out with 9MHz LTZ5 material found in the laboratory. Subsequently a Philips publication describing the PXE range of materials was found and some PXE5 discs, 0,2mm thick were ordered from Philips in Switzerland. Philips crystals are ordered not according to their frequency, but rather in sheets of a specified thickness. Knowing that we want a series resonant frequency of 9,0 MHz (the same as was used in the initial trials) the thickness of the transducer is calculated from the velocity of ultrasound in the crystal. From equation 4-51:

$$c = \frac{1}{\sqrt{s\rho}}$$

Since both stress and strain are in the 3-direction,

$$c_3 = \frac{1}{\sqrt{s_{33}\rho}}$$

The thickness of the crystal t is:

$$t = \tfrac{1}{2}\lambda$$

$$= \tfrac{1}{2}(c_3/f)$$

$$= \tfrac{1}{2}\cdot\frac{1}{f}\cdot\frac{1}{\sqrt{s_{33}\rho}}$$

Appendix 4-4 contains a list of PXE materials together with their piezoelectric constants. For PXE 5 we have:

$$s^E_{33} = 18{,}9 \times 10^{-12}\ \mathrm{m^2/N}$$

$$\rho = 7{,}6 \times 10^{3}\ \mathrm{kg/m^3}$$

Hence at 9,0MHz $t = 0{,}147$ mm

At the time the crystals were ordered there was still some uncertainty about the relationship between crystal frequency and thickness, since the obvious constant c_3 is not given in the Philips tables. Although 0,2mm crystals were ordered erroneously, numerous laboratory tests on these crystals indicated that a 0,2 mm crystal has a series resonance frequency of 9,1 MHz. It was explained later[52] that when the crystal is coated with a silver electrode, the silver diffuses into the ceramic material reducing the effective thickness of the crystal and therefore increasing the resonant frequency. One would imagine that such an electrode system (which was found to make the crystal 10% thicker) would in any case influence the theory developed in this chapter.

The Philips crystals were tried and proved to be much less successful than the LTZ crystals. So a fresh look was taken at the differences between the various types of PXE material in an attempt to find a more suitable one.

PZT4 and PZT5 are the materials commonly quoted in medical ultrasonics textbooks and seem to be the most readily available. Philips manufactures a PXE41 which appeared to be an improved version of PXE4. PXE41 has a very high mechanical Q of 1000, making it more suitable for narrow bandwidth applications such as CWDU, since the detector is then more sensitive. PXE5 has a low Q of about 80, making it suitable for pulsed applications where a wide bandwidth is necessary. PXE 41 also has a much lower permittivity in the 33-direction, thus reducing the capacitative loading. It has a lower dielectric loss factor and a marginally higher receiving constant. It would therefore seem that PXE41 is a good choice for a CWDU instrument.

More crystals were ordered from Switzerland, but this time the order was for PXE41. The order caused the supplier some consternation It would appear that PXE41 cannot be manufactured in such thin sheets because of its brittleness. In fact, the only material available in this thickness is PXE5.

There is a valuable lesson here. On retrospect I should have stuck more rigorously to the "cut and try" approach and left the rather

complicated theory to the physicists. Ultimately the original LTZ material was used in spite of the fact that there were no specifications available for it.

The transducer material was mounted on a small block of chip-board with shellac. It was then cut into 2×2,5mm² rectangles with a 0,3mm thick diamond saw at a very slow speed. Two of these were removed with spirits and then clamped in a heat sink. A 38 gauge wire was soldered to each surface. Great care has to be taken not to get too much solder onto the surface and to keep the soldered area as small as possible so that the resonance characteristics and the ultrasonic field are not unduly compromised. Care also has to be taken not to prolong the procedure unnecessarily or to overheat the area, since the silver electrode dissolves readily in the solder.

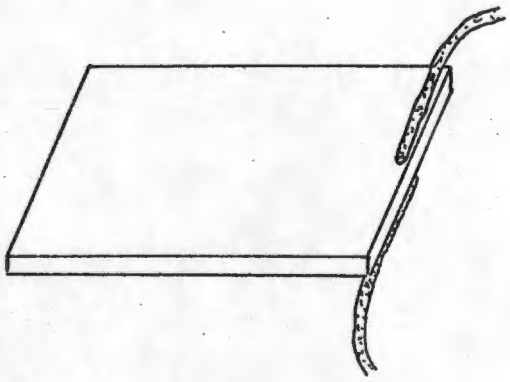

Fig.4-20

Fig.4-21

The two wires were cut and soldered onto a thin screened cable. The transducer was then mounted on a polystyrene block with Araldite quickset adhesive. The exposed parts of the wires were

also coated and the whole block was glued into a metal housing which is to be discussed in Chapter 7.

There are better ways of mounting such a transducer to improve the airbacking and reduce the effects of solder on the faces. However, this is a popular method because it is simple and ideally suited to prototyping. The housing was small and made of brass, which is generally not recommended because metals are such good reflectors of ultrasound. Ideally one would use a soft plastic and line it with an acoustic insulator. The principle is really the same as for loudspeakers mounted in loudspeaker boxes. However, space limitations and practical construction constraints precluded acoustic optimization of the housing.

Transducer housing and mounting is an enormous topic on its own and can not be covered in this work. For large scale production it would be worth devoting considerably more attention to this aspect.

CHAPTER FIVE

THE ELECTRONIC SYSTEM

We discussed the principle of extracting doppler signals from reflected ultrasound in Ch.4. Because of the large number of unknowns, it was decided to base the design on the characteristics a typical CWDU blood flow detector discussed by Baker[53].

Typically an instrument for shallow peripheral vascular applications transmits intensities of up to 600mW/cm^2, at between 8 and 10MHz. Low frequency instruments (2MHz) used in obstetrics have much lower intensity ratings, down to perhaps 10mW/cm^2. The lower frequency instruments are more penetrating and safety considerations dominate in obstetrics. As discussed in Ch.4, (Eq.4-17, page 40) the signal-to-noise ratio is directly proportional to the insonating power level.

Because of the very narrow bandwidth in CWDU systems, high Q air backed transducers are used for their sensitivity. They have typical impedances of 30 to 100 ohms and require 3 to 10V$_{pp}$ driving voltage.

The receiver requires about 50dB voltage gain. Signal-to-noise ratio is a very important consideration, since the doppler shifted signal is 40 to 60dB below the leakage component level. Doppler sidebands are typically 1 to 10µV at the input to the receiving amplifier. This requires proper impedance matching between the transducers and the input transistor to optimize the signal-to-noise ratio. Typically, 0,2 to 0,4µV equivalent noise can be expected with a good design. The final signal-to-noise ratio will be in the order of 20 to 30dB for vessels 1 to 5cm deep.

Fig.5-1 is a block diagram of the system that was finally implemented. An r.f. receiving amplifier was put into the prototype although multiplier sensitivity is about 3µV. An attempt was made to drive the multiplier directly through a centre-tapped transformer, but the signal was found to be too weak to be acceptable in practice.

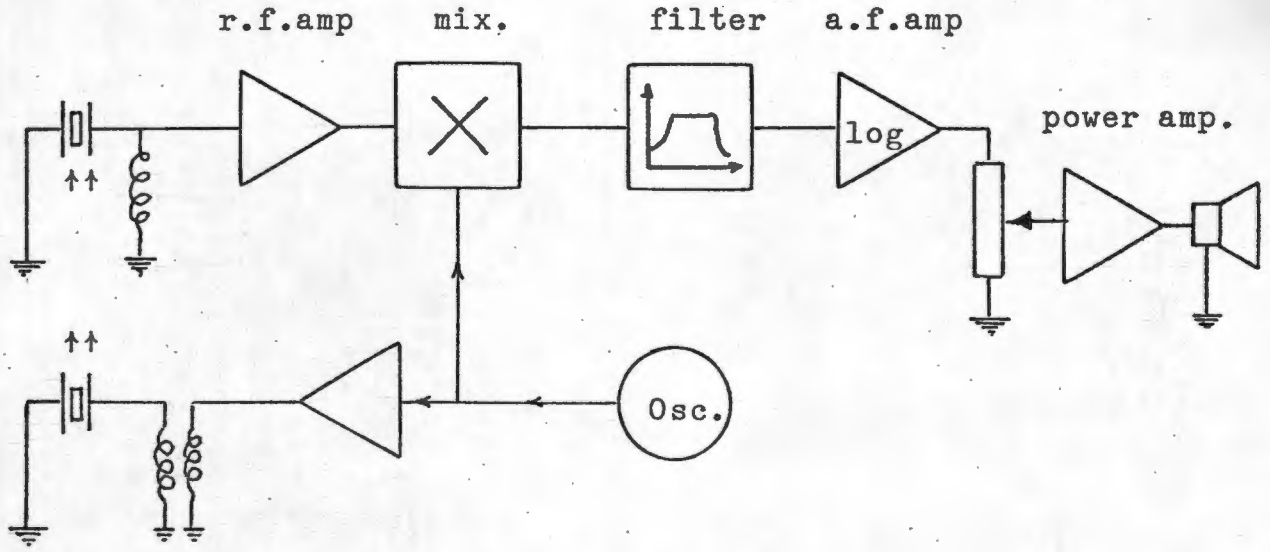

Fig.5-1

The output from the multiplier was passed through an a.f. bandpass filter to prevent unwanted r.f. from getting into the audio amplifier. Very powerful low frequency signals one associates with transducer movements were also filtered off, since these are prone to saturate the power amplifier.

No AGC is provided because signal intensity is considered an essential element in locating vessels. On retrospect, however, some degenerative feedback may have helped overcome stability problems that were experienced when prototyping. Instead of feedback a logarithmic amplifier was included to cope with the large anticipated dynamic range without saturating the amplifier.

§5.1 THE OSCILLATOR

Fig.5-2 is a circuit diagram of the Hartley oscillator[54] used in the circuit. The MFE131 Motorola Dual Gate MOSFET has excellent thermal characteristics making this circuit very stable. It is designed for amplifiers up to 200MHz. Of particular interest when prototyping is the dual gate feature which enables the gain to be controlled very easily by simply adjusting the d.c. potential on gate 2. This is typically between 1 and 4 volts. The higher the bias level, the greater is the gain.

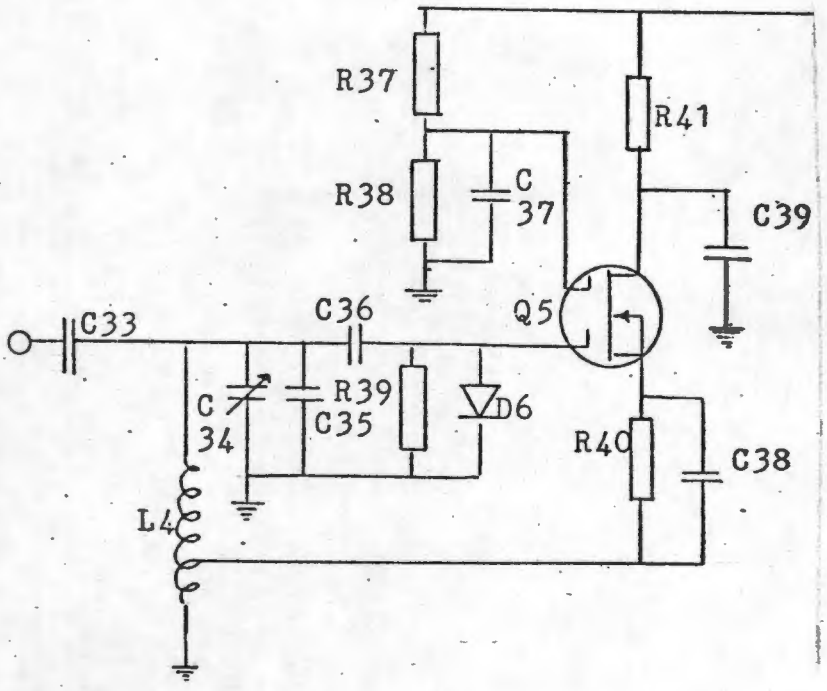

R37	180k
R38	100k
R39	47k
R40	270Ω
R41	1,0k
C33	100pF
C34	47pF preset
C35	82pF
C36	47pF
C37	10nF
C38	47nF
C39	47nF
D6	1N4148

Fig.5-2

The inductor used was built on a Micrometals T37-6 core. A 30 turn toroid of 0,4mm (27 gauge) enamelled copper wire, tapped at 6 turns from the cold end was wound onto the core.

§5.2 R.F. AMPLIFIER

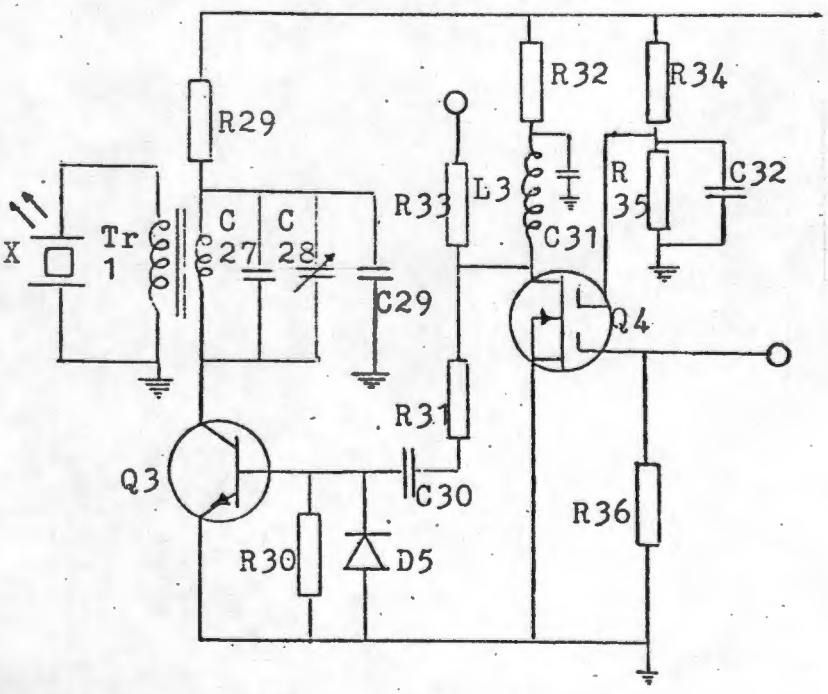

R29	100Ω
R30	1,0k
R31	1,0k
R32	100Ω
R33	10k
R34	180k
R35	100k
R36	100k
C27	-
C28	47pF preset
C29	10nF
C30	10nF
C31	10nF
C32	10nF
D5	1N4148
L3	10µH

Fig.5-3

Output from the oscillator is about $6V_{pp}$. This is passed into a MOSFET buffer, the gain of which is set by R34/35. The r.f. is decoupled from the power supply by L3 and C31. The inductor, ofcourse also presents a dynamic load impedance.

The signal on the Drain of Q4 is about $15V_{pp}$. A small portion of this signal is taken to the mixer through R33, while the rest is used to drive Q3. Q3 is an inexpensive high speed switching transistor with an exceptionally low storage time of 13 ns. This is important in class C operation at high frequencies. Class C is associated with very high efficiencies and is appropriate when the load is a tuned circuit.

§5.3 R.F.OUTPUT TRANSFORMER

The design of the output transformer is based on the characteristics of the transducer. These characteristics can be obtained in two ways, firstly by calculation and secondly, by direct measurement.

Calculation

The Resistance R of the crystal at resonance is obtained by combining equations 4-44, 4-49 and 4-59. Thus:

$$R = \frac{\rho' c' t^2}{A\, e^2} \qquad (5\text{-}1)$$

where
- ρ' = density of the physiological medium
- c' = velocity of sound in that medium
- A = area of the transducer
- t = thickness of the transducer
- e = piezoelectric stress constant.

e Is not given in the table of Philips materials (Appendix 4-4), but from equation 4-42 we know that:

$$e_{33} = \frac{d_{33}}{s^E_{33}}$$

which from the Philips tables works out to be 20,3 C/m^2. The

thickness t was measured to be 0,20mm. The characteristic impedance for various physiological materials $\rho' c'$ is as follows:

muscle: $1,7 \times 10^6$ kg/m^{2}s

water: $1,52 \times 10^6$ kg/m^{2}s

fat: $1,35 \times 10^6$ kg/m^{2}s

We have to take some average since the insonated tissue is not homogenous. Assuming that c' is $1,5 \times 10^6$ kg/m^{2}s, then

$$R = \frac{1,5 \times 10^6 \times (0,20 \times 10^{-3})^2}{2 \times 2,5 \times 10^{-6} \times (20,3)^2}$$

$$= 29\ \Omega$$

The capacitance of the crystal C_0 is given by equation 4-62:

$$C_0 = \frac{\varepsilon \cdot A}{t}$$

where ε is the permittivity of the ceramic material. The relative permittivity of PZT5 is 1800. Hence the capacitance is:

$$C_0 = \frac{1800 \times 8,85 \times 10^{-12} \times 5 \times 10^{-6}}{0,2 \times 10^{-3}}$$

$$= 400\ \text{pF}$$

Since the crystal is driven at the series resonance frequency, values for L and C (see Fig.4-19) are of no concern since these two reactive components cancel each other.

Direct Measurement

The calculations above pertain to Philips PXE5 ceramic material. As was mentioned earlier, LTZ was used in preferance to PXE because performance appeared to be superior. The figures obtained for R and C could not be extrapolated to LTZ material. While agreement between measured and calculated values for PXE material was found to be good, substantial differences were found between values calculated for PXE and values measured on LTZ.

The radiation resistance R was found to be very difficult to measure in circuit because of distortion in the current wave forms. So the following circuit was built and driven with a commercial sine wave generator, delivering a clean sine wave of $18V_{pp}$ at 9,0MHz. The resistance R_L representing the mounting losses was previously ignored but has been included here. An inductance L

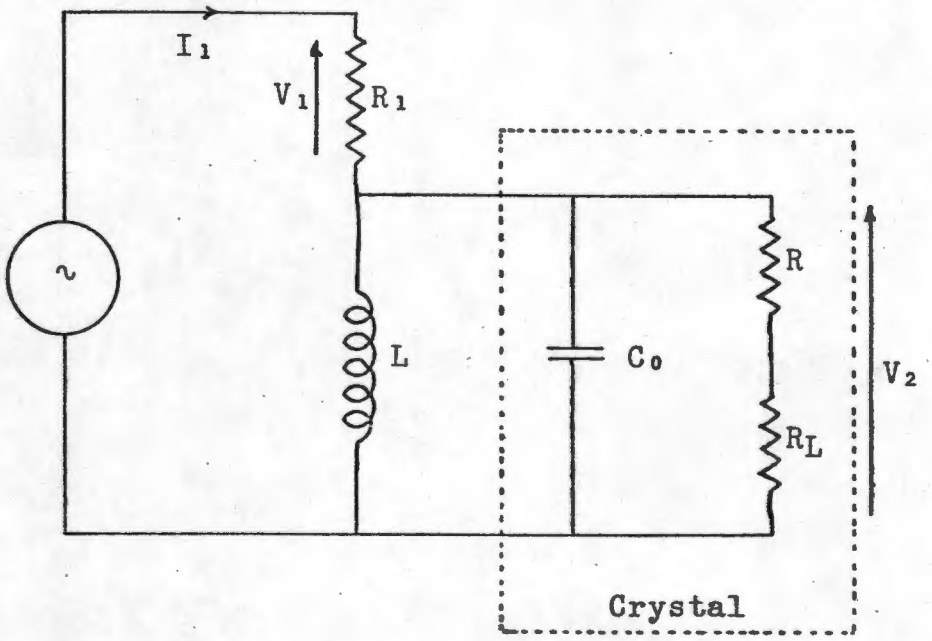

Fig.5-4

has been included to tune out C_0 as far as possible.

We have that:

$$\frac{I_1}{V_2} = \frac{V_1}{R_1} \times \frac{1}{V_2}$$

$$= \frac{1}{j\omega L} + j\omega C_0 + \frac{1}{R + R_L}$$

Both V_1 and V_2 were carefully measured in magnitude and phase on an oscilloscope. These measurements were taken 3 times with the crystal submerged in water and 3 times with the crystal out of water. Out of water the crystal is acoustically short circuited, since the impedance of air $(\rho'c')$ is very low. Thus R_L can be obtained quite readily. Submerged in water, the resistance of the crystal is the sum of R_L and R.

From these measurements R was found to be 230 Ω and R_L 1 300 Ω. These results are particularly useful when assessing the power output from the transducer. However, they were not found to be useful in designing the transformer. It was found necessary to do this by trial and error.

Tuning the secondary

Using a bridge, C_0 for the LTZ crystal was measured to be 105pF. The inductance of the secondary winding of the transformer (winding connected to the crystal) is given by:

$$L_2 = \frac{1}{4\pi^2 f_r^2 C_0} = 3\ \mu H$$

for a resonant frequency of 9MHz.

A Micrometals toroidal core T50-6 which has an inductance of 40μH per 100 turns, was used as a former. Since $L \propto N^2$ (where N = turns)

$$\frac{L_2}{L_{100}} = \left(\frac{N_2}{100}\right)^2$$

Hence $$N_2 = 100 \times \left(\frac{L_2}{L_{100}}\right)^{\frac{1}{2}}$$

$$= 100\ \sqrt{3/40}$$

$$= 27 \text{ turns}$$

Since measured values of inductance on these toroids was found to be a little higher than those specified by Micrometals Inc., only 25 turns were put on the secondary.

Tuning the primary

The primary coil consisted of 13 turns (by experimentation). Using the same principles as above, the inductance works out at 0,676 μH and the parallel tuning capacitance at 463 pF. In practice, however, for optimal tuning a capacitance of 220pF was used, parallelled by a tunable capacitor.

Output Power

Having constructed the circuit, two questions remain. Firstly, is there enough power available for adequate detection by the receiver? Secondly, is the power level within safe limits?

The first question was answered by trying the system out. There appeared to be sufficient power to detect even small veins.
To answer the second question, measurements were taken of the voltage generated across the crystal. This was found to be $20V_{pp}$ for the LTZ5 crystal. Thus:

$$I_{RMS} = \frac{V_{RMS}}{R + R_L} = 4{,}6 \text{ mA}$$

$$\text{Power} = I^2R = 4{,}9 \text{ mW}$$

$$\text{Intensity} = \frac{\text{Power}}{\text{Area}} = 100 \text{ mW/cm}^2$$

This is currently considered a safe dose even in obstetrics. However, with a more sensitive receiver it is very likely that this could be reduced. Since ultrasound may hold dangers of which we are not yet aware, it is as well to reduce output power to an absolute minimum. Optimization of the electronic circuit, however, goes beyond the scope of this work.

§5.4 TUNING THE RECEIVING CRYSTAL

The two crystals used are identical and the capacitance was measured to be 105pF. The required tuning inductance is about 3μH as was discussed in the previous section.

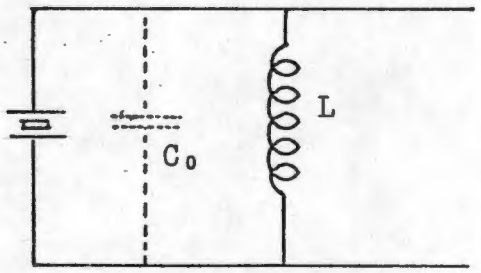

Fig.5-5

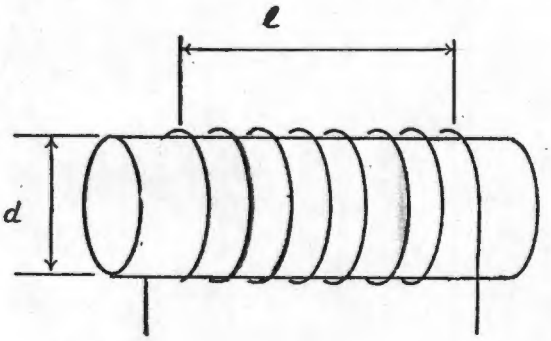

Fig.5-6

The inductor was wound onto a plastic bobbin, which could be suitably screened and tuned with a miniature ferrite screw. The inductance of a single layer solenoid without a core is given by[59]

$$L = \frac{kd^2N^2}{(3d+9\ell)} \qquad (5\text{-}2)$$

where $k = 7{,}874 \times 10^{-3}$

N = number of turns

Since $\ell = Nt$ (where t is the thickness of the wire) we have:

$$3dL + 9NtL - kd^2N^2 = 0$$

Hence:
$$N = \frac{9Lt \pm \sqrt{(9Lt)^2 + 12kd^3L}}{2kd^2} \qquad (5\text{-}3)$$

36 Gauge (0,21mm) wire was used. Thus t = 0,21. d Was measured to be 5,7mm. Substituting all these values into equation 5-3 we get N= 29 turns. Actually 27 turns were wound onto the bobbin, relying on the ferrite slug to make up the extra inductance that would be required for fine tuning.

§5.5 R.F. INPUT AMPLIFIER

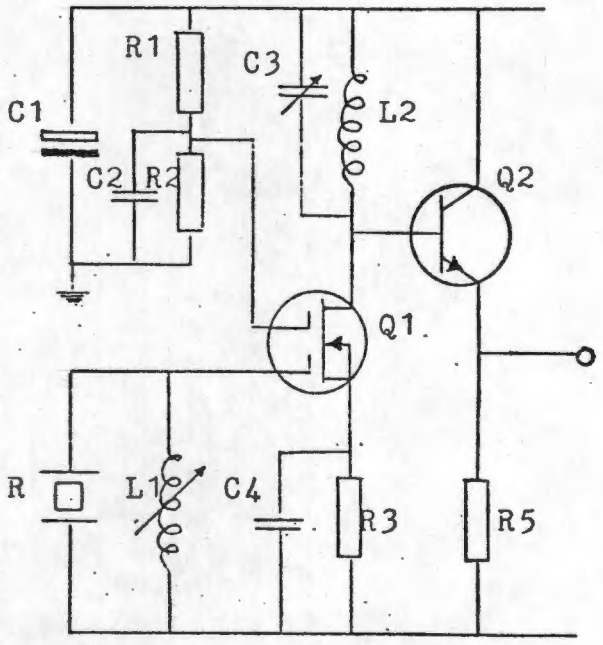

R1	100k
R2	47k
R3	56Ω
R5	5,6k
C1	1,0µF Tant
C2	10nF
C3	47pF Preset
C4	10nF
L2	10µH
Q1	MFE131
Q2	BFX89

Fig.5-7

The input stage consists of a common source dual gate MOSFET in a tuned amplifier arrangement, driving an emitter follower buffer. For prototyping the dual gate MOSFET is particularly attractive since it lends itself to AGC if this proves desirable. In the present circuit the gain has been fixed with the same voltage divider on G2 as was used in the oscillator circuit. C3 and L2 are tuned to provide a very high r.f. impedance for high gain. Voltage gain for this stage was measured to be about 20dB.

§5.6 THE MIXER [60]

The Motorola MC1496 balanced modulator is designed for use where the output is required to be a product of input voltage and a switching function. Since operation of the device is not obvious from the circuit diagram of Fig.5-9, it is discussed in a little more detail. Consider Fig.5-8, which is a functional diagram of the device itself, together with externally applied d.c. bias circuitry.

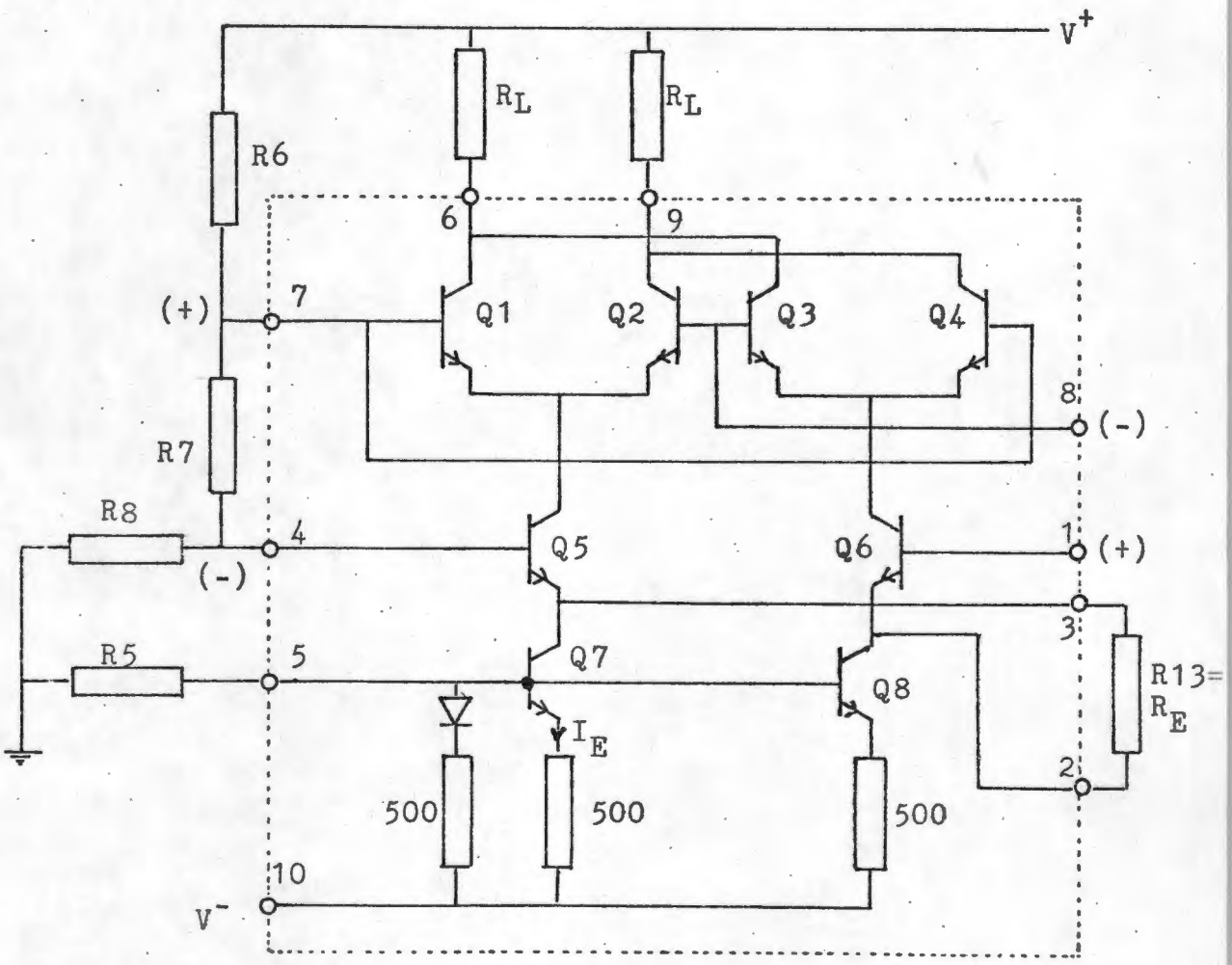

MC1496

Fig.5-8

For the sake of simplicity, base currents are ignored with respect to the magnitude of collector currents. A differential amplifier consisting of Q5 and Q6 drives a dual differential amplifier composed of Q1, Q2, Q3 and Q4. Q7 and Q8 are constant current sources.

The 1496 is usually driven with a high level carrier switching the

two upper amplifiers on and off. The signal input, however, is kept small enough to operate in the linear mode. The resulting output signal then contains only sum and difference frequency components and amplitude information of the modulating signal. Emitter degeneration resistance between pins 2 and 3 is set externally to tailor the linear dynamic range of the modulating input signal. This resistor also determines device gain.

$$V_{m(peak)} = I_e R_E \qquad \text{(ref.60)}$$

Since I_e is equal to the current into pin 5 (I_5) we can write:

$$V_{m(peak)} = I_5 R_E \qquad (5\text{-}4)$$

It can be shown[60] that provided the carrier input is greater than 100mV, the conversion gain of the single ended output for each fundamental sideband is:

$$A = \frac{0,637\ R_L}{R_E + 2R_e} \qquad (5\text{-}5)$$

For the differential output this is 6dB higher. At room temperature

$$r_e = \frac{26 \text{ ohms}}{I_5 \text{ (mA)}}$$

D.C. Bias

Current levels are set by controlling I_5 (where subscripts refer to pin numbers.) Hence:

$$I_5 = I_6 = I_9 = I_{10}/3$$

The manufacturer recommends that I_5 is set at 1mA. If the voltage divider is designed for a minimum current of 1mA, then base currents can be ignored. The bases should be biased as follows:

$$(V_6, V_9) - (V_7, V_8) \geq 2V$$

$$(V_7, V_8) - (V_1, V_4) \geq 2,7V$$

$$(V_1, V_4) - (V_5) \geq 2,7V$$

A negative voltage of -4,7V was generated to supply pin 10. The positive supply was regulated at +8V. Bearing in mind the biasing constraints mentioned above, R5, R6, R7 and R8 were chosen as in Fig.5-9. The load resistors were made small enough to ensure operation in the linear region. Some additional resistors have been inserted into the base circuits. These do not affect the d.c. bias but isolate signals.

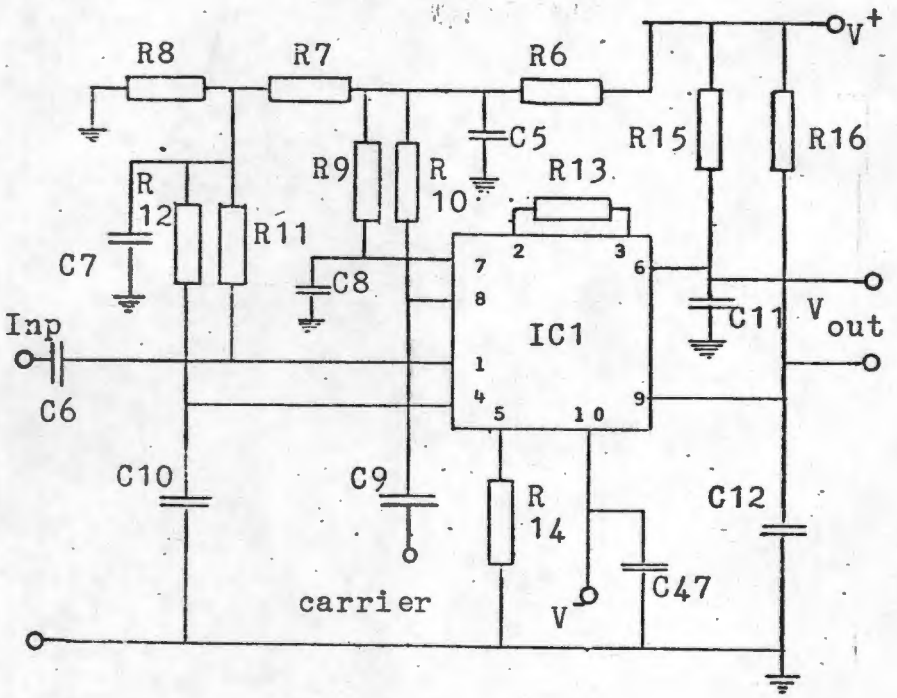

R6	1,8k
R7	1,0k
R8	220Ω
R9	1,0k
R10	1,0k
R11	1,0k
R12	1,0k
R13	560Ω
R14	3,3k
R15	2,7k
R16	2,7k
C5	100nF
C6	100nF
C7	100nF
C8	100nF
C9	100nF
C10	100nF
C12	4,7nF

Fig.5-9

We have that: $I_5 = I_e = 1mA$

$r_e = 26\Omega$

$R_E = 560\Omega$ (see below)

$R_L = 2k7$

The maximum voltage at the input was found to be 500mV. Hence:

$$R_E = V_{m(peak)} / I_5 \simeq 560\Omega$$

The conversion gain is

$$A = \frac{2 \times 0,637 \times 2k7}{(560 + 2 \times 26)}$$

$$= 5,6 \quad \text{(or 15dB)}$$

§5-7 THE PASSBAND FILTER

The purpose of the filter stage is to cut out any r.f. as well as the low frequencies associated with movement of the transducers on the skin. Consider Fig.5-10.

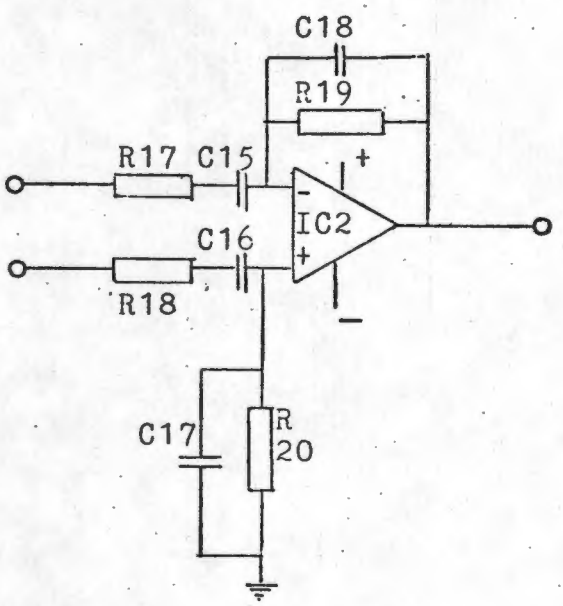

R17	10k
R18	10k
R19	47k
R20	22k
C15	100nF
C16	100nF
C17	1,0nF
C18	1,0nF

Fig.5-10

The gain of this amplifier is :

$$A(dB) = 20 \log \frac{z_0}{z_i}$$

where z_0 and z_i are the feedback and input impedances respectively. From this we can show that

$$A(dB) = 20 \log(R19.C15) + 20 \log\omega - 20 \log \frac{\omega}{1/R17.C15} - 20 \log \frac{\omega}{1/R19.C18}$$

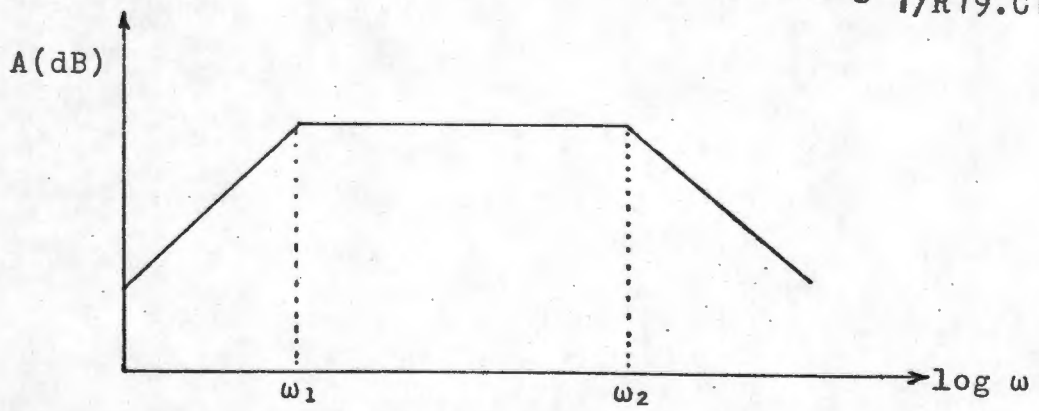

Fig.5-11

The lower corner frequency was established experimentally, the governing factor being low frequency stability and sufficient attenuation of transducer movement noise. For the components chosen this corner frequency is 1 kHz. The higher corner frequency was chosen at 20kHz, this being less critical. For this filter midband gain is 14dB, while the gain at 1Hz is -26dB.

§5.8 THE LOGARITHMIC AMPLIFIER

Consider Fig.5-12

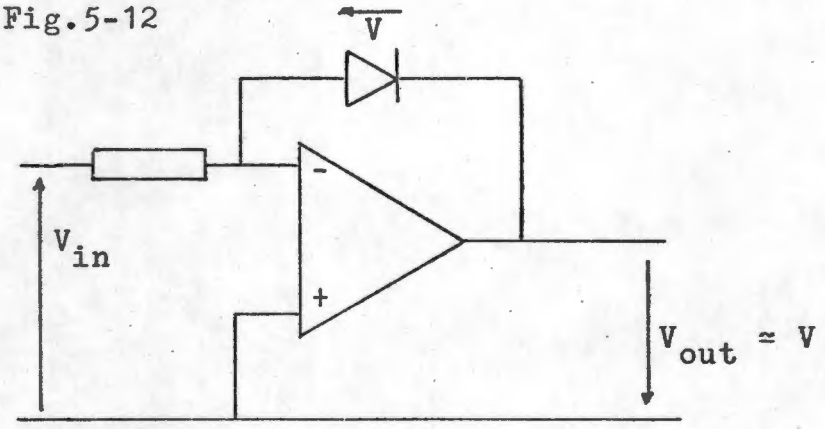

Fig.5-12

The current into R_{in} is equal to the current through the diode. Hence, from the diode equation we have:

$$\frac{V_{in}}{R_{in}} = I_s(\exp(V/V_T) - 1)$$

where $V_T = kT/q \simeq 25mV$ at room temperature

For the 1N4148 $I_s = 10mA$

$$\text{hence} \quad V_{out} \simeq V = V_T \ln\left(\frac{1}{I_s} \times \frac{Vin}{R_{in}} + 1\right)$$

$$= 0{,}025 \ln\left(100 \frac{V_{in}}{R_{in}} + 1\right)$$

A bipolar version of this amplifier was built (Fig.5-13). The positive input was d.c. biased to midway between the positive rail and ground. A feedback capacitor and resistor are included to smooth out high audio frequency noise and to linearize the zero

crossing points. Circuit values were chosen experimentally to optimize performance.

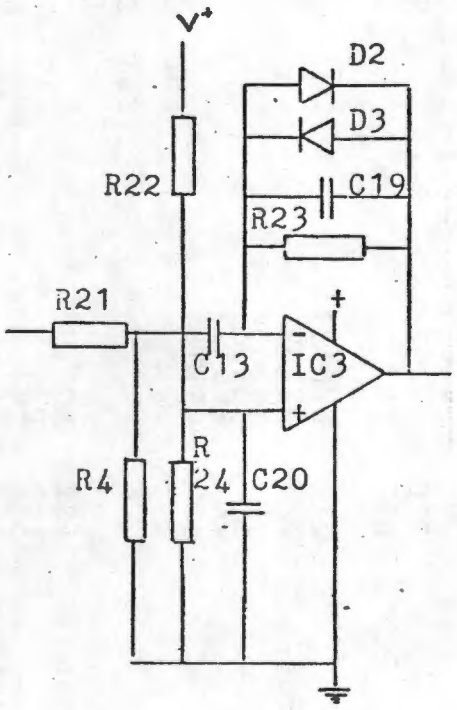

R4	1,2k
R21	10k
R22	10k
R23	100k
R24	10k
C13	100nF
C19	10nF
C20	10nF
D2, D3	1N4148

Fig.5-13

§5.9 A.F. POWER AMPLIFIER

An LM388 1,5W audio power amplifier was configured as suggested by the manufacturer[61]. Gain is set with R27 to close on 46dB. This was selected experimentally, circuit stability being the major constraint on the gain.

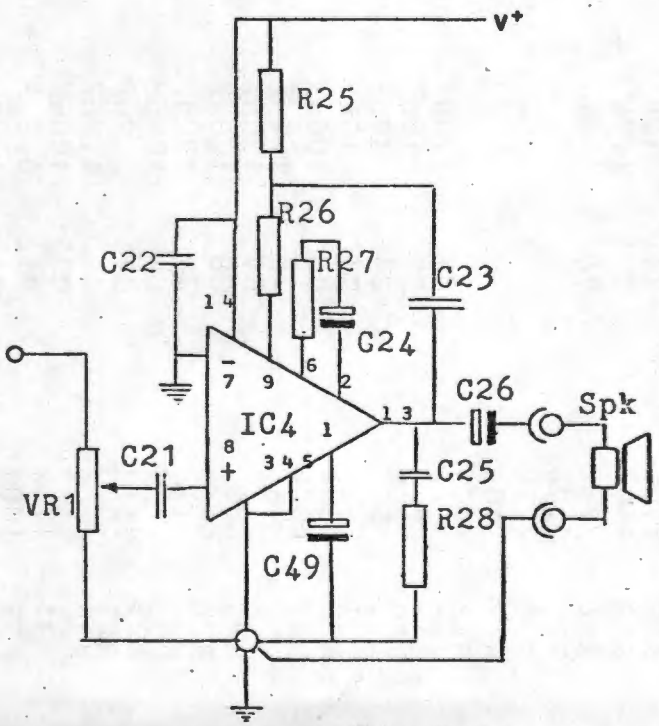

VR1	10k
R25	680Ω
R26	680Ω
R27	12Ω
R28	2,7Ω
C21	100nF
C22	10nF
C23	10µF
C24	10µF
C25	47nF
C26	220µF
C49	10µF
Spk	8Ω

Fig.5-14

Component List

R1	100k	R33	10k	C16	100nF	C48	100µF	L1	27 Turns 36G wire on screened 5,5mm Bobbin
R2	47k	R34	180k	C17	1,0nF	C49	10µF		
R3	56Ω	R35	100k	C18	1,0nF	C50	1000µF		
R4	1,2k	R36	100k	C19	10nF	C51	10nF	L2	10µH
R5	5,6k	R37	180k	C20	10nF			L3	10µH
R6	1,8k	R38	100k	C21	100nF			L4	30T of 27G Cu wire, tapped at 6T, on T37-6 toroidal core.
R7	1,0k	R39	47k	C22	10nF				
R8	220Ω	R40	270Ω	C23	10µF	D1	1N4001		
R9	1,0k	R41	100Ω	C24	10µF	D2	1N4148		
R10	1,0k	R42	1,0k	C25	47nF	D3	1N4148		
R11	1,0k	R43	10k	C26	220µF	D5	1N4148		
R12	1,0k	R44	10k	C27	220pF	D6	1N4148	Tr1	2 windings on T50-6 toroidal core. N1:25T 27G N2:13T 27G
R13	560Ω	R45	4,7k	C28	47pF Preset	D8	1N4001		
R14	3,3k	R46	220Ω	C29	10nF	D9	1N4001		
R15	2,7k			C30	10nF	D10	6V2 Zen.		
R16	2,7k	RV1	10k Preset*	C31	10nF	D11	LED		
R17	10k			C32	10nF				
R18	10k			C33	100pF	Q1	MFE131		
R19	47k	C1	1,0µF Tant	C34	47pF Preset	Q2	BFX89	R	2×2,5mm LTZ5
R20	22k	C2	10nF	C35	82pF	Q3	2N2369	X	2×2,5mm LTZ5 both 9MHz
R21	10k	C3	47pF Preset	C36	47pF	Q4	MFE131		
R22	10k	C4	10nF	C37	10nF	Q5	MFE131		
R23	100k	C5	100nF	C38	47nF			Spk	8Ω 66mm ϕ
R24	10k	C6	100nF	C39	47nF				
R25	680Ω	C7	100nF	C40	10nF			Sw1	Cherry E63 100mA µSwitch
R26	680Ω	C8	100nF	C41	22µF Tant	IC1	MC1496		
R27	12Ω	C9	100nF	C42	3,3nF	IC2	741	Bat	10×NCC24 1,5V Eveready NiCd.
R28	2,7Ω	C10	100nF	C43	1,0µF Tant	IC3	741		
R29	100Ω	C11	4,7nF	C44	1,0µF Tant	IC4	LM388		
R30	1,0k	C12	4,7nF	C45	100nF	IC5	LM2930-8TB	Plug	2pin polarized Radio spares 466-472,466-488 466-343
R31	1,0k	C13	100nF	C46	1,0µF Tant	IC6	555		
R32	100Ω	C14	6,8µF Tant	C47	10nF	IC7	741		
		C15	100nF						

Fig.5-15 ULTRAGUIDE CIRCUIT DIAGRAM

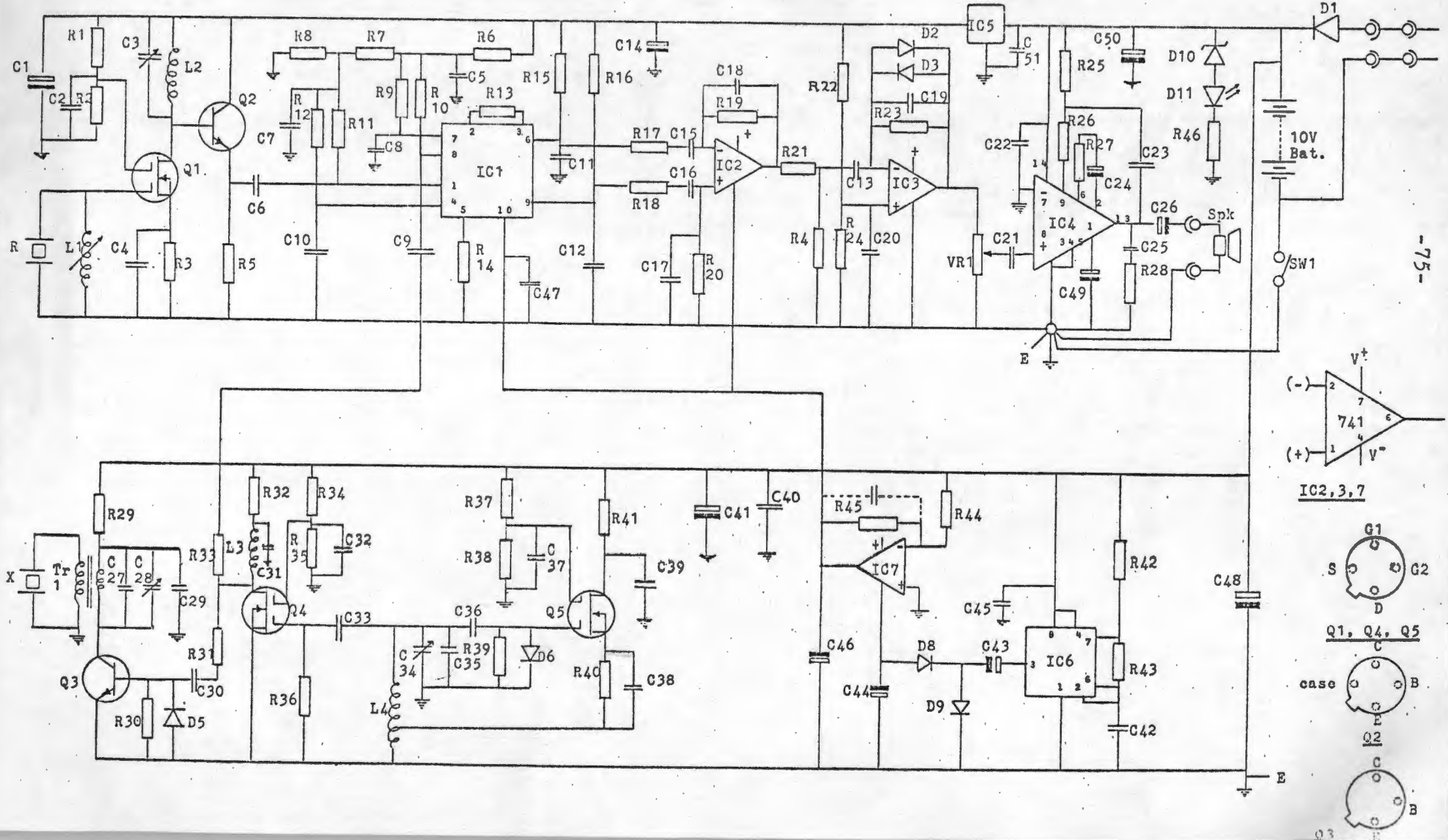

§5.10 NEGATIVE VOLTAGE GENERATOR

10 Volts is not really sufficient for IC1 to function properly. So a negative voltage of -4,7V was generated using IC6 (555 multivibrator) and a diode pump. The output was crudely regulated with reference to the positive rail by means of an operational amplifier. IC2 was also supplied with the negative voltage. This negative voltage generator caused some trouble by interfering with the 9MHz signal, causing an irritating, frequency unstable whistle at the output. Careful screening of the inverter circuit was tried as well as using completely separate power supplies for both the inverter and the negative rail. However, as long as the 555 was oscillating, the whistle was present. It has been minimized by carefully tuning the multivibrator to get the interference out of the audio spectrum. This has been largely successful. It is suspected that one or more of the harmonics generated by the multivibrator is modulating the very sensitive receiver by electromagnetic interference resulting in the a.f. noise.

The 555 multivibrator runs at about 22kHz.

§5.11 POWER SUPPLY

Power is supplied by eight 1,2V Eveready NCC24 rechargeable NiCd cells. They have a capacity of 240mAH. Current consumption is about 120mA. Since the instrument is switched on intermittently, it has the potential to give continuous service for a full day.

Regulator

It was found that the only efficient means of decoupling the very sensitive receiver from the power circuits was by means of an 8V regulator. The LM2930 is excellent for this application since it requires only a 0,6V drop from the raw supply to the regulated output.

Charger

A trickle charger was built to deliver a constant current of 25mA. An LED indicates whether or not the batteries are receiving charge.

§5 12 DEVELOPMENT OF THE CIRCUIT

The circuit of Fig.5-15 was developed from an initial design which was built on an experimental printed circuit board for testing. A platform was built to hold the P.C. board and a scaffold to hold the two transducers was constructed. The transducers were fitted into empty 0,22 cartridge cases and mounted on swivel joints so that they could be fixed into any position.

Fig.5-16

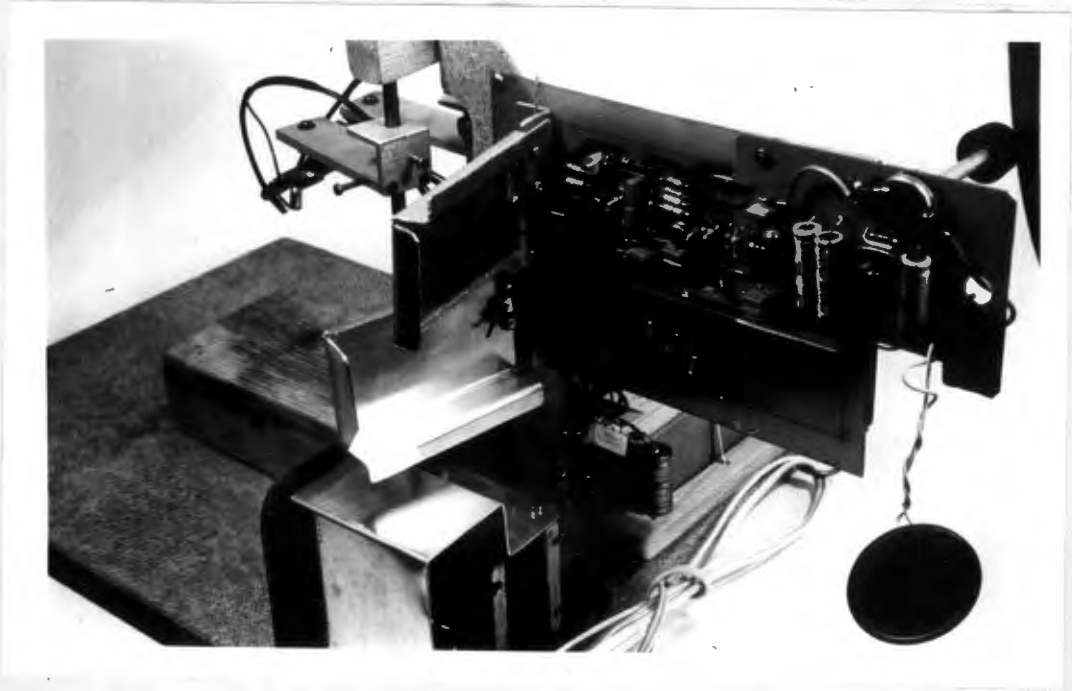

Fig.5-17

Various diameter silastic tubes immersed in a water bath were used to simulate blood vessels. A fish tank pump was used to pump water through these tubes. Particles of talcum powder were mixed into the water to serve as reflectors of ultrasound.

The purpose of this exercise was not only to develop the electronic system, but also to experiment with the directivity and sensitivity of ultrasound, and to acquire a feel for the subject. These tests showed, for example, that tubes less than a millimeter in diameter could be located very easily, even with very slow flowrates of a few millimeters per second.

§5.13 PERFORMANCE

Apart from an occasional return of the interference whistle attributed to the negative voltage generator, the circuit appeared to be very sensitive and functioned well. There is little doubt, however, that there is much room left for improvement. A different approach could result in a current saving which could reduce the battery pack. Component count could certainly be reduced, the need for a negative voltage could well be eliminated and perhaps sensitivity could be further increased without losing stability. Indeed, a pencil blood-flow detector is on the market. It is the size of a pen-light torch and uses a single pen-light cell which is said to last for 40 hours of operation [62].

Apart from these aspects, noise reduction could be accomplished through better design and the filtering could be improved to allow more of the lower frequencies through without sacrificing gain or stability.

Nevertheless, as a prototype this circuit is more than adequate. It can certainly be used to prove whether or not the mechanical needle guidance system is effective.

CHAPTER SIX

THE MECHANICAL SYSTEM

The mechanical system developed for this project is the heart of the needle guide. It is the original nature of this system that makes it the most important part of this work.

It should be pointed out here that it evolved from a very simple concept with some basic limitations, into a rather complex mechanism. While every effort was made at keeping the device simple, requirements that were thought should not be subject to compromise, were those involving biomedical aspects. A great deal of the complexity can therefore be ascribed to a recognition of the need for the device to be clinically acceptable in the first instance.

§6.1 REQUIREMENTS

It has been shown in Chapter 3 that needles are commonly inserted at an angle to the skin of from 5 to 35 degrees. Often, however, arterial blood samples are taken with needles inserted at 90°. A truly universal guide has to be able to guide needles into tissue at these angles to a depth of around 60mm, this being the depth at which one occasionally finds the Subclavian vein. In addition the guide should be able to cope with some of the very short needles such as the butterfly needle one finds in intravenous infusion sets.

DEVELOPMENT STAGES

§6.2 COMMON AXIS

The guidance system was developed through a number of stages. Initial concepts were based on the work of Mozersky. However, there are no needle guides in common use in hospitals today,

and one wonders why Mozersky's system failed to gain popularity. It will be remembered that he used a two transducer probe with a central canal through which needles were inserted between the transmitted and reflected beams. This approach certainly has merit when the procedure involves nothing more than collecting specimens or administring intravenous injections. However, as soon as it becomes necessary to separate the needle from the probe without first withdrawing the needle from the patient, the system runs into difficulties. Instead of a canal through the probe, some sort of groove would have to be made.

A model was constructed of a proposed guide in which the needle passes through a groove between the two transducers. A little catch allows the needle to be locked into the groove. This very primitive system as initially envisaged is illustrated in Fig.6-1.

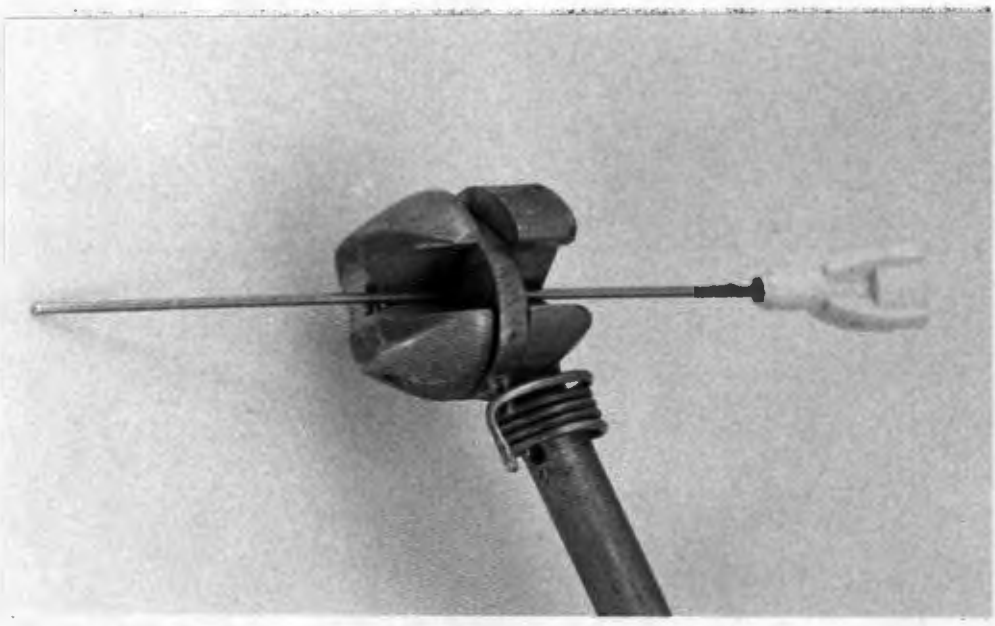

Fig.6-1

It soon became apparent that the proposed system suffered from a number of weaknesses. In the first instance, the length of the guide along which the needle slides has to be as great as possible to optimise the axial stability of the needle. On the other hand it also has to be as short as possible to accommodate the full range of needles commonly used.

The second drawback revolves around the whole principle of guiding a needle along the axis of the beam.

1. When ultrasonic beams enter sheets of media in which the velocities differ, they tend to get scattered by reflection as a result of acoustic impedance changes. They also undergo refraction. Refraction is a recognized problem in, for example, ultrasonically guided aspiration biopsy. What is particularly serious in blood flow detection at shallow angles is the problem of total internal reflection. Consider for example, ultrasonic waves travelling from fat into muscle. (The beam has to travel through fat and muscle to get to the blood).

$$\frac{\cos \theta}{\cos \theta'} = \frac{c}{c'} \qquad \text{(Snell's law)}$$

where:

θ is defined in Fig 6-2

θ' is the angle of the refracted ray

c and c' are the velocities of sound in fat and muscle respectively.

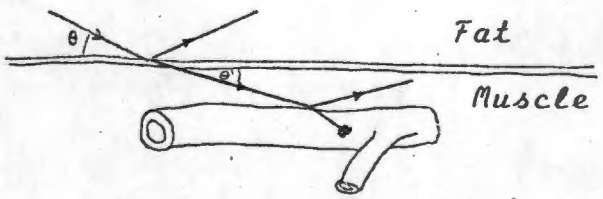

* Refraction
* Multiple reflection

Fig. 6-2

The velocity of sound in fat is 1443 m/s at 1,8MHz and that in muscle is 1580 m/s.(These figures apply to fresh pig samples[65]).

The critical angle of incidence occurs when the refracted angle is zero.

$$\theta' = 0$$

$$\cos \theta' = 1$$

$$\theta_{crit} = \text{arc cos } \frac{c}{c'} = 24^{\circ} .$$

This is very important when one considers that most of the vessel punctures are done at angles substantially less than 24 degrees.

2. In practice, small vessels that have to be punctured are inevitably superficial, the deeper ones being larger. Tiny superficial vessels which have to be approached at a very shallow angle, are located some considerable distance from the ultrasonic source. This has three drawbacks:

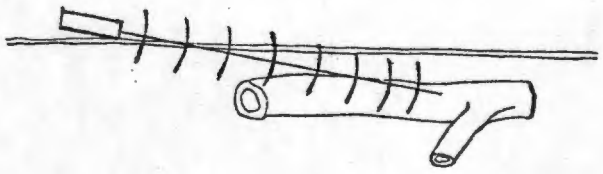

Fig.6-3

a. The beam tends to diverge (at about 5^{o} in our case), making it impossible to pin-point small distant vessels. Deep vessels are not affected by divergence since they are always much larger.

b. One can expect smaller signals to be reflected from the smaller vessels since there are fewer reflectors in the target volume. This is made worse by attenuation in the tissue.

c. It is axiomatic that it is difficult to aim at small targets that are far away.

3. Vessel identification may be nebulous in a very vascular area. One could conceivably confuse two vessels overlying one another, since the two beams overlap each other along their entire useful lengths (Fig.6-4).

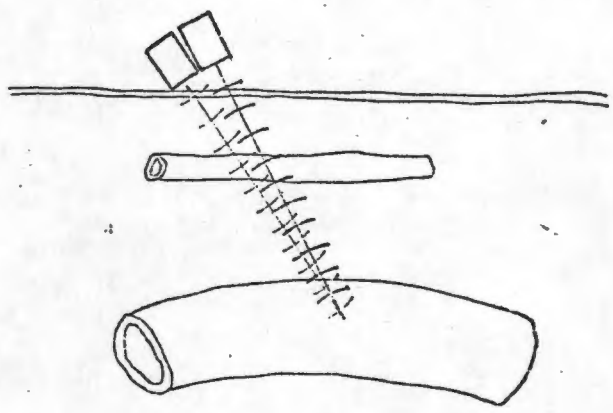

* Difficult to identify overlying vessels

Fig. 6-4

4. Sterilization could be a problem since the probe has to touch the skin at the point of incision.

5. Since the transducers are in the same housing or at best just very close to each other, the signal to leakage ratio (Ch 4) is small making detection of very small signals from deep vessels difficult.

§6.3 SEPARATION OF NEEDLE AND BEAM AXES

A totally new approach was developed in order to overcome these problems. Essentially the idea was to separate the ultrasonic beam from the axis of the needle (Fig 6-5a). In this way:

a. The needle could be inserted at any convenient shallow angle while the ultrasonic beam could be applied at an angle which best suits the properties of ultrasound.

b. The transducers could be located much closer to the target area.

c. Vessel identification can be made precisely if the beams intersect at only one "point".

d. Sterilization is less of a problem when the transducers are well away from the point of skin incision.

e. If the two transducers are seperately housed, transmitted power can be increased closer to the physiological limit. The higher signal to leakage ratio would enable easier recovery of weak signals from the deeper targets.

However, separating the beam axis from the needle axis brings about its own set of problems. The major problem is that the two axes must intersect, and furthermore, the intersection point must take place at the target.

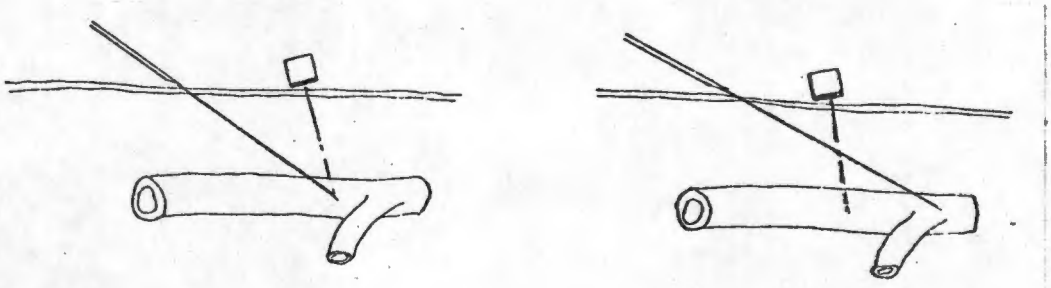

Cross at Target

(a)

Cross, but not at Target

(b)

Fig.6-5

This can only be achieved if the transducers are separated from each other by a reasonable distance and the intersection point of the beams is fixed to coincide with the axis of the needle.

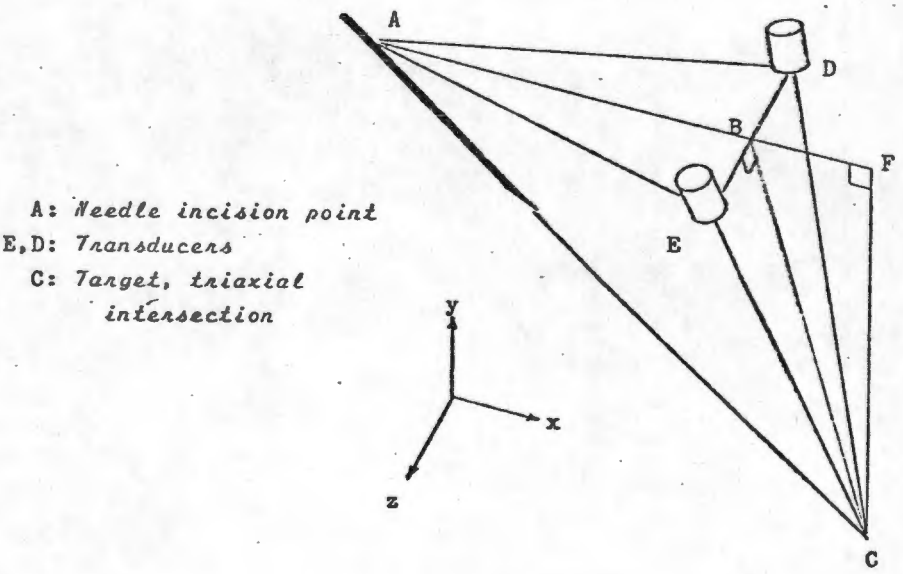

A: *Needle incision point*
E,D: *Transducers*
C: *Target, triaxial intersection*

Fig.6-6

§6.4 FIXED TRIAXIAL INTERSECTION

The possibility of building a system with a fixed intersection point was considered. It might well work, particularly if each puncture procedure has a particular fixed geometry dedicated to it. Thus the guide might consist of an electronic box with detachable guide heads for various procedures. Alternatively, in order to accommodate vessels at various depths, the needle support mechanism could be made to slide along the needle axis as illustrated in Fig.6-7. This arrangement will be examined more closely below.

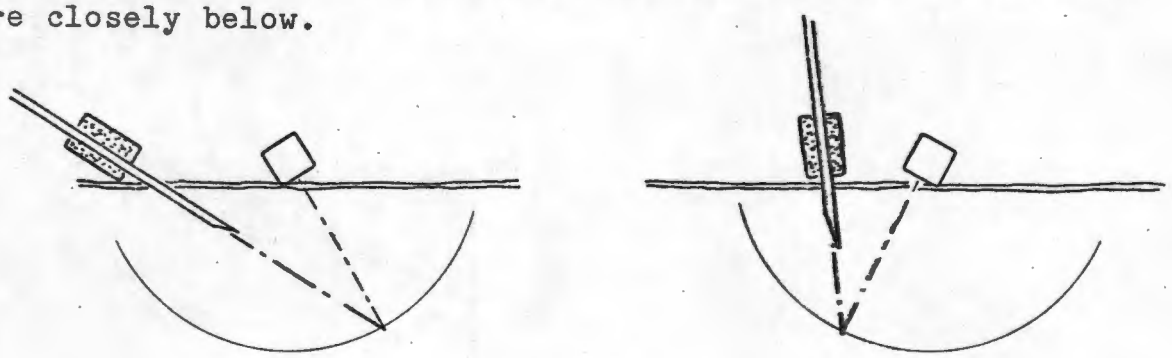

Fig.6-7

The first suggestion, a box with detachable components is not deemed suitable in a medical environment.

a. The set would have to be kept together, implying that some components could get lost.

b. The wrong head might be used for a particular procedure, leading to frustration.

c. A patient may be of such a size and shape that his blood vessels are located outside the range of a head prescribed for a particular procedure.

d. The extra complication of having to select and fit a head may make the device unacceptable to a large number of medical practitioners.

The second suggestion was actively pursued for a while. A model was made of the adjustable "foot guide" system (Fig.6-9). The mechanism consisted of three separate members which slid one into the other, parallel to the axis of the needle (Fig.6-8).

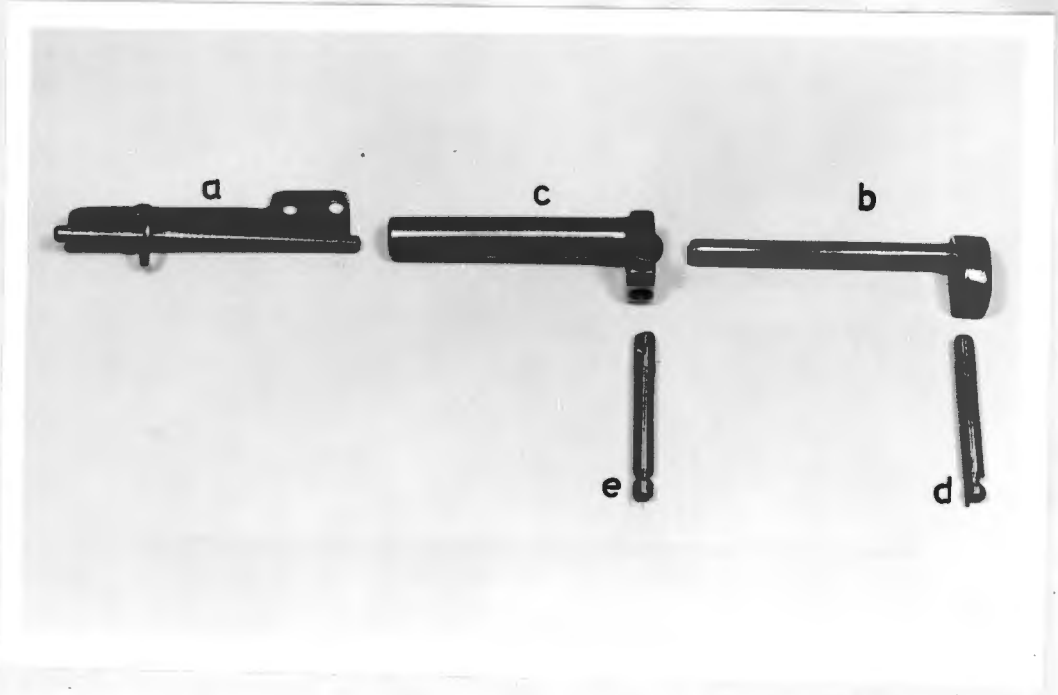

Fig.6-8

The innermost member (a) is simply a brass rod with a flange attached down its length. The flange presents a means for attaching the guiding element to the main housing and at the same time prevents axial rotation of the other two elements that slide over it.

The central element (b) slides over this rod. A slot cut along its length accommodates the flange. A rod (d) is attached at right angles to the base of this member. The needle runs through a groove at the end of the rod, and is held down by a spring clip. Rod (d) we call the foot guide stub.

The outermost element (c) slides over the two members (a) and (b). It has an identical guiding rod, but because it is associated with the head of the needle we call it the head guide stub (e).

The assembled unit is illustrated in Fig.6-9.

The system works as illustrated in Fig.6-7. Bearing in mind that the two axes of the ultrasonic beams and the axis of the needle remain fixed, one rocks the transducers over the area of interest and listens for doppler sounds. Once the operator is satisfied that the vessel has been accurately located, the central element is slid down until the foot guide and tip of the needle just touch the skin. The needle is then pushed into the tissue by

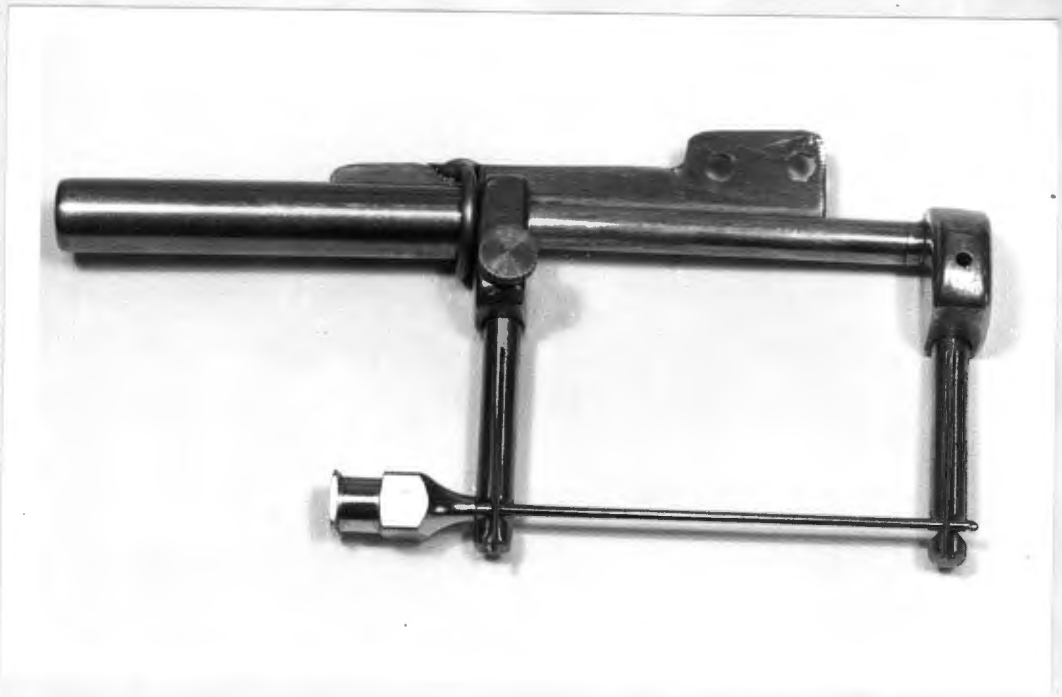

Fig.6-9

sliding the outer element down, parallel to the axis of the needle. During this procedure the needle slides over the foot guide, through the skin and ultimately into the target area.

It soon became obvious that this system was not sufficiently versatile.

1. The distance of the vessel from the transducer is always fixed. Since the Subclavian can be found at a depth of 60 mm (the deepest vessel to be located), the focus would have to be set a 60 mm. Not only would such a long focus make shallower Subclavians difficult if not impossible to locate, but all superficial vessels would also be difficult if not impossible to locate.

2. The system would be very difficult to operate because of the lack of versatility in the method that would have to be used when *scanning* for vessels at various depths.

However, one good point to have emerged from this model, was the unique two point needle support system discussed above. The system has the following important advantages over the earlier suggestion:

1. The needle is guided down along a rigid shaft parallel to its axis. The direction along which the needle is inserted

can therefore be precisely defined, and there is no need to rely on the rigidity of the needle.

2. The needle should enter the tissue straight along the correct axis without any deviation, because at the crucial initial stage of entry, the needle is supported at its ends.

3. Even short needles can be accommodated, because the two supports close up tightly together at a time when axial guidance is no longer important, i.e.: when the needle has already cut a tract into the tissue.

3. The parts holding the needle can be made disposable, making sterilization easy.

4. The bulk of the apparatus is well away from the point of incision.

This principle was ultimately to be used in the prototype.

While on the subject of the actual guidance mechanism, it should be mentioned that an attractive alternative was a system based on that just described, but without the foot guide. Instead, a small light is focussed on the skin at a point through which the needle has to travel to reach the target. It would then be up to the operator to pivot the needle on the head guide until the tip was on the light spot. The principle is exactly the same as above but now the foot guide becomes the initial incision spot itsself. There are some important advantages to this system:

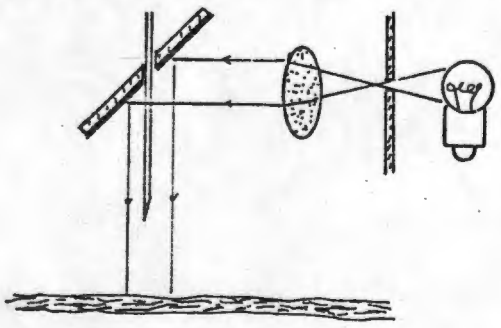

Fig.6-10

1. There is no contact with that part of the needle that enters the tissue.
2. Absence of a foot-guide makes it even easier to accommodate shorter needles.
3. Sterilization is much easier.

However, an inherent flaw in this system is that the guide and tissue have to be kept very still relative to each other for the duration of the puncturing procedure. Any small movement or lapse in concentration on the part of the operator could cause a significant deviation in the axis of the needle from the direction of the target.

§6.5 INDEPENDENT NEEDLE AXIS

It became clear that some system would have to be devised whereby the needle axis could be made adjustable relative to the axes of the ultrasonic beams. The following diagram represents the geometry of the needle and transducers all aimed at a target.

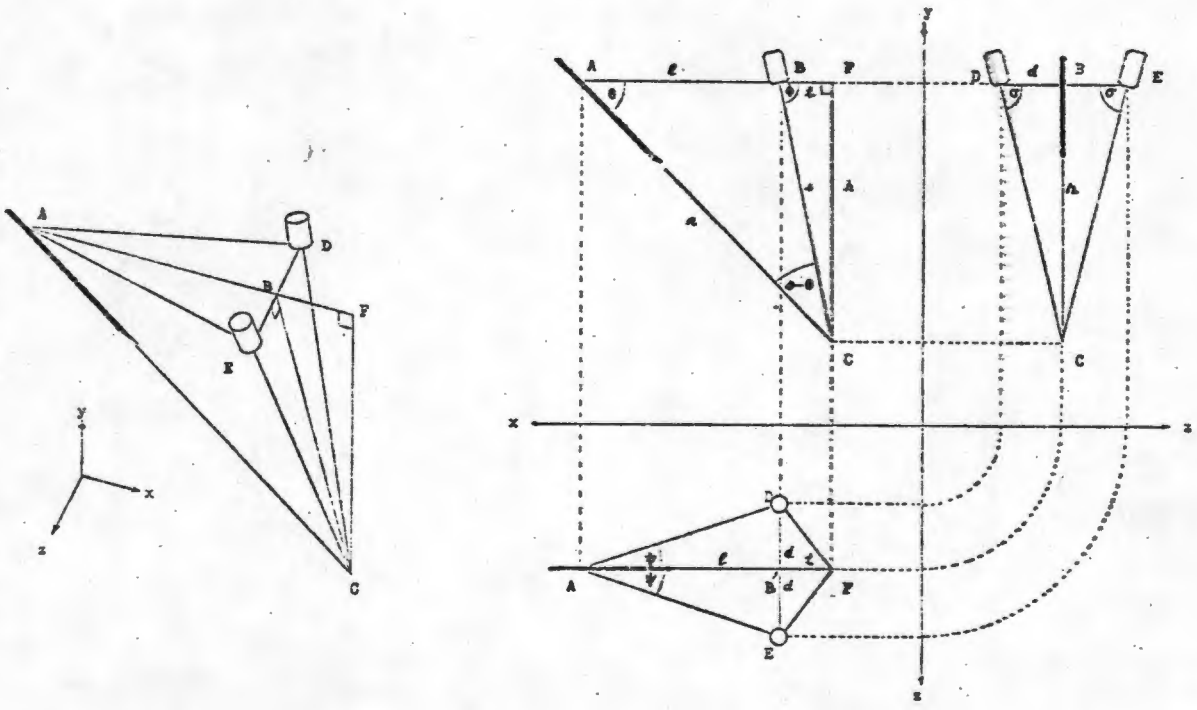

Fig.6-11

The axis of the needle n passes through the incision point A on the skin plane, to point C which we call the triaxial intersection point because the axes of the ultrasonic beams originating at D and E also pass through this point.

The question which now arises is whether it is possible to devise a scheme whereby the intersection point of the two beams could be arbitrarily altered to accommodate vessels at various

depths, and at the same time ensure that the axis of the needle still passes through that intersection point.

Firstly we need to establish how to manipulate the transducers in order to alter the depth h, where $h = d\tan\sigma$.
There are three alternatives:

a. The transducers can be rotated, making σ the variable.

b. The transducers are moved towards each other for locating shallow vessels and away from each other for deep vessels. This means that d is the variable.

c. Both σ and d are variable.

Having a variable σ has an advantage in that the transducers can be kept well away from the skin incision, even for shallow vessels. In addition the ultrasonic coupling gel would tend to stay in one place during depth scanning. However, any adjustment to angle σ will alter the angle of incidence and reflection of the ultrasonic beam. This means that subjective assessment of the signal strength can no longer be relied on to give any useful information, since the returned signal can be expected to change with this angle.

A second point against the variable σ scheme is that the system would have to be able to accommodate a very large range of angles between incident and reflected beams at the target. It is difficult to envisage how well superficial vessels could be located, because this angle would become very obtuse for shallow vessels.

Finally it will be shown later that it is difficult to link the needle axis mechanically to angle σ.

If σ is kept constant and d is made the variable, none of these difficulties arise. Perhaps the most important point in favour of the variable d system is the ease with which it can be implemented.

The needle Axis

The next step is to investigate what has to be done to the needle axis to ensure intersection at the triaxial intersection point. Again there are three alternatives. With reference to Fig.6-11:

a. The angle of entry θ can be made adjustable or
b. The distance ℓ can be varied or
c. Both θ and ℓ can be made adjustable.

Fixing ℓ and making θ variable means from a purely functional point of view that the operator is able to insert the needle at any angle to the skin, but is unable to chose the incision point on the skin relative to the vessel puncture site. In general, superficial vessels tend to be punctured at a shallow angle, with the skin incision point relatively far away from the vessel puncture site. The converse is true for deeper vessels. The sort of flexibility that will allow the operator to do that is not possible with this system.

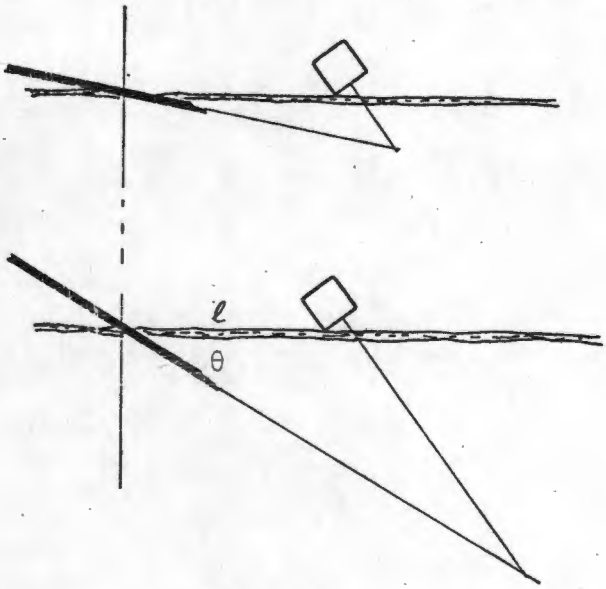

Fig.6-12

Fixing θ and making ℓ the variable means that the operator can chose the incision point of the needle, but cannot chose the angle of entry. The only way around this problem is to use this system in conjunction with the adjustable foot-guide mechanism discussed earlier. Nevertheless, even with this system the distance ℓ would become very large for deep vessels. In the case of

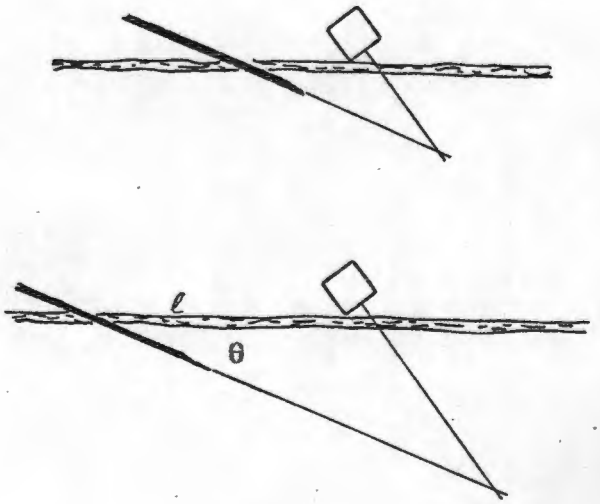

Fig.6-13

Subclavian cannulation, for example, this would not work since there is only a very small anatomical window through which to operate.

The second problem associated with such a system is that the particular angle of needle entry the operator may choose, automatically dictates the angle at which the ultrasonic beam enters the tissue. Finding arteries with the beam at right angles, say, to the blood flow would not be a problem since pulsation of the arterial walls gives a very powerful signal on which one can home in, but veins do not pulsate sufficiently for the detection of wall movements.

In the light of these limitations it can be argued that:

The optimum solution is one which allows complete freedom of movement of the needle, where both the skin incision location and the angle of entry can be chosen independently of the angle between the ultrasonic beam and the surface of the skin. The only proviso is that the integrity of the triaxial intersection point must be maintained.

§6.6 TRIAXIAL INTERSECTION INTEGRITY

Consider the geometry of Fig.6-11.

$$\langle BCA = (\phi-\theta)^{\circ}$$

and with reference to ΔABC

$$\frac{\sin(\phi-\theta)}{\ell} = \frac{\sin(180^{\circ}-\phi)}{r} = \frac{\sin\phi}{r}$$

$$r = \frac{\ell \sin\phi}{\sin(\phi-\theta)}$$

$$h = r\sin\theta = \frac{\ell \sin\phi}{\sin(\phi-\theta)} \sin\theta$$

$$d = \frac{h}{\tan\sigma} = \frac{\ell \sin\phi \cdot \sin\theta}{\sin(\phi-\theta)\tan\sigma} \qquad (6\text{-}1)$$

Translocation of needle along the x-axis

Equation 6-1 tells us that if we fix ϕ and σ and keep θ constant, then d becomes directly proportional to ℓ. This is intuitively obvious, since a change in ℓ then gives rise to a picture which is related to Fig.6-11 by similar triangles.

We can therefore consider AD as a locus along which D moves as ℓ is varied. Mechanically this can be implemented very readily. One simply machines a slot (guide rail) into a plate (guide rail platform) which is attached at point A. A pin attached to the transducer housing D fits into the slot and runs freely in it. Relative to ground reference, however, it is constrained to move in the z-direction only.

In order to get a feel for what was happening in three dimensions, a model was built from pieces of perspex and brass rod.

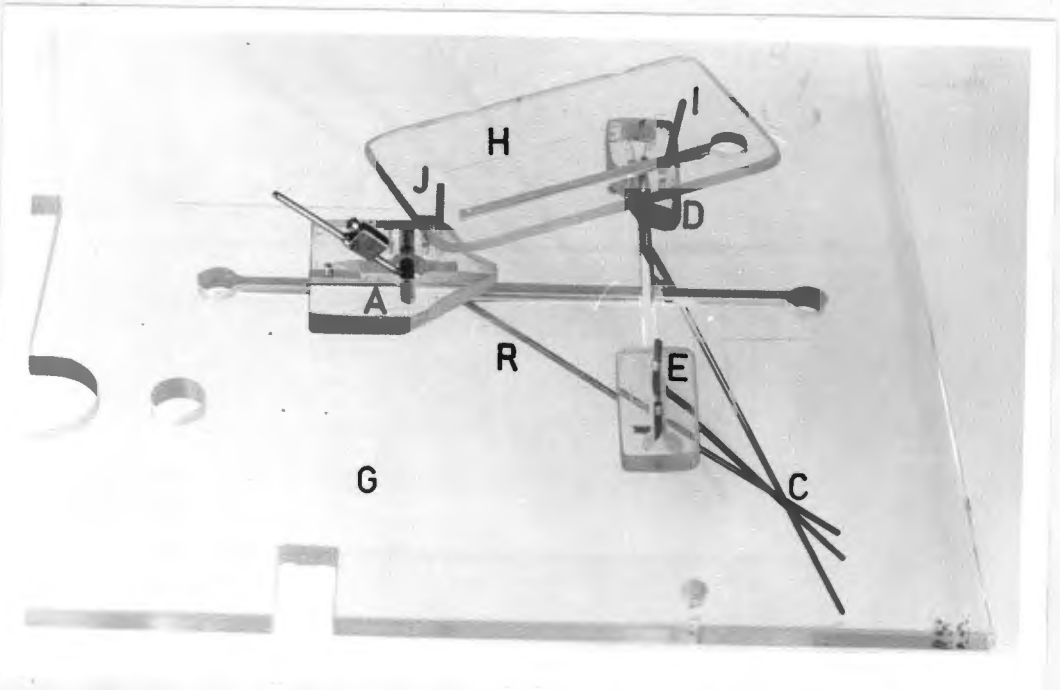

Fig.6-14

R represents the axis of the needle. D & E are the two transducers with the long brass rods representing the axes of the ultrasonic beams. A short vertical brass rod I represents the pin that slides along the guide rail. G is the plane of the skin. A cross has been cut into this plane with

the long axis representing the locus of the needle sliding bodily along the skin surface. The short axis of the cross represents the locus of the two transducers as they move to and away from each other. *H* is the guide rail platform.

In this photograph the guide rail which operates transducer *E* is missing. This was left out for simplicity since the model is symmetrical about the vertical plane in which the needle axis moves. The triaxial intersection point always lies in this plane and any analysis based on one transducer will hold for the other.

Another point that needs to be mentioned here is that the slot representing the guide rail falls neither directly over the needle incision point *A*, nor over the transducer *D*. This is quite in order provided that the guide pin in the transducer housing *I*, the origin of the needle axis platform *J*, the needle incision point *A* and the transducer *D* itself all form a parallelogram.

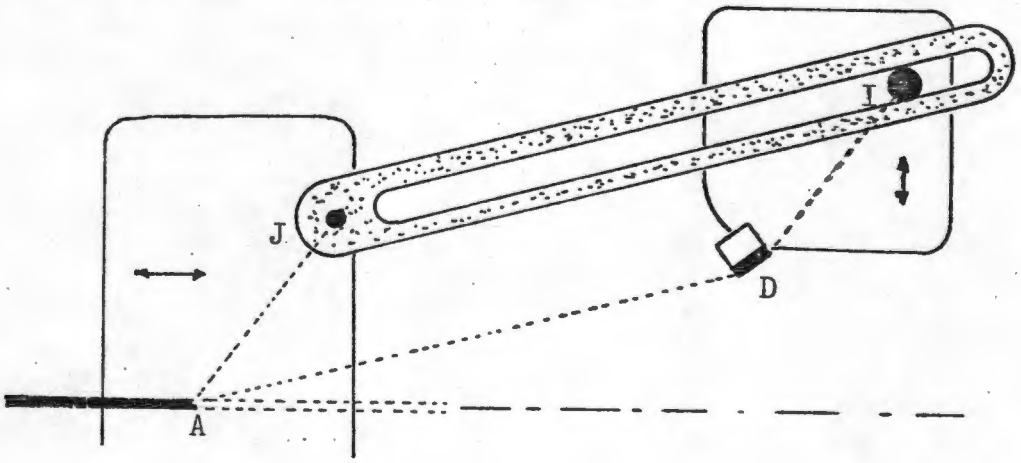

Fig.6-15

The three moving parts on this model move in the following way:

1. The needle and guide rail are constrained from rotating.

2. As the needle axis platform slides forward along the major axis, the guide rail slides over the guide pin *I* on the transducer platform, causing it to slide inwards along the minor axis.

3. Integrity of the triaxial intersection point is maintained as it rises towards the surface plane.

4. The triaxial intersection point drops when the needle axis platform slides backwards.

In Fig.6-16 an idea of a practical implementation has been sketched. The needle passes through two notches *A* and *K* cut into the guide stubs. The two guide stubs can slide towards each other along brass rod *L*, which is firmly attached to guide rail platform *H*. As the guide rail slides across *I* and *M*, transducers *D* and *E* are forced to move towards or away from each other. Meanwhile, the needle can be pushed down inbetween the transducers.

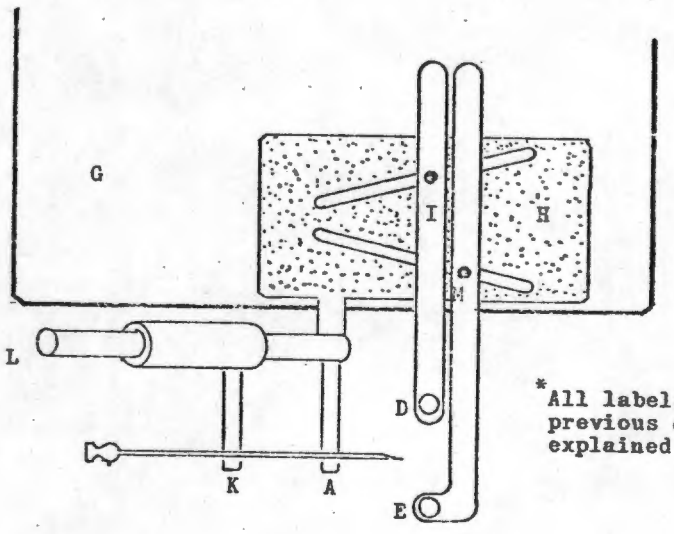

*All labels are consistent with previous drawings and are explained in the text

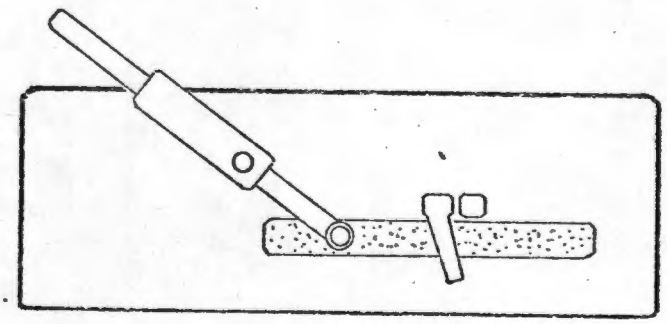

Fig.6-16

Rotation of the needle about the z-axis

Having established a mechanism for moving the transducers in sympathy with needle movement along the x-axis, we now look at a method for relating the *angular* position of the needle to the position of the transducers.

We have from equation 6-1

$$d = \frac{\sin\phi \quad \ell\sin\theta}{\tan\sigma \quad \sin(\phi-\theta)}$$

It is not immediately obvious from this expression how one could relate d to θ mechanically and keep ℓ as a variable at the same time. But by working with the model it soon became clear that it might be possible to relate ψ (the angle between the guide rail and the x-axis) mechanically to θ. In fact

$$\psi = \text{arc } \tan(d/\ell)$$

$$= \text{arc } \tan\left[\frac{\sin\phi \ \sin\theta}{\tan\sigma \ \sin(\phi-\theta)}\right] \qquad (6\text{-}2)$$

which is fortunately independent of 'ℓ'.

While the expression looks messy, it is clear that a profiled cam could be used to mechanically link θ with the angle of the guide rail ψ. Every point on this cam would have to be calculated according to equation 6-2.

Some thought was given to the possibility of making σ variable instead of d when adjusting the system for vessels at various depths. From equation 6-1 we can write:

$$\sigma = \text{arc} \cdot \tan\left[\frac{\ell \ \sin\phi \ \sin\theta}{d \ \sin(\phi-\theta)}\right] \qquad (6\text{-}3)$$

Equation 6-3 was rearranged, broken down and carefully related to the model, but the link between this equation and the mechanical solution could not be found.

§6-7 DEVELOPMENT OF A PRACTICAL CAM SYSTEM

Development of a satisfactory cam arrangement was a process that took unexpectedly long. What follows is an account of the major steps in the development of the system.

The problem was one of linking rotation of the needle about the z-axis to rotation of the guide rail about its y-axis pivot. (The axes are defined in Fig 6-11). A simple gear system is clearly not possible since the relationship between ψ and θ is not linear.

The Wire Cam

Dozens of possibilities for doing this spring to mind almost immediately. The first promising idea was one in which a loop of stiff wire in the form of a semi-circle was linked to the needle axis R as illustrated.

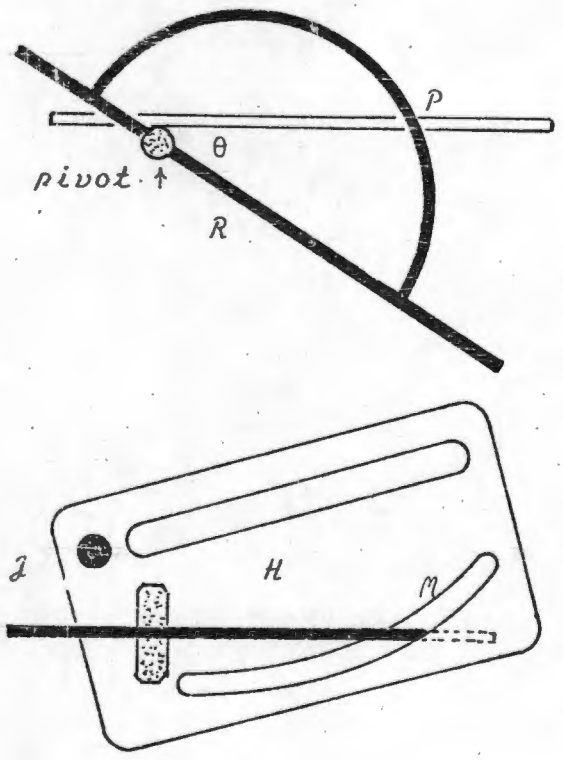

Fig.6-17

The intersection of the loop with the surface plane is denoted by P. It will be seen that as θ changes, so P moves along the surface of this plane. The guide-rail driving the transducer is cut into a platform H which rotates about pivot J, which in turn, is part of the needle axis platform. The cam-follower profile M cut into the guide rail platform is calculated from Eq.6-2 and from a knowledge of P for the various values of θ. P is readily calculated from the geometry of Fig6-17.

The model was built with $\sigma=75^{\circ}$ and $\phi=40^{\circ}$, and is illustrated in Fig.6-18. After playing with it for a while, it soon became clear that this was a poor design.

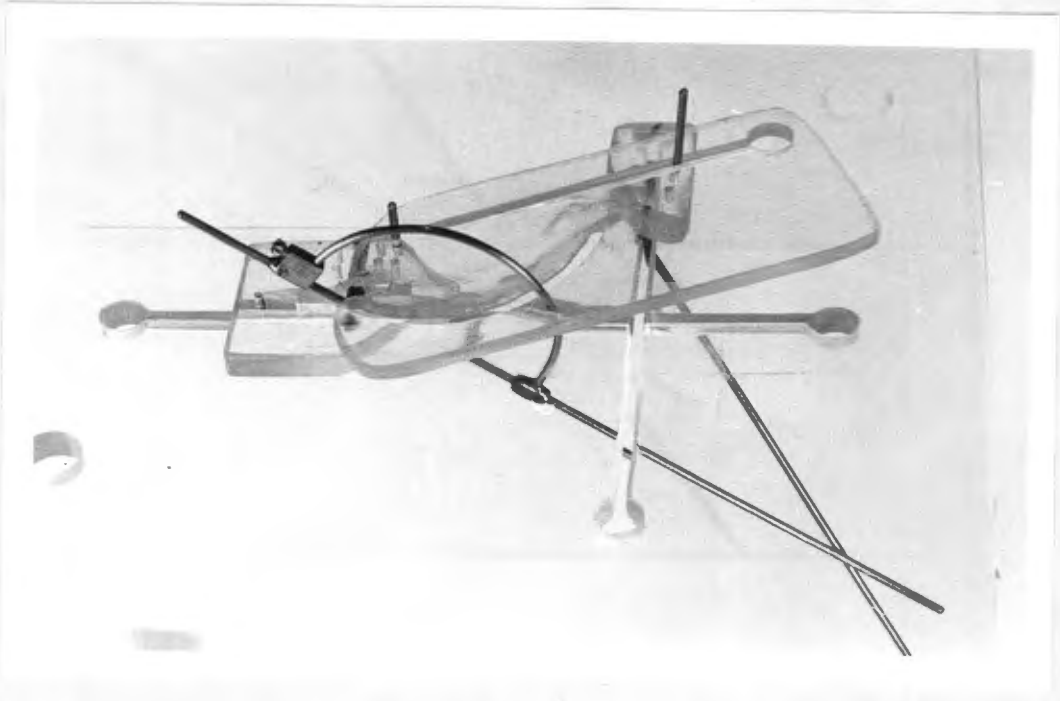

Fig.6-18

1. The sliding action of the wire through the slot in the guide rail platform tended to jam the system at certain angles. This results from the fact that the wire has to be pulled through the slot at an acute angle to the surface of the platform. If it entered at right angles then *P* would not move along the x-axis.

2. The driving element was made a wire arc rather than a profiled cam, since the system had to operate in both directions. Mechanically this is not a simple arrangement to implement.

3. The system gave the impression of being mechanically clumsy.

The Involute Cam

The next major advance was made when a cam was developed, attached to the needle axis *R* and sliding at all times at right angles to the cam follower *CF* which was cut into the guide rail platform *H* (see Fig.6-19). A spring return mechanism was to ensure that the system would operate in both directions. The principle of operation can be established from this diagram, bearing in mind that both members are only capable of rotating about their respective pivots *A* and *J*.

Profiling the cam and its follower is done as follows:

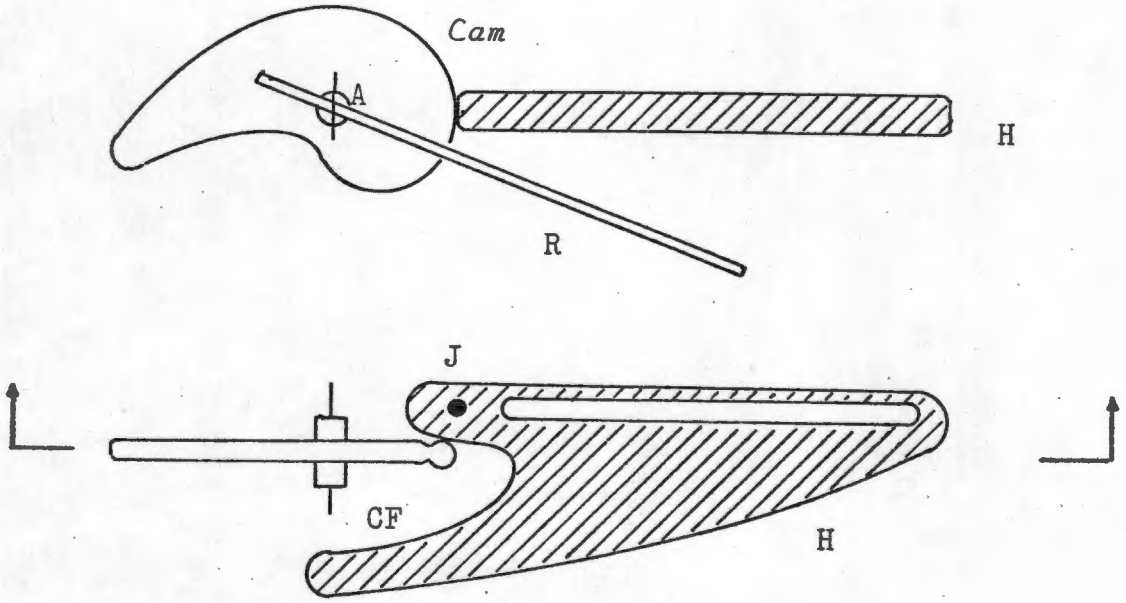

Fig.6-19

We still have the same relationship between θ and ψ given by equation 6-2, and plotted in Fig.6-20 for $\sigma = 75^{\circ}$ and $\phi = 40^{\circ}$. The reason for chosing these values is not important at this stage since we are only dealing with a model. What rather surprisingly turned out to give trouble was profiling the cam on the needle pivot axis, to ensure a meeting with the follower at right angles for all values of θ . In fact, unless one realizes that this profile is nothing more than an involute, the problem appears to be impossible to solve.

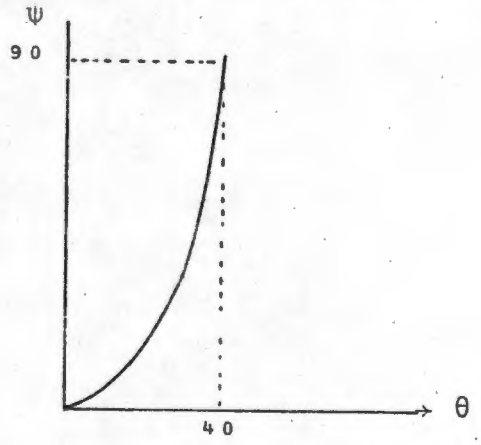

Fig.6-20

It will be remembered that the involute is the locus of the end of a string that is being unwrapped from around a cylinder of diameter 2a.

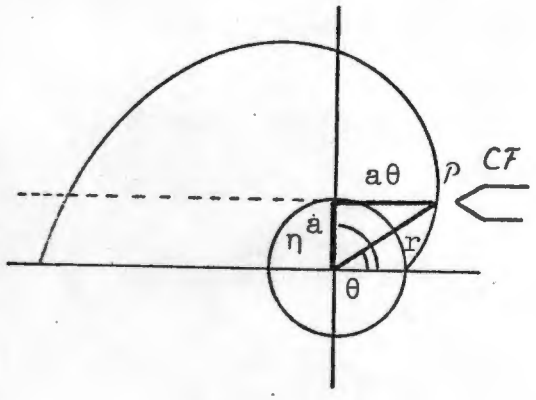

Fig.6-21

Hence:

$$r^2 = a^2 + (a\theta)^2$$

$$r = a(1 + \theta^2)^{\frac{1}{2}} \qquad (6\text{-}4)$$

$$\eta = \theta - \text{arc tan}\,\frac{a\theta}{a}$$

$$= \theta - \text{arc tan}\theta \qquad (6\text{-}5)$$

Since both 'r' and η are functions of the variable θ only, a table can be drawn up of r vs. η. These are marked off on a suitable disc, and from this the involute profile can be cut. The contact point P between the cam and cam follower must be located a distance 'a' above the needle pivot axis.

The profile on the cam follower can also be readily calculated. Since the horizontal displacement of P along the x-axis is given by $a\theta$ and ψ corresponding to each θ is given by equation 6-2, a unique spot can be found on the guide rail platform for each P. The line joining these dots is the cam follower profile.

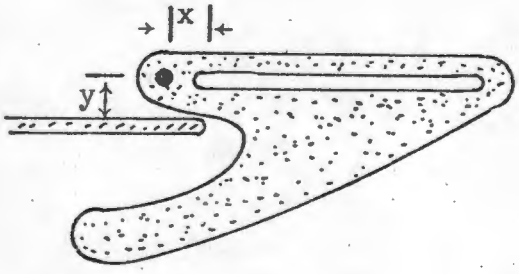

Fig.6-22

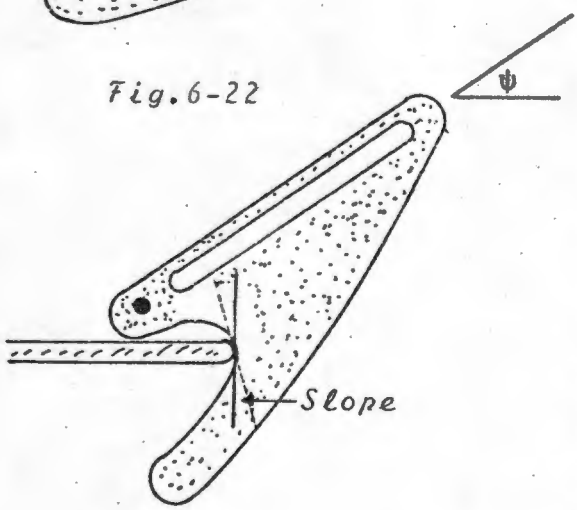

Fig.6-23

Several cam follower profiles were calculated based on some arbitrary guide rail pivot points. Consider point $P(x,y)$, the point at which the cam and cam-follower meet when $\psi = 0$. Four profiles were calculated for $P = (0,a)$; $(0,\frac{1}{2}a)$; (a,a) and $(a,\frac{1}{2}a)$ where 'a' is a constant. Of the four it was decided to build the last one into the model. The criterion used for judging these schemes was based on the need to obtain a maximum slope at the tail end of the cam follower, where the mechanical advantage is smallest. ($\frac{d\psi}{d\theta}$ is very large at large values of ψ - see Fig.6-20.)

Clearly the greater the slope at this end, the less is the risk of jamming. Fig.6-24 illustrates the outline of the guide rail platform that was actually cut for this model.

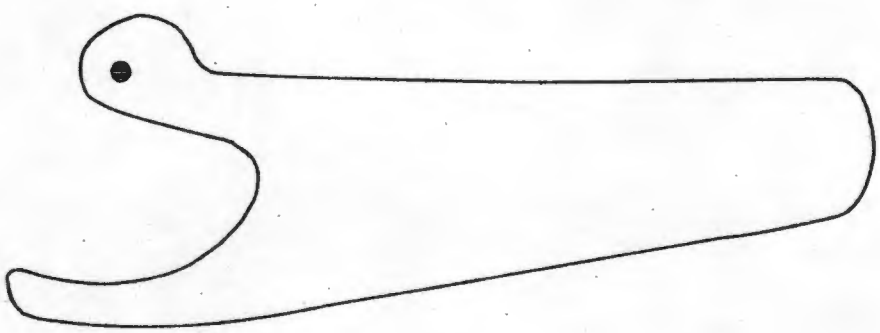

Fig.6-24

Before discussing the model that was built, we need to recap on an important concept. It should be understood that there are three platforms that move relative to the base. The first represents the transducer housing and ultrasonic beam and slides along the z-axis only. For the sake of simplicity the other transducer platform has been left out. The second platform carries the needle axis and is constrained to slide along the x-axis of the base only. Finally, the guide rail platform pivots on the needle axis platform.

At this stage ideas on the practical implementation of the system were considered, and it was decided to incorporate these into the model. Referring back to Fig. 6-16, it will be seen that if $\mathcal{G}$ represents the box in which the "mechanical computer" is housed, three elements have to protrude from the housing and move relative to it. The first two are the bars carrying the transducers. Since these slide axially out of the box they are easily sealed with 'O' rings. What presents a major sealing problem, however, is the shaft that holds the sliding mechanism which clamps the needle, since this moves radially along the outside of the box. The possibility of using a concertina seal was not seriously considered for a medical instrument. One solution lay in having the shaft holding the needle transport mechanism enter the back of the box axially as illustrated in Fig.6-25. While this idea

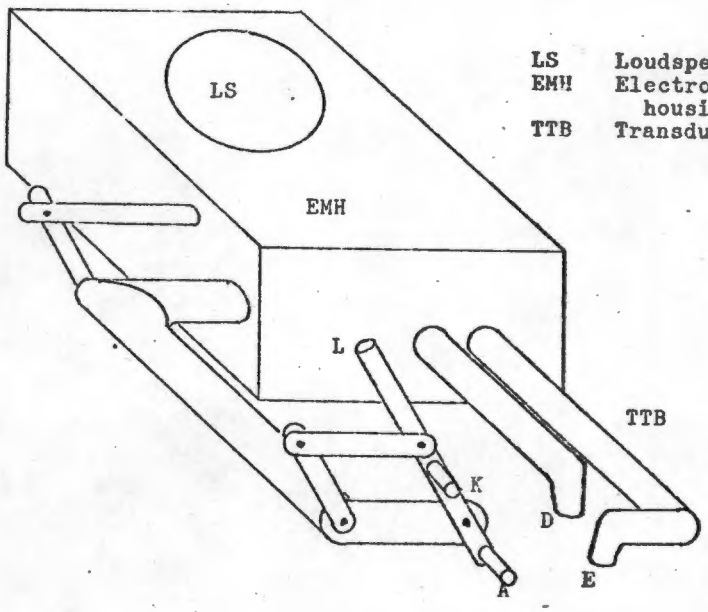

Fig.6-25

was to be dropped later, it served as a basis for the prototype.

The principle is well illustrated in Fig.6-27, which is a photograph of the model. It was built on the same base as was used previously, but in addition to the base a new needle axis platform had to be constructed (Fig.6-26). A cam idler was installed between the involute profile at *N* and the cam follower at *Cf*.

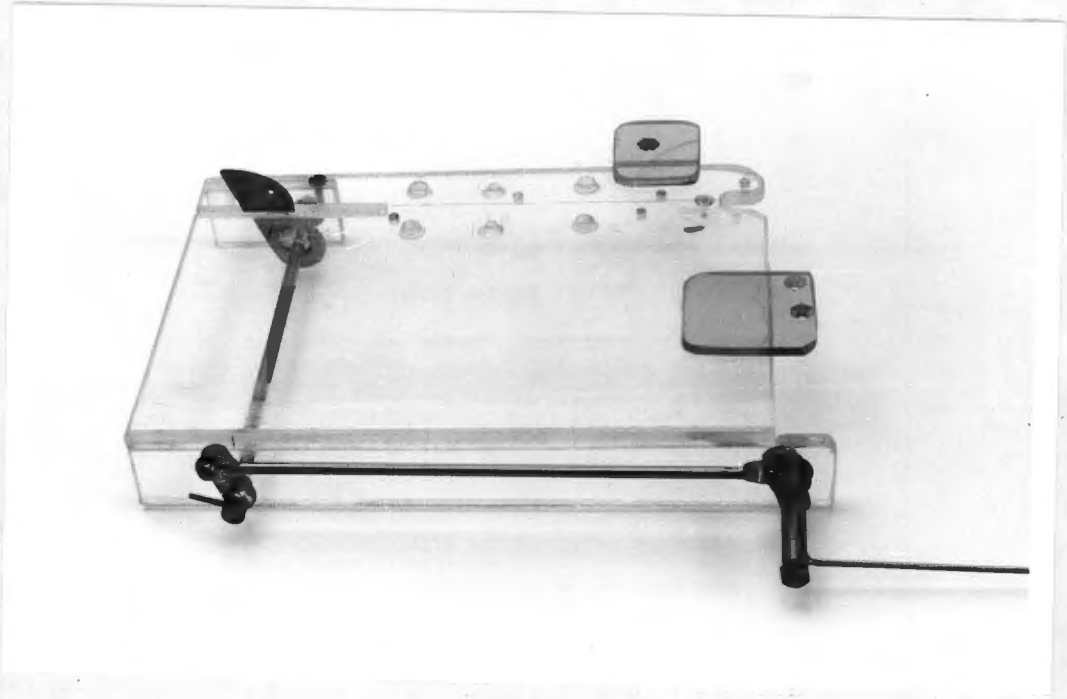

Fig.6-26

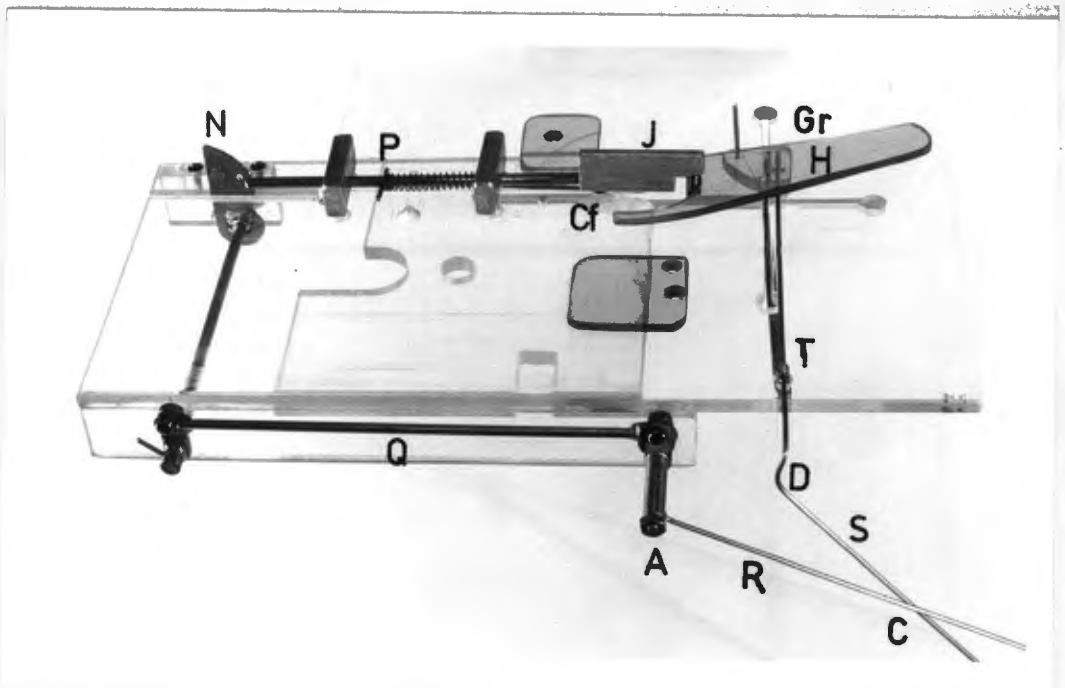

Fig. 6-27

The system operates as follows: As needle axis *R* pivots about axis *A* it transmits the angle through which it has turned to *N* via pushrod *Q*. The involute edge of *N* slides in a notch at the end of idler *P*. A return spring mounted on *P* ensures that the two surfaces never part. The other end of the idler fits into the cam follower surface *Gr* of the guide rail platform *H*. A roller at its extremity was installed to reduce friction in order to prevent jamming. Now, as *R* is turned about axis *A*, the guide rail edge *Gr* pushes the transducer platform outwards. Return spring *7* (poorly illustrated here) ensures a meeting of the two surfaces. Thus it can be seen how sliding of the needle axis platform in the x-direction, or angular rotation of the needle about the axis *A* causes the ultrasound beam *S* to move in the z-direction, thus maintaining the triaxial intersection point *C*.

Not alltogether unexpectedly the system tended to jam for large values of ψ (Fig. 6-23). In addition, the return spring mechanism tended to load a portion of the system that was already experiencing a mechanical disadvantage. The third problem area could only be identified by working with the model. It was obviously going to be very difficult to make the system accurate. The forces operating the follower had a tendency to push the cam idler out of alignment. Any minute movement here was reflected in a very large angular misalignment of the guide rail platform.

The Intermediate Scroll System

The tendency of the system to jam was viewed with great concern. The peculiar relationship between θ and ψ (Fig.6-20), meant that at small angles there would always be a mechanical advantage from θ to ψ while at large angles the reverse was true. At this point it was therefore decided to introduce an intermediate stage. This would inevitably complicate the system, but there is no doubt that any attempt made at resolving this mechanical advantage problem would be well worth while.

The principle was to make an intermediate part that would drive both the needle axis and the guide rail platform with a mechanical advantage towards both these elements for all angles. The new concept is best discussed by referring to a photograph of the model that was built (Fig.6-29). The platform used in the previous model was altered slightly to accommodate the new mechanism (Fig.6-28).

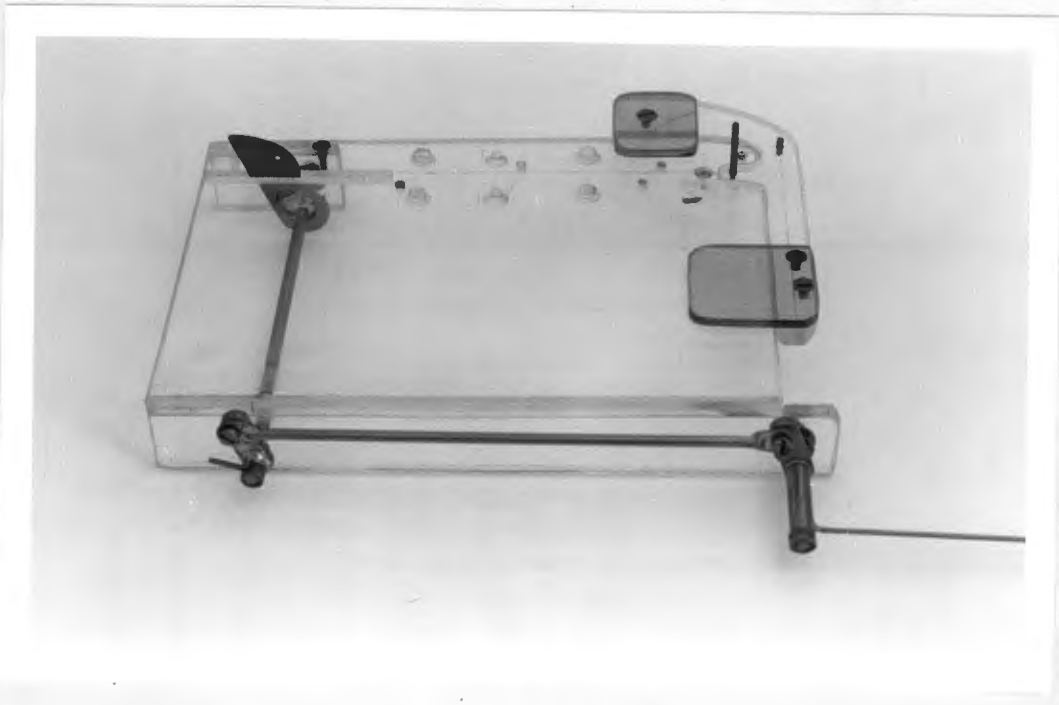

Fig.6-28

The cam idler was replaced by a link P (Fig.6-29) which was attached at one end to the involute lever by means of a pin. (The involute surface was therefore no longer utilized). The other end fitted into the slot of a scroll (scroll pin S_P, Fig. 6-30). By turning the scroll, the link P is pushed or

pulled in the x-direction, pulling lever *N* and thereby setting the needle axis to any desired angle. Because of the forward mechanical advantage it was not possible to turn the scroll by tilting the needle. In fact, the scroll was designed to go around a full 360° for a 40° tilt in the needle.

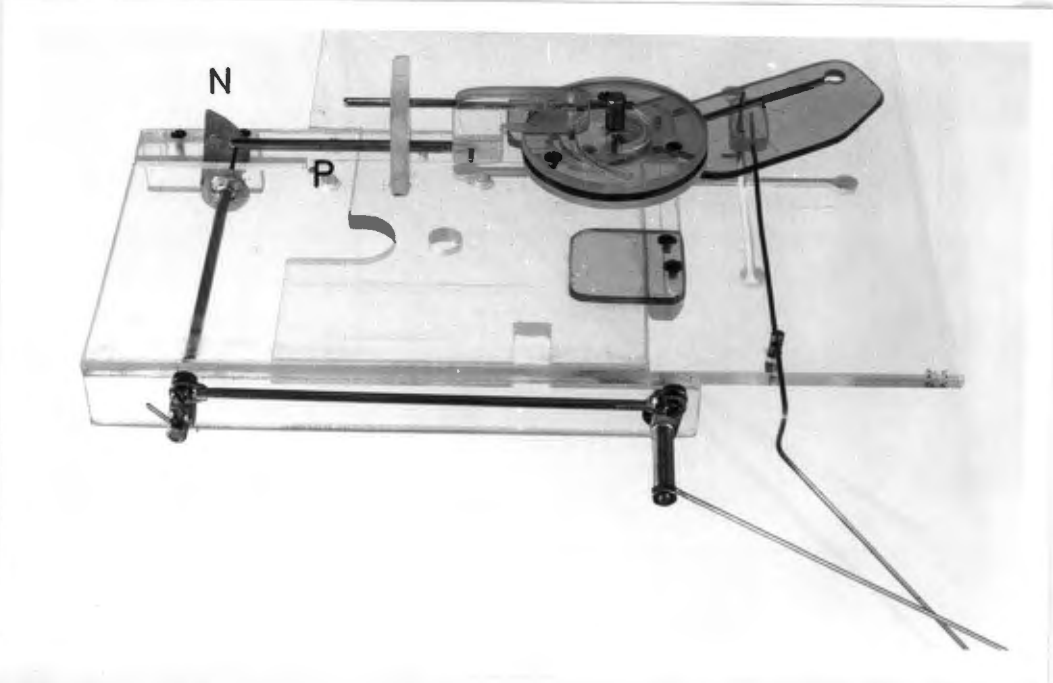

Fig.6-29

Fig.6-30

The scroll system was composed of two separate scrolls with an isolating disc sandwitched between them (Fig 6-31). The purpose of the top scroll has been discussed above. The lower scroll was used to turn the guide rail platform. Thus, by turning the scroll through 360°, both the needle axis angle and the guide rail platform could be set together.

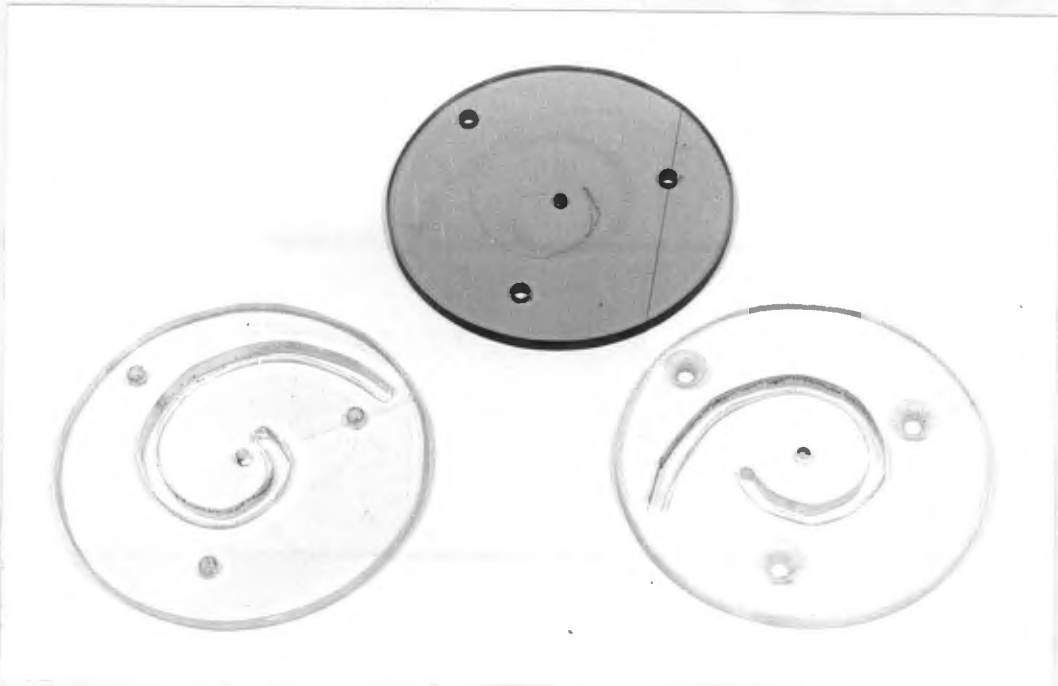

Fig.6-31

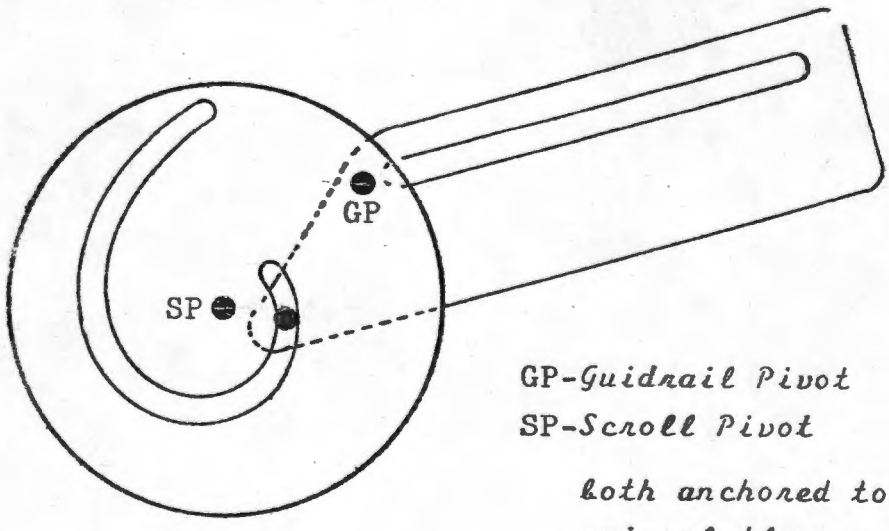

GP-*Guidrail Pivot*
SP-*Scroll Pivot*

both anchored to needle axis platform.

Fig.6.32

For this model the lower scroll driving the guide rail platform was made a linear function of the scroll position. Thus if η is the angle through which the scroll rotates and k is a constant,

$$\psi = k \cdot \eta$$

Since for each ψ there is a unique θ given by equation 6-2, a table can be drawn up between the displacement of link P and then the upper scroll can be cut accordingly.

An exact geometrical analysis will not be given here. A comprehensive calculation for a similar scroll which was used in the prototype is given in appendix 6-1.

By this stage the model was very pleasing. All possible problems appeared to have been ironed out. The fact that the needle could not be tilted without setting the scroll was found to be superior in concept, since the operator would not have to worry about keeping the angle steady while pushing the needle home.

The next step was to build a *model* of the *prototype* (as opposed to the concept). During construction it became painfully obvious that the rear entry into the box had a serious drawback. Since the needle axis platformwas to be a U-shaped structure (Fig.6-25), any small forces at the needle could throw the axis of the needle right off the beam intersection point. To make this U-shaped structure completely rigid did not appear to be a practical solution.

A second disappointing aspect was the clumsy system of links and pushrods located in the needle axis platform. This would have involved a complicated mechanical arrangement to implement in practice.

Since the basic concept appeared to be sound, however, there was no need for any further development along these lines. Only the practical implementation would require further attention.

§6-8 PRE-PROTOTYPE MODEL

The next stage in the development of the guide was marked by an intense search for some alternative way of linking the needle axis platform to the external needle guide slide whilst ensuring a satisfactory seal.

During this stage I learnt of the existence of a clockmaker. While visiting him it became clear that custom made gears could form an important basis for the design, since they vastly improved design flexibility.

There appeared to be only one alternative to the rear entry problem, and that was front entry. Since entry had to take place well behind the transducer transport bars, a recess had to be cut into the base of the box. This is illustrated in Fig. 6-33.

Fig.6-33 is a diagram (not an accurate mechanical drawing) of the internal mechanical arrangement necessary to maintain triaxial intersection between needle axis and the axes of the ultrasonic beams. The needle transport slide and the transducer mountings have been omitted in this drawing. The system operates as follows:

(Note: Labels no longer conform to previous drawings.)
The needle axis platform (b) slides through seals (o) and (p) in the x-direction. Position control knob (f) engages a thread on the plafrom position shaft (u), so that x-direction movement is controlled by this knob. For example, clockwise rotation of the knob would cause the needle axis platform to slide back towards the knob.

(j) And (k) are the two transducer transport bars. The needle transport slide (not shown) is attached to shaft (q). The needle axis angle control knob (e) is linked through the drive shaft (v), a worm (d) and a gear (g) to shaft (q). As this knob is turned, so the needle axis angle θ tilts from about 5° through to about 40°. At the same time the angular position of the scroll (h) is controlled also through the angle drive shaft, a second worm (c) and a gear, by the needle axis angle control knob. The angular position of the scroll is therefore directly linked to the angle of the needle axis. A spiral groove is

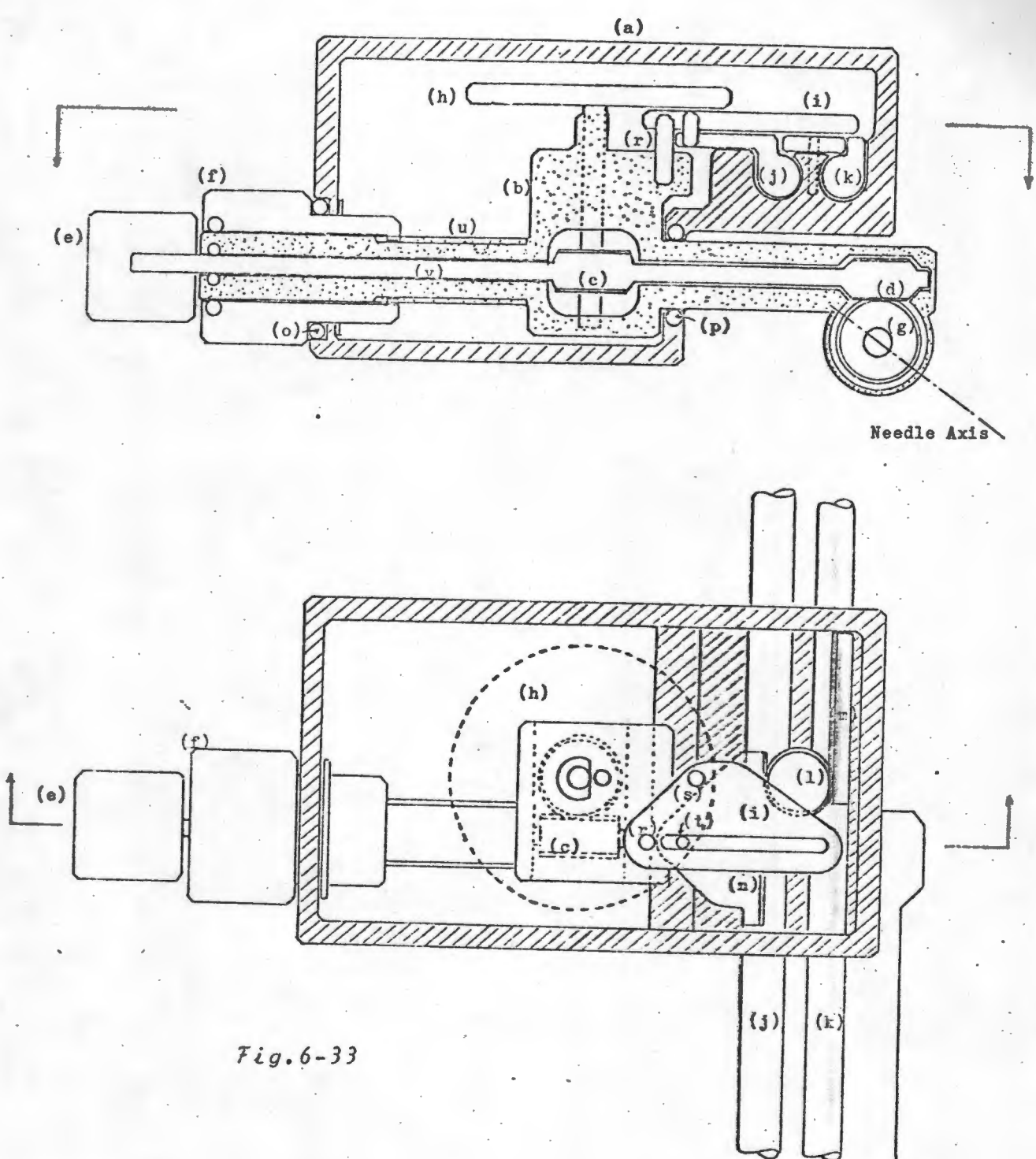

Fig.6-33

(a) Aluminium box
(b) Part of needle guide platform
(c) Scroll drive worm
(d) Needle axis angle drive worm
(e) Needle axis angle control knob
(f) Position control knob
(g) Needle axis angle drive gear
(h) Scroll disc
(i) Guide rail platform
(j) Inner transducer transport bar
(k) Outer transducer transport bar
(l) Pinion
(m) Rack
(n) Rack
(o) PTFE seal
(p) PTFE seal
(q) Needle Axis angle shaft
(r) Guide rail platform pivot
(s) Guide rail platform crank roller
(t) Transducer transport bar crank roller
(u) Needle axis platform position shaft
(v) Needle axis angle control shaft

cut into scroll disc (h).

The guide rail platform (i) rotates about its centre of rotation (r). A pin (s) attached to the guide rail platform is free to slide in the spiral groove. As the disc (h) rotates, the guide rail platform will swing about (r). The exact relationship between the angle through which the needle axis tilts and the guide rail platform swings is determined by the geometry of the spiral.

Roller (t) is attached to a platform which in turn forms part of the transducer transport bar (j). A rack (n), also attached to the bar, drives pinion (l) as bar (j) slides along its axis in the z-direction. As the pinion rotates it drives rack (m) in the opposite direction to (n), thereby establishing reciprocal movement between (j) and (k).

With proper calibration, the system incorporates all the principles that have been established earlier for maintaining triaxial intersection between beam and needle axes.

Design of the system reached a fairly advanced stage when it was decided to build a model as illustrated in Fig.6-34.

Fig.6-34

The model showed up some serious operational weaknesses in the system. These weaknesses resulted from poor location of the transducer transport bars. Because they slid out of the housing next to each other they tended to:

1. Obscure the skin incision point.
2. Obstruct the external needle transport slide mechanism.
3. Make mounting of the transducer housings awkward, because of the complicated bends in the transducer transport bars.
4. Give rise to difficulties in designing a rack and pinion system that would function correctly and which could readily be assembled.

§6.9 PROTOTYPE MODEL

A new look at the instrument from an operational point of view gave rise to the system illustrated in the model of Fig.6-35. This model represents no more than the mechanical part of the instrument. As can be seen, the two transducer transport bars no longer interfere with the view of the skin incision point. There is also far less apparatus around the transducer in contact with the skin of the patient. The transducers are housed neatly and the support mechanism does not get in the way.

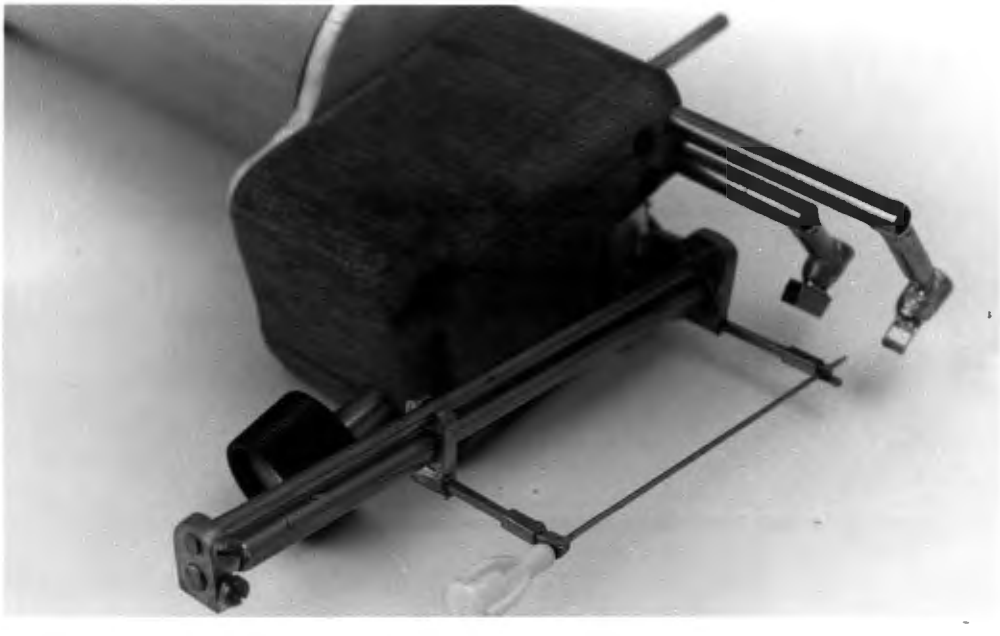

Fig.6-35

Jamming

Consider Fig.6-33. The two transducer transport bars in the final model (Fig.6-35) were to be located one over the other, either in position (j) or (k). Position (j) had to be excluded as an alternative, since in that position the guide rail platform could not be accommodated. For this reason position (k) was chosen. One of the main problems with this system was the fact that the two transducer transport bars had to be much further away from the guide rail platform roller (t) than before. This means that the axial force applied to the bars is not on the axis, but some distance away from it. This results in a moment being applied to the bar which can result in jamming.

Consider now the following diagramatic representation of the bar.

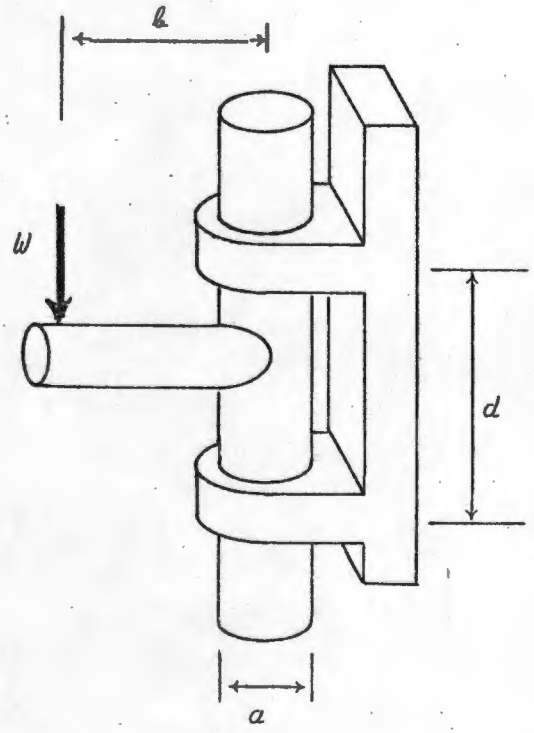

Fig.6-36

Normally we would expect a force W to cause the bar to slide through the two ring supports at either end. Intuitively we might worry about the system jamming. The question is "When and why would it jam?".

Jamming of the system would be considered a catastrophe!

If W is applied on the axis of the bar, the bar will definitely slide for large enough W. However, if W is applied far away from the axis, the system will almost certainly stick. (This principle is employed in some common workshop clamps.) There must therefore be some radial distance from the centre of the bar at which a force being applied causes the bar to be on the point of sliding/sticking. From an analysis of the force diagram we can show that for large values of ℓ the reactions are statically indeterminate. For

small values of ℓ i.e.: when the system slides, the problem becomes one of dynamic equilibrium. But at the critical distance, when the bar is at the point of sticking/sliding, then the problem reduces to one of static equilibrium, which is analysed in Appendix 6-2. From this analysis we have that the critical distance is given by

$$\ell_{crit} = \frac{d}{2\mu} \qquad (6\text{-}6)$$

where μ is the coefficient of friction and $\psi = 0$.

Therefore for sliding to take place $\ell < \ell_{crit}$ and for sticking $\ell > \ell_{crit}$. The interesting result here is that whether or not the bar will stick depends on ℓ, d and μ. It is, in fact, independent of W. This independence of W implies jamming, for irrespective of the applied load, the system will remain stuck if ℓ is large enough.

In the final instrument the transducer transport bar is not subjected to an axial force only. One of the problems here is that the guide rail exerts a force on the roller at an angle ψ (the same angle that the guide rail makes with the x-axis).

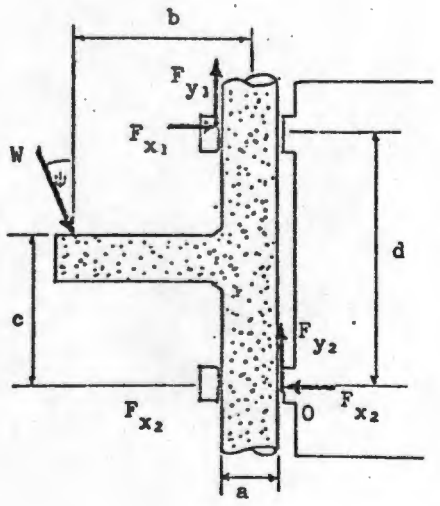

Fig.6-37

Consideration of Fig.6-37 will show that the forces have been arranged for small ψ. It was shown in appendix 2 that for small ψ

$$\ell = \frac{d}{2\mu} + (c - \tfrac{1}{2}\mu a - \tfrac{1}{2}d)\tan\psi$$

As ψ increases from 0 to a point beyond which $F_{x_1} = 0$, the forces F_{x_1} and F_{y_1} will flip to the other side of the bar. Under these conditions the two reactions become parallel. The system is therefore improperly constrained and thus statically indeterminate. Mathematically what this means is that there are not sufficient independent equations to solve

for the reactions. The result of this analysis is that we now know that for some values of μ the system will jam. In fact, if we put some real values into equation 6-6, we can calculate a maximum value for μ. From drawings of the final model we have: ℓ = 27mm and d = 45mm. Substituting these into equation 6-6 we get that μ = 0,83. We could make the rings from material with a low coefficient of friction, such as PTFE which has a μ = 0,1, in which case we would be safe from jamming. However, any bit of clotted blood on the transducer transport bar could change this effective coefficient of fricition. While μ is not often greater than unity it certainly can be and one could conceive that foreign material could produce such a result.

In addition it must be remembered that when ψ goes beyond a certain limit, the reactions become parallel and then there is no knowing what the system will do since it is statically indeterminate.

Solution to Jamming

It was decided not to take any chances with jamming, and the following arrangement was devised:

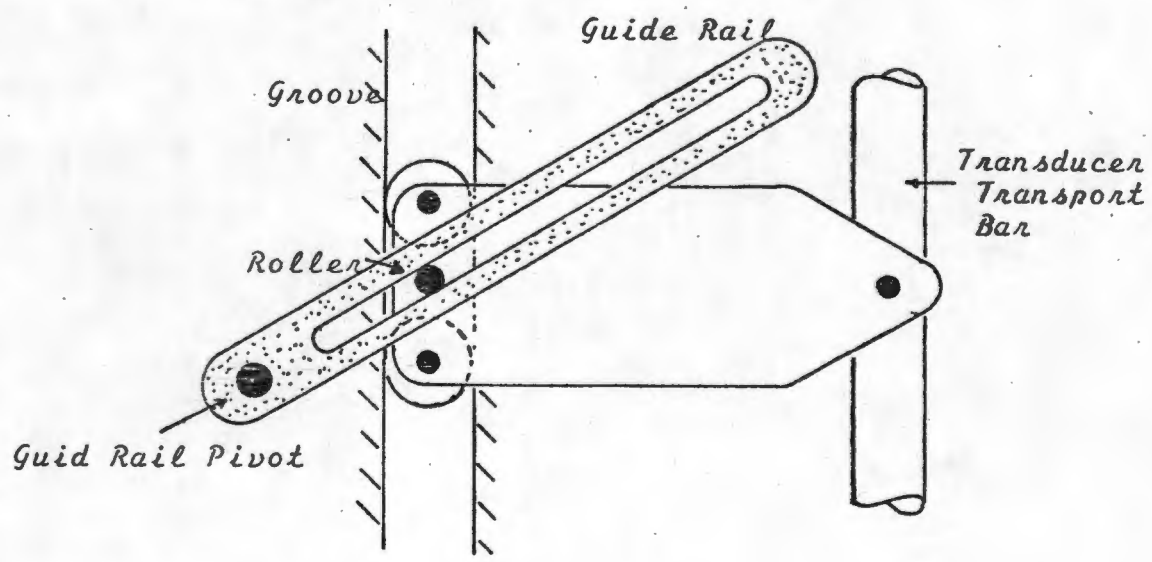

Fig. 6-38

The guide rail pushes on a roller, which is not mounted on the transducer transport bar as in Fig.6-33, but on a float rolling freely in a groove parallel to the transducer transport bars. The coefficient of rolling resistance is always much less than that of sliding resistance, and in addition can be carefully controlled since the float is inside a sealed box. In principle, therefore, it should be possible to eliminate jamming.

The transducer transport bar is driven so close to its axis, that jamming here is also extremely unlikely. When constructing the system it must be remembered that the bar may only be driven at a point about which the driving arm can rotate. If this precaution is not observed the theory will break down and jamming may occur.

Some of the other advantages of the rolling float system are that:

1. While it looks more complicated, it can in fact be readily made and assembled.
2. The pinion can be kept clear of the guide rail.
3. Important friction areas can be lubricated.

§6.10 NEEDLE AXIS PLATFORM POSITION SHAFT

In the model of Fig.6-33 the needle axis platform position shaft and the needle axis angle control shaft were concentric. This idea was thought to be ideal from an operational point of view, and it was thought that it would be relatively simple to build. It turned out,however, that the advance mechanism was very awkward to construct and there were fears about its reliability. The difficulties arose because of the need to be able to dismantle the structure.

A second troublesome feature was the fact that the needle axis angle control knob remained stationary relative to the needle guide platform. This meant that during various stages of operation the two knobs would be axially displaced relative to one another. In addition some form of clutch was thought to be essential for the needle axis angle control knob, to prevent damage to the scroll and guide rail mechanisms. The only site for the clutch was inside the control knob, and this seemed a clumsy arrangement.

By separating the two shafts, the two knobs would lie next to each other. The results of such a change were that:

a. Two seals were needed instead of three.
b. The advance screw was immeasurably simplified.
c. The two knobs were always flush up against the housing.
d. The unit was much easier to assemble.
e. The diameter of the needle axis angle control shaft could be increased.
f. The clutch system was relatively simple to implement.

The clutch consists of a brass sleeve fitting over the angle control shaft. A slot runs along the length of the sleeve. At the

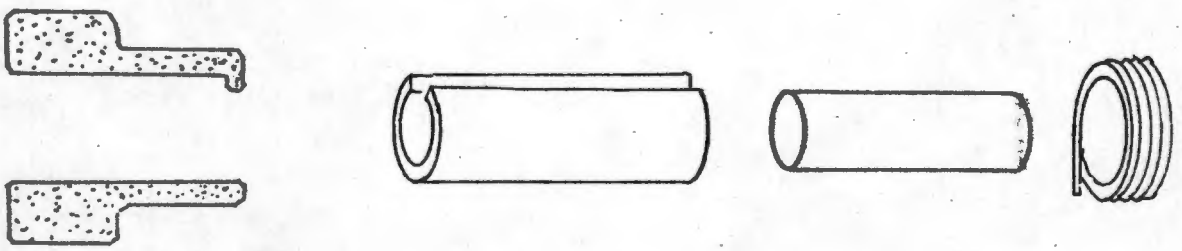

Fig. 6-39

knob end it is driven by a tongue from the knob which fits into the slot. The other end is compressed over the shaft by a spring, the tension of which can be set for the best possible yield point.

This arrangement seemed to be so much easier to construct, and since operational inferiority over the pre-prototype system was by no means established, this system was to be implemented in the prototype.

§6-11 THE EXTERNAL NEEDLE GUIDE SLIDE

The first arrangement ever considered was discussed earlier and illustrated in Fig.6-34. While it was neat and fairly compact, it did suffer from two fundamental drawbacks. Firstly, it did not provide a smooth action and had a tendency to jam. Secondly, the groove at the back of the two concentric cylinders slid over the attachment plate of the guid pole, providing angular locking so that the head and foot guide stubs were prevented from rotating about the cylinders' axes. This groove had to be very tight to provide satisfactory locking because of its close proximity to the axis. This requirement is at variance with the need for a loose fit to prevent jamming.

A further point worth mentioning is that with a satisfactory arrangement having been developed for flexible angle and position control of the needle, the requirement for a three part slide fell away.

The second system that was tried is illustrated in Fig. 6-40. Since it is possible to obtain high precision hexagonal brass tubing that slide one within the other, a model was made using this material. Again this is a very neat and compact system. but suffers from the same drawbacks as the first design. It was felt that angular stability could not be maintained while assuring smooth sliding action.

Fig.6-40

The third design embodies the principles discussed in Appendix 6-2. It is illustrated in Fig.6-35.

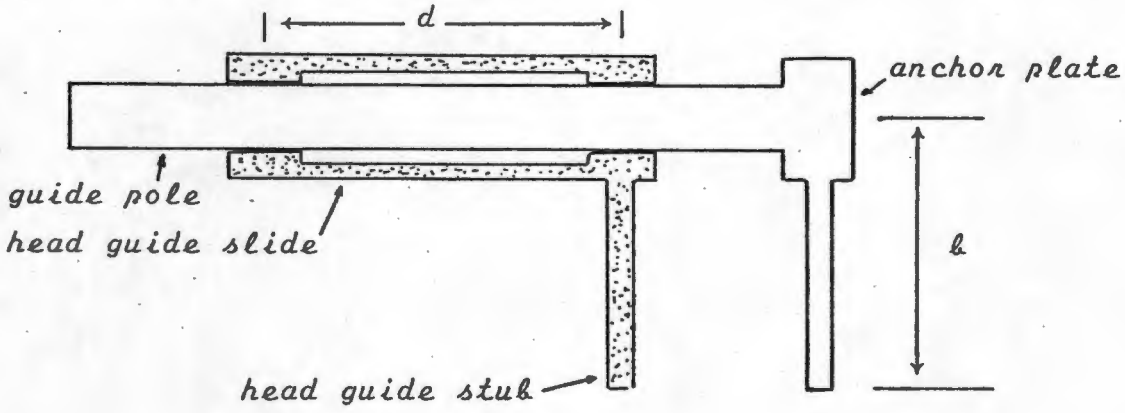

Fig.6-41

Care was taken to ensure that the sliding supports were at the two ends of the head guide slide. *d* Was made as long as reasonably possible. Angular locking action was provided by a separate locking pole some distance away from the guide pole (See Fig.6-35). This arrangement makes for a very positive locking action and does not affect the smoothness of the slide. The only problem that was found was that the radial locking pole tended to foul the transducer transport bars at steep angles, so in the prototype the two poles were lain next to each other.

§6-12 NEEDLE HEAD AND FOOT GUIDE STUBS

Soon after the project was started, it was decided that:

1. The head and foot guide stubs should be removable and sterilizable or disposable, since the sterile needle is to pass through these stubs.
2. Both guide stubs must be polarized to prevent incorrect assembly.
3. The guide stubs have to 'click' reliably into place before the needle is loaded.
4. It must be possible to load and remove the needle quickly and easily.
5. Account must be taken of the variations in needle diameter.
6. The two guide stubs must be interchangeable.

There were scores of different ideas that came to mind. At first a solution was sought that would enable needles of different thicknesses to be accommodated by one standard guide stub. The type of arrangement illustrated in Fig. 6-42 was incorporated in the first model (Fig.6-8 and 6-9). The 'V'-notch cut into one end of the stub was to accommodate the needle. A spring clip over the needle would ensure that it was held down during insertion but could nevertheless be removed fairly readily. At the other end of the stub a notch was to be cut to allow it to be homed with a fair degree of certainty.

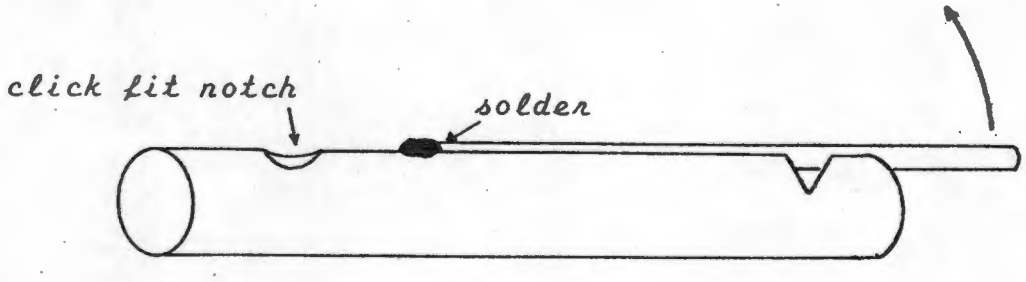

Fig.6-42

The foot guide stub (*d* in Fig.6-8) is held into the housing or anchor plate by a 'click' fit arrangement. A spring and ball were soldered into the housing to ensure this action. The head guide stub was held into the anchor plate by a screw with a knurled rim, so that the two systems could be compared.

Neither arrangement was regarded as being satisfactory.

1. Locking action of the stub in the anchor plate was not fool-proof in the case of the screw-lock.
2. The click fit was too complicated to make.
3. Both anchor plates were too difficult to clean.
4. The needle was not that easy to remove from the guide stubs.
5. The anchor plates were bulky. This prevented them from getting close together, an essential feature when inserting short needles.

The second arrangement illustrated in Fig.6-35 was fabricated from a number of precision cut square section tubes. This stub also had a V-notch to retain the needle. A freely moving slide

prevented the needle from dropping off. A click fit arrangement on the other side ensured that the stub would stay in the correct place in the anchor plate.

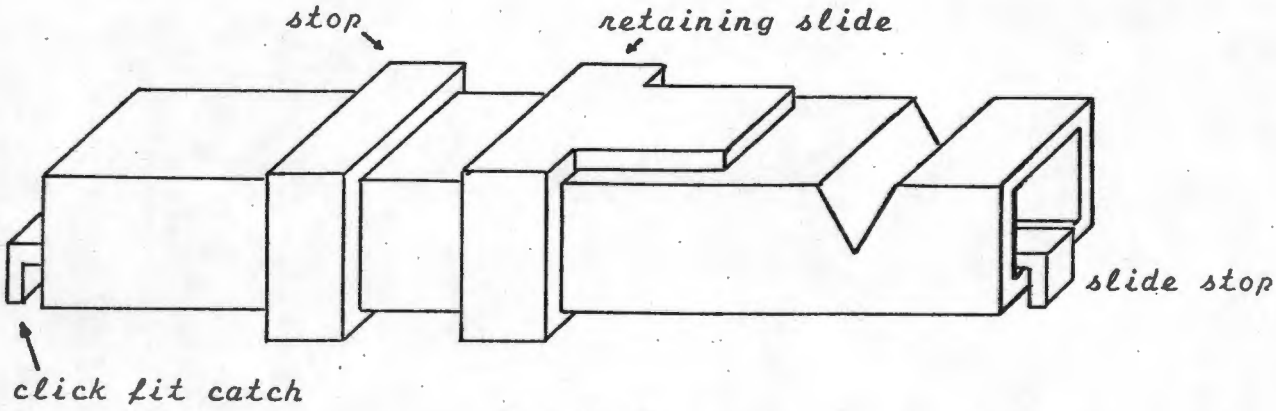

Fig.6-43

The system was rejected for the following reasons:

1. While it might be possible to injection mould the stub, it gave the impression of being too 'fiddly.'
2. Although the needle dropped out very easily when required. it was awkward to load.
3. Polarizing the stub was going to be difficult.
4. Cleanability was better than before, but still not satisfactory.

The idea of having a single guide stub for all diameter needles was dropped. A much simpler arrangement was finally devised.

A thin stainless steel stub was anchored firmly and permanently on each anchor plate. A plastic sleeve was to fit over the stub. At the end of the sleeve there was a hole, the size of which depended on the needle that was to be used.

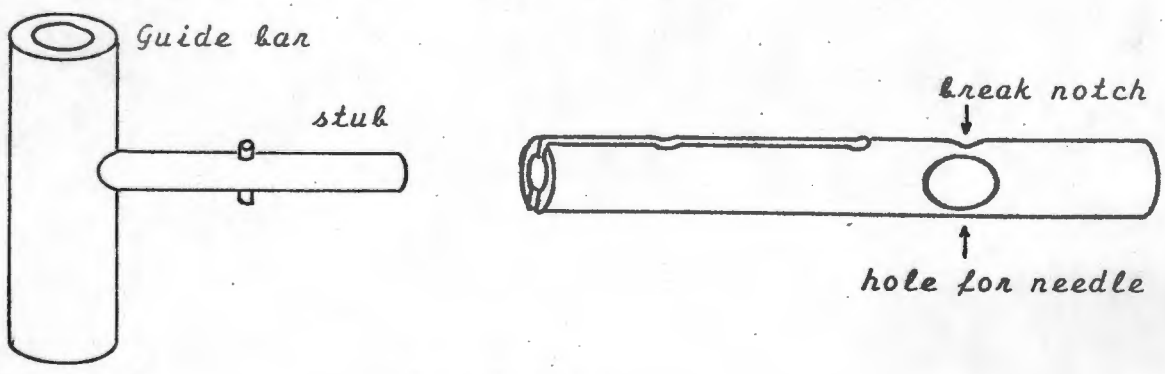

Fig.6-44

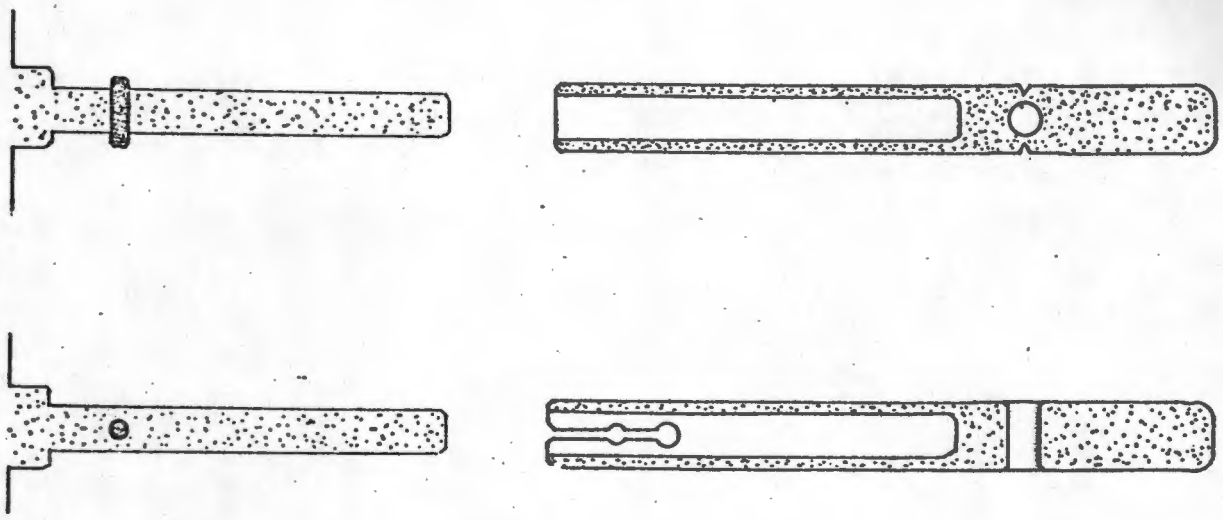

Fig.6-45

Some of the interesting features of this arrangement are:

1. It is very easy to clean.
2. The stainless steel stub provides rigidity to the sleeve to a point very close up to the needle, while at the same time being slender.
3. A pin through the stub provides polarization and locking for the sleeve.
4. The sleeve provides sterility over most of its length.
5. The needle is easily removed by breaking the end of the sleeve off at its weakest point, i.e.: at the needle hole.
6. Since the sleeve can only be used once, it has to be replaced by a sterile one. A used sleeve is broken.
7. The sleeve looks as if it could be injection moulded economically.

Drawbacks:

1. Since these sleeves are disposable, they have to be fabricated or hand moulded for initial testing.
2. Each needle has to be matched by its own gauge guide sleeve. This problem could be reduced if the needles were packed with a set of guide sleeves.
3. There could be difficulty in threading the needle through the holes, particularly for fine gauge needles.

Difficulties associated with threading of the needle could be overcome if the needle were pre-threaded into the needle guide sleeves with the whole assembly held together correctly by a disposable cartridge. In order to load the needle one would then push the two guide stubs together, break the sterile needle pack, clip the two sleeves over the stubs simultaneously, discard the cartridge and pull back the head guide slide. This procedure would be very simple and could be executed in a few seconds.

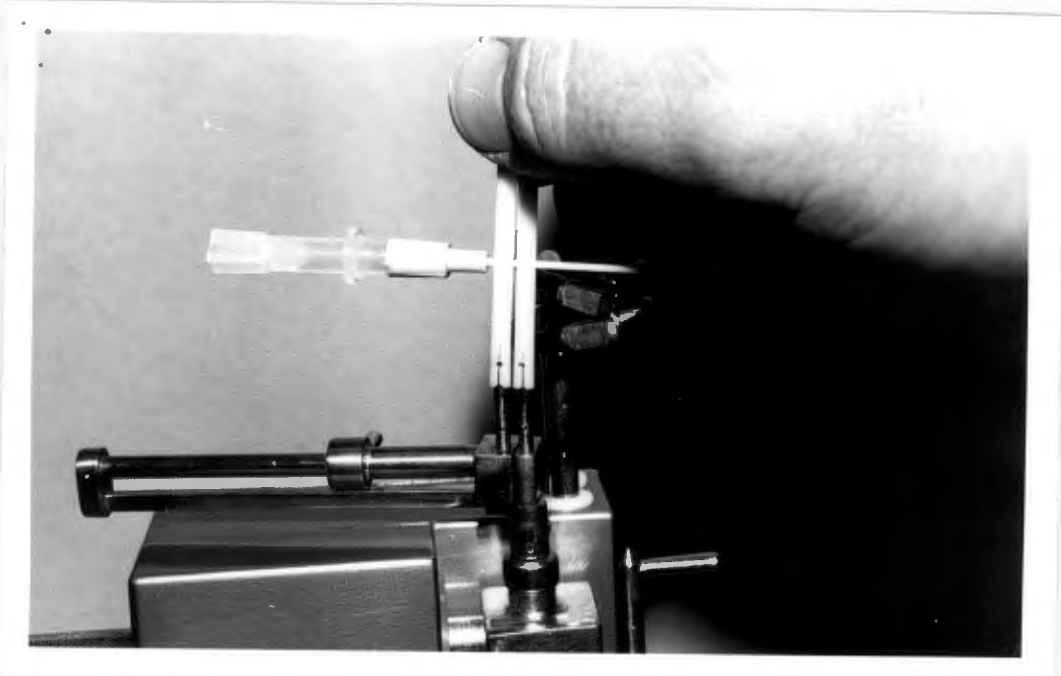

Fig.6-46

This then summarizes the principles involved in the design of the prototype. While great care was taken to optimize the chances of the instrument being successful, it is not regarded as the final solution. It can in all probability be greatly simplified mechanically. What is more important than the optimization of the mechanical arrangement, is whether or not the instrument is clinically acceptable. At this stage this turns out to be the only major consideration.

CHAPTER SEVEN

CONSTRUCTION

A model was built of the system as finally envisaged (Fig.7-1). This was shown to the two anaesthetists most interested in the development of the instrument. Two criticisms were noted. Firstly, the two needle supports discussed earlier and illustrated again in Fig 7-1 were criticised as being awkward. For this reason the system discussed at the end of chapter 6 was developed. The second criticism was based on a feeling that the needle support mechanism and transducer should be further away from the bulk of the equipment in order to improve accessibility. This was very difficult to achieve in practice, requiring a complete redesign, and it was thought that the system as it stood had sufficient merit to warrant construction and a trial. It was therefore decided to construct the instrument as planned.

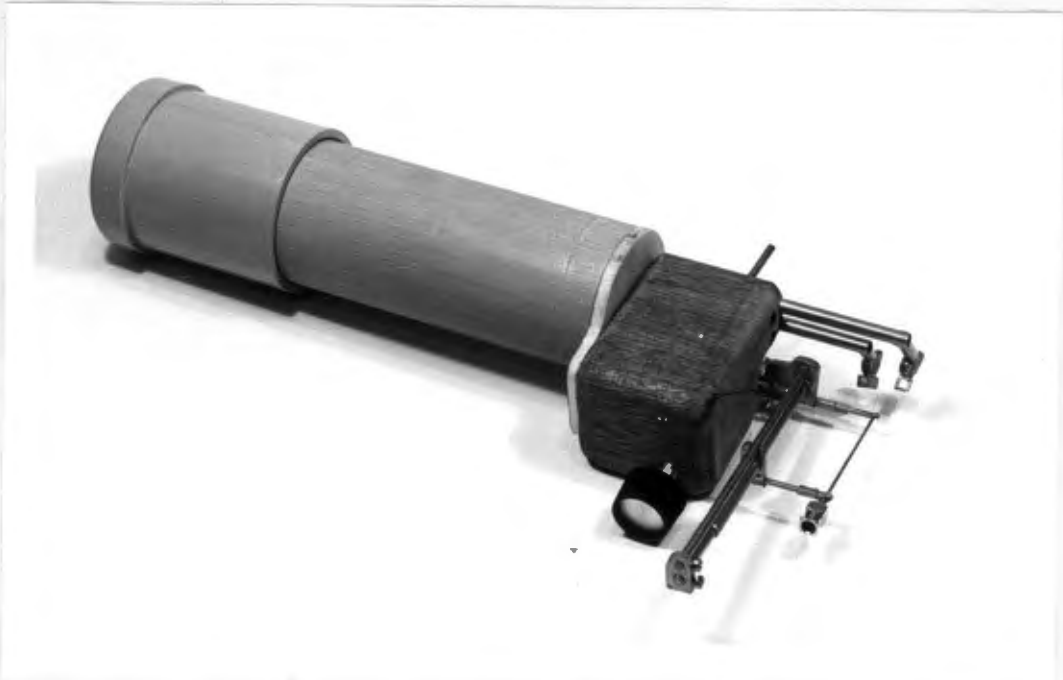

Fig.7-1

Most of the concepts illustrated in the following drawings have been discussed earlier. *The names of the parts are descriptive in themselves and appear listed on Page 125a . Next to each part is a list of pages on which the item appears.*

§7.1 THE MECHANICAL SYSTEM

Fig.7-2 is a drawing of the mechanical system, excluding the transducer housings and external needle guide slide. It is based on the pre-prototype model discussed in some detail in section 6.8. A complete understanding of the system from this drawing alone is difficult, but together with drawings of the individual parts and photographs which follow, it should be possible to get a picture of the mechanism.

The two control knobs 70, and 71 have been so arranged that they always remain flush up against the back wall of the housing. The needle position control knob 71 simply screws into the needle axis platform body 78, thereby sliding the whole platform backwards and forwards relative to the main housing. The needle axis angle control knob 70 controls the angle at which the needle tilts, relative to the housing. The worm 84 drives a gear at the end of shaft 82, which rotates scroll disc 79. The scroll itself is not shown. It controls the angle of the guide rail platform 80, which pivots on the needle axis platform body. A roller running in the guide rail is anchored to the rolling float, which in turn drives the upper transducer transport bar 9 and a pinion 17 by means of a rack. The pinion drives a second rack which is attached to the lower transducer transport bar 10.

At the end of the needle axis angle control shaft 75 is a second worm 92, which drives a gear to which the shaft controlling the needle axis angle is attached. In this way the needle axis angle and guide rail platform angle are linked.

No Description of Part: (Fig.7-....)

1 Upper mechanical housing: 2,(3),4
2 Lower mechanical housing: 2,(3),4
3 Lid for mechanical housing: 2,(3)
4 Sealing bush: 2
5 Sealing bush: 2,(3),(24)
6 Sealing bush: 2
7 Sealing bush: 2,(3)
8 Sealing bush: (3)
9 Rolling float rail: 2,(3),13
16 Rolling float: 2,(12),14,
17 Pinion: 2,13,23
18 Linking plate: 2,(9),14
19 Rollers: 2,(12),14
20 Rack: 2,23
21 Rack: 2,23
22 Guide rail roller: 2
23 Guide rail roller shaft: 2,14
30 Up.Transducer Transport bar: 2,(5),6
31 Lower Transducer Transport bar: 2,(5),6
32 Angular locking slide: 2,(9),10
33 Angular locking slide: 2,(9),11
34 Lower transport bar rack support: 2,(9),11
35 Upper transport bar linking plate support: 2,(9),10
36 Upper transducer transport sleeve: 2,(9),10
37 Lower transducer transport sleeve: 2,(9),11
40 Transducer housing: (5),6
41 Ball swivel joint: (5),6
42 Clamping screw: 6
45 Transducer housing: (5),7
46 Ball swivel joint: (5),7
47 Clamping screw: 7
51 Guide pole: (27),28
52 Locking pole: (27),28
53 Foot guide anchor plate: (27),28
54 Head guide anchor plate: (27),28
55 Guide slide upper bearing collar: (27),28
56 Upper stabilizing collar: (27),28
57 Foot guide stub: (27),28
58 Head guide stub: (27),28
59 Foot guide sleeve: (27),28
60 Head guide sleeve: (27),28
61 Guide slide: (27),28
62 Manual locking screw: (27),28
70 Needle axis angle control knob: 2,(24)
71 Needle position control knob: 2,(24)
72 Retaining collar: 2,(24)
73 Retaining collar: 2,(24)
74 Needle axis platform position screw: 2,(24)
75 Needle axis angle control shaft: 2,17,(22),23,21
76 Clutch sleeve: 2,(22)
77 Clutch tension spring: 2,(22)
78 Needle axis platform body: 2,(15),17
79 Scroll disc: 2,(16),17,(18)
80 Guide rail platform: 2,(18),19
81 Guide rail platform pivot: 2,(15),17,19
82 Scroll shaft: 2,(16),17,(22)
83 Scroll drive gear: 17,(22)
84 Scroll drive worm: 2,(22),23
85 Angle control shaft retaining clip: (16),17,(25)
86 Retaining screw for retaining clip: 17,(25)
89 Gear housing cover: 21,(26)
90 Needle axis angle control sleeve: 2,(15),21
91 Gear Housing: 2,(20),21
92 Needle axis angle drive worm: 2,(22),23
93 Needle axis angle drive gear: 21,(22),23
94 Needle axis shaft: 21,(22)
95 Needle axis sleeve: (20),21
96 Seal: 21

Note 1: Figures in parentheses indicate photographs.

Note 2: Parts are not necessarily numbered in all the drawings indicated.

Rev: B

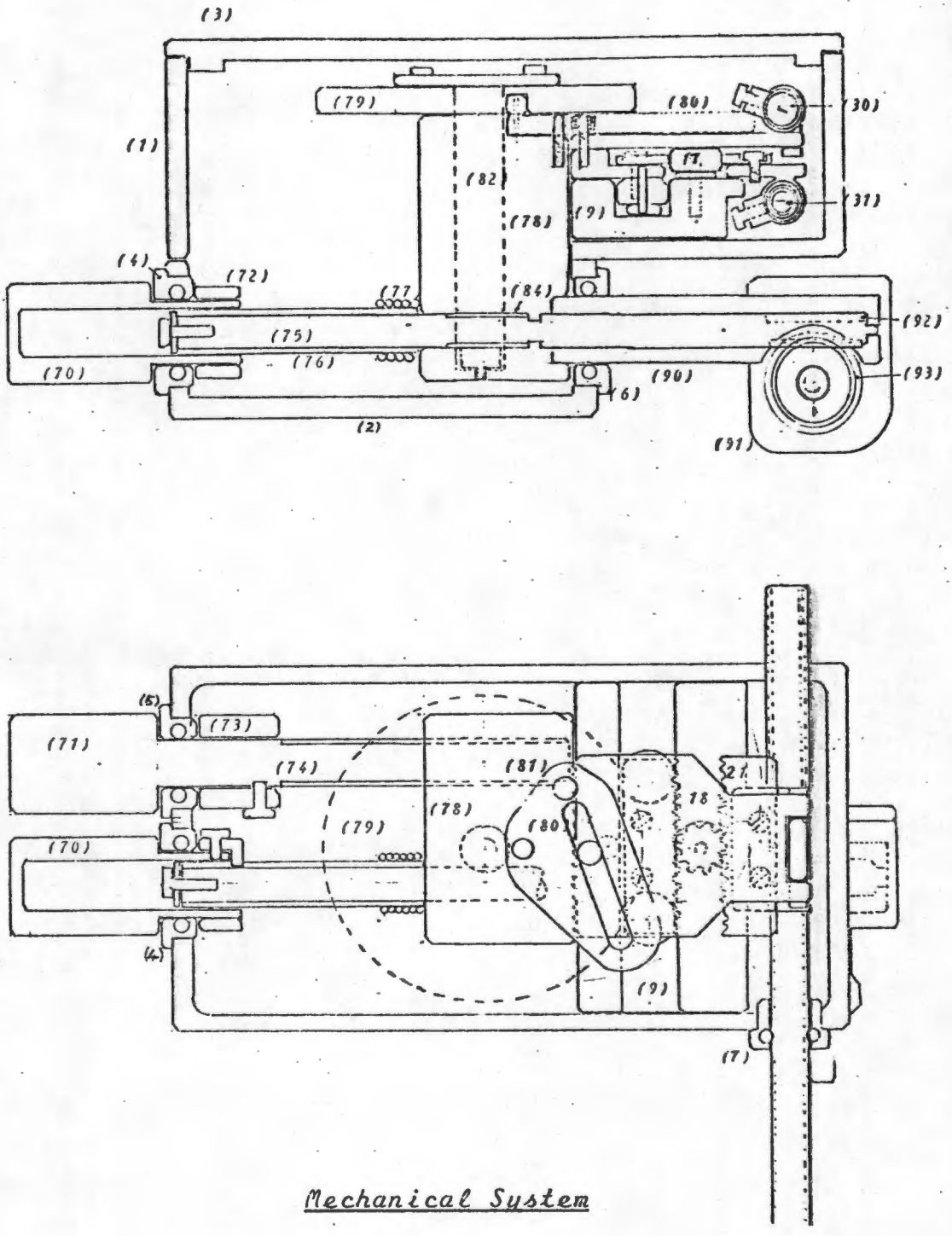

Mechanical System

Fig.7-2

Scale: 1,27:1

Housing

The housing was machined from a section of half-hard Aluminium, which was subsequently anodised. The three parts were screwed together with brass screws. The photograph shows three of the nylon bushes in place. A sealing lip was milled onto the lid and the centre hollowed to accommodate the moving scroll.

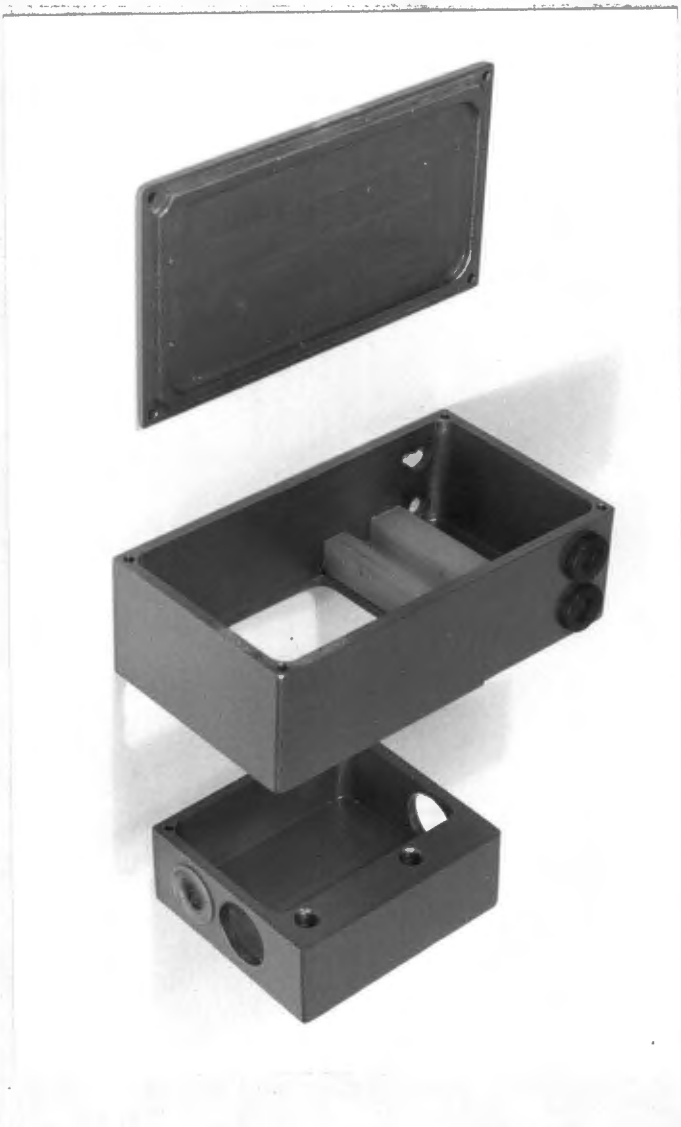

Fig.7-3

Rev: A

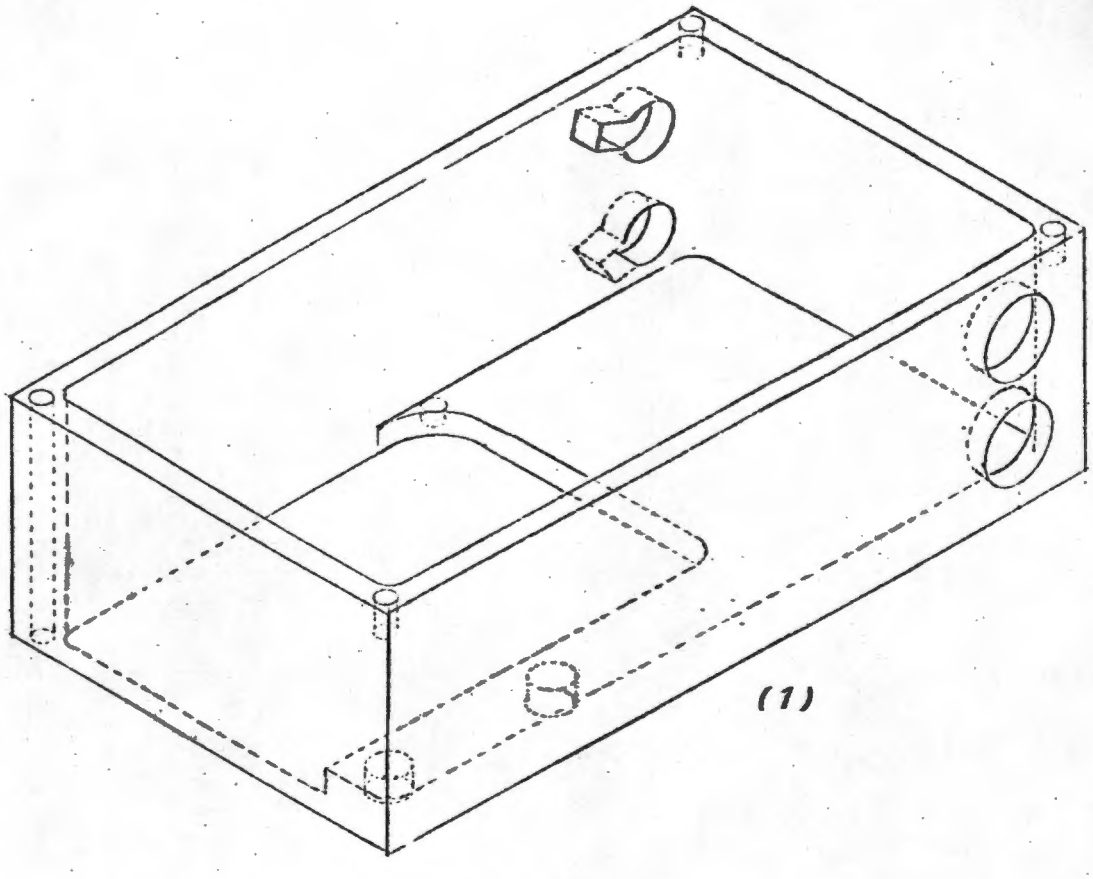

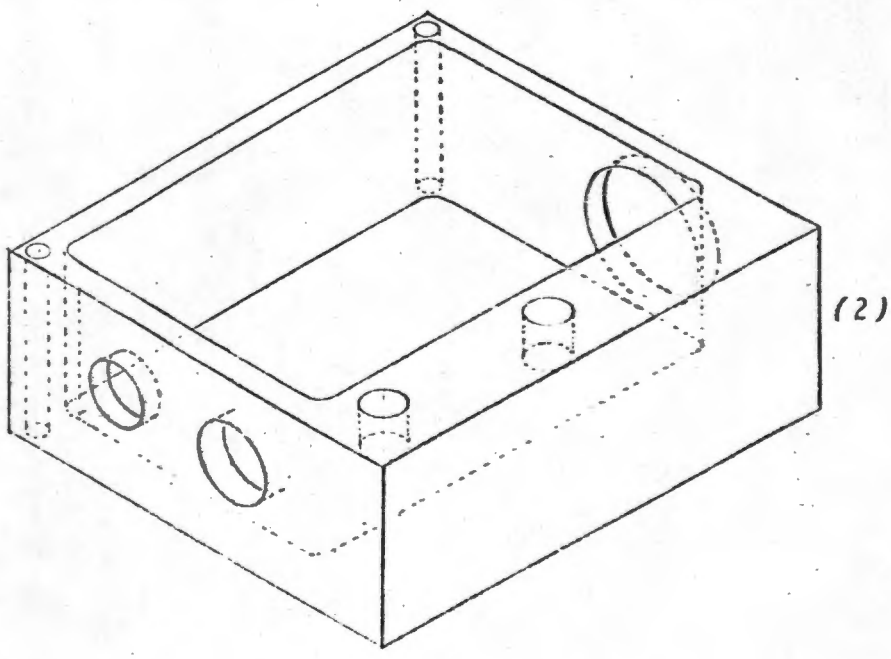

Upper and Lower Mechanical Housing

Fig.7-4

Scale: 1,27:1

Transducer Transport Bars (30 & 31)

The two transducer transport bars were built from 5mmϕ brass tubes. A short piece of stainless steel was fabricated into a hollow cylinder and silver soldered onto the end of each tube. A chrome plated ball bearing fits inside and projects from one end as illustrated in Fig.7-6 and 7-7. A 4mm square section of brass 40 was carefully soldered onto the ball 41. An internal screw 42 adjusted from the other end of the stainless steel housing, clamps the ball.

A transducer was mounted on a polystyrene block as discussed in Chapter 4 and glued into the square section transducer housing. The face of the transducer was made flush with the edge of the square tubing. The function of the ball-in-socket joint is to allow alignment of the transducers.

The two transport tubes go right through the upper mechanical housing and into the electronic box. Two bushes 7 & 8 that were designed to contain PTFE seals, provide a bearing surface where the bars enter the housing.

Fig.7-5

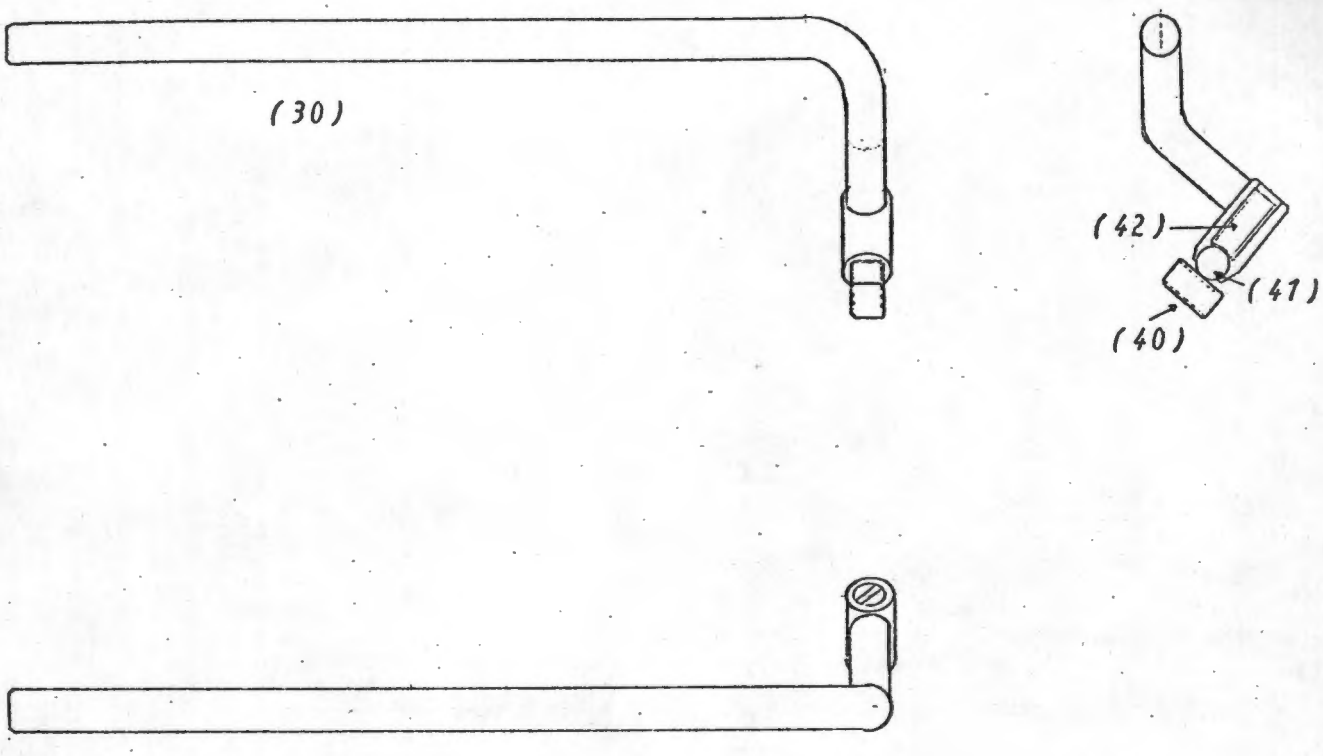

Fig.7-6 Upper Transducer Transport Bar

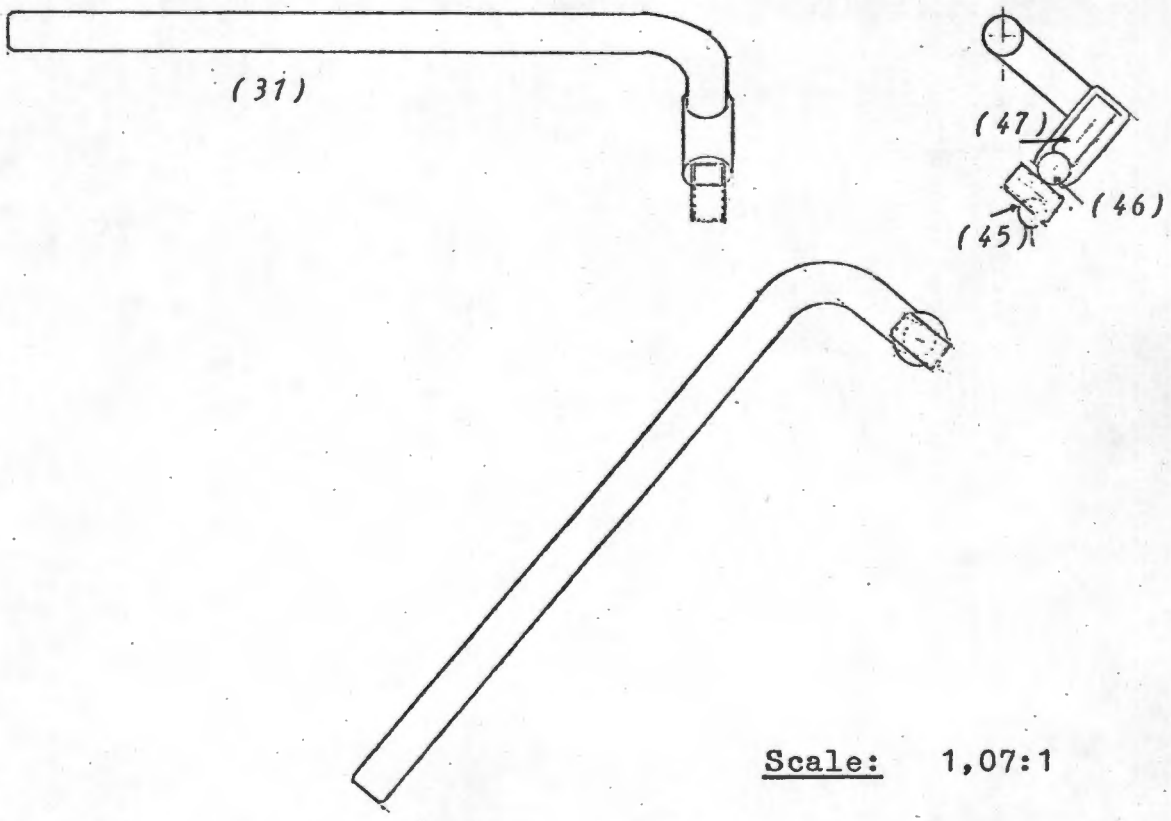

Scale: 1,07:1

Fig.7-7 Lower Transducer Transport Bar

Upper and Lower Transducer Transport Sleeves (36 & 37)

The two transducer transport bars are sleeved at the exit from the mechanical housing by means of a locking sleeve. The sleeve has three functions. Firstly, it prevents rotation of the transducer transport bars by keying into the housing. Secondly, it provides an adjustment for rotational and axial positioning of the transducer transport bars. Two screws tapped into the key (or locking slides 32 and 33) and accessible from outside the mechanical housing, lock the transport bars into any desired position. Finally the sleeve provides a driving point for the internal mechanical system.

The lower transducer transport sleeve 37 has a rack support 34 which a rack is mounted (rack not shown). The upper sleeve 36 is driven by a linking plate 18 which is attached to the rolling float 16 and clips into the linking plate support 35 of the upper transport sleeve. As discussed earlier, this coupling may not be solid since it could present a jamming problem.

Fig.7-9

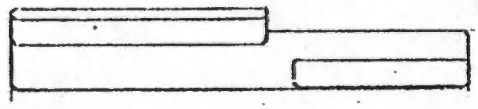

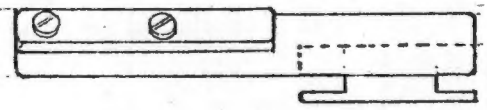

Upper Transducer Transport Sleeve (36)

Fig. 7-10

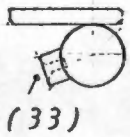

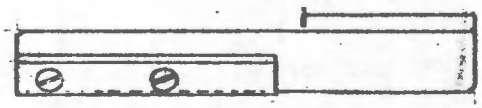

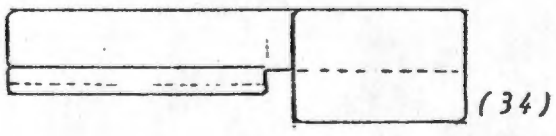

Lower Transducer Transport Sleeve (37)

Fig.7-11

Scale: 1,5:1

Rolling Float 16

The rolling float serves to eliminate jamming problems associated with translocation of the transducer transport bars. Two nylon rollers 19 on the underside of the float, roll in a rail 9 the body of which is screwed down to the base of the upper mechanical housing. The rail is cut into a polypropylene block.

A rack 20 (not shown) is attached to the float by means of two adjusting screws. The pinion 17 is mounted on the float rail block. Linking plate 18 is attached to the float and fits over the rack. Midway between the two screws holding this plate down is a stainless steel stub that screws into the body and accommodates a tiny nylon roller which rolls in the slot of the guide rail platform 80.

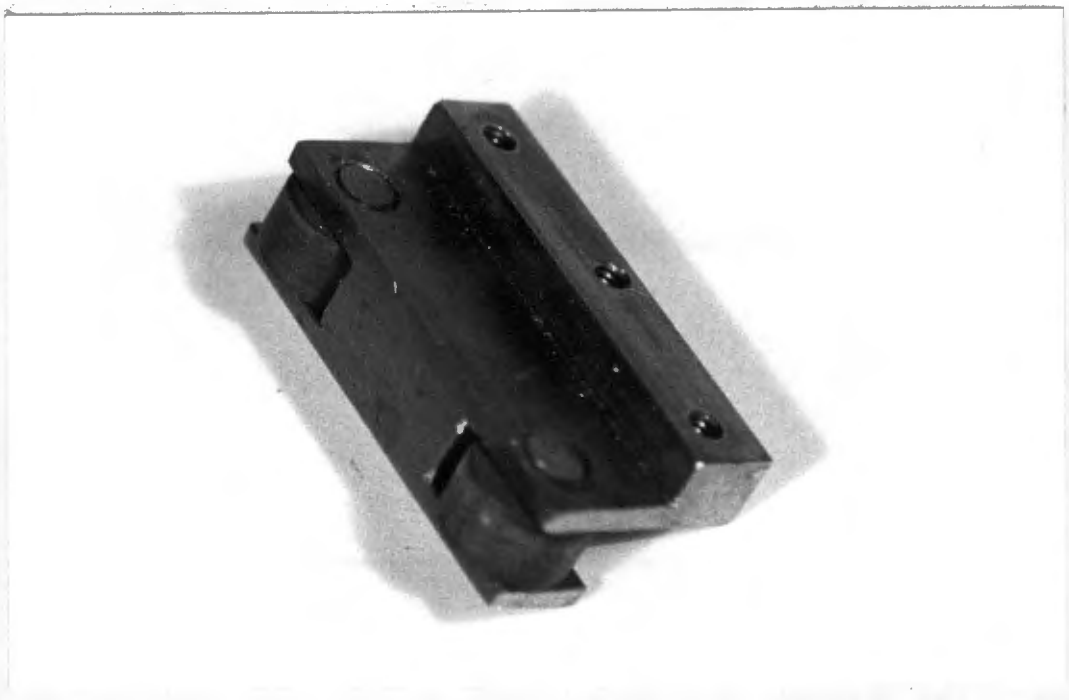

Fig.7-12

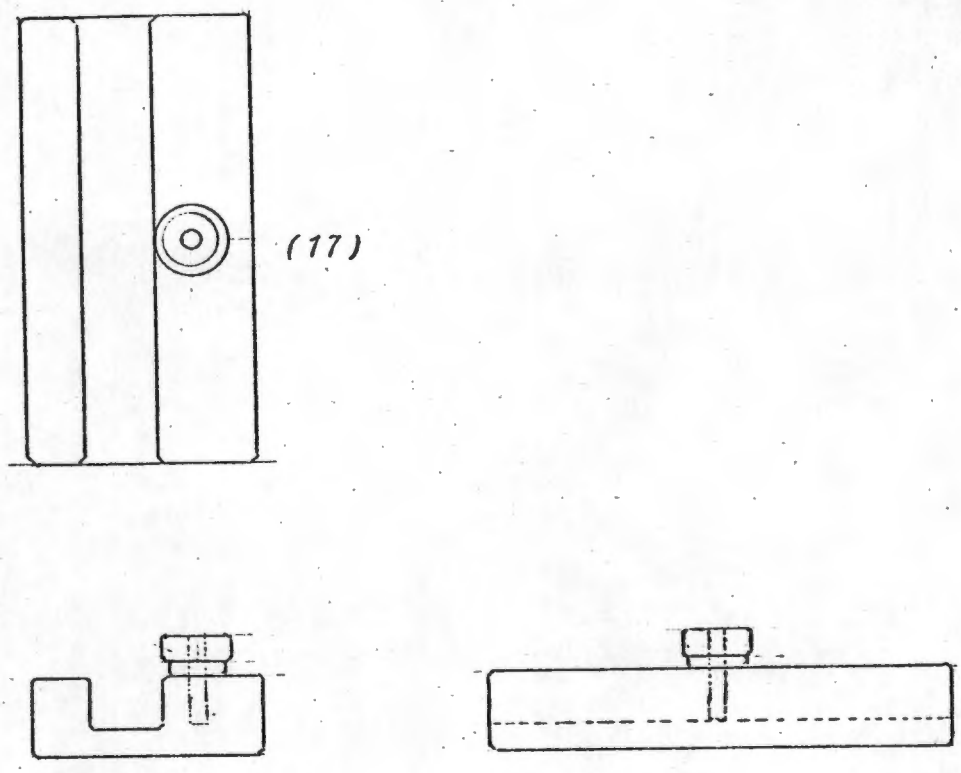

Fig.7-13 Rolling Float Rail (9)

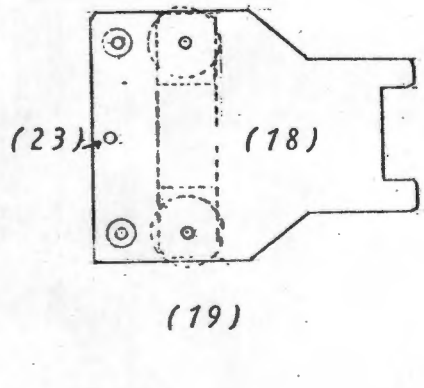

Fig.7-14 Rolling Float (16)

Scale: 1,43:1

Needle Axis Platform Body 78

This part supports the scroll shaft 82 (Fig.7-16) and serves as a gear box that links it to the needle axis angle control shaft 75. It also supports the guide rail platform pivot 81. The needle axis angle control sleeve 90 is silver soldered to the body and therefore forms an integral part of it.

Fig.7-15

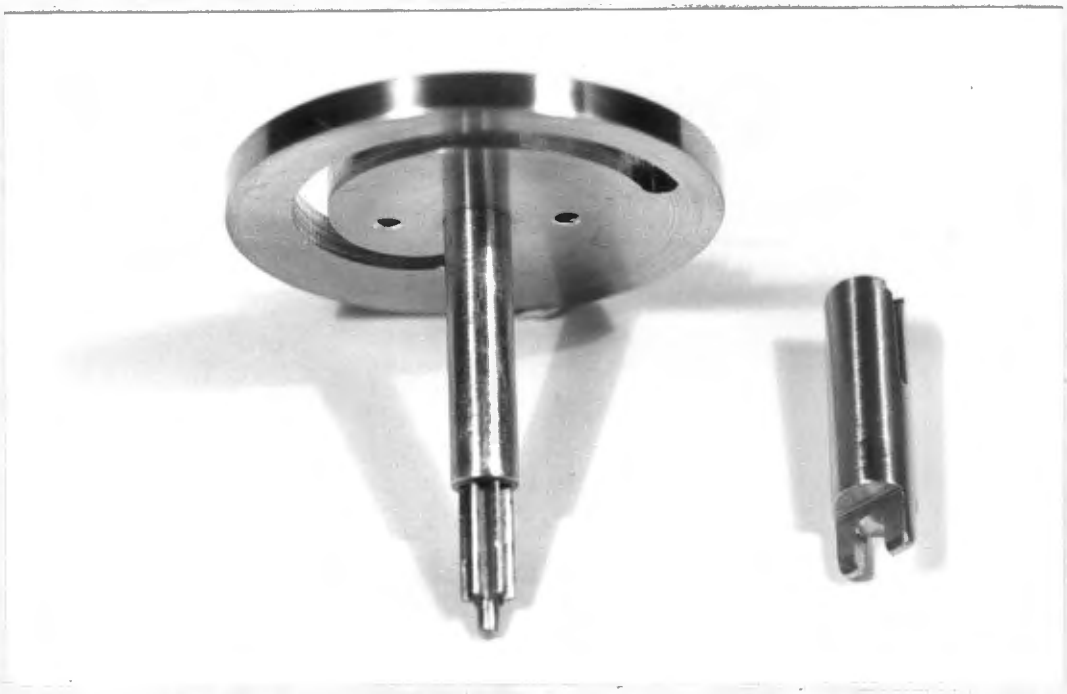

(82) (85)

Fig.7-16

Rev: B

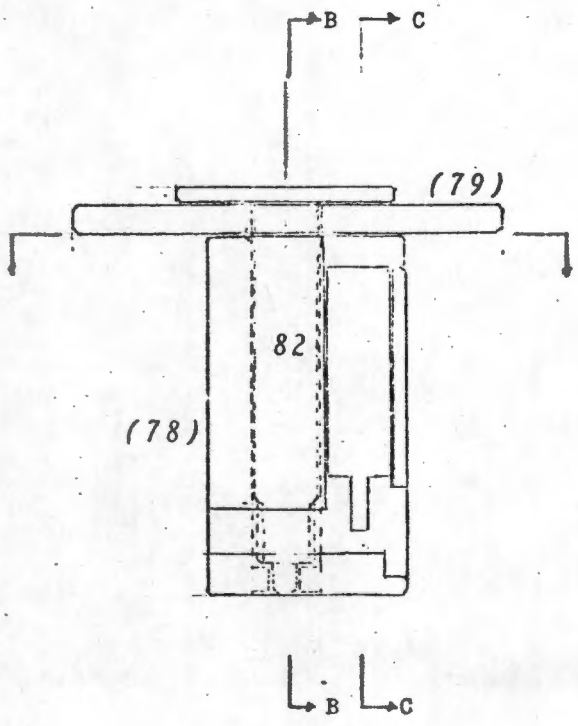

View 'B'

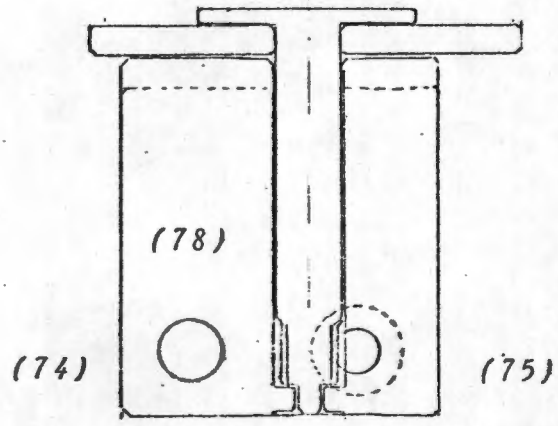

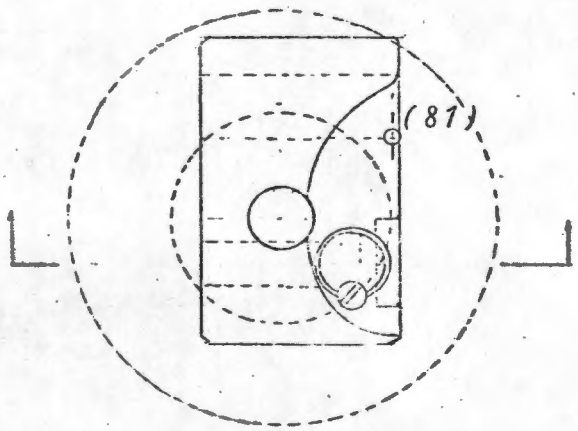

View 'C'

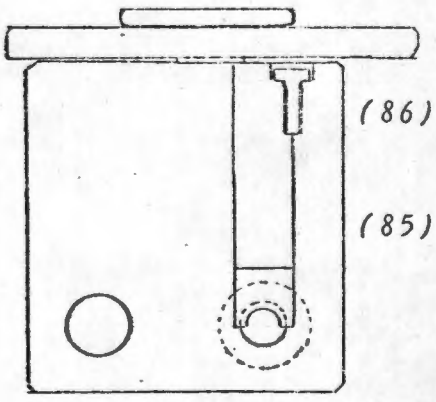

Needle Axis Platform Body

Fig.7-17 Scale: 1,45:1

The needle axis angle control shaft 75 runs through the sleeve. It is constrained from moving axially by a retaining clip 85 which fits over a notch in the shaft. The retaining clip in turn is held down by a retaining screw 86. Another hole in the needle axis platform body is tapped to accommodate the needle axis platform position screw 74.

The Scroll 19

The scroll was cut with a numerically controlled milling machine according to the formula given in appendix 6-1 into the end of a brass bar. The 3mm thick disc containing the scroll groove was then cut off.

(79) *Scroll*

(80) *Guide Rail Platform*

Fig.7-18

The scroll shaft 82 fits accurately into a hole in the centre of the scroll disc. A rim around the top of the shaft has two slots through which screws pass into the scroll disc. In this way it is possible to set the position of the disc accurately. There is no other place along the gear chain where this can be done.

The Guide Rail Platform 80

The guide rail groove was cut into the guide rail platform. A brass shim was soldered over the top of the platform to retain the nylon wheel which runs in the groove.

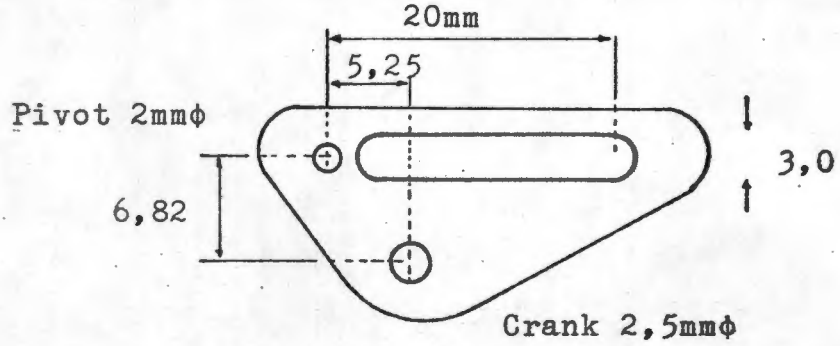

Fig.7-19

The Gear Housing 91

The gear housing was fabricated from brass to link the needle axis shaft 94 to the needle axis angle control shaft 75. A needle axis sleeve 95 has been silver soldered to the basic block. A seal 96 could have been put into this sleeve, but was left out of the prototype model.

The block is screwed onto the needle axis angle control sleeve with two screws located under the lid. It could not be permanently attached since it has to be removable for assembly purposes. A fairly tight nylon disc was pushed under the lid of the housing to retain the gear while assembling the system.

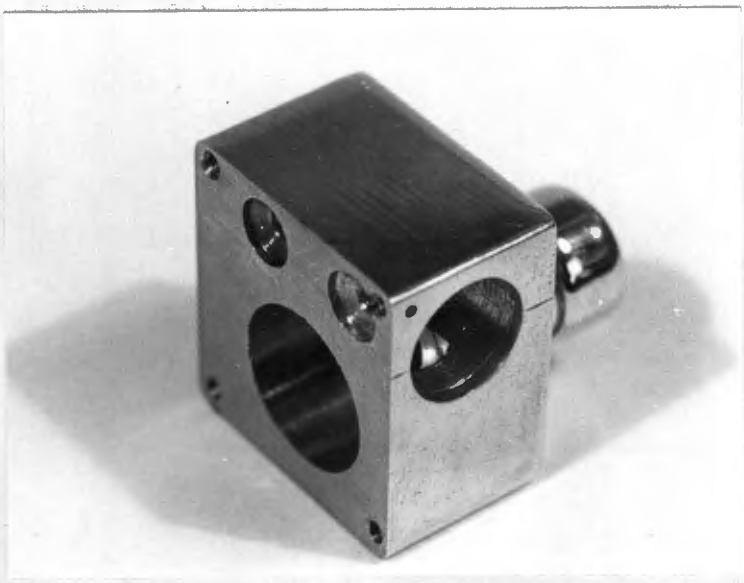

Fig.7-20

Rev: A

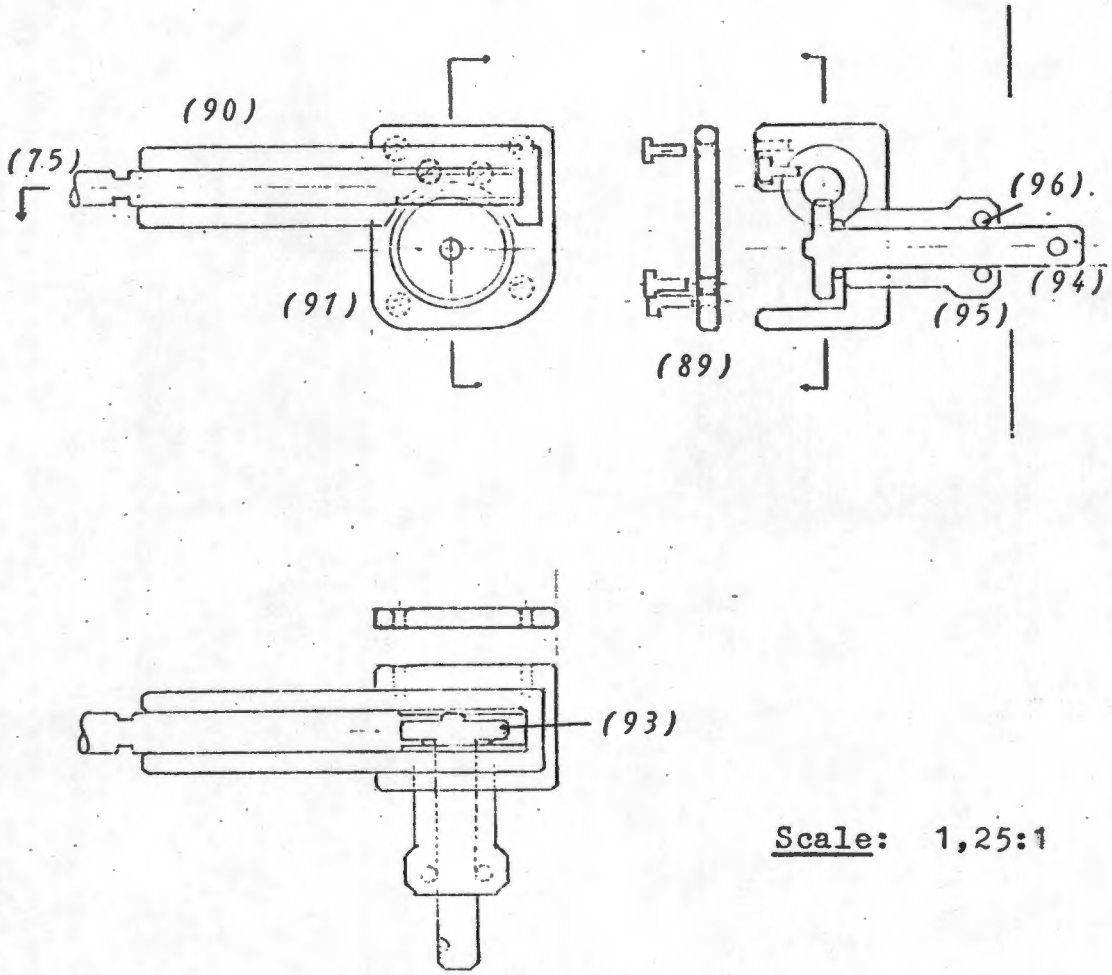

Scale: 1,25:1

Gear Housing & Related Parts

Fig. 7-21

Needle Axis Angle Control Shaft 75

The first shaft that was tried was made of brass, but after the coarse worm developed cracks it was decided to remake it from steel.

The clutch sleeve 76 fits over the shaft as was discussed in §6.10. It was machined with one end closed and perforated with a small hole to accommodate a loosely fitting retaining screw. This screw is tightened up against the bottom of the tapped hole in the end of the shaft.

Fig.7-22

The needle axis shaft 94 and needle axis angle drive gear were turned from a single piece of brass. The scroll drive gear 83 could have been cut directly onto the scroll shaft 82, but was infact cut on a separate steel shaft and pressed into the scroll shaft.

A supporting bearing on the ends of both the scroll shaft and the needle axis angle control shaft is essential to prevent the tendency of these gears to ride on each other.

Shaft: Mild Steel. Two worms to be cut to mate with corresponding Gears as shown.

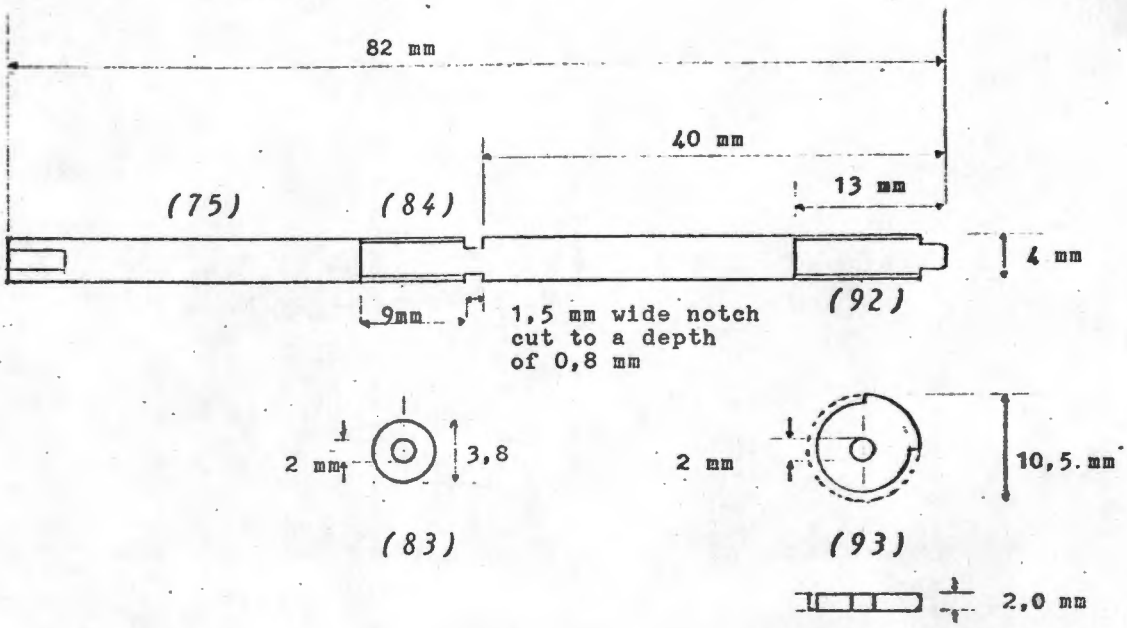

Gear 1 3,8 mm diameter
6 teeth
Mild Steel

Gear 2 10,5 mm diameter - Brass
45 teeth per circumference but the gears need only be cut around 25% (90 degrees) of the cog. The rest of the gear should preferably be milled away to protect the worm during incorrect assembly

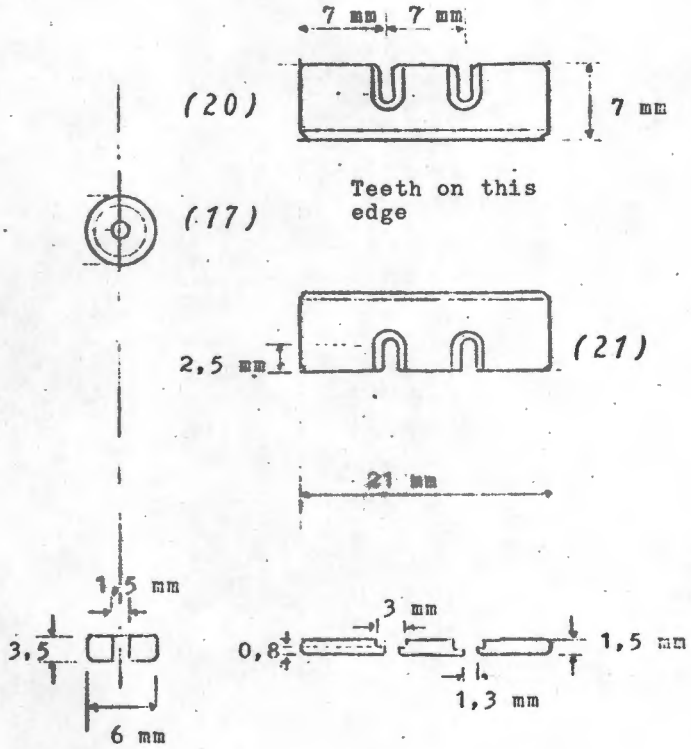

TWO Racks

The Two racks are to be identical. The Number of teeth per unit length is not important, as long as they mate with the pinion.

ONE Pinion

A single Pinion, also made of brass, 6 mm in diameter.

Gear Systems

Fig.7-23

Control Knobs 70 & 71

The needle position control knob 71 is integral with the needle axis platform position screw 74. It is knurled and made of stainless steel. A nylon bush and washer together form the bearing surfaces between the knob and aluminium housing. A retaining collar 73 and the knob together constrain the screw from moving axially relative to the housing.

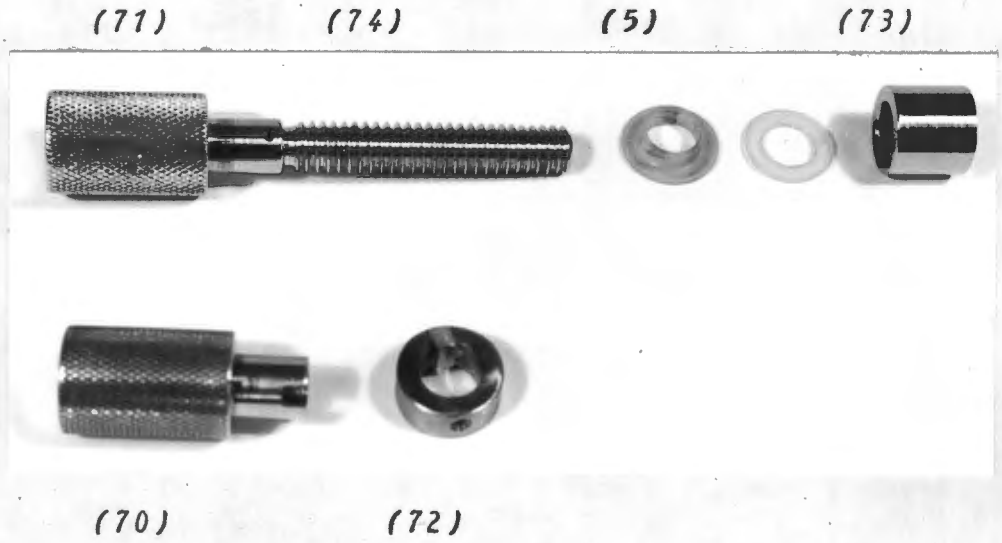

Fig.7-24

The needle axis angle control knob 70 is also made of stainless steel and is hollowed to accommodate the clutch sleeve 76. A similar bush to that described above is not shown in Fig.7-24. The retaining collar 72 on the knob has a lip that fits into the slot cut into the clutch sleeve.

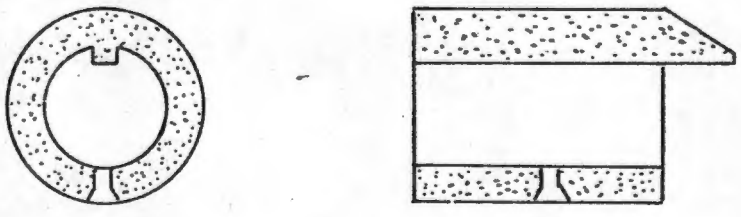

Needle Axis Platform

Fig.7-25 shows the needle axis platform assembled, but with the scroll disc not fully lowered over the guide rail. Fig.7-26 shows the other side of the same thing, with the scroll disc in place. In the background the external needle guide slide can be seen attached to the needle axis shaft.

Fig.7-25

Fig.7-26

External Needle Guide Slide

Development of this component was discussed in § 6.11. The guide pole 51 is 80mm long, which is long enough for a 40mm deep puncture. Any needle requiring to go deeper than that can be removed from the guide and pushed the rest of the way without it. The guide pole was not made any longer to protect the gears from excessive accidentally applied moments.

Nylon bushes, which may still be replaced with PTFE, were fitted to both ends of the guide slide 61. With these low coefficient of friction materials a jamming problem was thought unlikely to occur, the slide being 33 mm long.

The two guide stubs were made of 2,5mmϕ brass rods, 16mm long. The sleeves were fabricated from Acetal rods, although no final decision has yet been taken on the material that will finally be used.

The guide slide is fitted with a locking screw 62, which can be tightened by hand to lock it. This is useful when the needle and the sleeves are fitted and during vessel searches.

The whole assembly is pushed onto the needle axis shaft. A 1,2mmϕ steel screw passes into the shaft and locks the assembly to it.

Fig.7-27

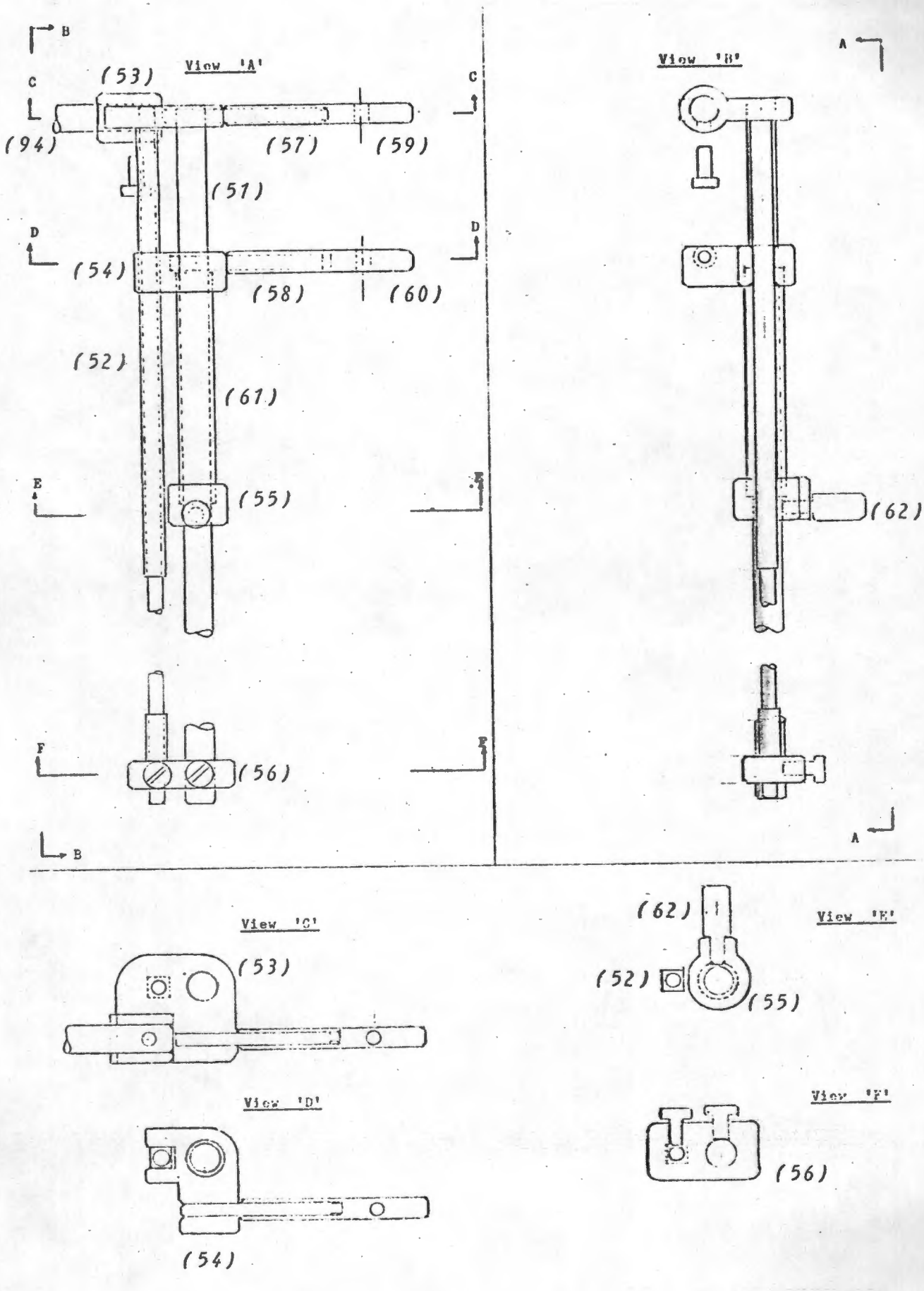

Fig.7-28

Scale: 1,32:1

(See text for specific measurements)

§7.2 DISASSEMBLY OF MECHANICAL SYSTEM

The mechanical system is dismantled very easily. No parts are difficult to access and no special tools are needed apart from a long, slender screw-driver which is required for adjusting the transducer transport bars. The four 1,2mmϕ retaining screws have to be accessed from the space between the interface plate and the mechanical housing.

When the lid is opened two plastic blocks will be found supporting the needle axis platform body, preventing it from rotating or rocking about the needle axis angle control shaft. These were added afterwards.

Dismantling should be done in the following order:

Separate electronic box (to be discussed).
Lift out scroll assembly (79/82)
Lift out guide rail (80)
Remove linking plate (18)
Remove pinion (17)
Remove transducer transport bars (30&31)
Remove rolling float (16)
Remove control knobs (70&71)
Remove bush (4)
Lift out retaining clip (85) with screw provided nearby.
Remove lid to gear housing (89)
Remove needle axis shaft and gear(93/94)
Remove needle axis angle control shaft (75)
Remove gear housing (91)
Remove bush (6)
Remove needle axis platform body (78)

Reassembly is roughly the reverse of the dismantling procedure.

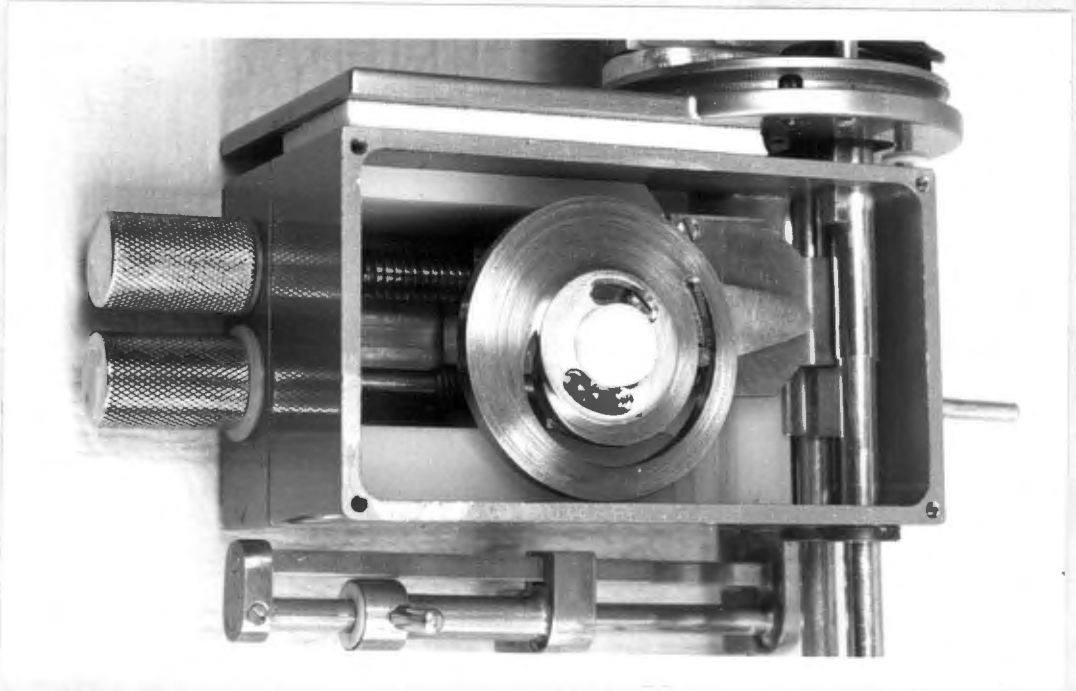

Fig.7-29 *Internal mechanical arrangement assembled*

§7.3 ELECTRONIC BOX

The electronic system is housed in a 50mm diameter, grade 4, PVC pipe. The pipe is clamped onto the interface plate as shown in Fig.7-31.

The interface plate is machined from a single piece of half-hard aluminium. The groove illustrated in Fig.7-30 accommodates a silicone rubber seal. The interface plate has an opening through which the transducer transport bars penetrate the electronic box. An aluminium T-section is screwed to the plate and supports the printed circuit boards.

The plate is stuck to the mechanical housing with mirror tape. This makes separation tedious, although assembly is easy. What is very important, however, is that the mirror tape, being spongy, introduces a certain amount of acoustic decoupling between the speaker and the transducers.

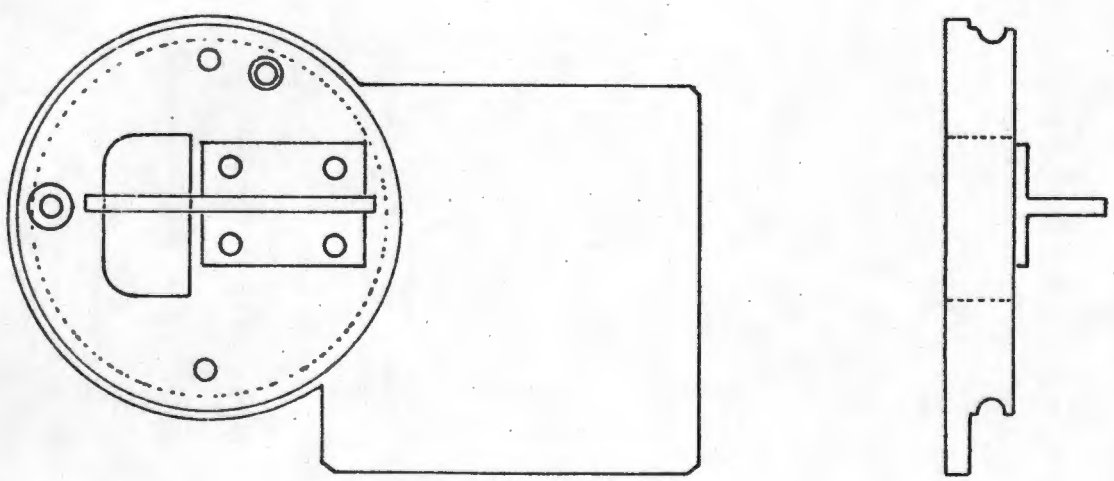

Fig.7-30 Interface Plate

The speaker housing is made from a section of Nylon. Two silicone-rubber rings and a neoprene ring are the only contact between the speaker housing and the electronic box (Fig.7-31). This is the second stage of acoustic decoupling.

A third stage of acoustic decoupling is introduced by mounting the speaker in a ring of neoprene rubber. The speaker with its ring

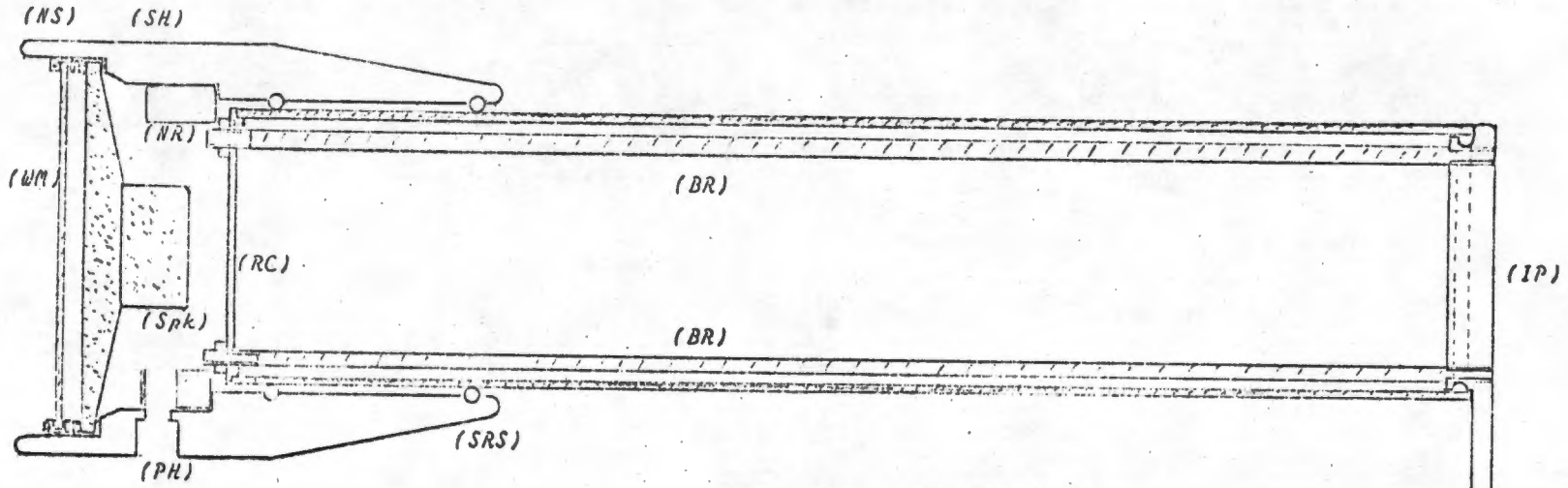

BR	Brass Rod
IP	Interface Plate
NR	Neoprene Ring
NS	Neoprene seal
PH	Plug Hole
RC	Retaining clip
SH	Speaker Housing
Spk	Loudspeaker
SRS	Silicone Rubber Seal
WM	Wire Mesh covered by Silicone rubber sheet

Fig.7-31 Electronic box and speaker housing

of rubber fits into the back of the loudspeaker housing. A brass ring covered in wire mesh and overlain with a sheet of silicone rubber is mounted in exactly the same way as the speaker, to ensure a water-tight seal. The back of the speaker is covered in a layer of fibre-glass insulation for further acoustic decoupling.
A small hole in the speaker housing is fitted with one of the three plugs listed in the electronics parts list, for charging the batteries.

The electronic box opens as follows:

1. Slide the speaker housing off the PVC pipe and unplug the internal speaker plug and charging plug.
2. Undo the two 5,5mm nuts holding the retaining clip to the housing. Remove the clip.
3. Slip the PVC pipe off.
4. Unscrew the upper support rod from the interface plate.
5. Swing the upper PC board upwards to open.

Fig.7-32

The following are some of the features of this housing arrangement:

1. The box can be opened within a matter of seconds. The only tool necessary is a 5,5 mm spanner, but a knurled nut or special screw could be used to replace the nuts.

2. A special support arrangement was built so that the PCB's remain rigidly attached to the interface plate when the opened system is handled.
3. Acoustic decoupling takes place at 3 separate places. None of the acoustic instabilities encountered in the work bench model were present in the prototype.
4. The whole unit is completely sealed and can, in principle, be completely submerged in water for washing.

§7.4 PRINTED CIRCUIT BOARDS

All the electronic components are located on two PCB's. The upper board is hinged so that all the tracks and components are immediately accessible without the need for desoldering anything.

The boards are laid out as in the Circuit diagram. The upper board contains the inverter, Oscillator and r.f. output amplifier. The lower board contains the receiver, demodulator, filter, preamplifier and main amplifier. Eight rechargeable NiCd cells are divided evenly between the two boards and soldered directly onto the tracks. This obviates the need for a special battery housing and ensures short power leads.

An aluminium screen, sandwitched between two pieces of cardboard lies between the boards and plugs into the mounting platform on the interface plate. Electrical contact is therefore ensured.

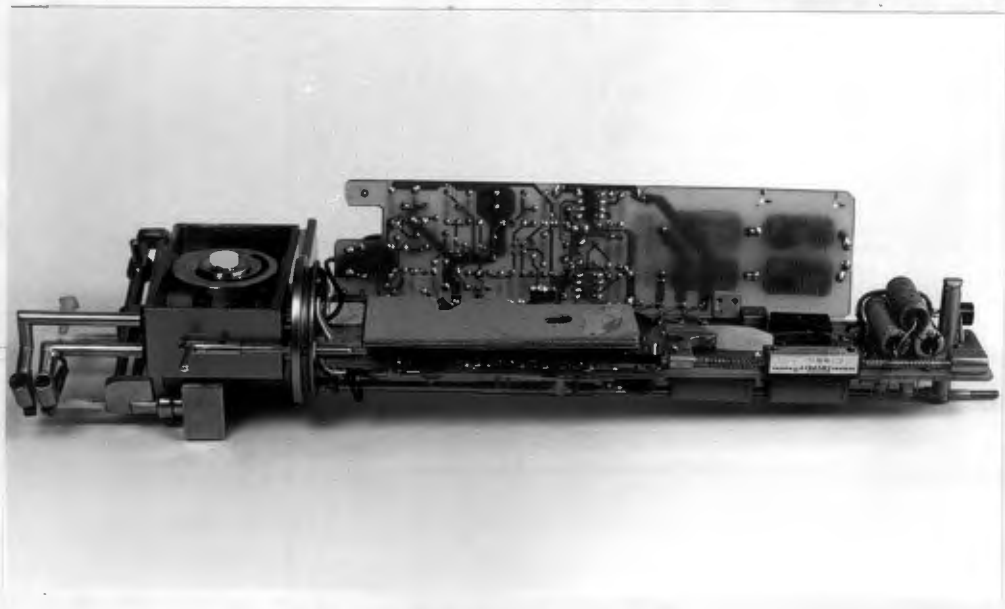

Fig.7-33

On/Off Switch and Volume Control

The on/off switch and volume control potentiometer were mounted directly on the printed circuit board as illustrated in Fig.7-32. A stainless steel rod pierces the interface plate and runs between the two boards to where it activates both the microswitch and gain potentiometer. The latter is a modified BOURNS multiturn trimpot, converted into a sliding potentiometer.

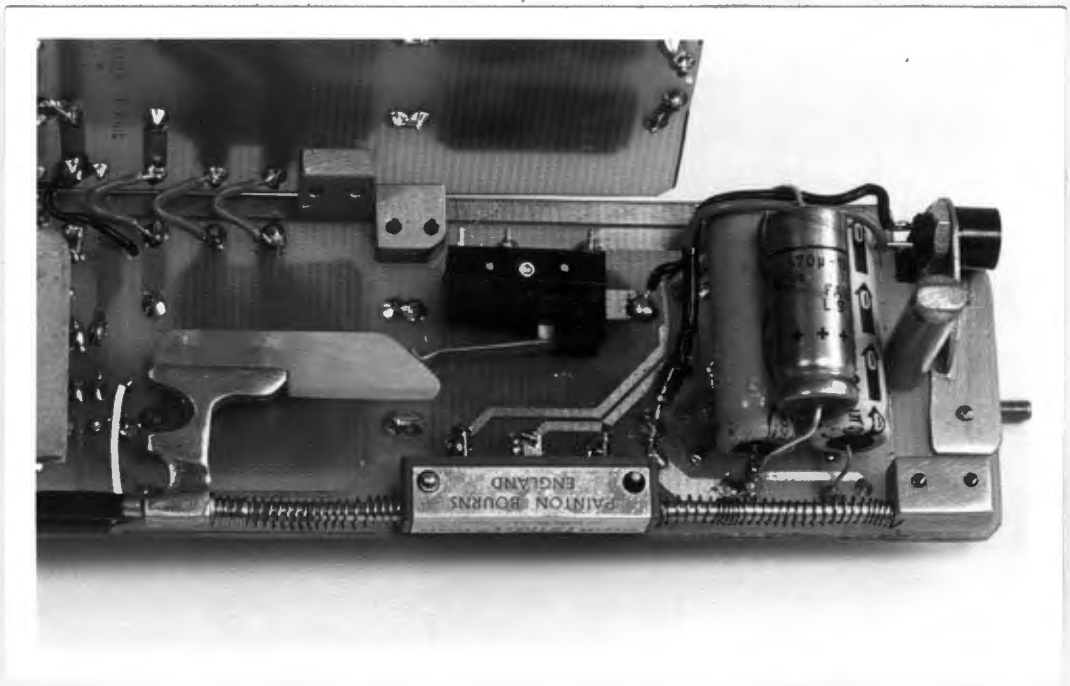

Fig.7-34

The philosophy behind this arrangement is that the operator should be able to grasp the instrument with his left hand and operate the switch and volume control with his index finger. Not only does this leave his right hand free to manipulate the needle, but it ensures that the device is off when not in use. A dual spring return system ensures that the trigger is returned to the off-position. By pulling it into the housing with the index finger, the device is switched on, this being indicated by the illumination of an LED on the interface plate. Pulling the trigger further increases the amplifier gain.

Component List

R1	100k	R33	10k	C16	100nF	C48	100µF	L1	27 Turns 36G wire on screened 5,5mm Bobbin
R2	47k	R34	180k	C17	1,0nF	C49	10µF		
R3	56Ω	R35	100k	C18	1,0nF	C50	1000µF		
R4	1,2k	R36	100k	C19	10nF	C51	10nF	L2	10µH
R5	5,6k	R37	180k	C20	10nF			L3	10µH
R6	1,8k	R38	100k	C21	100nF				
R7	1,0k	R39	47k	C22	10nF			L4	30T of 27G Cu wire, tapped at 6T, on T37-6 toroidal core.
R8	220Ω	R40	270Ω	C23	10µF	D1	1N4001		
R9	1,0k	R41	100Ω	C24	10µF	D2	1N4148		
R10	1,0k	R42	1,0k	C25	47nF	D3	1N4148		
R11	1,0k	R43	10k	C26	220µF	D5	1N4148		
R12	1,0k	R44	10k	C27	220pF	D6	1N4148	Tr1	2 windings on T50-6 toroidal core. N1:25T 27G N2:13T 27G
R13	560Ω	R45	4,7k	C28	47pF Preset	D8	1N4001		
R14	3,3k	R46	220Ω	C29	10nF	D9	1N4001		
R15	2,7k			C30	10nF	D10	6V2 Zen.		
R16	2,7k	RV1	10k Preset*	C31	10nF	D11	LED		
R17	10k			C32	10nF				
R18	10k	C1	1,0µF Tant	C33	100pF	Q1	MFE131		
R19	47k	C2	10nF	C34	47pF Preset	Q2	BFX89	R	2×2,5mm LTZ5
R20	22k	C3	47pF Preset	C35	82pF	Q3	2N2369	X	2×2,5mm LTZ5 both 9MHz
R21	10k	C4	10nF	C36	47pF	Q4	MFE131		
R22	10k	C5	100nF	C37	10nF	Q5	MFE131		
R23	100k	C6	100nF	C38	47nF			Spk	8Ω 66mm ϕ
R24	10k	C7	100nF	C39	47nF				
R25	680Ω	C8	100nF	C40	10nF			Sw1	Cherry E63 100mA µSwitch
R26	680Ω	C9	100nF	C41	22µF Tant	IC1	MC1496		
R27	12Ω	C10	100nF	C42	3,3nF	IC2	741	Bat	10×NCC24 1,5V Eveready NiCd.
R28	2,7Ω	C11	4,7nF	C43	1,0µF Tant	IC3	741		
R29	100Ω	C12	4,7nF	C44	1,0µF Tant	IC4	LM388		
R30	1,0k	C13	100nF	C45	100nF	IC5	LM2930-8TB	Plug	2pin polarized Radio spares 466-472,466-488 466-343
R31	1,0k	C14	6,8µF Tant	C46	1,0µF Tant	IC6	555		
R32	100Ω	C15	100nF	C47	10nF	IC7	741		

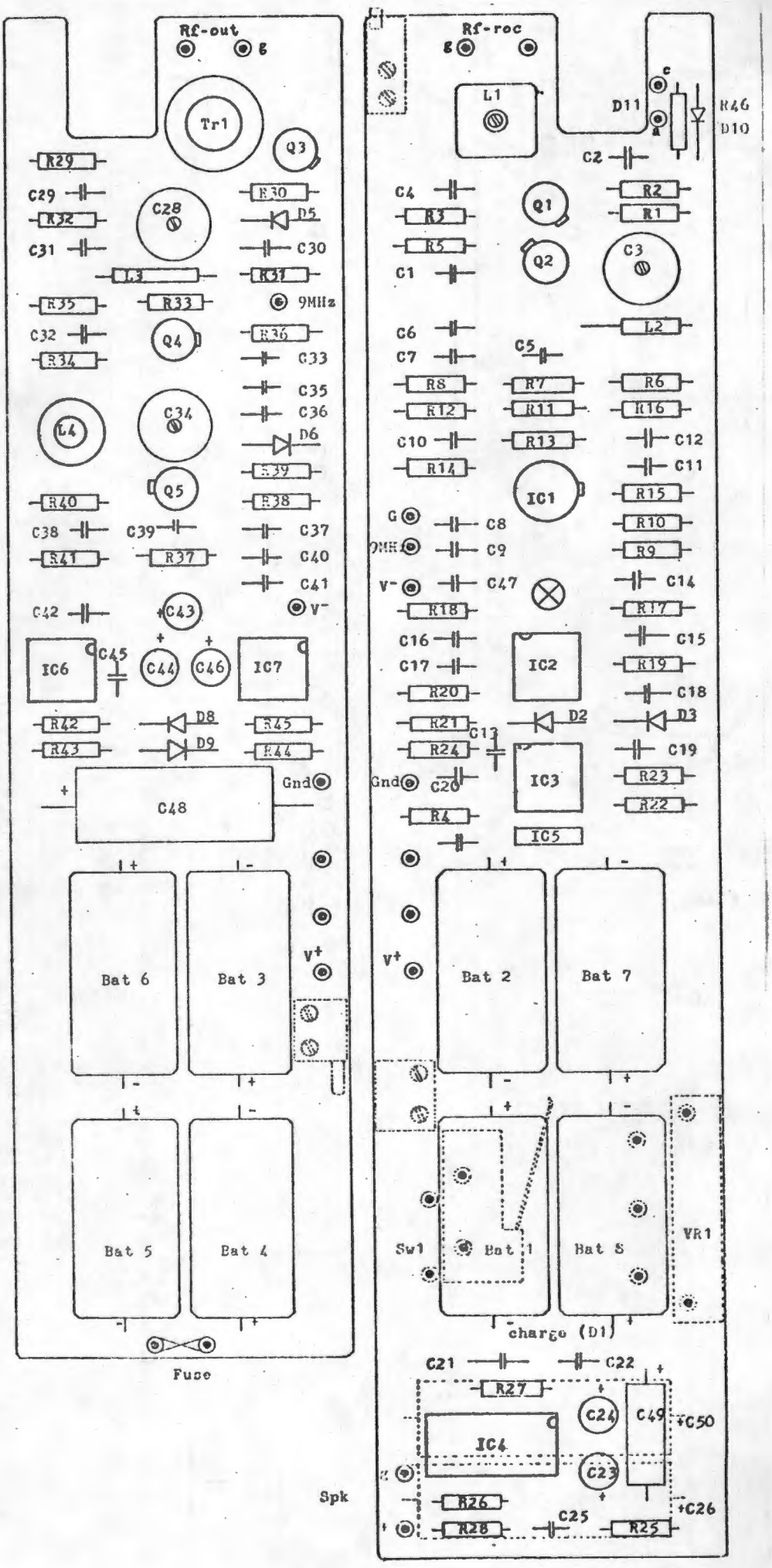

Fig.7-35 Component Layout

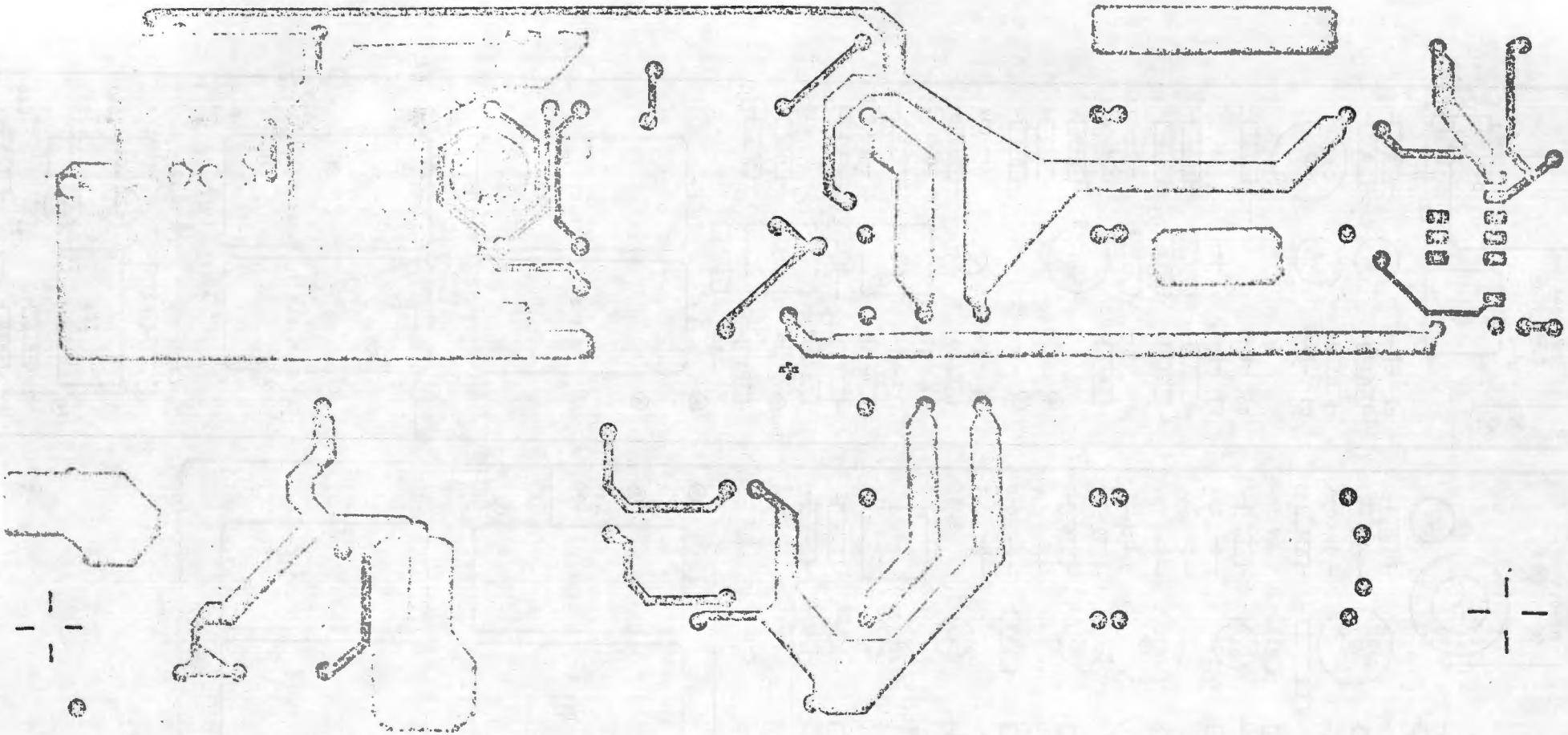

Fig.7-36 *P.C.Board; component side* Scale: 1,25:1

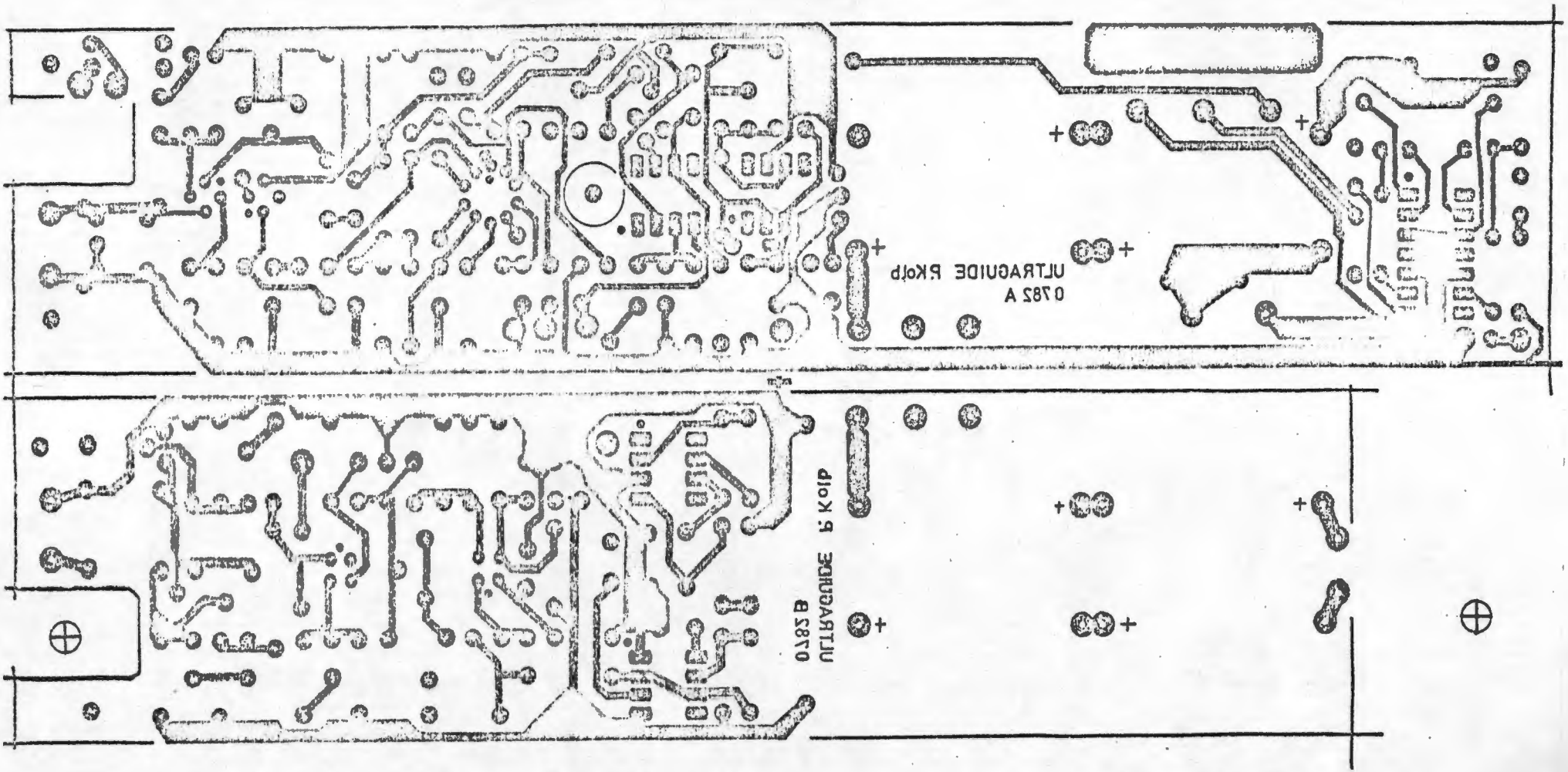

Fig.7-37 *P.C.Board; Track side* Scale: 1,25:1

Charger

A Charger was built for the ultraguide (Fig.8-3). Output is 20 to 25mA, i.e.: 10% of the Amp-hour rating of the NCC24 NiCd batteries. The simple circuit was built on a printed circuit board and housed in an attractive sealed plastic box suitable for a hospital environment. The same care was taken in constructing the charger as was taken with the Ultraguide itself.

An LED next to the output cable indicates whether the batteries are being charged.

§7.5 TRANSDUCER ALIGNMENT

This proved to be a task as difficult as had originally been expected. Several days were spent on this problem. While in a production model transducers would be aligned on a jig and moulded into the plastic housing so that no further adjustment would be necessary, this procedure is not suitable for prototyping. Apart from the need for flexibility in being able to preset the transducers for experimental purposes, a jig would require an enormous outlay in time and money and could only be justified for use in mass-production.

To a first approximation the transducers were aligned by sighting the two dimensional projections of the transducer housing through a protractor. The transducers are set with $\sigma = 70^0$ and $\phi = 40^0$. Any change in these angles would require the machining of a new scroll disc. Having fixed these angles roughly, the transducer transport bars were adjusted by loosening the retaining screws in the angular locking slides (parts no.32 and 33; page 125a). The transducers could thus be symmetrically positioned about the needle axis. At the same time the angular position of the transducer transport bars was set by viewing them from the side and rotating them. The transducer transport bars were then locked into position with a very long screw-driver pushed through an opening in the mirror tape between the interface plate and mechanical housing.

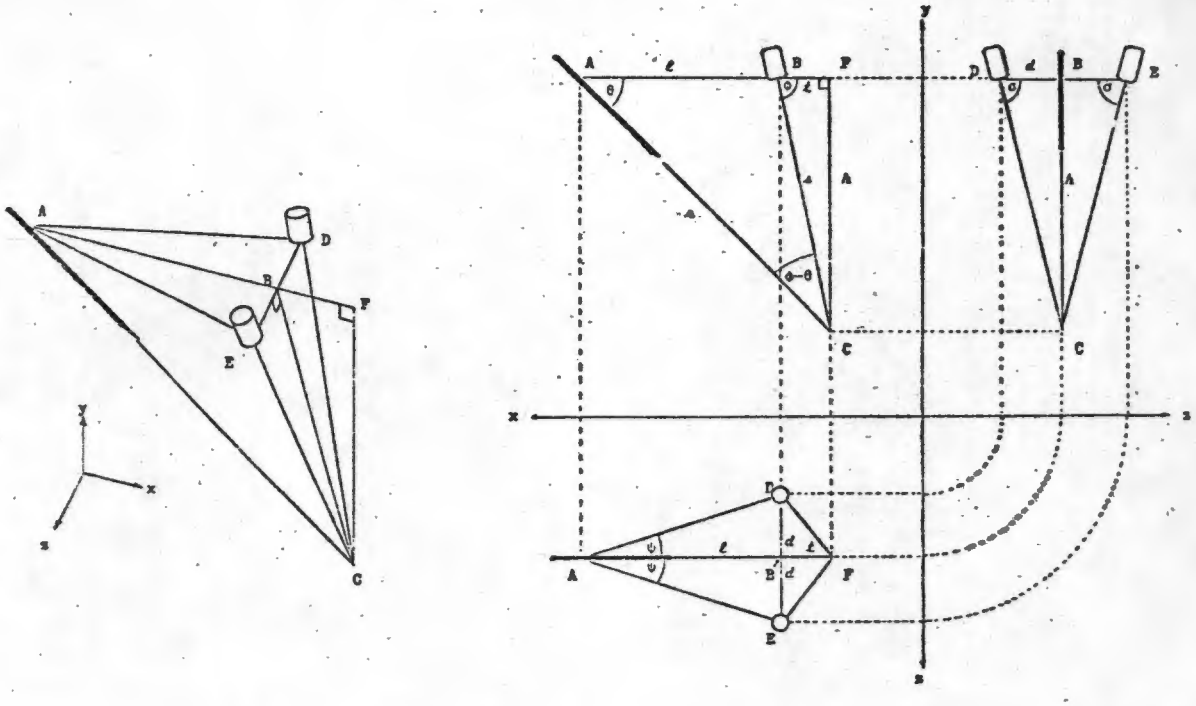

Fig.7-38

The distance ℓ (Fig.7-38) is measured between the guide rail pivot (88) and the guide rail roller (22) in a direction parallel to the position and angle control shafts. This distance should co-incide with that between the axis of the foot guide sleeve (59) and the centres of the transducer faces.

The angular position of the needle axis can be crudely sighted with a protractor. Alternatively, and this is the preferred method, the needle axis is set to zero by aligning it with the mechanical housing. The needle axis angle moves through 8° for every turn of the control knob. By turning the needle axis through 5° (i.e.: 5/8 turns of the control knob) the zero position of the scroll can be found. Provision is made for enabling the scroll to be set into the correct position.

d Can be obtained from equation 6-1 (§6.6) and checked on the instrument for various values of ℓ and θ. The two transducer transport bars were first set with $\theta = 13^{\circ}$ and $\ell = 18{,}2$mm, making $d = 2{,}1$mm.

The next step was to separate the two transducers and aim them at a remote target. For this purpose a brass tube with a 1mm bore

was connected to a fish tank pump. A small window was filed into the tube, and the whole thing was covered in silastic tubing. Water containing talcum powder particles was slowly passed through this tube. The guide was clamped in a stand and the transducers were dipped into a water tank. A very long 20 gauge needle mounted on the slide was used to position the target. By

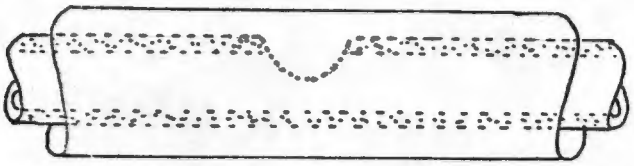

Fig.7-39

pre-setting θ and ℓ, r can be obtained (§6.6) and the window in the brass tube can be positioned very accurately at the tip of the needle. The geometry was set as follows: $\theta = 29^{o}$, ℓ = 16,7mm and hence r =56,4mm. The two transducers could then be aligned for maximum doppler intensity.

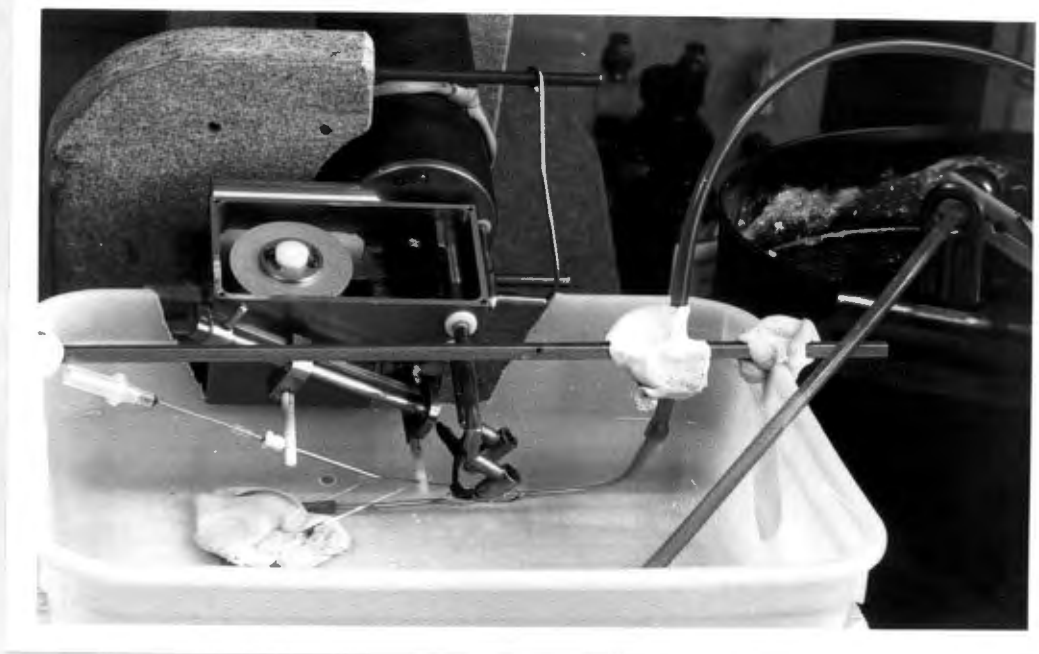

Fig.7-40

After this alignment was complete, θ and ℓ were changed and the target was moved around for a new maximum intensity. Triaxial

intersection could then be assessed by passing the needle down the guide sleeves and checking whether it hit the target. The results appeared to be very satisfactory, but for shallow targets it was difficult to see exactly what was happening because of refraction at the surface of the water.

Alignment Difficulties

Apart from the obvious tedium involved in the iterative procedure required for transducer alignment, there were some other difficulties that had to be faced:

1. In spite of the care taken in construction, there was at least 1mm of mechanical slack in d. Differentiating equation 6-1 (p92), we get:

$$\frac{\Delta h}{\Delta d} = \tan\sigma$$

   i.e.: because of the 1mm slack, the uncertainty in the depth of the vessel is 2,7mm.

2. The axis of the needle axis shaft (94) was located about 1,5mm below the centre of the transducer faces. The initial design specified that the transducers should be vertically adjustable to permit accurate positioning, but construction was so difficult that it was decided rather to tackle that problem if and when it arose.

3. There was play of a few degrees in the needle axis shaft (94).

4. Perhaps the most serious difficulty was that d was limited to a minimum of 2mm because the transducers physically interfered with one another. Thus the minimum distance which can be accommodated between the transducers and the vessels to be located is theoretically 10mm.

5. Working in shallow water imposes restrictions on optical alignment dictated by the refractive interface between air and water.

Slack in the system could not be eliminated by simple spring loading, since the moving parts were already a little stiff and could easily have jammed. Two alternatives remained. One was to set the two

transducer transport bars to the mid-point of the slack. However, the arrangement adopted was to align the transducers with all the slack entirely to one side. In other words, for vessel detection requiring a great deal of accuracy one would set the needle axis position and angle in such a way that the transducers are on the point of separating. This arrangement also has the advantage of offsetting some of the range limitations imposed by the physical dimensions of the transducers. At close ranges one could impinge into the slack area, knowing that the needle axis no longer passes exactly through the intersection point of the two beams. For shallow vessels this type of smudging can be tolerated if the vessel is in the same vertical plane as the needle. This principle also holds for deeper vessels, so that the needle axis angle and position adjustments can be approached from either side without affecting accuracy to any significant extent.

CHAPTER EIGHT

EVALUATION

§8.1 PRE-TRIAL EVALUATION

Physical

As already stated earlier, it is my view that an extremely important function of the biomedical engineer is to ensure not only that his creations are technically sound, but that they blend in well with the medical environment and especially that they are so attractive to the end user that he will want to use them. In line with the importance attached to aesthetics and ergonomics, the instrument was housed in a neat, rigid carrying case. A polysyrene mould was cut and glued and covered in felt to ensure that the presentation was attractive and that the instrument could not be damaged in transit.

Fig.8-1

The instrument itself (arguably) looks attractive. Aluminium parts were anodised in gold to make it look expensive and therefore to elicit some care and respect when handling. All brass parts were neatly finished off and polished.

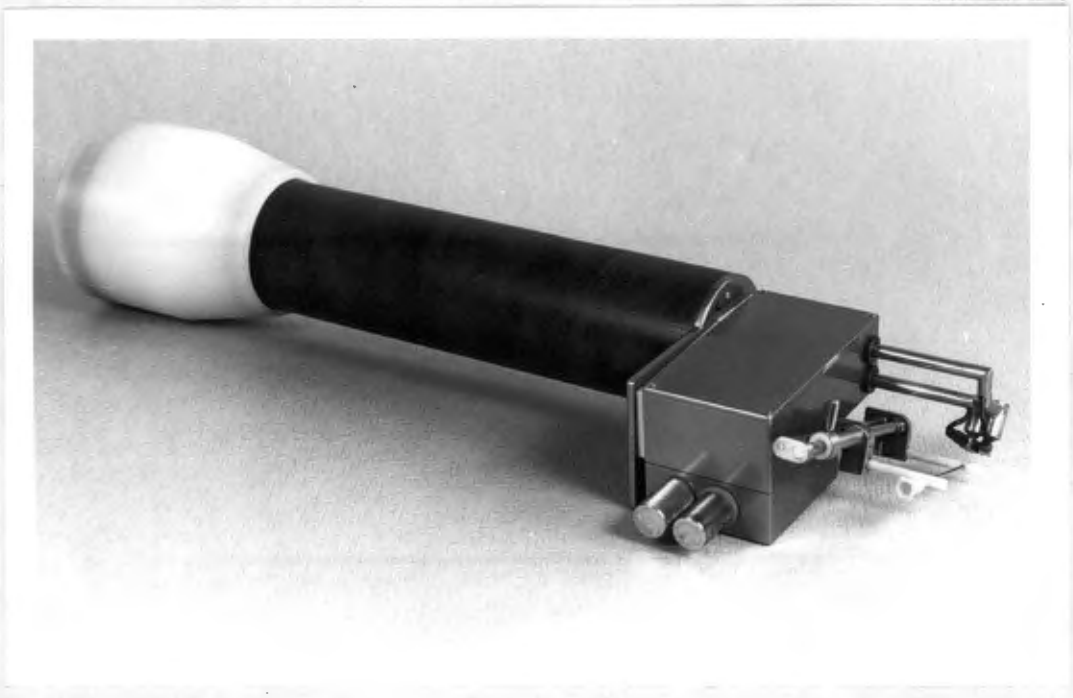

Fig.8-2

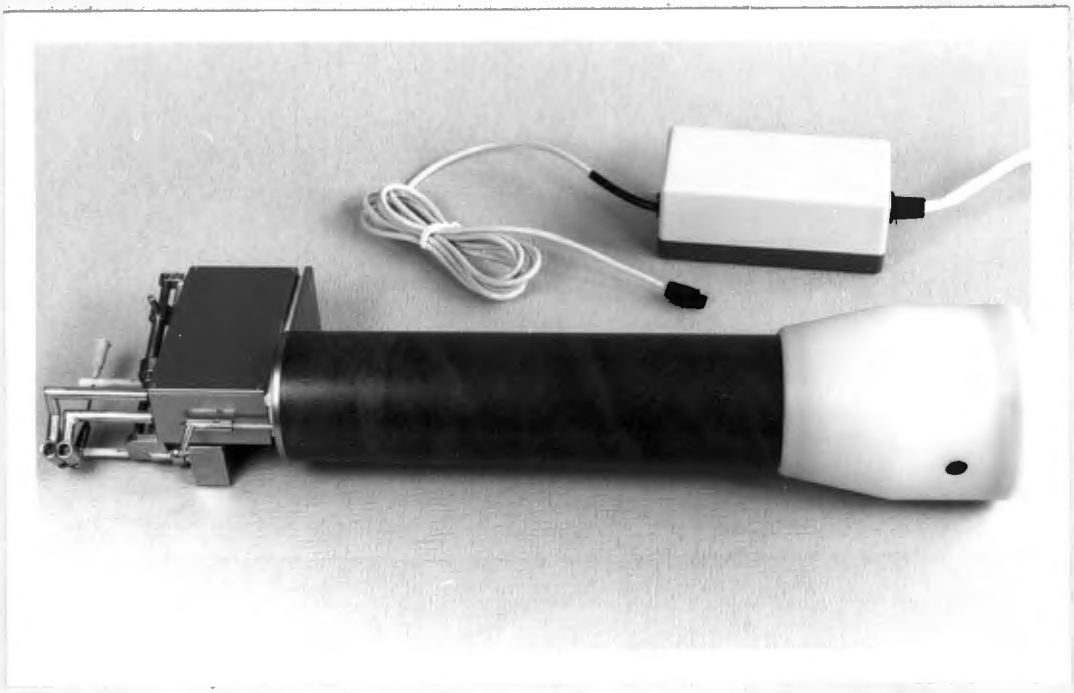

Fig.8-3

Functional

The instrument is quite easy to hold, can be picked up with one hand and is ready for action immediately. The on-off switch and volume control are very conveniently located. The feature that it need not be connected to other equipment should make it attractive to use.

Physically, a drawback is that it is still too heavy and bulky although this criticism was less frequently encountered than was expected. Its bulk, most regrettably, precludes it from use on the Subclavian Vein in its present form, since the electronic box gets in the way. Perhaps a flexible joint between the electonic box and the mechanical housing would enable the instrument to fit into this part of the anatomy. Alternatively, a drastic reduction in size could have the same effect.

It is absolutely essential that any future instrument will have to be sufficiently rugged to withstand dropping and bumping. This was one of the first reactions from an anesthetist. The prototype has to be handled very gently and is far too delicate for the rigours of clinical conditions. The vulnerable parts are, ofcourse, the transducers and the guide slide. The instrument is also vulnerable internally. While there is a clutch to protect the scroll disk from being overwound, there is no such clutch on the position screw. In addition, operators have to be careful that the transducers are not driven too close together, since the transducer transport bars could well be forced out of their preset positions. Effective blocking or mechanical fusing are needed. However, none of these problems is insurmountable.

A minor criticism is that the control knobs are too close together. Although this problem was foreseen early on in the design stages, a compromise solution was not thought desirable.

The guide sleeves were relatively easy to make with the help of a new jig designed and built in the mechanical workshop. The jig (Fig.8-4) ensures that each sleeve is identical, an important aspect in this instrument.

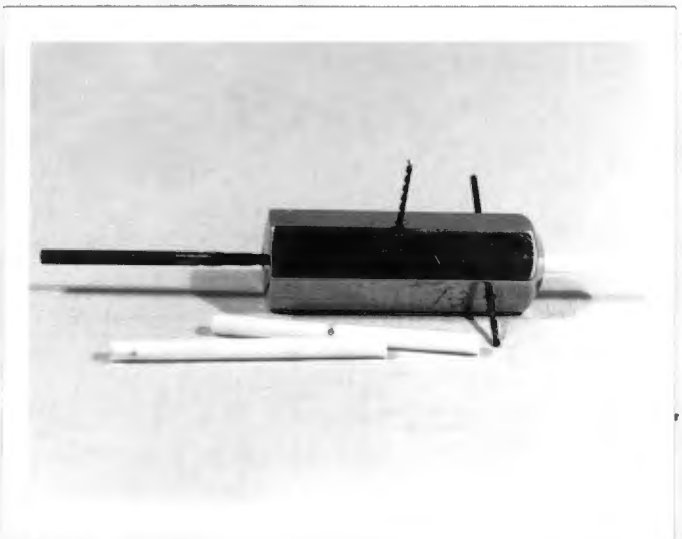

Fig.8-4

The sleeves were kept sterile in an alcohol-hepatane solution in small pill bottles, from which they could be slipped onto the guide stubs without contamination. For procedures requiring greater sterility, they could be pushed into place using a sterile glove or alcohol swab, while in other cases the sleeve was long enough to be handled at both ends without contaminating the hole through which the needle passes.

Threading the needle was also found to be less of a problem than initially expected. What was awkward was ensuring that the bevelled edge was up, since the needle has to be sheathed in the guide sleeve during the vessel search. All needles, especially thin ones, should in any case have a bevel mark on the head for doctors with poor vision.

The sliding mechanism which guides the needle functioned well, but incorporation of PTFE bearings rather than nylon would make the slide smoother. Since nylon is extremely hygroscopic, the possibility exists that it could swell up and cause the slide to seize.

That there is room for improvement in the electronic system is without question. Perhaps the most disturbing feature of the prototype is the whistle that was described earlier and which manifests itself from time to time. Noise reduction would improve the instrument at low signal levels. For detecting venous flow the gain usually has to be turned up a little higher than for arterial blood flow. The lower 3dB cut-off frequency of the band-pass filter may also be a little too high, particularly for venous blood flow detection.

An independent attenuator, reducing the gain for shallow vessels and allowing it to rise for deep vessels could readily be controlled by the position of the transducer transport bars, and should be considered for inclusion in future models.

While the built in loudspeaker is excellent for demonstrations and eliminates the additional operation of fitting an ear-piece, there are circumstances under which the use of an optional ear-piece would be desirable. It will be shown later that the patient could be distressed by the sound of his blood flow. There are also particularly noisy wards (especially where there is an abundance of ventilators), where private hearing is essential. One neat solution might be to have a clip on the end of the instrument which would hold a stethoscope bell over the loudspeaker cover. Since all doctors always seem to carry stethoscopes, it would eliminate the hygiene problem and the possibility of losing the earpiece.

Range

In line with information obtained from doctors (Appendix 3-2), the angle of the needle was made variable from 5^{o} to 35^{o}. It is not necessary, however, for the instrument to lie flat on the skin, since it can be tilted so that the needles can be inserted at any angle up to 90^{o}. The distance between the skin incision point and the transducers can be varied from 4mm to 15mm, which is again in line with information obtained from doctors. Having said that, however, it should be noted that because of physical constraints on moving the transducers close together, the minimum distance of a vessel from the transducers is about 10mm. This is theoretical. In practice vessels much closer than this can be identified through the side lobes of the beams. One can also lift the transducers from the surface of the skin for very superficial vessels, provided that there is sufficient coupling gel. We should mention that the geometry of the transducers may not be ideal, and that a scheme should be devised for effectively bringing the sound sources closer together.

The maximum depth of a vessel that the mechanical system can deal with is 55mm with the present transducer geometry, but this

can be increased if necessary by changing the angles of the transducers. The limitations on range are more likely to result from attenuation of ultrasound at 9 MHz. For deeper vessels a lower frequency should be used.

Technical

The ease with which the instrument opens and the accessibility of the various parts proved to be very useful during the final stages of development and testing, and especially for the transducer alignment procedure.

The question of slack in the system is less serious than was at first supposed. For paediatric work, however, it would have to be designed out of the system. The slack is largely due to an accumulation of small tolerances, necessary for smooth operation. It is essentially a design fault and cannot be blamed on poor craftsmanship.

While the mechanism does not jam, there are unnecessarily high forces between the guide rail and transport bars, especially when angle ψ is large. While the design allows both the guide rail and the needle axis angle to be driven with considerable mechanical advantage, there is no such advantage from the guide rail to the transducer transport bars. This could have been remedied by, for example, attaching a friction wheel to both control shafts in order to "sweep" the transport bars in the required direction.

§8.2 CLINICAL TRIALS

The following section is a report on initial clinical trials, the difficulties that were encountered and how these difficulties were addressed. The trials are expected to continue until sufficient information becomes available for a final design to be proposed.

After transducer alignment was completed, the instrument was taken to a senior anaesthetist who had earlier expressed a willingness to help with the testing. His initial concern was about the difficulty one might experience in keeping the instrument steady, particularly if the doctor has a tremor, as is not uncommon during

operations. I pointed out that the instrument was rather heavy and that the inertia may, in fact, damp out any minor tremor.

He thought that there was little point in trying the instrument out on animals, since it could do no damage to the patient.

The first test was done on a young cardiac patient prior to surgery. A 20 gauge teflon catheter/needle was to be inserted into her radial artery. The vessel was healthy and the pulsations were strong. Unexpectedly it was suggested that *I* locate the vessel. I had anticipated that the anaesthetist himself would operate the device. There was little difficulty in finding the artery, and the needle was gradually and successfully pushed in by the anaesthetist at the first attempt. This led to considerable excitement in the theatre. Since I was responsible for guiding the needle, this was effectively my first vessel puncture. It is interesting to note that the needle guide enabled a complete novice to effect such a puncture successfully.

The second ~~trial~~ test was on the radial artery of an elderly female cardiac patient, also prior to surgery. The pulse was weak and I was told that this was to be a difficult one. Inspired by the previous success, we approached the vessel as before. Although the doppler sounds were clear, we missed the vessel. This experience was sobering and led to a re-examination of a number of aspects. The following factors were thought to have contributed to this failure:

1. The vessel was very small, estimated by the anaesthetist to have been similar in size to the 20 gauge needle that was used.
2. Because the vessel was so small, the instrument should have been more effectively supported.
3. We discovered that the 20 gauge needle used in this test was about 20% thinner than the 20 gauge needle used in the first test! Since the guide sleeves were prepared for what was thought to be a standard 20 gauge needle, there was considerable play between the needle and its supports.

4. For such a small vessel the skin incision point was much too far from the target.

A special support attached to a clamp was made at the recommendation of the anaesthetist. The clamp was to be attached to a drip stand or similar vertical pole. I was extremely reluctant to clamp the instrument, since it has to be manouvreable when searching for a vessel. The instrument was therefore simply to rest on the support. Since the use of the support would tend to complicate the preparation before puncture, it should not be used unless absolutely necessary. Anything that complicates the use of the guide detracts from its value as it would tend to discourage people from using the instrument.

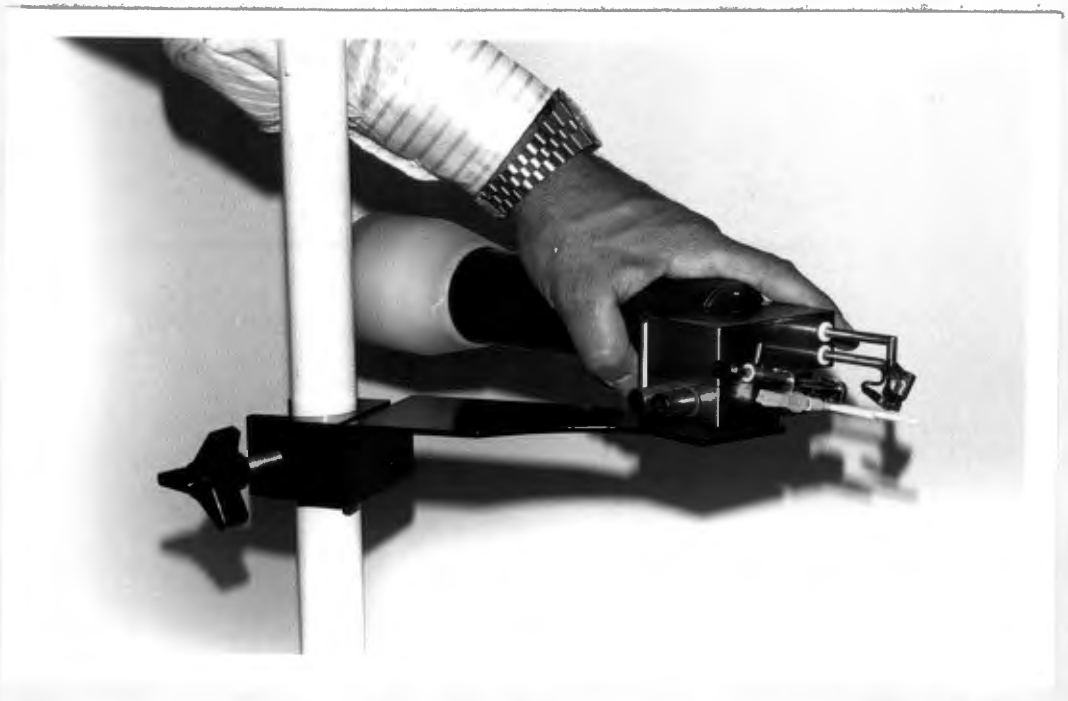

Fig.8-5

The needle alignment was checked and was found to be marginally out. Over the next three days the transducers were re-aligned. A possible reason for the misalignment was that a new guide sleeve manufacturing technique was employed. It was at this time that the new jig had been constructed for manufacturing these sleeves.

After exhaustive tests were carried out in the water-tank, a 1mm bore silastic tube was imbedded in a small plate of gelatine.

Practice runs were performed on this, and after these appeared to be satisfactory a further clinical trial was carried out.

The instrument was taken to a consultant in the respiratory unit at the hospital. He was very helpful and arranged for me to have access to the respiratory intensive care unit.

The third test was performed on an elderly, slightly built respiratory patient. A blood sample had to be taken for routine blood gas analysis. The stand was not available for this procedure. I located the vessel as before, while a young doctor leaned over my shoulder to push the needle home. We lost the doppler sounds during the attempt and missed the vessel twice. The attempt was then aborted.

It became imperative to find out exactly what was happening to the needle to establish the reasons for us missing. Back in the workshop a length of 1mm bore silastic tubing and a 2,5mm bore plastic tube were suspended on a specially constructed stand and immersed to varying depths in 2,5 liters of double strength gelatine. The gelatine, once set, was covered with a little water and a wet cloth. Water containing talcum powder was once again pumped through these tubes. The needles that were used were filled with ink and food-colouring. As the needle was withdrawn

Fig.8-6

after a blind puncture attempt through the cloth, a streak of clearly visible dye was left behind in the furrow. In this way it was possible to examine the path of the needle at leisure and without any obstruction. From these tests it became clear that the guide was off-centre by about 0,5mm for shallow vessels. After very careful examination of the transducers, the two transport bars were shifted slightly to one side and the transducers were carefully re-aligned. Subsequent tests done on the jelly indicated that the instrument was remarkably accurate when used correctly, even when the needle and the vessel were not in the same plane. The following points emerged and should serve as ground rules for using the instrument:

1. While scanning for a vessel, side-to-side searches are not sufficient. Depth searches have to be carried out at the same time. If the vessel lies before or beyond the triaxial intersection point, lateral scans tend to give a smudged output, and the centre of the vessel is difficult to identify. If, however, the depth is adjusted correctly, a very clear and unambiguous peak is obtained at the centre of the vessel. (If the transducers are aligned in a way such that the two beams fail to intersect properly, the same effect is observed.)

2. Once the peak intensity has been found, this must be maintained during the puncture procedure. If the signal fades, it means that the vessel has been pushed aside. One then withdraws the needle slightly, re-aligns and tries again.

3. If the bevelled edge is not held upwards, the needle stands a good chance of pushing the vessel away and missing the lumen all together. In fact the needle should always go in bevel up, and once blood is drawn it should be rotated through 180^{o} to reduce the chance of it piercing the back wall.

4. Very shallow punctures appear to get deflected easily, although this argument was not supported by the anaesthetist who was working with me.

5. The operator of the guide should perform the puncture himself. The instrument is not magical and has to be used with some sensitivity.

In all three trials thus far, every one of these rules was violated.

The fourth test was on the radial artery of the same patient on whom the third test had been done. This time no doctor was present, but a nurse supervised the procedure. Although the patient was conscious, a little more time and care was taken than before. No mounting post for the bracket was available, but the instrument rested satisfactorily on the patient's wrist. The site of the radial artery was carefully scanned in both depth and from side-to-side. When the midpoint of the vessel was found, the sound of flowing blood became suddenly so intense that the staff were startled and the patient started to shake with terror. After reducing the sound volume, I successfully impaled the vessel myself. However, while breaking the guide sleeves, the needle was drawn out by the heavy tube hanging from its end. Clearly someone should have been helping by holding onto the needle.

This incident underlined the need for these tests to be carried out in conjunction with an enthusiastic co-worker. Nursing staff in the ICU in question, while very helpful and friendly, are not enthusiastic over the instrument. They draw blood from radial arteries several times a day and thus clearly consider the instrument to be redundant in their circumstances.

By the time of writing there were no further punctures performed, although there are two further incidents worth mentioning. In the department of radiology, two consultants were very enthusiastic about the instrument. They thought that it would be useful to them personally in two to three percent of femoral artery catheterizations, and for students in general.

The first patient considered for the Femoral trial was suspected of having an occluded Aorta. Faint blood flow signals were detected in the Femoral Artery with the instrument, although there was no palpable pulse. A subsequent angiogram obtained after Aortic injection of dye confirmed the lesion in the Aorta and that Femoral catheterization was therefore contra-indicated. The

Femoral blood flow detected earlier on with the instrument was found to be entirely due to collateral circulation.

A second patient was prepared for Femoral catheterization, but when I saw the sterility procedure that had been followed, I had serious misgivings about the infection hazard the guide might pose to the patient. The test was called off at the last moment pending further investigations into this problem. The catheterization was done conventionally without the guide.

Venous blood flow:

While ultrasonically guided venipuncture has not yet been attempted with this instrument, it in fact can detect venous blood flow quite readily. Small superficial veins as well as deeper ones such as the Femoral can be successfully located. However, since venous flow is extremely slow, augmentation may be necessary in the form of deep breathing or localized squeezing of tissue distal to the puncture site.

Sterility:

The question of sterility cropped up in most discussions with medical personnel. Most doctors considered that the instrument would not pose an infection hazard to their patients. The fact that needle entry into the skin takes place at a site some distance removed from the transducers, seems to reassure most of them. One doctor was not reassured and so the department of Bacteriology was approached. One of the doctors working in that department was very impressed with the instrument and considered it to be safe from cross infection, but pointed out that nothing was ever 100% safe. He suggested that the professor be consulted. The professor was available only after the femoral test mentioned earlier had been cancelled. He volunteered that he was very impressed with the instrument, particularly with the following features:

1. The instrument was sealed and could therefore be washed. He considered that careful washing solved 90% of all sterility problems.
2. The design of the sterile guide sleeves and the proposed

method for mounting them on the guide stubs with a disposable cartridge, was entirely satisfactory.

3. The skin incision point was removed from the transducers.
4. The instrument had a nice finish.

He recommended that we proceed with tests including Femoral catheterizations, but that we observe the following precautions:

1. Keep the instrument clean.
2. Wipe the transducers with alcohol swabs before each procedure.
3. Put an extra sterile cloth down over the area where the instrument is to make contact with the patient or other sterile objects. This cloth should be removed after the instrument has performed its function.

He promised to arrange a meeting with senior theatre sisters so that a protocol for using the instrument in theatres can be confirmed.

While dangers of bacterial cross infection were negligible, precautions would have to be taken against viral cross infections. In the unlikely event of the instrument getting contaminated with hepatitis infected blood, it would have to be fully sterilized prior to further use. The solution here is to ensure that the instrument is not used on hepatitis cases, or that it is wrapped as far as possible in a plastic bag, or that future models are made from materials that are resistant to sterilizing agents such as Gluteraldehyde so that it can be effectively disinfected.

Finally he suggested that any production model should be free from cracks, crevices or sharp protrusions where germs and spores can lurk. In other words, every part should be easily washable. The one criticism he had of the prototype was that there were too many such sites and that the transducer wires and supports should be covered. This was, ofcourse, not practical to arrange on the prototype since it would have compromised experimental flexibility.

Coupling Gel

A second problem discussed with various personnel was the use of ultrasonic coupling gel. Sterile "Aquasonic 100" manufactured by Parker Laboratories Inc., is sold in 15gm sachets for about R2-00 a piece. This is commonly used as a coupling medium in ultrasonically guided biopsy procedures.

Because "Aquasonic" is so expensive and difficult to obtain in small quantities, consideration was given to using sterile "K-Y" lubricating gel, which is much less expensive and freely available throughout the hospital in convenient 2,5ml sachets. Suppliers of Ultrasound equipment are reported to discourage people from using "K-Y" as it is alleged to damage the epoxy coating on transducers. Manufacturers of epoxies, on the other hand, claim that these adhesives are remarkably resistant to chemicals such as water, oils, solvents, detergents etc.

From the point of view of safety to patients, "K-Y" was found to consist of 10% glycerine in Hydroxyethylcellulose preserved with Methyl Paraben [66]. While one would not inject this into arteries, needles would be wiped clean by passing through the tissue and any contaminant in the lumen would be expelled when the first drops of blood flush it out. So far nobody has objected to the use of "K-Y" gel from a clinical point of view.

The composition of Aquasonic could not be established, but it is remarkably like "K-Y." It is perhaps a little thicker, suggesting that there may well be no glycerine in it.

As was explained earlier, clinical trials are to be continued indefinitely. We will continue trying to evolve a technique for using the instrument, uncovering its short comings and establishing for which procedures the instrument is particularly suited and under what circumstances it should be used.

CHAPTER NINE

ULTRAGUIDE — THE FUTURE?

Initial indications are that the instrument would *definitely* be useful for routine arterial punctures in obese patients and in patients with proximal occlusive arterial diseases. It would *probably* be useful for routine venipuncture in obese patients, for deep veins such as the Femoral and in patients with a very black skin where veins cannot readily be seen. It would almost certainly be generally useful to inexperienced medical personnel and to those doctors that have persistant difficulties in locating vessels. The instrument in its present form is probably not useful for puncturing tiny scalp veins in infants and vessels which are easy to locate but difficult to puncture for other reasons. It would also not be used routinely by personnel experienced in a particular procedure. It would perhaps be most useful to anaesthetists in preparing patients for surgery.

The puncturing of Subclavian Veins, as has already been mentioned, is not possible with the instrument in its present form. A decision as to whether to desing an instrument dedicated to deep vessel location such as the Subclavian and the Aorta, or whether to make the present instrument more versatile, has still to be taken. There may be certain advantages in having a low-frequency, long range instrument, where the needle passes down the length of the ultrasonic beam. Based on this principle, ultrasonically guided Subclavian puncture has been done successfully before.

Although we are still in the process of evaluating the instrument's potential usefulness, initial contact with medical personnel has been encouraging. Inspite of conservatism normally attributed to the medical profession, doctors on the whole have been remarkably receptive to the instrument. Thus far everything has pointed to a successful future for ultraguide.

Further Development

A considerable amount of further development will have to be done. On a technical level, the scroll system will have to be replaced by a simpler one, such as a revolving cylinder containing the cam slot for driving the guide rail platform. This would reduce the bulk in the mechanical housing, and remove the need for one set of gears. The transducer transport bars could be driven more effectively by better utilization of the mechanical advantage afforded by the control knobs.

Both the size and the weight should be reduced down to 25 to 50% of the prototype.

One of the most important new features that should be considered is a full covering of the transducers. There appears to be no reason why the transducers and all related moving parts should not be fully enclosed in a sturdy, drop-proof shroud. The ultrasonic beam could be passed right through the base of the cover, which could be made of "pc" rubber, i.e.: rubber having a characteristic acoustic impedance approximately the same as that of physiological tissue. This would make the instrument very much easier to clean, would enable it to be gas-sterilized and would ensure that the transducers are protected from damage. In addition, friction and sealing problems associated with transducer movement would be completely eliminated. Finally, the instrument could be made to look a lot more streamline.

A dynamic triangulation diagram appearing under a transparent mechanical housing cover, would be a simple feature to include and would provide the operator with useful depth and range information.

Further development should concentrate not only on building new found requirements into the guide, but should also attempt to reduce the mechanical complexity in order to make it economical. If the instrument is to be sold as a general purpose tool, it should be within the general-purpose tool price-range.

At this stage it is difficult to see why a perfected needle guide should not one day, indeed, be found in every theatre, ICU and in every ward where vessel punctures are performed.

APPENDIX 1-1

Comments on the proposed needle guide from various medical Doctors

A summary of comments from medical personnel on the proposed needle guide is listed below. All the interviews were recorded, and in the order in which they took place. Since many of the interviews were fairly casual and no warning was given that they would be quoted, it was decided not to mention the names of the people interviewed.

Anaesthetist

He said that it can take from five minutes to half an hour to find an artery. He would like to be associated with the project and would certainly use the needle guide.

Paediatrician (Registrar)

He admitted to having trouble in finding the radial artery. Arterial blood samples are usually obtained by locating the artery by trial and error. He would use the needle guide.

M.D. (DVT Clinic)

He rarely does any puncturing. As a houseman he used to do about five or six per week, but he usually found the artery fairly quickly. He would not need a needle guide.

M.D. (Angiography)

Supplied estimates on time taken for various percutaneous puncture procedures:

	Novice	Expert
Internal Jugular Vein	>½hour	"1st Stab" on average
Subclavian Vein	2 hours→all day	2 minutes on average
Femoral Artery	3 minutes ave.	5 seconds on average
Femoral Vein	20 minutes ave. to 1 hour	5 seconds on average

He has done about 150 Jugular veins and estimates that 3 % still give him trouble,i.e: take longer than half an hour. When questioned he said he would use a needle guide for those difficult ones provided it was not too complicated or expensive.

Two Paediatricians (Registrars)

They were both very enthusiastic about the proposed needle guide and said they would use it in at least 50% of their cases. It would be particularly useful for collecting multiple samples of arterial blood, since arteries become increasingly hard to find as the number of available puncture sites decreases.

Two Paediatricians (Housemen)

They were also very enthusiastic about the guide and said that they had just been discussing the possibilities of obtaining such a device before I arrived.

Paediatrician (Senior Consultant)

He considered himself to be an expert in venipuncture although he had not had to do any for over a year. He thought the guide might be "nice to have around" but not really terribly useful. He was worried that it might prevent younger doctors from getting experience.

Paediatrician (Experienced Consultant)

According to him, they had some 10 000 children per year with intravenous drips in the oupatient diarrhoea room alone. However, he did not think that a needle guide would be useful in Haematology, since there were so many punctures performed that the technique was mastered relatively quickly. He thought, however, that it might have potential as a training device for inexperienced doctors. It might also be useful to general practitioners who do not perform venipuncture on a regular basis, in general surgery and in wards where non-routine punctures are performed.

Senior Anaesthetist

He was not only very enthusiastic about the proposed needle guide, but he was also convinced that all sixty four anaesthetists in the department would support the project. He felt that the guide would be particularly useful on cardiac patients where the set-up time averages about one hour.

Senior Anaesthetist

Fully endorsed the views expressed above.

Anaesthetist

He described the idea as "fantastic" and was convinced that it would be very useful.

Anaesthetist

He described the proposed guide as a "reasonable thing" and superb for infants.

Anaesthetist

Expressed enthusiasm for the idea.

Prof.(Clinical Sciences)

He did not think that there was a need for such a device, but he would give the project his full support if others thought there was.

Consultant (Coronary Care Unit)

He did not think the guide was a necessity, but he would certainly find use for it if it turned out to be a "pretty slick device".

APPENDIX 2-1

SURVEY ON PERCUTANEOUS PUNCTURE (Adults)

PLEASE COMPLETE AND RETURN TO:
P.J.Kolb (Dept. Biomedical Engineering)
33 Bastart Road, Observatory. Tel.: 685117
before 19th June 1981.

VESSEL (Name)	PROCEDURE	FREQUENCY OF PROCEDURE (1 - 10) *	VESSEL		ANGLE OR DISTANCE OF INCISION	REMARKS/DIAGRAMS
			Diameter (mm)	Depth (mm)		
			±	±	±	
			±	±	±	
			±	±	±	
			±	±	±	
			±	±	±	
			±	±	±	
			±	±	±	
			±	±	±	
			±	±	±	
			±	±	±	
			±	±	±	
			±	±	±	
			±	±	±	

FREQUENCY OF PROCEDURE

Score: 10 if procedure is known to be very common
1 if procedure is known to be rare

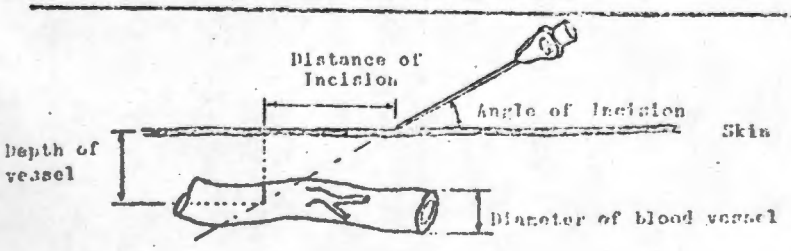

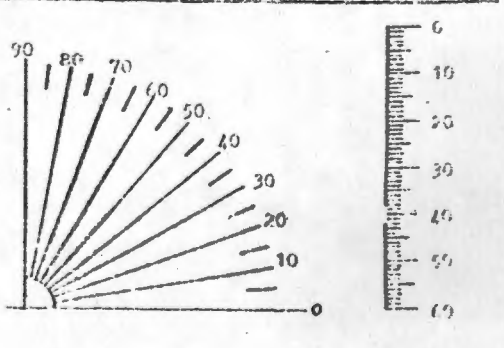

APPENDIX 2-2

Summary on survey of percutaneous puncture (Scale 3:1)

Veins: -Radial
-Median Cubital
-Basilic
-Forearm Veins
-Superficial veins

f = 9

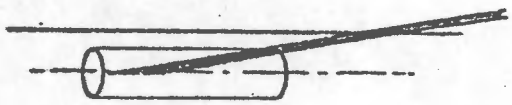

Dorsalis Pedis Artery f = 4

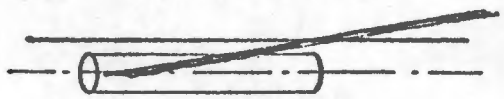

Dorsal Veins of Hand f = 10

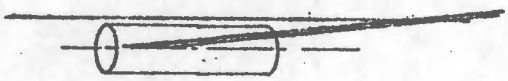

Radial Artery f = 7

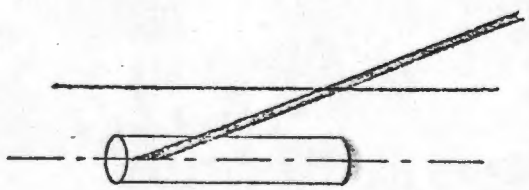

External Jugular Vein f = 6

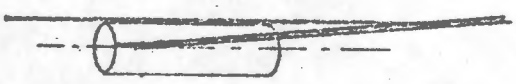

Internal Jugular Vein f = 5

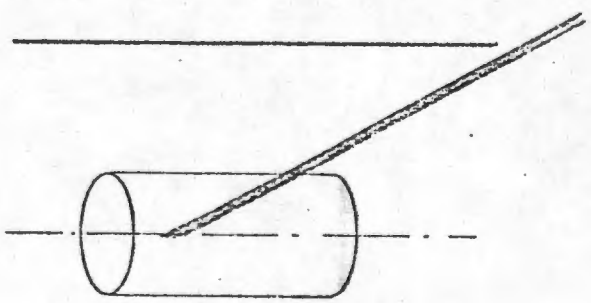

Femoral Artery f = 1

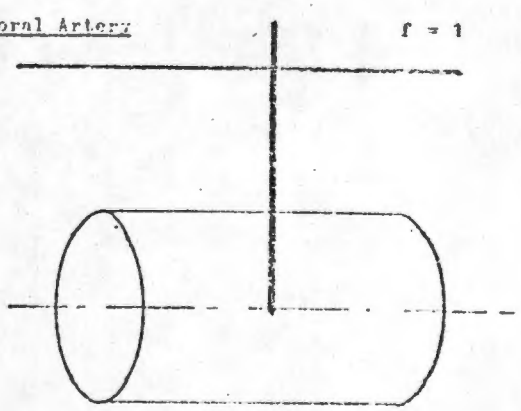

APPENDIX 4-1

The Doppler Principle

Consider a stationary source of sound waves S and a target R moving at velocity u away from the source.

Let:

λ_0 = wavelength of transmitted wave
f_0 = frequency of transmitted wave
f_1 = frequency as observed by target

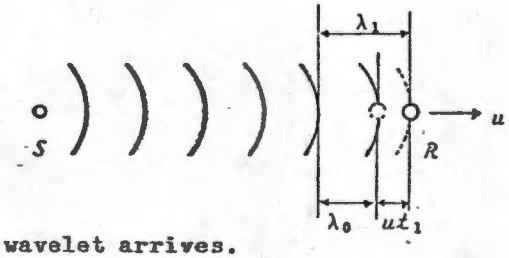

The wavelength as seen by the target is equal to the wavelength transmitted + the distance travelled by the target when the next wavelet arrives.

$$\lambda_1 = c.t_1$$
$$= \lambda_0 + u.t_1$$

where

$$t_1 = \frac{1}{f_1}$$

$$\frac{c}{f_1} = \frac{c}{f_0} + \frac{u}{f_1}$$

$$f_1 = \frac{(c - u)}{c} . f_0$$

Now let a stationary observer record the frequency reflected off the target. The wavelets are separated in time by

$$t_1 = \frac{1}{f_1}$$

Since the second wavelet is given off a distance $u.t_1$ after the first, the new wavelength is

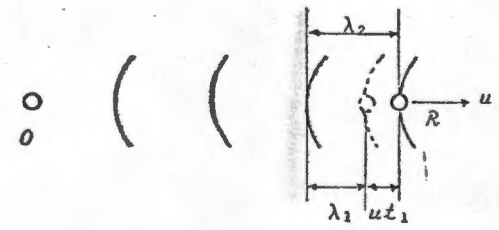

$$\lambda_2 = u.t_1 + c.t_1$$
$$= \frac{(u + c)}{f_1}$$

$$f_2 = \frac{c}{\lambda_2} = \frac{c}{(u + c)} . f_1$$

$$f_2 = f_0 \frac{(c - u)}{(c + u)}$$ where the target travels away from the source and

$$f_2 = f \frac{(c + u)}{(c - u)}$$ where the target travels towards the source

The doppler beat frequency is given by the difference between f_2 and f_0

$$\Delta f = \frac{2.u}{(c + u)} . f_0$$ (where u is negative when the target moves towards the source)

When the velocity of the target is not in the direction of the propagating waves, then that component of the velocity which is must be substituted for u. Thus

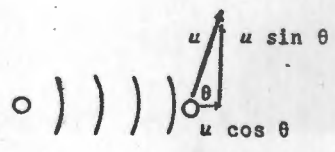

$$\Delta f = \frac{2.u.\cos\theta}{(c+u\cos\theta)} . f_0 = \frac{2.u f_0}{c} \cos\theta \quad \text{for } u << c$$

APPENDIX 4-2

Directivity and impedance functions for a circular piston

x	Directivity Functions ($x = ka \sin\theta$)		Impedance Functions ($x = 2ka$)	
	Pressure	Intensity	Resistance	Reactance
	$\frac{2J_1(x)}{x}$	$\left[\frac{2J_1(x)}{x}\right]^2$	$R_1(x)$	$X_1(x)$
0.0	1.0000	1.0000	0.0000	0.0000
0.2	0.9950	0.9900	0.0050	0.0847
0.4	0.9802	0.9608	0.0198	0.1680
0.6	0.9557	0.9134	0.0443	0.2486
0.8	0.9221	0.8503	0.0779	0.3253
1.0	0.8801	0.7746	0.1199	0.3969
1.2	0.8305	0.6897	0.1695	0.4624
1.4	0.7743	0.5995	0.2257	0.5207
1.6	0.7124	0.5075	0.2876	0.5713
1.8	0.6461	0.4174	0.3539	0.6134
2.0	0.5767	0.3326	0.4233	0.6468
2.2	0.5054	0.2554	0.4946	0.6711
2.4	0.4335	0.1879	0.5665	0.6862
2.6	0.3622	0.1326	0.6378	0.6925
2.8	0.2927	0.0857	0.7073	0.6903
3.0	0.2260	0.0511	0.7740	0.6800
3.2	0.1633	0.0267	0.8367	0.6623
3.4	0.1054	0.0111	0.8946	0.6381
3.6	0.0530	0.0028	0.9470	0.6081
3.8	+0.0068	0.00005	0.9932	0.5733
4.0	−0.0330	0.0011	1.0330	0.5349
4.5	−0.1027	0.0104	1.1027	0.4253
5.0	−0.1310	0.0172	1.1310	0.3232
5.5	−0.1242	0.0154	1.1242	0.2299
6.0	−0.0922	0.0085	1.0922	0.1594
6.5	−0.0473	0.0022	1.0473	0.1159
7.0	−0.0013	0.00000	1.0013	0.0989
7.5	+0.0361	0.0013	0.9639	0.1036
8.0	0.0587	0.0034	0.9413	0.1219
8.5	0.0643	0.0041	0.9357	0.1457
9.0	0.0545	0.0030	0.9455	0.1663
9.5	0.0339	0.0011	0.9661	0.1782
10.0	+0.0087	0.00008	0.9913	0.1784
10.5	−0.0150	0.0002	1.0150	0.1668
11.0	−0.0321	0.0010	1.0321	0.1464
11.5	−0.0397	0.0016	1.0397	0.1216
12.0	−0.0372	0.0014	1.0372	0.0973
12.5	−0.0265	0.0007	1.0265	0.0779
13.0	−0.0108	0.0001	1.0108	0.0662
13.5	+0.0056	0.00003	0.9944	0.0631
14.0	0.0191	0.0004	0.9809	0.0676
14.5	0.0267	0.0007	0.9733	0.0770
15.0	0.0273	0.0007	0.9727	0.0880
15.5	0.0216	0.0005	0.9784	0.0973
16.0	0.0113	0.0001	0.9887	0.1021

Ref 24

APPENDIX 4-3

Program to generate field intensity patterns for U.S.transducers

The following Computer program plots the field pattern of a circular transducer of radius a and operating frequency ℓ , both parameters having to be entered. The highest intensity ratio relative to I_0 must also be entered as well as the number of -5dB plots required.

For the plots in chapter four:

a = 1
ℓ = 9,1 and 5,0
I/I_0 = 10
Number of plots = 6
Scale Factor. = 1

```
C       PLOT SOUND INTENSITY DISTRIBUTION FOR U.S. TRANSDUCER
        DIMENSION W(45),DF(45),Y(2,45),X(45)
        DF(1)=1.00
        DF(2)=.9950
        DF(3)=.9802
        DF(4)=.9557
        DF(5)=.9221
        DF(6)=.8801
        DF(7)=.8305
        DF(8)=.7743
        DF(9)=.7124
        DF(10)=.6461
        DF(11)=.5767
        DF(12)=.5054
        DF(13)=.4335
        DF(14)=.3622
        DF(15)=.2927
        DF(16)=.2260
        DF(17)=.1633
        DF(18)=.1054
        DF(19)=.0530
        DF(20)=.0068
        DF(21)=.0330
        DF(22)=.1027
        DF(23)=.1310
        DF(24)=.1242
        DF(25)=.0922
        DF(26)=.0473
        DF(27)=.0013
        DF(28)=.0361
        DF(29)=.0587
        DF(30)=.0643
        DF(31)=.0545
        DF(32)=.0339
        DF(33)=.0087
        DF(34)=.0150
        DF(35)=.0321
        DF(36)=.0397
        DF(37)=.0372
        DF(38)=.0265
        DF(39)=.0108
        DF(40)=.0056
        DF(41)=.0191
        DF(42)=.0267
        DF(43)=.0273
        DF(44)=.0216
        DF(45)=.0113
        W(1)=0
        DO 4 I=1,20
        W(I+1)=W(I)+.2
4       CONTINUE
        DO 6 I=21,44
        W(I+1)=W(I)+.5
6       CONTINUE
7       TYPE 'ENTER RADIUS OF DISC (MM)'
        READ(11,105) A
        TYPE 'ENTER FREQUENCY (MHZ)'
```

```
      READ(11,105) F
      TYPE 'ENTER SCALE FACTOR'
      READ(11,105) SF
    9 TYPE 'ENTER 1ST INTENSITY RATIO (FROM 10. DOWN)'
      READ(11,105)AIRAT
      TYPE 'ENTER NUMBER OF PLOTS (UP TO 7)'
      READ(11,115)MFIN
C
C     INITIALIZE PLOTTER
C
      CALL PLOTS(0,0,0)
      CALL FACTOR(SF)
      CALL PLOT(-1.,A,3)
      CALL PLOT(0.,A,2)
      CALL PLOT(0,-A,2)
      CALL PLOT(-1.,-A,2)
C
C     DEFINE CONSTANTS
C
      PI=4.*ATAN(1.)
      ALAMD=1500./F/1000.
      AK=2.*PI*A/ALAMD
      AAK2=AK*A/2.
      XMIN=A*A/ALAMD
      WRITE(12,100)A,F,SF,ALAMD,AK,AIRAT,AAK2,XMIN
C
C     PLOT FAR FIELD/NEAR FIELD BOUNDARY
C
      DUMX=XMIN-.2
      DUMY=A-.4
      CALL PLOT(DUMX,A,3)
      CALL PLOT(XMIN,A,2)
      CALL PLOT(XMIN,DUMY,2)
      CALL PLOT(DUMX,-A,3)
      CALL PLOT(XMIN,-A,2)
      CALL PLOT(XMIN,-DUMY,2)
      CALL PLOT(0.,0.,3)
C
C     START OF CALCULATIONS AND PLOTS FOR 7I/10 FACTORS
C
      DO 70 M=1,MFIN
      SQRAT=SQRT(AIRAT)
      DO 10 I=1,45
      THET=ASIN(W(I)/AK)
      R=AAK2*DF(I)/SQRAT
      X(I)=R*COS(THET)
      Y(1,I)=R*SIN(THET)
      Y(2,I)=-Y(1,I)
   10 CONTINUE
      WRITE(12,100)(X(I),Y(1,I),I=1,10)
      WRITE(12,100)(X(I),Y(1,I),I=11,20)
      WRITE(12,100)(X(I),Y(1,I),I=21,30)
      WRITE(12,100)(X(I),Y(1,I),I=31,40)
      WRITE(12,120)(X(I),Y(1,I),I=41,45)
      DO 60 J=1,2
      DO 60 I=1,45
      IF(X(I)*SF.LT.30.)GO TO 15

      X(I)=30./SF
      GO TO 50
   15 IF(I.EQ.1)GO TO 50
      CALL PLOT(X(I),Y(J,I),2)
      GO TO 60
   50 CALL PLOT(X(I),Y(J,I),3)
   60 CONTINUE
      AIRAT=AIRAT/SQRT(10.)
   70 CONTINUE
      TYPE'MORE?  NO=0,  FULL RUN=1,  TO INIT RAT=2'
      READ(11,115)MORE
      IF(MORE.EQ.1)GO TO 7
      IF(MORE.EQ.2)GO TO 9
      STOP
  105 FORMAT(F10.5)
  100 FORMAT(5(2F10.5," *"))
  115 FORMAT(I1)
  120 FORMAT(5(2F10.5," *")/)
      END
```

APPENDIX 4-4: Piezoelectric properties of Philips PXE materials

Principal properties of present grades of PXE materials.
Unless otherwise specified the values given are nominal ones measured at 20 °C ± 5 °C.

property and symbol[1]	unit	PXE4[2]	PXE5	PXE6[3]	PXE7	PXE11[3]	PXE21	PXE22	PXE41	PXE42[4]	PXE51[3][4]
thermal data											
Curie temperature[5]	°C	265	285	370	320	400(180)[6]	270	270	315	325	220
specific heat	J/kg °C	420	420	420	420	420	420	420	420	420	420
thermal conductivity	W/m °C	1,2	1,2	1,2	1,2	1,2	1,2	1,2	1,2	1,2	1,2
mechanical data											
density ϱ_m	10^3 kg/m³	7,50	7,60	7,70	7,75	4,5	7,75	7,75	7,90	7,80	7,70
compliance s_{33}^E	10^{-12} m²/N	13,5	18,9		15,8	9,5	18,6	18,6	14,6		17,8
compliance s_{11}^E	10^{-12} m²/N	11,8	15,4	10,2	12,5	8,1	15,1	15,1	12,2	11,8	14,5
compliance s_{55}^E	10^{-12} m²/N		38,5		35,8	24,4			32,0		
Poisson's ratio σ		≈ 0,3	≈ 0,3	≈0,3	≈ 0,3	≈ 0,3	≈ 0,3	≈ 0,3	≈ 0,3	≈ 0,3	≈ 0,3
mechanical quality factor for radial mode Q_m^E		≈ 500	≈ 80	≈1000	≈ 80	≈ 270	≈ 80	≈ 80	≈ 1000	≈ 750	≈ 50
frequency constants[7] N_p^E	Hz·m or m/s	2300	2000	2460[8]	2200	3600	2000	2000	2200	2250	2050
frequency constants[7] $N_3^D = \frac{1}{2}v_3^D$	Hz·m or m/s	2050	1850		2000	2900	1900	1900	2000		1950
frequency constants[7] $N_1^E = \frac{1}{2}v_1^E$	Hz·m or m/s	1620	1460	1800	1640	2650			1620		
frequency constants[7] $N_5^E = \frac{1}{2}v_5^E$	Hz·m or m/s		930		970	1500			1020		
compressive strength	10^6 N/m²	> 600	> 600	> 600	> 600	> 600	> 600	> 600	> 600	> 600	> 600
tensile strength	10^6 N/m²	≈ 80	≈ 80	≈80	≈ 80	≈ 80	≈ 80	≈ 80	≈ 80	≈ 80	≈ 80
electrical data											
relative permittivity $\varepsilon_{33}^T/\varepsilon_0$ ϵ_r		1750	1800	600	700	400	1750	2250	1200	1300	2800
($\varepsilon_0 = 8{,}85 \cdot 10^{-12}$ F/m) $\varepsilon_{11}^T/\varepsilon_0$ ϵ_r			1800		1000	600			1130		
resistivity ϱ_{el} (25 °C)	10^{12} Ωm	0,1	1	0,1	1	100	0,1	0,1	0,05		0,1
time constant $\varrho_{el}\,\varepsilon_{33}^T$ (25 °C)	min	>25	> 250	> 9	> 100	> 6000	> 25	> 30	> 7		> 40
dielectric loss factor tan δ	10^{-3}	6	16	8	20	25	16	16	2,5	2,5	16
electromechanical data											
coupling factor k_p		0,55	0,58	0,32	0,52	0,43	0,62	0,62	0,56	0,55	0,66
coupling factor k_{33}		0,64	0,70		0,70	0,55	0,72	0,72	0,68		0,72
coupling factor k_{31}		0,32	0,34	0,19	0,31	0,25	0,37	0,37	0,33	0,32	0,39
coupling factor k_{15}			0,66		0,66	0,65			0,66		
piezoelectric charge constants d_{33}	10^{-12} C/N or m/V	292	384		220	100	385	438	268		480
piezoelectric charge constants d_{31}	10^{-12} C/N or m/V	− 138	− 169	− 44	− 86	− 47,5	− 180	− 202	− 119	− 120	− 234
piezoelectric charge constants d_{15}	10^{-12} C/N or m/V		515		370	235			335		
piezoelectric voltage constants g_{33}	10^{-3} Vm/N or m²/C	18,8	24,2		35,4	28,2	25	22,0	25,2		19,3
piezoelectric voltage constants g_{31}	10^{-3} Vm/N or m²/C	− 8,9	− 10,7	− 8,0	− 14,0	− 13,4	− 11,6	− 10,1	− 11,2	− 10,4	−9,5
piezoelectric voltage constants g_{15}	10^{-3} Vm/N or m²/C		32,5		42,0	44,0			33,5		

Notes

(1) Product properties are dependent on the dimensions and technology of the product and measuring signal level. Therefore a meaningful translation of the material properties is best done in consultation with the supplier.
Properties in the planar mode are measured on discs 16 mm diameter and 1 mm thick.
Properties in the 33-mode are measured on cylinders 6,35 mm diameter and 16 mm long.
Properties in the 15-mode are measured on plates 10 mm by 12 mm and 0,2 mm thick.

(2) Maintenance type only.

(3) Available on request.

(4) Preliminary data.

(5) Temperature at which the ε_{33}^T is maximum.

(6) In PXE11 there is a transition from the ferroelectric orthorhombic to the ferroelectric tetragonal phase at 180 °C. If the material passes through this temperature in either direction then it must be repoled.

(7) See Section 2.3.2.

(8) Fractional variation of N_p^E between 20 °C and 65 °C < 0,3%.

APPENDIX 6-1 Design of the Scroll

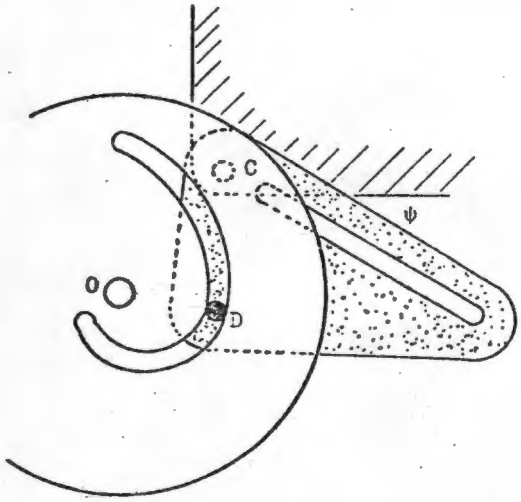

Fig:

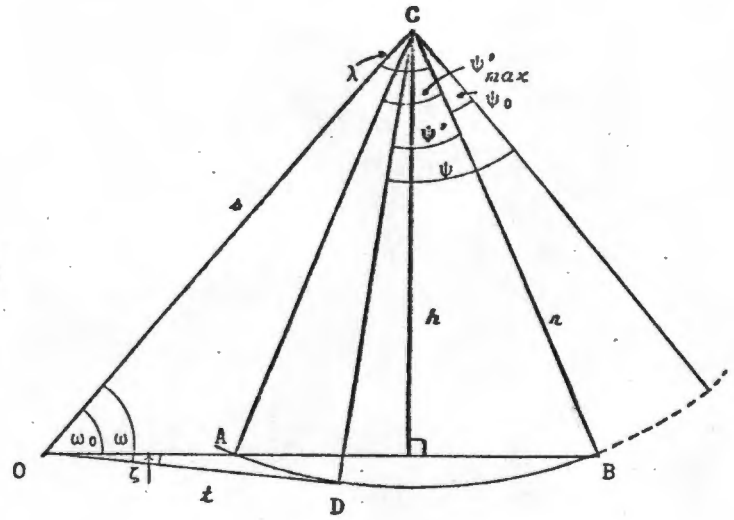

Fig:

The Scroll forms the link between the needle axis angle θ and the angle ψ the guide rail makes with the x-axis. The scroll and guide rail mechanism is illustrated in Fig: Fig: is a diagram representing the geometry of the system.

The Scroll rotates about it's centre O, while the guide rail platform rotates about C. As the scroll rotates, D slides along the spiral groove, turning the guide rail platform about C.

Definition of Terms:

θ, σ, ϕ and ψ were defined in Chapter 6. The relevant diagram is repeated here.

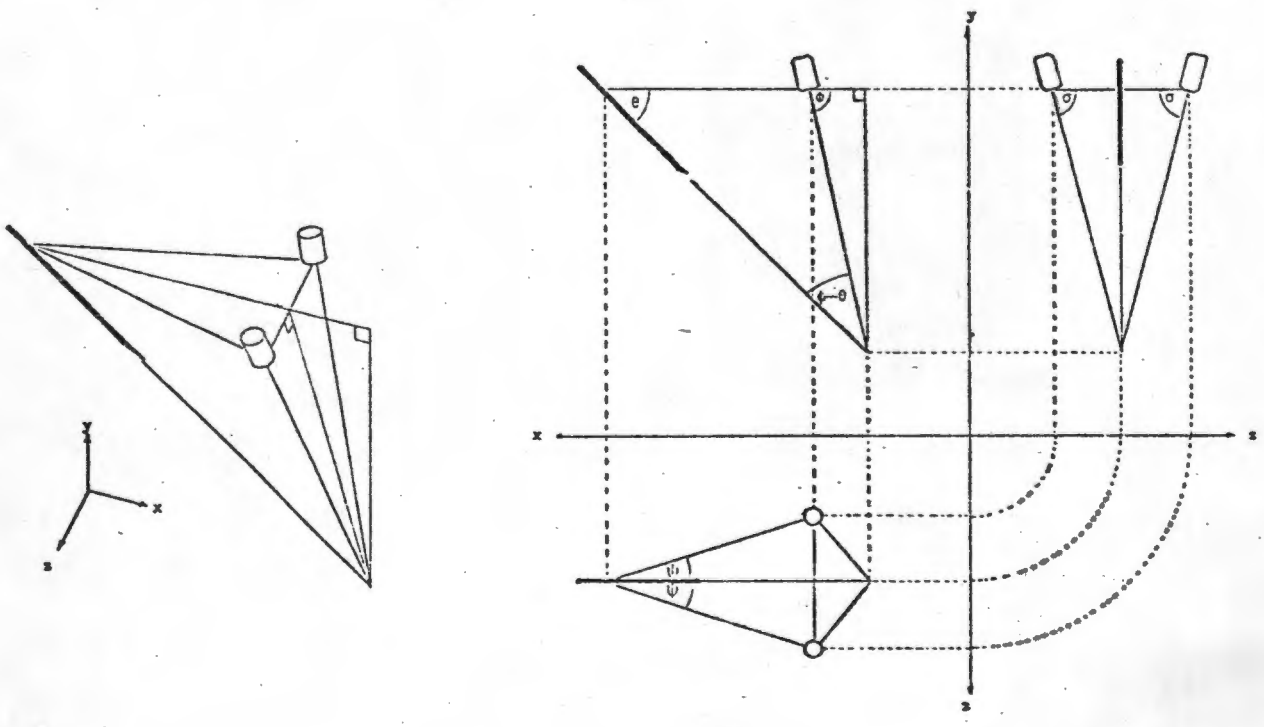

Fig:

θ_0 is the minimum value of θ .

η is the angle through which the disc rotates from its zero position. The gear ratio between the two sets of gears on the angle drive shaft TNSRAT is predefined. Therefore $\eta = TNSRAT \cdot (\theta - \theta_0)$.

ξ is the angle between the zero axis of the disc and line OD. It is numerically equal to η when D is at A or B, but takes into account the curvature of the path of point D as it moves between A and B.

ψ_0 is the angle ψ when $\theta = \theta_0$.

$\psi'max$ is the angle ψ when D coincides with A. .

$\Delta\eta$ is the step increase in η between successive points calculated along the spiral.

A,B are the limits of D.

Calculation

The following quantities are fixed and must be defined for a particular scroll:

Angles: σ, ϕ, θ_0

Lengths: r, OA, OB

$\Delta\eta$ is the angular step length and establishes the coarseness of the groove.

$$\frac{AB}{2r} = \sin\left(\frac{\psi'max}{2}\right)$$

$$\psi'max = 2.\text{arc sin}\left(\frac{AB}{2r}\right)$$

We have established in equation: that

$$\psi_0 = \text{arc tan}\left(\frac{\sin\phi}{\tan\sigma}\,\frac{\sin\theta_0}{\sin(\phi-\theta_0)}\right)$$

$$\frac{AB/2}{h} = \tan\left(\frac{\psi'max}{2}\right)$$

$$h = \frac{AB}{2.\tan\{\frac{\psi'max}{2}\}}$$

$$\omega_0 = \text{arc tan}\left(\frac{h}{OA + AB/2}\right)$$

$$s = \frac{h}{\sin\omega_0}$$

$$\frac{OB}{\sin\lambda} = \frac{r}{\sin\omega_0}$$

$$\lambda = \text{arc sin}\left(\frac{OB}{r}\sin\omega_0\right)$$

These quantities are all constant for a particular scroll.

Since the following expressions are all functions of θ they have to be evaluated for all values of θ .
We had earlier:

$$\eta = \text{THSRAT} \cdot (\theta - \theta_0)$$

$$\psi = \arctan\left[\frac{\sin\phi}{\tan\sigma}\,\frac{\sin\theta}{\sin(\phi-\theta)}\right]$$

$$\psi' = \psi - \psi_0$$

$$\ell = \left(s^2 + r^2 - 2rs\cos(\lambda - \psi')\right)^{\frac{1}{2}} \qquad \text{(Cosine Rule)}$$

$$\omega = \arcsin\left[\frac{r}{\ell}\sin(\lambda - \psi')\right]$$

$$\zeta = \omega - \omega_0$$

$$\xi = \eta + \zeta$$

The spiral is described in polar coordinates by ℓ and ξ.
A computer program was written in FORTRAN to generate a table of cartesian coordinates for the spiral. This data was punched into a Numerically Controlled (N.C.) milling machine.

The symbols used in the analysis above were converted into FORTRAN variables according to the following table:

Symbol	Fortran
r	R
s	S
AB	AB
OA	OA
OB	OB
h	H
ℓ	T
ψ (rad)	PSI
ψ'(rad)	PSID
ψ'max(r)	PSIDM
ψ_0(rad)	PSIØ
η (deg)	AET
η (rad)	ETA
$\Delta\eta$(deg)	ADET

Symbol	Fortran
σ (deg)	ASIG
σ (rad)	SIG
θ_0(deg)	ATHØ
θ (rad)	TH
θ_0(rad)	THØ
$\Delta\theta$(deg)	ADTH
$\Delta\theta$(rad)	THD
ϕ (deg)	APHI
ϕ (rad)	P
ω (rad)	OMEG
ω_0(rad)	OMEGØ
λ (rad)	BL
ξ (deg)	AXI
ξ (rad)	XI

FORTRAN Program for Calculating the coordinates of the Spiral groove forming the Scroll

When the Program runs it asks for θ_0, σ, ϕ and $\Delta\eta$. These have to be entered, each on a new record in F10.2 format. Then R, OA, OB and TNSRAT have to be entered in the same way.

```
C       PROJECT. SCROLL FOR ULTRAGUIDE
C       THIS PROGRAM CALCULATES X,Y COORDINATES OF GROOVE IN THE SCROLL.
C       REFER SECTION.
C       **********************
C
    1   WRITE(10,100)
        READ(11,200)ATHO,ASIG,APHI,ADET
        WRITE(10,150)
        READ(11,250)R,OA,OB,TNSRAT
        WRITE(12,320)ATHO,ASIG,APHI
        WRITE(12,330)R,OA,OB,TNSRAT
        WRITE(12,300)
        WRITE(12,310)
C
        PI=4 *ATAN(1. )
        FACT=PI/180.
        SIG=FACT*ASIG
        P=FACT*APHI
        THO=FACT*ATHO
        AB=OB-OA
        PSIDM=2. *ASIN(AB/2. /R)
        B1=SIN(P)/TAN(SIG)
        B2=SIN(THO)/SIN(P-THO)
        PSIO=ATAN(B1*B2)
        H=AB/2. /TAN(PSIDM/2. )
        OMEGO=ATAN(H/(OA+AB/2. ))
        B4=SIN(OMEGO)
        S=H/B4
        BL=ASIN(OB/R*B4)
        U=S*S+R*R
        V=2. *S*R
        ATH=ATHO
        TH=THO
        ADTH=ADET/TNSRAT
        CALL PLOTS(0,0,0)
        CALL PLOT(12. ,12. ,-3)
        CALL FACTOR(.5)
        XCORD=-S*COS(OMEGO)
        YCORD=S*SIN(OMEGO)
        CALL SYMBOL(R,0. ,2. ,10,0. ,-1)
        CALL SYMBOL(XCORD,YCORD,1. ,5,0. ,-1)
        CALL SYMBOL(0. ,0. ,2. ,3,0. ,-1)
C
        DO 10 I=1,360
        ETA=TNSRAT*(TH-THO)
        B3=SIN(TH)/SIN(P-TH)
        PSI=ATAN(B1*B3)
        PSID=PSI-PSIO
        T=SQRT(U-V*COS(BL-PSID))
        OMEG=ASIN(R/T*SIN(BL-PSID))
        DZ=OMEG-OMEGO
        XI=ETA+DZ
        AXI=XI/FACT
        AET=ETA/FACT
        APSI=PSI/FACT
        X=T*COS(XI)
        Y=T*SIN(XI)
```

```
      WRITE(12,350)ATH,APSI,AET,AXI,T,X,Y
      IF(I.NE.1)GO TO 66
      CALL PLOT(X,Y,3)
      GO TO 67
   66 CALL PLOT(X,Y,2)
   67 ATH=ATH+ADTH
      TH=TH+ADTH*FACT
      IF(T.LT.OA)GO TO 12
      AA=I
      IF((AA/5.-I/5).LT..001)WRITE(12,318)
   10 CONTINUE
   12 WRITE(12,315)
      CALL PLOT(0.,0.,3)
      TYPE 'MORE?  YES=1     NO=0'
      READ(11,660) MORE
      IF(MORE.EQ.1)GO TO 1
      STOP
C
  100 FORMAT(/T10,"THETA 0"/T10,"SIGMA"/T10,"PHI"/T10,"DEL ETA"/)
  150 FORMAT(/T10,"R"/T10,"OA"/T10,"OB"/T10,"TNSRAT"/)
  200 FORMAT(3(F10.2/)F10.2)
  250 FORMAT(3(F10.2/)F10.6)
  300 FORMAT(T6,"THETA",T17,"PSI",T26,"ETA",T37,"XI",T47,"T",T57,
     +"X",T67,"Y")
  310 FORMAT(T6,65("*")/)
  315 FORMAT(/T6,65("*")//)
  318 FORMAT()
  320 FORMAT(/T20,"THETA0=",F10.2/T20,"SIGMA =",F10.2/T20,"PHI    ="
     +,F10.2/)
  330 FORMAT(/T20,"R      =",F10.3/T20,"OA     =",F10.3/T20,"OB     ="
     +,F10.3//T20,"TNSRAT=",F10.6//)
  350 FORMAT(4F10.2,3F10.3)
  660  FORMAT(I1)
       END
```

OUTPUT FROM PLOTTER

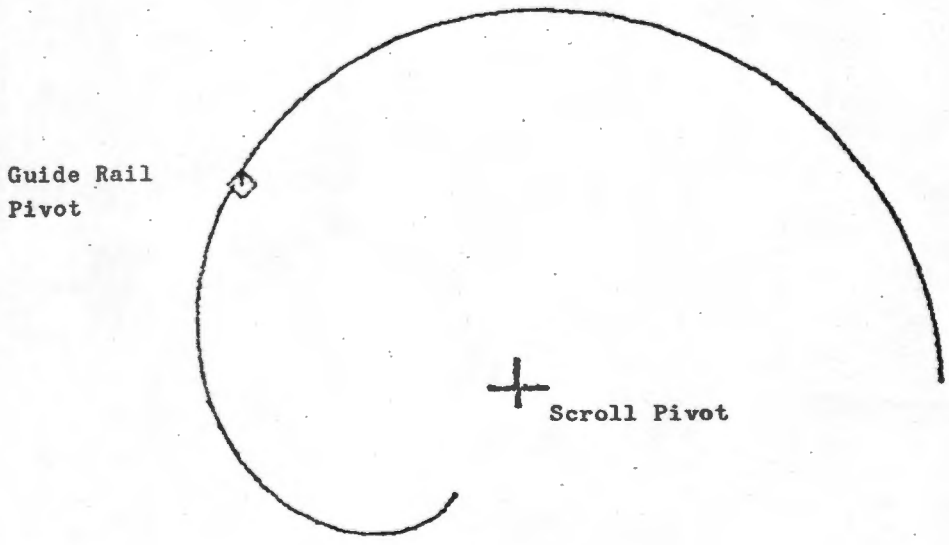

THETA0= 5.00
SIGMA = 70.00
PHI = 40.00

R = 8.600
OA = 4.500
OB = 14.500

TNSRAT= 7.500000

THETA	PSI	ETA	XI	T	X	Y
5.00	2.04	.00	-.00	14.500	14.500	-.000
5.27	2.16	2.00	2.04	14.485	14.476	.516
5.53	2.28	4.00	4.08	14.470	14.433	1.031
5.80	2.41	6.00	6.13	14.455	14.372	1.543
6.07	2.54	8.00	8.17	14.439	14.292	2.052
6.33	2.67	10.00	10.22	14.423	14.195	2.558
6.60	2.80	12.00	12.26	14.407	14.078	3.059
6.87	2.93	14.00	14.31	14.391	13.944	3.556
7.13	3.06	16.00	16.35	14.374	13.793	4.047
7.40	3.20	18.00	18.40	14.357	13.623	4.532
7.67	3.34	20.00	20.45	14.340	13.437	5.009
7.93	3.48	22.00	22.49	14.323	13.233	5.480
8.20	3.62	24.00	24.54	14.305	13.013	5.942
8.47	3.77	26.00	26.59	14.287	12.776	6.396
8.73	3.92	28.00	28.64	14.269	12.523	6.840
9.00	4.06	30.00	30.69	14.250	12.254	7.274
9.27	4.22	32.00	32.74	14.232	11.970	7.698
9.53	4.37	34.00	34.80	14.213	11.671	8.111
9.80	4.53	36.00	36.85	14.193	11.358	8.512
10.07	4.69	38.00	38.90	14.173	11.030	8.901
10.33	4.85	40.00	40.96	14.153	10.688	9.277
10.60	5.01	42.00	43.01	14.133	10.334	9.641
10.87	5.18	44.00	45.07	14.112	9.967	9.991
11.13	5.35	46.00	47.13	14.091	9.587	10.326
11.40	5.52	48.00	49.18	14.069	9.196	10.647
11.67	5.69	50.00	51.24	14.047	8.794	10.954
11.93	5.87	52.00	53.30	14.025	8.381	11.245
12.20	6.05	54.00	55.36	14.002	7.959	11.520
12.47	6.24	56.00	57.42	13.979	7.527	11.779
12.73	6.42	58.00	59.48	13.955	7.086	12.022
13.00	6.61	60.00	61.55	13.931	6.637	12.248
13.27	6.81	62.00	63.61	13.907	6.181	12.458
13.53	7.00	64.00	65.68	13.882	5.717	12.649
13.80	7.20	66.00	67.74	13.856	5.248	12.824
14.07	7.41	68.00	69.81	13.830	4.773	12.980
14.33	7.62	70.00	71.88	13.804	4.293	13.119
14.60	7.83	72.00	73.95	13.777	3.809	13.239
14.87	8.04	74.00	76.02	13.749	3.322	13.342
15.13	8.26	76.00	78.09	13.721	2.831	13.426
15.40	8.49	78.00	80.16	13.692	2.339	13.491
15.67	8.72	80.00	82.24	13.663	1.845	13.538
15.93	8.95	82.00	84.31	13.633	1.350	13.566
16.20	9.19	84.00	86.39	13.602	.856	13.575
16.47	9.43	86.00	88.47	13.571	.362	13.566
16.73	9.68	88.00	90.55	13.539	-.130	13.538
17.00	9.93	90.00	92.63	13.506	-.620	13.492
17.27	10.19	92.00	94.71	13.473	-1.107	13.427
17.53	10.45	94.00	96.80	13.439	-1.591	13.344
17.80	10.72	96.00	98.88	13.404	-2.070	13.243
18.07	10.99	98.00	100.97	13.368	-2.544	13.124
18.33	11.27	100.00	103.06	13.331	-3.012	12.987
18.60	11.56	102.00	105.15	13.294	-3.474	12.832
18.87	11.85	104.00	107.24	13.256	-3.929	12.660
19.13	12.15	106.00	109.34	13.216	-4.376	12.471
19.40	12.45	108.00	111.43	13.176	-4.814	12.265
19.67	12.77	110.00	113.53	13.135	-5.243	12.043
19.93	13.09	112.00	115.63	13.093	-5.663	11.805
20.20	13.41	114.00	117.73	13.049	-6.072	11.551
20.47	13.73	116.00	119.83	13.005	-6.469	11.282
20.73	14.09	118.00	121.94	12.959	-6.855	10.998
21.00	14.44	120.00	124.04	12.913	-7.229	10.700
21.27	14.80	122.00	126.15	12.865	-7.589	10.388
21.53	15.17	124.00	128.26	12.815	-7.936	10.062
21.80	15.55	126.00	130.38	12.765	-8.269	9.724
22.07	15.93	128.00	132.49	12.713	-8.587	9.374
22.33	16.33	130.00	134.61	12.659	-8.890	9.012
22.60	16.73	132.00	136.73	12.604	-9.178	8.640
22.87	17.15	134.00	138.85	12.548	-9.449	8.257
23.13	17.58	136.00	140.98	12.490	-9.703	7.864
23.40	18.02	138.00	143.10	12.430	-9.941	7.463

23. 67	18. 47	140. 00	145. 23	12. 369	-10. 161	7. 053
23. 93	18. 93	142. 00	147. 37	12. 305	-10. 363	6. 636
24. 20	19. 40	144. 00	149. 50	12. 240	-10. 546	6. 212
24 47	19. 89	146. 00	151. 64	12. 173	-10. 712	5. 783
24 73	20. 39	148. 00	153. 78	12. 104	-10. 858	5. 348
25 00	20. 91	150. 00	155. 92	12. 032	-10. 985	4. 910
25 27	21. 44	152. 00	158. 06	11. 959	-11. 093	4. 468
25 53	21. 98	154. 00	160. 21	11. 883	-11. 181	4. 023
25. 80	22. 54	156. 00	162. 36	11. 805	-11. 250	3. 577
26. 07	23. 12	158. 00	164. 51	11. 724	-11. 299	3. 131
26. 33	23. 71	160. 00	166. 67	11. 641	-11. 327	2. 684
26. 60	24. 32	162. 00	168. 83	11. 555	-11. 336	2. 239
26. 87	24. 95	164. 00	170. 98	11. 466	-11. 324	1. 797
27. 13	25. 60	166. 00	173. 15	11. 374	-11. 293	1. 357
27. 40	26. 27	168. 00	175. 31	11. 280	-11. 242	. 922
27. 67	26. 96	170. 00	177. 48	11. 182	-11. 171	. 492
27. 93	27. 67	172. 00	179. 64	11. 080	-11. 080	. 069
28. 20	28. 40	174. 00	181. 81	10. 976	-10. 970	-. 347
28. 47	29. 15	176. 00	183. 98	10. 867	-10. 841	-. 755
28. 73	29. 93	178. 00	186. 16	10. 755	-10. 693	-1. 153
29. 00	30. 73	180. 00	188. 33	10. 639	-10. 527	-1. 541
29. 27	31. 55	182. 00	190. 50	10. 519	-10. 343	-1. 917
29. 53	32. 41	184. 00	192. 67	10. 395	-10. 142	-2. 280
29. 80	33. 29	186. 00	194. 84	10. 267	-9. 924	-2. 630
30. 07	34. 20	188. 00	197. 01	10. 134	-9. 691	-2. 965
30 33	35. 13	190. 00	199. 18	9. 996	-9. 442	-3. 284
30. 60	36. 10	192. 00	201. 34	9. 854	-9. 178	-3. 586
30. 87	37. 09	194. 00	203. 50	9. 707	-8. 902	-3. 871
31. 13	38. 12	196. 00	205. 65	9. 555	-8. 613	-4. 136
31. 40	39. 18	198. 00	207. 80	9. 397	-8. 313	-4. 383
31. 67	40. 28	200. 00	209. 93	9. 235	-8. 003	-4. 608
31. 93	41. 41	202. 00	212. 06	9. 066	-7. 684	-4. 812
32. 20	42. 57	204. 00	214. 17	8. 893	-7. 358	-4. 994
32. 47	43. 77	206. 00	216. 26	8. 713	-7. 026	-5. 154
32. 73	45. 00	208. 00	218. 34	8. 528	-6. 689	-5. 290
33. 00	46. 27	210. 00	220. 39	8. 338	-6. 350	-5. 403
33. 27	47. 58	212. 00	222. 42	8. 141	-6. 010	-5. 491
33. 53	48. 93	214. 00	224. 41	7. 939	-5. 671	-5. 556
33. 80	50. 31	216. 00	226. 37	7. 732	-5. 335	-5. 596
34. 07	51. 73	218. 00	228. 28	7. 519	-5. 004	-5. 612
34. 33	53. 19	220. 00	230. 14	7. 301	-4. 679	-5. 604
34. 60	54. 69	222. 00	231. 95	7. 078	-4. 363	-5. 573
34. 87	56. 22	224. 00	233. 68	6. 850	-4. 057	-5. 520
35. 13	57. 78	226. 00	235. 34	6. 619	-3. 764	-5. 444
35. 40	59. 38	228. 00	236. 90	6. 384	-3. 486	-5. 348
35. 67	61. 02	230. 00	238. 36	6. 146	-3. 224	-5. 232
35. 93	62. 68	232. 00	239. 70	5. 906	-2. 980	-5. 099
36. 20	64. 37	234. 00	240. 89	5. 665	-2. 756	-4. 950
36. 47	66. 10	236. 00	241. 92	5. 424	-2. 553	-4. 786
36. 73	67. 84	238. 00	242. 77	5. 185	-2. 372	-4. 611
37. 00	69. 61	240. 00	243. 41	4. 949	-2. 215	-4. 425
37. 27	71. 39	242. 00	243. 80	4. 717	-2. 082	-4. 233
37. 53	73. 20	244. 00	243. 93	4. 493	-1. 974	-4. 036

****

The x-y coordinates generated by the FORTRAN program were used by Mr.A.Sass of the Department of Mechanical Engineering at U.C.T., to program a numerically controlled milling machine. The following is a listing of the program:

```
%N1G90G71X0.0Y75.0T1M6
N2X14.5Y0.0Z2.0
N3G1Z-3.5F200
X14.476Y0.516
X14.433Y1.031
X14.372Y1.543
X14.292Y2.052
X14.195Y2.553
X14.079Y3.059
X13.944Y3.556
X13.793Y4.047
X13.623Y4.532
X13.437Y5.009
X13.233Y5.480
X13.013Y5.942
X12.776Y6.396
X12.523Y6.840
X12.254Y7.274
X11.970Y7.693
X11.671Y8.111
X11.353Y8.512
X11.020Y8.901
X10.663Y9.277
X10.334Y9.641
X9.967Y9.991
X9.587Y10.326
X9.196Y10.647
X8.794Y10.954
X8.381Y11.245
X7.959Y11.523
X7.527Y11.779
X7.086Y12.022
X6.637Y12.243
X6.181Y12.453
X5.717Y12.649
X5.248Y12.824
X4.773Y12.980
X4.293Y13.119
X3.809Y13.239
X3.322Y13.342
X2.831Y13.426
X2.339Y13.491
X1.845Y13.538
X1.350Y13.566
X0.856Y13.575
X0.362Y13.566
X-0.130Y13.538
X-0.620Y13.492
X-1.107Y13.427
X-1.591Y13.344
X-2.070Y13.243
X-2.544Y13.124
X-3.012Y12.987
X-3.474Y12.832
X-3.929Y12.660
X-4.376Y12.471
X-4.814Y12.265
X-5.243Y12.043
X-5.663Y11.805
X-6.072Y11.551
X-6.469Y11.282
X-6.855Y10.998
X-7.229Y10.700
X-7.589Y10.388
X-7.936Y10.062
X-8.269Y9.724
X-8.587Y9.374
X-8.890Y9.012
X-9.178Y8.640
X-9.449Y8.257
X-9.703Y7.864
X-9.941Y7.463
X-10.161Y7.053
X-10.363Y6.636
X-10.546Y6.212
X-10.712Y5.783
X-10.858Y5.348
X-10.985Y4.910
X-11.093Y4.468
X-11.181Y4.023
X-11.250Y3.577
X-11.299Y3.131
X-11.327Y2.684
X-11.336Y2.239
X-11.324Y1.797
X-11.293Y1.357
X-11.242Y0.922
X-11.171Y0.492
X-11.080Y0.069
X-10.970Y-0.347
X-10.841Y-0.755
X-10.693Y-1.153
X-10.527Y-1.541
X-10.343Y-1.917
X-10.142Y-2.282
X-9.924Y-2.636
X-9.691Y-2.965
X-9.442Y-3.284
X-9.178Y-3.586
X-8.902Y-3.871
X-8.613Y-4.136
X-8.313Y-4.383
X-8.003Y-4.608
X-7.684Y-4.812
X-7.358Y-4.994
X-7.026Y-5.154
X-6.689Y-5.293
X-6.350Y-5.403
X-6.010Y-5.491
X-5.671Y-5.556
X-5.335Y-5.596
X-5.004Y-5.612
X-4.679Y-5.604
X-4.363Y-5.573
X-4.057Y-5.520
X-3.764Y-5.444
X-3.486Y-5.343
X-3.224Y-5.232
X-2.980Y-5.099
X-2.756Y-4.953
X-2.553Y-4.786
X-2.372Y-4.611
X-2.215Y-4.425
X-2.082Y-4.233
X-1.974Y-4.036
G0G90X0.0Y75.0M2
E
*
```

APPENDIX 6-2

An expression is to be obtained for determining the maximum distance from the centre of a rod supported at both ends by rings, such that slipping will still occur, when the applied force is not parallel to the axis of the rod.

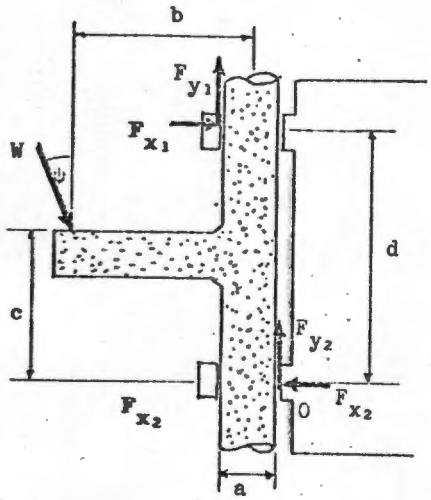

At the point of slipping:

$\sum F_x = 0$

$$F_{x_1} + W \sin \psi = F_{x_2} \qquad (1)$$

$\sum F_y \equiv 0$

$$F_{y_1} + F_{y_2} = W \cos \psi \qquad (2)$$

$$F_{y_1} = \mu F_{x_1} \qquad (3a)$$

$$F_{y_2} = \mu F_{x_2} \qquad (3b)$$

$\sum M_0 = 0$

$$W \cos \psi (b+a/2) - F_{y_1} a = F_{x_1} d + W c \sin \psi \qquad (4)$$

from (1) $\quad -F_{x_1} + F_{x_2} = W \sin \psi$

from (2)&(3) $\quad \mu F_{x_1} + \mu F_{x_2} = W \cos \psi$

$$- \mu F_{x_1} + \mu F_{x_2} = \mu W \sin \psi$$

therefore $\quad 2\mu F_{x_1} = W(\cos \psi - \mu \sin \psi)$

$$F_{x_1} = \frac{W}{2\mu} (\cos \psi - \mu \sin \psi) \qquad (5)$$

from (4) $\quad W \cos \psi (b+a/2) - \mu F_{x_1} a = F_{x_1} d + W \sin \psi \, c$

subst (5) $\quad W \cos \psi (b+a/2) - (\mu a + d) \cdot \frac{W}{2\mu} (\cos \psi - \mu \sin \psi)$

$$= c W \sin \psi$$

$$W \cos \psi \, (b+a/2) - \cos \psi (\mu a + d) \frac{W}{2\mu} = \sin \psi \, (c W - (\mu a + d) \frac{W}{2})$$

$$((b+a/2) - \frac{1}{2\mu}(\mu a + d)) W \cos \psi = (c - \frac{\mu a}{2} - d/2) W \sin \psi$$

$$(b - \frac{a}{2} + \frac{a}{2} - \frac{d}{2\mu}) = (c - \frac{\mu a}{2} - \frac{d}{2}) \tan \psi$$

$$\boxed{b = \frac{d}{2\mu} + (c - \frac{\mu a}{2} - \frac{d}{2}) \tan \psi}$$

As ψ increases from 0 to some critical value, F_{x_1} decreases until it is zero. Thereafter Thereafter F_{x_1} increases from zero on the radially opposite side of the shaft. At this moment of "flipping":

$$F_{x_1} = F_{y_1} = 0$$

$$F_{x_2} = W \sin \psi \qquad \mu F_{x_2} = W \cos \psi$$

$$\tan \psi = 1/\mu$$

From (4) $\quad W \cos \psi \, (b+a/2) = c W \sin \psi$

Therefore $\quad b = c \tan \psi - a/2 = c/\mu - a/2$

REFERENCES

1. A.W. Jongens, Acoustics Lab., UCT: private communication.
2. I.P.Murray: Complications of invasive monitoring; Medical Instrumentation; Vol.15 No.2; March-April 1981; pp85-89.
3. V.C.Roberts: A review of non-invasive measurement of blood flow; Biomedical Engineering; August 1974; pp332-335.
4. B.Jacobson, J.G.Webster: Medicine and Clinical Engineering; Prentice-Hall Inc.,1977; p186.
5. B.Y.Lee, F.S.Trainor, D.Kavner, J.Madden: A clinical evaluation of a non-invasive electromagnetic flowmeter; Angiology; April 1975; pp317-328.
6. E.W.Powers, W.W.Frayer: Laser doppler measurement of blood flow in the microcirculation; Plastic and Reconstructive Surgery; Feb.1978; pp250-255.
7. Phung Le-Cong, R.H.Lovberg: Analysis of a dual beam laser velocimeter applied to microcirculation studies; Rev.Sci. Instrum.; Vol.51 part 5; May 1980; pp565-574.
8. W.M. Phillips, S.S.Furby, W.S.Pierce: Laser doppler anemometer studies in unsteady ventricular flow; Trans. Am. Soc. Artif. Organs: Vol.25; 1979; pp56-60.
9. H.H.Holm; J.K.Kristensen: Ultrasonically guided percutaneous puncture technique:
10. Preface to ref.9.
11. H.H.Holm, J.K.Kristensen, S.N.Rasmussen, A.Northeved, H.Barlebo: Ultrasound as a guide in percutaneous puncture technique; Ultrasonics; March 1972; pp83-86.
12. H.H.Holm, J.F.Pedersen, J.K.Kristensen, S.N.Rasmussen,S.Hancke, F.Jensen: Ultrasonically guided percutaneous puncture; Radiologic Clinics of North America; Vol.8 No3; Dec.1975; pp493-503.
13. D.J.Mozersky, D.E.Hokanson, D.S.Sumner, D.E.Strandness Jr: Ultrasonic visualization of the arterial lumen;Surgery; Vol.72 No.2; pp253-259.
14. D.J.Mozersky, R.M.Olson, H.G.Coons, C.O.Hagood Jr.: Doppler controlled needle director - a useful adjunct to Angiography; Radiology; Vol.109; October 1973; pp221-222.
15. R.Petzoldt, H.Lutz, R.Ehler: Puncture of veins and arteries assisted by ultrasound: Ultrasound in Medicine and Biology; Vol.2; 1976; pp331-333.

16. H.Wallman: Private communication.
17. D.W.Baker, F.K.Forster, R.E.Daigle: Doppler principles and techniques; from Ultrasound: Its applications in Medicine and Biology; Ed. F.J.Fry; Elsevier Scientific Publishing Co.; 1978; pp172-174.
18. O.C.J.Lippold, F.R.Winton: Human Physiology; p214; Churchill Livingstone; 7th edition 1979.
19. D.A.McDonald: Blood Flow in Arteries; p53; Edward Arnold; 2nd edition 1974.
20. A.C.Burton: Physiology and Biophysics of the Circulation; p63; Year Book Medical Publishers; 1965.
21. Ref.19, p60.
22. Ref.20, p66.
23. P.N.T.Wells: Biomedical Ultrasonics; p124; Academic Press; 1977.
24. L.E.Kinsler, A.R.Frey: Fundamentals of Acoustics: p175; J.Wiley and Sons; 2nd edition.
25. J.P.Woodcock: Ultrasonics; p19; Ed. J.M.Lenihan; Pub. Adam Hilger Ltd; 1979.
26. Ref. 24,p171.
27. Ref. 24,p170 and 171.
28. Ref.23, p31.
29. Ref.24, p176.
30. Ref.23, p124.
31. Ref.25, p18.
32. Ref.23, p33.
33. Ref.24, p325.
34. K.K.Shung, A.Rubens, A.Sigelmann, J.M.Reid: Scattering of ultrasound by blood; IEEE Transactions on Biomedical Engineering; Vol.BME-23 No.6; November 1976; pp460-467.
35. Ref.23, p120.
36. Ref.23, p121.
37. K.K.Shung, A.Rubens, A.Sigelmanm, J.M.Reid: Angular dependence of scattering of ultrasound from blood; IEEE Transactions on Biomedical Engineering; Vol.BME-24 No.4; July 1977; pp325-330.
38. Ref.17, p178.
39. Ref.23, p21.
40. Ref.17, p180.

41. J.van Randeraat, R.E.Setterington: Piezoelectric Ceramics; p9; Philips publications; 2nd Edition. 1974.
42. Don Belincourt; Piezoelectric crystals and ceramics; from Ultrasonic Transducer Materials; Ed. O.E. Mattiat; Plenum press; 1971; p72.
43. Ref.42, p66.
44. Ref.42, p66-71.
45. Ref.41, p11.
46. Ref.41, p10.
47. J.Blitz: Fundamentals of Ultrasonics; Butterworth & Co., 1963.
48. Ref.24, p61.
49. Ref.47, p13.
50. Ref.47, p14.
51. Ref.42, pp90-107.
52. H.Vlutters; private communication.
53. Ref.17, p183.
54. S.Reich: Application Notes AN-4590; RCA Solid State Division.
55. Ref.23, p136.
56. Ref.23, pp421-468.
57. Ref.23, p466.
58. Ref.17, p180.
59. R.P.Turner: Electronic Conversions, Symbols and Formulas; Foulsham-Tab Ltd., 1977; p53.
60. R. Hejhall: Application Notes AN-531; Motorola Semiconductor Products Inc.
61. National Semiconductor Data Book: Linear;1980; p10-39.
62. Advertising brochure: Hayashi Denki Co., Ltd."Mini Pen-sized Blood Flow Detectors": Supplied by Protea Electro-Medical Services.
63. P.P.Lele: Safety and Hazards in the current applications of Ultrasound in Obstetrics and Gynecology; Ultrasound in Med. and Biology; Vol 5;1979; pp307-320.
64. J.Hobbins, R.Berkowitz, C.Hohler; How safe is Ultrasound in Obstetrics?; Contemporary Ob-Gyn; Vol.14 special issue; 1979; pp 63-74.
65. D.E.Goldman, T.F.Hueter; Tabular data of the velocity and absorption of HF sound in mammalian tissues; Journal of the Ac.Soc. of America, Vol.28 no.1; Jan.1956; pp35-37.
66. Martindale; The Extra Pharmacopoeia; 27th Ed. p924.

ACKNOWLEDGEMENTS

SUPERVISION:	J. Amoore
MECHANICAL CONSTRUCTION:	M. Price
GEARS:	B. Parker
SCROLL MACHINING:	A. Sass

The direct contributions of these people are gratefully acknowledged.

I also wish to thank the following people for their assistance: A. Jongens (Acoustics), T. Hughes, T. Priday, M.Sketch, Dr. Ozinski (Anaesthetics), Dr. D.Morrell (Anaesthetics), Dr. P.Potgieter (Respiratory), Dr. Wright (Neuroanatomy), Dr. Harris-Jones(Radiology), Dr.B. Knight (Bacteriology), Prof.A.A.Forder (Bacteriology), Dr. Straughan (Pharmacology), Dr.E. Bateman (Respiratory) and the many others who have contributed by way of comment and encouragement.

In addition I want to thank the department of Biomedical Engineering at U.C.T. Medical School, for making available the workshop where most of the construction work was done.